COMILLAS
UNIVERSIDAD PONTIFICIA

Escuela Técnica Superior de Ingeniería ICAI

ASSESSMENT OF ELECTRICITY GRID REQUIREMENTS FOR THE ENERGY TRANSITION

Author: Leslie Herding
Director: Michel Rivier Abbad
Co-director: Rafael Cossent Arín

MADRID | April 2025

Leslie Herding
ASSESSMENT OF ELECTRICITY GRID REQUIREMENTS FOR THE ENERGY TRANSITION

ASSESSMENT OF ELECTRICITY GRID REQUIREMENTS FOR THE ENERGY TRANSITION

Author:

Leslie Herding

Director: Michel Rivier Abbad

Co-director: Rafael Cossent Arín

Doctoral Program: Power Systems

Instituto de Investigación Tecnológica

Escuela Técnica Superior de Ingeniería ICAI

Universidad Pontificia Comillas

Madrid, April 2025

CONSTANCIA REGISTRAL DEL TRIBUNAL DEL ACTO DE LA DEFENSA DE TESIS DOCTORAL

Title: Assessment of electricity network requirements for the energy transition

Author: Leslie Herding

Director: Michel Rivier Abbad

Co-director: Rafael Cossent Arín

Faculty: Escuela Técnica Superior de Ingeniería ICAI

Committee members:

President:	Signature:
Member:	Signature:
Member:	Signature:
Member:	Signature:
Secretary	Signature:

Date:

DECLARATION

I declare that this thesis was composed by myself, that the work contained herein is my own except where explicitly stated otherwise in the text, and that this work has not been submitted for any other degree or professional qualification.

Leslie Herding

Madrid, April 2025

ACKNOWLEDGEMENTS

This thesis would not have materialised if it hadn't been for the support of countless colleagues, friends, and family who have accompanied me during these five and a half years.

Primero de todo quiero darles las gracias a mis supervisores, Rafael Cossent y Michel Rivier. Os estoy enormemente agradecida por haber elegido compartir vuestra experiencia conmigo. Me habéis guiado a encontrar ese equilibrio tan difícil de conseguir que cuida todos los detalles, pero aun así nunca pierde el panorama general de la vista. Con ello no solo me habéis apoyado en desarrollar esta tesis doctoral, sino también me habéis apoyado a lo largo del camino que recorrí para convertirme tanto en la persona como en la investigadora que soy hoy en día.

Quiero dar las gracias también a tantos otros que han formado parte de este recorrido. A Tomás Gómez y José Pablo Chaves Ávila por compartir su experiencia conmigo y a Andrés Ramos por guiarme en mis primeros pasos en el mundo de la optimización. Quiero agradecerle también a Santiago Bañales por su apoyo, paciencia y sus consejos.

Gracias a los miembros del tribunal interno, Tomás Gómez, Pablo Dueñas y Matteo Troncia por su feedback constructivo para la mejora de este documento.

Quiero extender mis gracias a la Universidad Pontificia Comillas y al IIT por acogerme durante estos últimos cinco años y medio. He de dar las gracias a tod@s mis compañer@s del IIT que han compartido este camino conmigo. David, Shilpa, Leandro, Enrique, Marco, Leo, Miguel Ángel, gracias por incontables desayunos, cafés y conversaciones.

Agradezco el apoyo recibido por la Cátedra Iberdrola de Energía e Innovación, el programa RETOS COLABORACIÓN del Ministerio de Ciencia e Innovación y la Agencia Estatal, y la ayuda económica a la movilidad de la Universidad Pontificia Comillas.

Aitor, deseo expresar mi más profunda gratitud por tu apoyo incondicional en este camino. Gracias por celebrar todos los logros conmigo y por no dudar en empeñar nuevas aventuras conmigo. A tu lado siento que puedo con todo, hasta con una tesis doctoral.

Diese Arbeit wäre nicht möglich ohne Euch, die mich auf diesem Weg begleitet habt. Mama, Papa, danke für die bedingungslose Uberstützung auf diesem nicht immer geradlinigen Weg. Danke für all eure Geduld sowie unzählige Fahrten und Flüge durch Deutschland und Europa, wohin auch immer das Leben mich gerade getrieben hat.

Danke Michelle, Sarah und Daniel, nicht nur für all die gemeinsame Zeit in Köln, sondern auch und gerade für unzählige Stunden auf der anderen Seite des Bildirms. Ebenfalls bedanken möchte ich mich bei Volker Nickich und Simon Caron für die Unterstützing meiner ersten Schritte in der Welt der Forschung.

Gostaria ainda de estender a minha gratidão aos amigos e colegas que conheci no INESC TEC, no Porto. Pedro, Renan, Fabio, obrigada por partilharem comigo parte deste percurso.

Leonel, obrigada pelos inúmeros conselhos que me deste ao longo destes últimos anos. Ajudaste-me, sem dúvida, a tornar-me a pessoa e a investigadora que sou hoje. Obrigada por me teres despertado a paixão por um novo campo de investigação.

I would further like to extend my gratitude to the friends and colleagues I met at the National Renewable Energy Laboratory. Tarek, thank you for your guidance during this journey. Thank you for sharing your optimism with me. It has given me the curiosity and the courage to tackle new topics and tools.

Thank you to each and every one of you!

ABSTRACT

The rising threat of climate change is changing the world we live in. Society is facing an increase in land and ocean temperatures, more frequent extreme weather events, higher risks of droughts, and heavy precipitation events. The participation of greenhouse gases in global warming has been scientifically proven. In an effort to limit the increase of global mean surface temperature to below 2 ºC and 1.5 ºC if possible, governments have developed ambitious plans to decrease their greenhouse gas emissions by decarbonising their economies in the course of the Paris Agreement.

The power industry represents 28% of global 2023 greenhouse gas emissions. Hence, the transition towards using zero-emission energy generation technologies is of interest. Electricity can be generated carbon-free via nuclear energy and from renewable sources such as solar or wind power. Energy demands for heating and cooling, as well as transportation, can be decarbonised via electrification. Some industrial applications can be decarbonised via biofuels and hydrogen. These applications lead to an increase in final electricity consumption to be covered by electricity, which further drives the need to invest in carbon-free electricity generation sources.

Renewable energy sources (RES) are expected to cover the main part of the future electricity demand due to a decrease in cost experienced over the last decade. This requires a significant rollout of RES generation capacity to substitute existing fossil generation capacities while at the same time meeting additional demand from electrification. However, optimal locations for renewable energy generation are often found in areas distant from electricity demand centres, requiring electricity grids to connect generation and consumption. Geographically dispersed renewable generators challenge the paradigm of electricity transmission grids, historically built to connect centralised generation sites to demand centres. New electricity transmission assets are necessary to guarantee the security of supply in a decarbonised energy system. Those new assets require investments as well as time to perform lengthy permitting processes.

Another part of the energy transition is the increasing participation of distributed energy resources (DER). Those resources refer to assets connected to the distribution grid, including technologies such as distribution-connected renewable generation (i.e. distributed generation), electric vehicles and heat pumps. The growing importance of distributed resources and their decentralised character challenge the electricity grid at the transmission as well as at the distribution level. They require transmission assets to supply or evacuate their power and additional distribution assets due to increased usage of those networks. Furthermore, in situations where local generation surpasses demand, reverse power flows towards the transmission grid occur, challenging distribution grid infrastructure historically built for one-directional power flows.

The built-out of new electricity infrastructure is often referred to as a potential bottleneck for the energy transition. Apart from the beforementioned requirements for new assets and their related costs, the permitting process has turned grid expansion into a time-consuming process, jeopardising the timely connection of renewable energy resources to the electricity networks.

This thesis seeks to contribute to the efficient integration of renewable generation into electricity transmission and distribution networks. Two research lines are identified in line with the challenges described previously. The first research line (Papers 1 to 3) assesses the grids' reinforcement requirements for integrating high shares of RES and DER. A methodology for evaluating renewable energy-related transmission and distribution network investment costs is developed and later applied to determine the impact of different transmission grid characteristics on the network costs related to integrating high amounts of renewables. Furthermore, this thesis proposes a model to estimate the distribution grid expansion requirements associated with integrating distributed energy resources. The research line concludes with a quantification of electricity grid reinforcement requirements on the transmission and distribution levels. The results show that the economic order of magnitude of grid investment needs is far below the investments required for expanding RES capacity. However, the completion of the necessary grid assets on time is determined to be a more significant bottleneck than the incurred costs.

The second research line of the thesis (Papers 4 and 5) is dedicated to increasing the use of the existing electricity grids to accelerate the electricity grid integration of new resources. The research focuses on flexible connections and the hybridisation of renewable generation technologies downstream of the grid connection point. First, several concepts of calculating a network node’s capacity to connect new assets, i.e. hosting capacity, are evaluated to quantify the potential of relaxing the conservative calculation criteria currently in place. The analysis shows that a dynamic definition of electricity grid hosting capacity could unlock over 60% more annual energy injection into existing electricity grids. The second part of this research line assesses the implications of hosting capacity calculation criteria relaxation and hybridisation of RES technologies on investment into renewable generation capacity. The research suggests that the alternative hosting capacity concepts allow to significantly increase expected profits obtained from an investment into RES capacity. This research line concludes that relaxing hosting capacity calculation criteria and hybridising RES generation technologies represent two efficient ways to enhance the use of existing electricity networks.

This thesis contributes to the ongoing research of efficiently integrating renewable and distributed energy resources into electricity transmission and distribution grids. The works presented in this thesis represent technical and economical contributions to the research field. The findings obtained in this thesis are of help to regulators, system operators, and investors alike to foster the rapid rollout of renewable electricity generation capacities required for a successful decarbonisation of the energy sector.

RESUMEN

Los efectos del cambio climático están transformando el mundo en el que vivimos. La sociedad enfrenta un aumento de las temperaturas terrestres y oceánicas, eventos climáticos extremos más frecuentes y mayores riesgos de sequías y precipitaciones intensas. La contribución de los gases de efecto invernadero emitidos como resultado de la actividad humana al calentamiento global ha sido científicamente demostrada. En un esfuerzo por limitar el aumento de la temperatura media global por debajo de los 2 ºC y, si es posible, a 1.5 ºC, los gobiernos han desarrollado planes ambiciosos para reducir sus emisiones de gases de efecto invernadero mediante la descarbonización de sus economías en el marco del Acuerdo de París.

El sector energético representó el 28% de las emisiones globales de gases de efecto invernadero en 2023. Por lo tanto, la transición hacia el uso de tecnologías de generación de energía sin emisiones es esencial. La electricidad libre de carbono puede generarse mediante energía nuclear y la generación renovable mediante, entre otras, energía solar o eólica. Las demandas térmicas para calefacción y refrigeración, y el transporte pueden descarbonizarse mediante la electrificación. Asimismo, algunos procesos industriales se pueden descarbonizar mediante el uso de biocombustibles o hidrógeno. Estas aplicaciones aumentarán el consumo final de electricidad, que deberá ser cubierto por fuentes libres de carbono para evitar un aumento de las emisiones, impulsando aún más la necesidad de invertir en generación de electricidad libre de emisiones.

Se espera que las renovables cubran la mayor parte de la demanda energética futura gracias a la disminución de costes experimentada en la última década. Esto requerirá la instalación masiva de capacidad de generación renovable para sustituir las capacidades fósiles existentes y para cubrir la creciente demanda eléctrica debido a la electrificación. Sin embargo, los emplazamientos óptimos para esta generación a menudo se encuentran en áreas alejadas de los centros de demanda, lo que requiere que las redes eléctricas conecten la generación con los centros del consumo. Los generadores renovables geográficamente dispersos alteran el paradigma de las redes de transporte, históricamente diseñadas para conectar la generación centralizada con los centros de demanda. Es, por tanto, necesario expandir la red de transporte para garantizar la seguridad del suministro en un sistema energético descarbonizado. Esto requiere inversiones y tiempo para llevar a cabo los prolongados procedimientos de tramitación y obtención de los permisos correspondientes.

Otra consecuencia de la transición energética es el crecimiento de los recursos energéticos distribuidos, esto es, nuevos usuarios de la red de distribución que incluyen tecnologías como la generación renovable (es decir, generación distribuida), vehículos eléctricos y bombas de calor. La creciente relevancia de los recursos distribuidos y su carácter descentralizado suponen un desafío tanto a nivel de transporte como de distribución. Por un lado, la red de transporte ha de suministrar o evacuar su potencia, y, por otro lado, la red de distribución experimenta un uso más

intensivo. Además, en situaciones donde la generación local supera la demanda, pueden producirse flujos de energía inversos hacia la red de transporte, creando posibles problemas en la operación de unas redes que históricamente se diseñaron para soportar flujos de energía unidireccionales.

A menudo se menciona un desarrollo insuficiente de nueva infraestructura eléctrica como un posible cuello de botella para la transición energética. Además de los requisitos mencionados para nuevos activos y los costes asociados, la tramitación y obtención de permisos ha convertido la expansión de la red en un proceso largo y costoso, poniendo en peligro la conexión en los plazos requeridos de la generación renovable y las nuevas demandas a las redes eléctricas.

Esta tesis busca contribuir al ámbito de la integración eficiente de la generación renovable en las redes de transporte y distribución de electricidad. Para ello, se identifican dos líneas de investigación complementarias. La primera línea (artículos 1 a 3) tiene como objetivo evaluar las necesidades de refuerzo de las redes para integrar altos niveles de penetración de renovables y recursos distribuidos. Se desarrolla una metodología para evaluar los costes de las redes de transporte y distribución asociados con la integración de la energía renovable, y luego se aplica para evaluar el impacto de diferentes características de la red de transporte sobre estos costes. Además, se desarrolla un modelo para estimar los costes de la red de distribución causados por la integración de recursos energéticos distribuidos. Esta línea de investigación concluye con una cuantificación de los requerimientos de refuerzo de las redes de transporte y distribución eléctrica. Los resultados obtenidos muestran que el orden de magnitud de los costes de red está muy por debajo de la inversión requerida para expandir la capacidad de generación renovable. Sin embargo, llevar a cabo estos refuerzos a tiempo es presumiblemente un cuello de botella más significativo que la inversión requerida.

La segunda línea de investigación de esta tesis (artículos 4 y 5) está dedicada a evaluar mecanismos para aumentar el uso de las redes eléctricas existentes como un medio para acelerar la integración en las redes eléctricas de nuevos recursos. La investigación se centra en conexiones flexibles y la hibridación de tecnologías de generación renovable aguas abajo del punto de conexión. En primer lugar, se evalúan varios conceptos de cómo calcular la capacidad de un nudo de red para conectar capacidad nueva, la llamada capacidad de acceso, para cuantificar el potencial de relajar los conservadores criterios de cálculo actualmente vigentes. El análisis muestra que una definición dinámica de la capacidad de acceso de la red eléctrica podría desbloquear más de un 60% más de inyección de energía anual en las redes eléctricas existentes. La segunda parte de esta línea de investigación evalúa las implicaciones de la relajación de los criterios de cálculo de la capacidad de acceso y la hibridación de renovables sobre la inversión en capacidad de generación renovable. La investigación muestra que los conceptos alternativos de capacidad de acceso permiten aumentar significativamente los beneficios esperados de una inversión en capacidad renovable. Esta línea de investigación concluye que la relajación de los criterios de cálculo de la capacidad de acceso y la hibridación de las tecnologías de generación renovables representan dos formas eficientes de mejorar el uso de las redes eléctricas existentes.

Mediante estos resultados, esta tesis contribuye al actual campo de investigación de la integración eficiente de la generación renovable y los recursos energéticos distribuidos en las redes de transporte y distribución de electricidad. Los trabajos presentados a lo largo de esta tesis representan aportaciones al campo de investigación tanto desde el punto de vista técnico como económico. Estas contribuciones pueden servir de ayuda tanto para los reguladores como para los operadores del sistema y los inversores, con el fin de fomentar el rápido despliegue de las capacidades de generación de electricidad renovable necesarias para el éxito de la descarbonización del sector energético.

TABLE OF CONTENT

LIST OF PUBLICATIONS

Journal publications

I. **L. Herding**, R. Cossent, M. Rivier, J. P. Chaves-Ávila, and T. Gómez, 'Assessment of electricity network investment for the integration of high RES shares: A Spanish-like case study', Sustainable Energy, Grids and Networks, Vol. 28, pp. 100561-1 - 100561-14, Dec. 2021, Q1, doi: 10.1016/j.segan.2021.100561.

II. **L. Herding**, R. Cossent, M. Rivier, and S. Bañales, 'Assessing the impact of renewable energy penetration and geographical allocation on transmission expansion cost: A comparative analysis of two large-scale systems', Sustainable Energy, Grids and Networks, Vol. 38, pp. 101349-1 - 101349-13, Jun. 2024, Q1, doi: 10.1016/j.segan.2024.101349.

III. **L. Herding**, M. Pérez-Bravo, R. Barrella, R. Cossent, and M. Rivier, 'Large-scale estimation of electricity distribution grid reinforcement requirements for the energy transition – A 2030 Spanish case study', Energy Reports, Vol. 12, pp. 5432 - 5444, Dec. 2024, Q2, doi: 10.1016/j.egyr.2024.11.026.

IV. **L. Herding**, L. Carvalho, R. Cossent, and M. Rivier, 'A security-aware dynamic hosting capacity approach to enhance the integration of renewable generation in distribution networks', *International Journal of Electrical Power & Energy Systems*, Vol. 161, pp. 110210-1 - 110210-13, Oct. 2024, Q1, doi: 10.1016/j.ijepes.2024.110210.

V. **L. Herding**, L. Carvalho, R. Cossent, and M. Rivier, 'Local renewable capacity investment planning under distribution grid hosting capacity uncertainty via Conditional Value-at-Risk',

Conference participations

I. **L. Herding**, J.P. Chaves, S. Bañales, R. Cossent, M. Rivier, T. Gómez, Do network investment costs outweigh the benefits of integrating high shares of renewable generation into electricity networks?, 9th International Conference on Integration of Renewable and Distributed Energy Resources - IRED 2022, Adelaide (Australia). 24-26 Oct. 2022.

II. **L. Herding**, R. Cossent, and M. Rivier, 'Enhancing RES Grid Connection via Dynamic Hosting Capacity and Hybridization', presented at the 2023 IEEE Belgrade PowerTech, Belgrade, Serbia: IEEE, 2023. doi: 10.1109/PowerTech55446.2023.10202726.

Other contributions

- The distribution cost model *DIstribution COst Model for the Energy Transition* (DISCOMET) is being registered as intellectual property of Universidad Pontificia Comillas.

ABBREVIATIONS

BC	Base Case
CC	Coupling Coefficient
COP	Conference of the Parties
CP	Clearing Price
CVaR	Conditional Value-at-Risk
D	Distribution
DER	Distributed Energy Resources
DG	Distributed Generation
DHC	Dynamic Hosting Capacity
DSO	Distribution System Operator
EU	European Union
EV	Electric Vehicle
FERC	Federal Energy Regulatory Commission
FOR	Forced Outage Rate
G&S	Generation and Storage
GEP	Generation Expansion Planning
GHG	Greenhouse gases
GIC	Grid Integration Cost
GWP	Global Warming Potential
HC	Hosting Capacity
HP	Heat Pump
HV	High Voltage
ICP	Investment Candidate Portfolio
IPCC	International Panel on Climate Change
IRA	Inflation Reduction Act
LAU	Local Administrative Unit

LV	Low Voltage
MCS	Monte Carlo Simulation
MV	Medium Voltage
NECP	National Energy and Climate Plan
NTC	Net Transfer Capacity
NUTS	Nomenclature of Territorial Units for Statistics
O&M	Operation and Maintenance
PDF	Probability Distribution Function
PV	Photovoltaics
RC	Rural concentrated
RCR	Relative Cost Reduction
RD	Rural dispersed
RES	Renewable Energy Sources
SDHC	Security-aware Dynamic Hosting Capacity
SHC	Static Hosting Capacity
SO	System Operator
SU	Semi-urban
T	Transmission
T&D	Transmission and Distribution
TEP	Transmission Expansion Planning
TTC	Total Transfer Capacity
U	Urban
USA	United States of America
UTS	Unit Transmission Savings
VaR	Value-at-Risk

1

INTRODUCTION

1.1 Background

Climate change represents a significant threat to modern society. Humanity is already facing its consequences, ranging from the increase of land and ocean temperatures, increased risks of both droughts and the intensity of heavy precipitation events, to more severe climate and weather extremes such as heatwaves [1]. To limit the effects of climate change on humankind, 196 parties signed the Paris Agreement in 2015. In this treaty, the parties agreed to pursue the limit of global warming to well below 2 ºC global mean surface temperature, aiming towards 1.5 ºC [2]. In recent years, the International Panel on Climate Change (IPCC) has pointed out that missing the 1.5 ºC target implies an increased risk of the loss of ecosystems, water and food scarcity, as well as an impact on human health by increasing heat-related mortality rates and diseases [1]. Consequently, a significant global effort is required to limit global warming to help limit the effects on our ecosystems. Lower rates of change allow the natural and human systems to adapt to changes.

However, the remaining carbon dioxide equivalent (CO_2-eq[1]) budget for reaching the 1.5 ºC target is very tight [1], and the emission of greenhouse gases (GHG) resulting from human activity is fuelling global warming [4]. Examples of GHG emitters are fuels such as gasoline, coal, oil and natural gas. These resources are employed for fuelling cars, industry, and electric power plants, among others [4]. In 2023, 28% of global CO_2-eq emissions were related to the power industry, 22% to industrial combustion and processes, 16% to transport, and 7% to buildings [5]. The remaining 27% is related to fuel exploitation, agriculture and

[1] Carbon dioxide equivalent (CO_2-eq) represents a measure to compare the global warming potential (GWP) of different greenhouse gases. The GWP of all GHG is converted to the equivalent GWP of CO_2, resulting in CO_2-eq [3].

waste. GHG emissions have reached an all-time high in 2023, with an increase of 1.9% with respect to 2022 [5].

One means of emission reduction is covering energy demand with zero-emission technologies. Renewable energy sources (RES) offer an opportunity for carbon-free energy generation [6], [7]. The benefits of extending the use of RES are numerous and extend beyond carbon-free energy generation. Direct advantages for the population include health benefits due to emission reduction and local job creation [8], [9], [10]. Further advantages include increasing energy security by reducing the dependency on fuel imports [11]. RES investment costs have decreased significantly over the last decade [12], converting them into an economical alternative to fossil fuel-based generation technologies exposed to fuel price volatility [13].

Thanks to the economic viability of electricity generation with RES, other final energy uses are to be decarbonised via electrification. The decarbonisation of private transport involves electric vehicles (EVs), while heating and cooling are decarbonised via heat pumps (HPs). A pathway towards the 1.5 ºC target involves 30% of final energy consumption to be covered by electricity in 2030, which implies electricity demand will grow in all economies around the globe [14]. The increase of final energy consumption to be covered by electricity further drives the need to invest in carbon-free electricity generation sources such as RES and nuclear energy [14].

As a consequence of the above, countries are pursuing the large-scale rollout of RES technologies to decarbonise their final energy consumption. In 2023, the COP28[2] participants signed the pledge to triple RES capacity until 2030 and ended the continued investment in unabated new coal-fired power plants to pursue the 1.5 ºC target [16]. In 2022, the United States of America (USA) introduced the Inflation Reduction Act (IRA). The IRA seeks energy security by establishing tax credits for various processes, from the manufacturing of RES-related products to the purchase of such by private citizens [17]. The IRA introduces tax credits for investment in zero-carbon electricity generation, as well as for heat pumps (HP) [18]. In Europe, the European Green Deal seeks to reduce the European Union's (EU) GHG emissions by at least 55% by 2030, consecutively reaching carbon neutrality by 2050 [19]. Within the Green Deal, the Fit-for-55 legislative package includes a series of proposals to align EU policies with the climate goals [20]. Correspondingly, the European Council updated the Renewable Energy Directive, aiming for 42.5% to 45% of the EU's total energy consumption to be covered by RES by 2030 [21]. The directive further seeks to reduce the GHG intensity of the transport sector, to gradually increase the use of RES in the industry, and to increase renewable targets of the heating and cooling sector [22].

[2] Conference of the Parties (COP) is a yearly meeting of countries that joined the United Nations Framework Convention on Climate Change. The Parties meet at COPs to assess progresses and negotiate common future objectives. The Paris Agreement is a result of the COP21 [15].

In Europe alone, these targets are expected to double electricity consumption from today to 2050 [23]. Those ambitious targets call for a significant amount of RES generation capacity to be installed throughout the Member States to serve these growing loads with carbon-free electricity. EU Member States publish their mid-term decarbonisation targets in the form of National Energy and Climate Plans (NECPs)[3] [24]. One part of those NECPs details the Member States' objectives in terms of speeding up the deployment of RES to decarbonise the electricity sector.

Electricity grids will be required to transport this emission-free electricity from generation sites to where it is consumed. Optimal locations for investing in RES generation with high generation potential, such as high wind speeds, are often found in areas far away from electricity demand, requiring new electricity transmission assets to connect generation and demand [25]. Additionally, RES installations are usually smaller and more dispersed throughout the territory [26], increasing the distances to be covered by a future decarbonised energy system [25]. This changes the paradigm of the electricity network sending power from centralised generation facilities to customers distributed throughout the territory. In a decarbonised electricity system, RES generation sites are also decentralised throughout the territory but not necessarily aligned with the geographical dispersion of demand. The German regulator is currently implementing the largest infrastructure projects of the energy transition, aiming to expand the transmission grid and connect the wind-rich north with the demand centres in the south [27], [28]. In the USA, high winds are found in the interior of the country, making it ideal sites for wind energy generation. However, the country's major loads are located along the coasts, hundreds of kilometres away from those generation sites [29]. Significant additions of electricity transmission infrastructure are required to connect the new generation sites with demand centres [30].

The construction of transmission lines connecting RES to national demand is only one part of the future requirements of the electricity system. An increasing degree of cross-border interconnection between the different transmission systems is crucial for the decarbonisation process [31]. A well-interconnected system links optimal RES generation sites with customers throughout a wide range of territories. Furthermore, local peaks and valleys of RES resource availability are geographically smoothed out as meteorological events are unlikely to affect the entirety of a large territory [32]. In consequence, transmission grid interconnection represents a means to enhance the security of supply [33].

Transmission grids are connected to the final customers via distribution networks. Traditionally, power from centralised power plants would flow from the transmission system to the distribution grids. However, distributed generation (DG) is on the rise as part of the energy transition. DG refers to generation capacity connected to distribution networks [34]. These installations are smaller and connect to lower voltage levels, namely low voltage (LV) and medium voltage (MV). When paired with assets for electrifying other loads, such as

[3] In the course of the NECPs, the Member States describe their ambitions for 2030, covering decarbonisation, energy efficiency, energy security, internal energy market, and research, innovation and competitiveness.

electric vehicles (EVs) and HPs, those resources are referred to as distributed energy resources (DER). DER allow consumers to become prosumers, i.e. produce and consume their own electricity [35]. This implies that DER participation increases in geographical areas where these consumers are located, i.e. industrial, commercial or residential areas. Contrary to utility-size transmission-connecting RES in remote areas with the highest renewable resource availability, there is usually an existing electricity grid in areas where DER are of interest.

Distribution-connecting RES can help defer the construction of new transmission grid lines to serve growing electricity demand due to the electrification of other energy demands, i.e. transport, heating and cooling. These new loads can be covered locally with DG, posing less strain on the transmission network by reducing the need to transport electricity from distant generation installations to the loads. Contrarily, reverse power flows due to excessive amounts of DG connected to a distribution system can be limited by supplying local, electrified loads [36]. However, in situations where local DG surpasses demand, power flows upstream from the distribution towards the transmission grid. This situation is referred to as reverse power flow because it is opposed to what the electricity grid infrastructure was initially designed for when built several decades ago [35]. In these situations, DG poses a burden on the transmission network for it to transport the electricity to other areas with load surplus. Hence, more transmission grid assents might be required to accommodate DG.

However, DER affect not only the transmission grid required to supply or evacuate their power, but also the local distribution networks they are connected to. Increasing demand requires more distribution lines and substations to transport power from the transmission grid to the end customers. The increasing role of DG requires electricity distribution assets to be able to manage bi-directional power flows. Consequently, the integration of DG especially challenges the operation of existing distribution grids historically built for one-directional power flows from the transmission grid to the load customers [35]. Hence, at the distribution level, upgrades of the existing infrastructure play an important role for integrating the local resources connected to the lower voltage levels.

As mentioned before, European electricity demand is expected to almost double from now to 2050. EVs and HPs are expected to increase twenty-fold, triggering a sixty-fold increase in public EV chargers. DG is expected to increase seven-fold in that timeframe, reaching 2,300 GW by 2050 [23]. All these new resources require reliable electricity grid connections to safely inject and withdraw energy. The annual investment rate into European electricity distribution grids needs to double to 67 billion EUR/yr from now until 2050 to keep up with modernisation, digitalisation and reinforcement requirements. Out of that, 29 billion EUR/yr (42%) alone are required to expand grid capacity for connecting new demand, and another 8 billion EUR/yr (12%) for connecting new generation capacity to the distribution grid [23].

However, the wired approach of enhancing grid capacity via building new assets is often costly and time-consuming, sometimes discouraging investment in RES due to a lack of available electricity grid capacity [37]. The readiness of distribution networks to integrate

DER, especially DG, represents a bottleneck to achieving the 2030 decarbonisation targets on the pathway to limiting global warming to 1.5 ºC [38].

Nevertheless, bottlenecks for efficiently integrating large amounts of RES are not just in the cost of upgrading the grid. The timely increase of the RES share in energy generation is of high importance for limiting global warming to 1.5 ºC. Yet, this objective is potentially jeopardised by lengthy permitting processes. Hence, permitting is a crucial part of streamlining the RES grid connection process, and backlogs in permitting put the power sector's decarbonisation targets at risk. Two mechanisms to mitigate the backlogs of future RES capacity grid connection are long-term planning and anticipatory investments as a means to prepare electricity grids for the energy transition [39]. The European Union's Member States are urged to ensure that national system operators' (SO) grid development plans adequately account for future RES and demand electrification needs [40], while transmission grids in the USA are already suffering a significant backlog of connection requests, saturating the existing grids [41]. Connection times are rising, leading the US Federal Energy Regulatory Commission (FERC) to review the grid connection process for streamlining the integration of new resources [42].

One means of reducing the magnitude of required grid reinforcement is enhancing the use of existing networks with grid-friendly flexibility. It allows the SO to adapt the customers' energy injection or withdrawal to variable operating conditions and is of particular interest for distribution networks. Despite investments required to increase the degree of digitalisation needed for a more flexible distribution grid, the economic savings in European distribution grids could ascend to 4 billion EUR/yr (6%) from now through 2050 [23]. Financial savings from reduced reinforcement costs add to the advantage of avoiding lengthy grid upgrade processes, which often need to be completed before connecting new resources [43]. In accordance with these benefits, EU Member States are recommended to create legal frameworks that allow electricity distribution system operators (DSOs) to use flexibility options [44], [45], [46].

The use of flexibility represents a non-wire alternative for enhancing the use of the existing electricity grid. It can help address the system's needs cheaper and faster than traditional wired expansion options [25]. Flexible connections, also denominated non-firm connections, represent one of these non-wire alternatives. They allow the SO to connect a customer to the network without providing the total requested grid capacity at all times [47]. Those flexible connection agreements enable the DSO to curtail the injection to or the withdrawal from the grid according to the grid's needs, representing a tool to speed up the integration of new DER into the grid. Non-firm connections are helpful in cases of underdeveloped local flexibility markets or as a temporary instrument to connect new grid users quickly [38]. Reinforcement might be deterred or avoided entirely with flexible connections [48]. Another means of enhancing the use of the existing electricity network's capacity is by hybridising different renewable technologies. Hybridisation describes the combination of various technologies downstream of a common grid connection point, i.e. combining a wind power plant with a battery storage system or combining wind and solar power. This allows the use of the complementarity of RES, if given at the location, to efficiently use the grid's capacity with sources that generate electricity at different times (of the day or year) [49].

This chapter has pointed out the rapid changes the electricity sector is facing in the context of the energy transition. The relevance of electricity transmission and distribution grid upgrades for a successful decarbonisation is clear. At the same time, the challenges of integrating new RES and DER into the electricity system need solutions. In the following chapter, the objectives of this thesis are presented in accordance with the challenges introduced.

1.2 Objectives

As introduced in 1.1, ramping up RES at the required speed for meeting the world's decarbonisation goals places particular focus on electricity networks to integrate the new generation capacity at decentralised sites. This thesis aims to assess electricity grid requirements to accommodate the amount of RES necessary to achieve the decarbonisation targets. Two main research lines and their respective objectives have been identified to carry out this evaluation:

I. Assessment of electricity grid reinforcement requirements

This first research line focuses on modelling procedures of electricity transmission and distribution grids to determine the impact of high RES shares and DER on reinforcement needs. The objectives are:

Obj. 1. Developing a methodology to assess RES network integration costs considering both transmission and distribution grid reinforcement requirements in high RES future pathways compared to low RES pathways.

Obj. 2. Assessing the impact of the geographical and voltage level dispersion of RES on electricity transmission grid reinforcement requirements.

Obj. 3. Assessing the large-scale impacts on electricity distribution grid reinforcement requirements for integrating DER.

II. Increasing the use of the existing electricity network

This second research line focuses on the electricity grid connection of RES. It aims to quantify the impact of more flexible grid connection options and RES hybridisation on the rapid and efficient electricity grid integration of RES. The objectives are:

Obj. 4. Understanding the benefits of relaxing the calculation criteria for how much generation capacity can be connected to a network node (i.e. hosting capacity).

Obj. 5. Development of a model to quantify the benefits of flexible connections and RES hybridisation for speeding up RES grid integration.

Obj. 6. Assessing the impact of the beforementioned hosting capacity concepts on investment decisions into new RES electricity generation assets.

By addressing both of these research lines, this thesis seeks to respond to the following **research questions**:

A) Do RES-driven electricity grid investment requirements outweigh the benefits of high RES future pathways?
B) How do different RES dispersions within the grid influence the magnitude of electricity transmission grid reinforcement requirements for integrating RES?
C) What are the distribution grid reinforcements for a nationwide integration of DER?
D) Can flexible connections and RES hybridisation help maximise the use of existing electricity grids?
E) How much electricity network hosting capacity can be unlocked via the relaxation of calculation criteria?
F) How do flexible connections and hybridisation affect the investment decisions regarding new RES capacity?

The outline of the thesis is presented in the following section.

1.3 Thesis outline

This thesis document is presented as a compilation thesis based on several research papers. Following the objectives and research questions described in the previous section, this thesis is structured according to its two research lines. Chapter 2 is dedicated to assessing electricity grid reinforcement requirements, and Chapter 3 evaluates the increase in the use of existing grids. Each chapter is then structured into sections in accordance with its objectives. Each of the previously mentioned objectives is addressed by a paper reported in the annexes of the thesis document. Chapters 2 and 3 provide a global and coherent vision of the developments and contributions performed in both research lines. The thesis document presents the research papers in a summarised form and seeks to highlight the contributions and the connections between the various academic papers. The details of the research can be found in the annexed papers.

First, the contributions to quantifying electricity grid reinforcement requirements are described in Chapter 2. In the first journal paper, a methodology for quantifying transmission, distribution and grid connection costs is presented (Obj. 1) [50]. The second journal paper assesses the impact of different RES dispersions on transmission grid reinforcement requirements via a comprehensive study of two large-scale systems (Obj. 2) [51]. The third journal paper proposes a large-scale model to estimate electricity distribution grid reinforcement requirements for integrating DER (Obj. 3) [52].

This thesis' contributions to the second research line are presented in Chapter 3. The fourth journal paper assesses five different concepts of electricity grid hosting capacity (HC), seeking the maximum injectable energy into existing electricity grids (Obj. 4) [53]. A conference paper proposes an investment model to determine the optimal RES capacity under varying HC and hybridisation scenarios (Obj. 5) [54]. The fifth and last journal paper of this thesis complements the concepts of HC derived in the fourth journal paper with an investor perspective [55]. The model previously presented as a conference contribution is enhanced. Portfolio optimisation is carried out to maximise profits derived for the different HC concepts (Obj. 6).

The findings presented throughout chapters 2 and 3 allow to formulate recommendations on regulatory design for speeding up RES electricity grid integration. These recommendations are presented in Chapter 4.

Finally, the conclusions respond to the research questions, sum up the contributions of this thesis and identify future research lines of interest. Figure 1 summarises the research lines and the corresponding journal publications. The citations are provided in the *List of publications*.

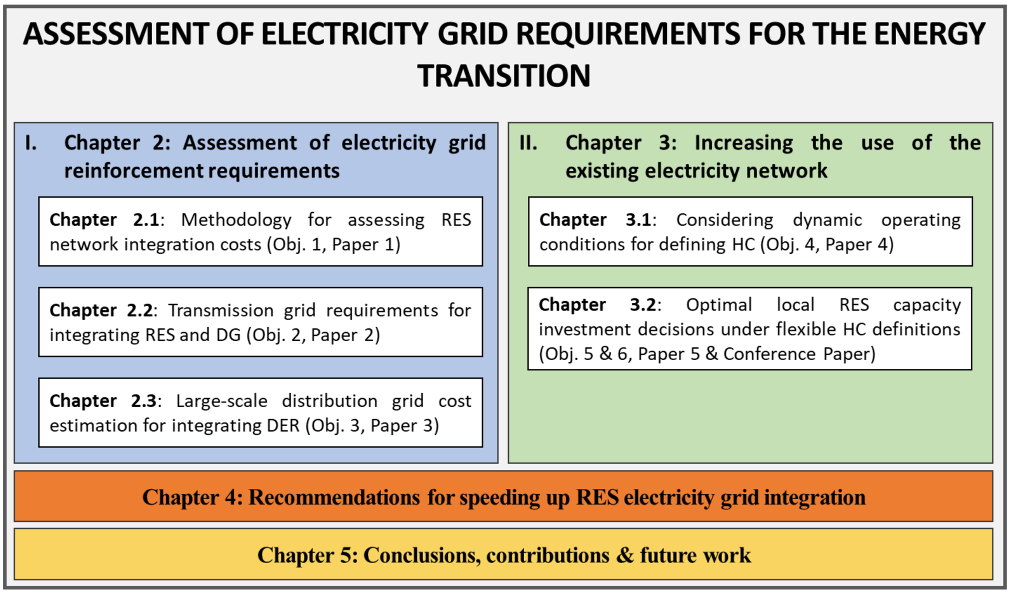

Figure 1: Research lines and journal papers of this thesis

2

ASSESSMENT OF ELECTRICITY GRID REINFORCEMENT REQUIREMENTS

The integration of high RES penetration levels challenges both electricity transmission and distribution networks. The intermittency of RES calls for large generation capacities to be installed and connected via long-distance transmission lines [25]. Integrating these large capacities of RES into electricity grids is expected to require significant investments in electricity grid infrastructure, as pointed out in 1.1. These new physical infrastructure needs are three-fold:

1) **Large-distance interconnections** to smooth out the effect of RES intermittency between different generation sites. Those interconnections often link several transmission systems.
2) **Transmission grid extensions** to connect geographically distributed utility-size RES to demand centres.
3) **Additional distribution grid assets** to adapt the networks to changing power flow directions due to DG and to integrate growing demand.

This thesis is concerned with the latter two and focuses on the reinforcement requirements of additional assets for integrating RES and DER in transmission and distribution networks. It seeks to identify the factors that influence the need for reinforcements and quantify reinforcement requirements. Large-distance transmission interconnections for the energy transition have been subject to a range of studies and are out of the scope for this thesis [30], [56].

The research papers in this research line seek to assess the economic order of magnitude of electricity grid requirements for the energy transition. The scope is set to the requirement for new assets (i.e. transformers, lines) for integrating RES. This thesis is concerned with evaluating the additional impact of RES and DER on electricity grid reinforcement requirements. Costs such as asset replacement and the digitalisation of electricity grids are considered costs which are going to be incurred independent of new RES generation assets due to the ageing electrical infrastructure and increased requirements for grid monitorisation. Hence, these cost terms are out of the scope of this thesis.

The three research papers associated with grid reinforcements assess grid expansion costs at the transmission and distribution level, including an estimation of connection costs. The first paper (annexed in 7.1) addresses Obj. 1 by proposing a methodology to assess the transmission and distribution grid reinforcement requirements for a given horizon target for a national scale-sized system [50]. The methodology is illustrated with a 2030 case study applied to a Spanish-like electricity system. The methodological approach, main findings, and contributions are summarised in Section 2.1.

The second academic publication (annexed in 7.2) addresses Obj. 2 by focussing on the transmission modelling component of the previously proposed methodology [51]. The contribution addresses two synthetic large-scale transmission systems with notably different characteristics and seeks to identify the main factors that may impact the transmission grid reinforcements to accommodate high RES penetration levels. Particularly, the impact of different RES placement scenarios throughout the two networks is evaluated. This paper further enhances the methodology to assess transmission grid expansion requirements for integrating RES. The methodological approach, main findings, and contributions are summarised in Section 2.2.

The third research paper (annexed in 7.3) addresses Obj. 3 and focuses on electricity distribution grid expansion, enhancing the work previously presented in Paper 1 [52]. The contribution proposes a methodology for the large-scale estimation of distribution grid reinforcement requirements for integrating DER. A 2030 case study is presented to demonstrate the model's functionality and highlight the distribution grid challenges related with the geographical dispersion of future DG capacities and load electrification. The methodological approach, main findings, and contributions are summarised in Section 2.3.

2.1 Methodology for assessing RES network integration costs

In this first contribution of this thesis [50], a methodology for calculating RES network integration costs is developed. The research paper presents the methodology and a 2030 case study on a synthetic Spanish large-scale network to show its functionality for determining RES network integration costs.

Figure 2 summarises the methodology for determining RES network integration costs. The methodology encompasses transmission and distribution grid requirements. Additionally, RES network integration costs contain an approach for estimating electricity grid connection costs of new generation assets. Each dimension of RES network integration costs is addressed via an individual methodology. As a final step of the methodology, RES network integration costs are assessed incrementally compared to pathways in which no new RES generation capacity is installed in the system. This part of the analysis allows to draw conclusions on the impact of high RES shares on future electricity system costs.

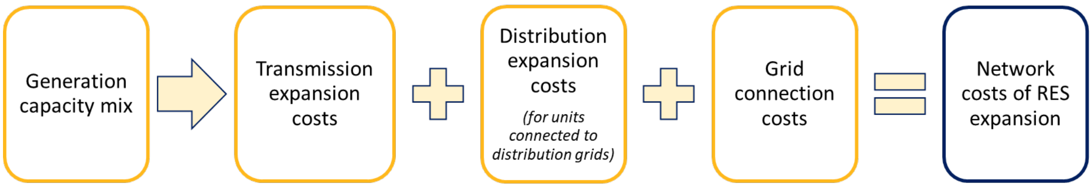

Figure 2: Cost dimensions considered for RES network integration costs

The starting point of the RES network integration costs evaluation methodology is a future electricity generation capacity mix obtained with the help of a Generation Expansion Planning (GEP) model[4]. The GEP model determines an economically optimal generation and storage (G&S) capacity mix. However, the GEP model optimises future G&S capacities for a single-node representation of the electricity system, meaning that electricity network restrictions are not considered at this stage of the analysis. The RES network integration costs methodology seeks to contribute a network perspective to the GEP optimisation. Hence, this first research paper contrasts the cost-optimal G&S capacity mix obtained from a single-node GEP model with a conservative estimation of electricity network investment requirements for an exemplary Spanish-like case study. GEP G&S capacity results represent an input to this contribution. G&S capacity expansion is modelled separately from transmission grid expansion. Generation and network investment decisions are made independently in the current regulatory framework in many deregulated electricity systems. Moreover, current regulation concerning grid investments and network access presents some asymmetries between transmission and distribution, which drive actual investment decisions by RES promoters away from the global optimum.

Transmission grid costs are assessed via a Transmission Expansion Planning (TEP) model[5]. A geographical allocation of G&S resources and load needs to be performed to determine the transmission grid reinforcement requirements for integrating the G&S capacity mix obtained via GEP. The allocation is carried out in proportion to the geographical distribution of existing capacity and resource availability. The geographical allocation is the first contribution of this work.

The TEP model employed in this contribution assesses the economic order of magnitude of transmission grid reinforcements required to integrate the G&S capacities and loads resulting from GEP. The model carries out optimal TEP, minimising total system costs. Those system costs include investments into new transmission grid assets and operating costs, i.e. fuel costs for thermal generation, CO_2 emission costs, and operation and maintenance costs. Secure transmission grid operation is assured by accounting for increased security margins of the transfer capacities of existing grid assets. For this, the

[4] https://www.iit.comillas.edu/technology_offer/3

[5] https://www.iit.comillas.edu/technology_offer/2

maximum loading of an asset is reduced to 67% of its thermal capacity [57]. This allows to reserve the remaining capacity as a security reserve in case of N-1 contingencies, ensuring system reliability and security of supply.

To maintain the computational burden of TEP manageable, the time resolution of the transmission expansion problem is expressed via representative load levels. The load levels are based on the clustering of four representative weeks as employed by the GEP model. Additionally, Monday through Friday are considered via a single daily profile representing weekdays. As a last step, the time-representation is reduced bi-hourly to further reduce the computational burden. This reduces the load levels considered in TEP to 144 representative snapshots which are modelled with their corresponding weight.

As a further means to reduce the computational burden, candidate transmission assets for expansion are pre-selected according to congestions and the difference in nodal prices over distance observed in the initial network. For this step, future generation and demand are allocated at the corresponding transmission nodes, and a first iteration without expansion is run. TEP is then carried out in an additional iteration step. In the expansion iteration, the TEP model is allowed to opt into continuous investment decisions to maintain the computational time at a reasonable magnitude. This is deemed suitable for the scope of this study as the objective is to evaluate the order of magnitude of reinforcement requirements rather than carrying out a detailed TEP. The candidate identification methodology is a contribution of this work.

Distribution grid expansion costs represent the second dimension of RES network integration costs. As stated in Figure 2, distribution-related reinforcements only apply to the amount of capacity connected in the form of distributed generation. Transmission-connecting utility-scale G&S capacities are considered to have no impact on distribution network reinforcement requirements. The share of RES connected to the distribution grid is determined based on historical values of the Spanish electricity system [58].

At the moment of publication, distribution grid expansion costs for integrating DER have been studied extensively in the literature. Hence, an estimation of distribution expansion costs for integrating DG is carried out as a part of this methodology. This estimation is based on the values provided by previous studies found in the literature. Those values express incremental unit costs for integrating DG, i.e. they are given in EUR/kW of DG to be integrated. It is important to note that different distribution grid configurations significantly impact expansion costs. Urban grids usually serve customers located closer to each other, resulting in lower unit costs of urban reinforcement than reinforcement in rural grid zones. Consequently, the employed unit expansion costs distinguish between urban, semi-urban and rural areas.

Electricity grid connection costs are modelled in accordance with a shallow connecting charging regime. This means that costs are computed from the generation site to the closest connection point with the network. Costs for upgrades required in the upstream grid are captured via the transmission and distribution cost terms. The connection cost estimation in this paper is based on already existing generation capacities and their distance to the closest node of the existing network, distinguishing different technologies and voltage levels. These distances are multiplied by the unit connection costs (EUR/km) extracted from Spanish regulation [59], [60].

As mentioned previously, this methodology seeks to analyse RES electricity grid integration costs in an incremental manner compared to alternative future pathways in which no new RES capacity is installed. Four different GEP scenarios are designed for this evaluation. These four scenarios are obtained by combining two load growth rates, i.e. 0% and 2.3% per year [61], and two generation technology options: a fully non-renewable pathway (i.e. no new solar or wind capacity is permitted) and a cost-minimising technology mix. The cost-minimising GEP provides the economically optimal G&S capacity expansion considering all available generation technologies. The scenarios lead to RES shares of around 80% in both demand growth cases. This scenario approach allows for the evaluation of the impact of economically optimal high-RES participations on electricity grid costs compared to a pathway with traditional thermal generation capacities. The resulting scenarios are named according to the corresponding annual demand growth rate and the technology pathway (0%_Non-RES, 0%_RES, 2.3%_Non-RES, 2.3%_RES). In the scenarios without demand growth (0%_Non-RES and 0%_RES), the impact of the technological change of the generation capacity mix towards renewables is analysed. The scenarios with demand growth (2.3%_Non-RES and 2.3%_RES) have been chosen for this case study to increase the generation capacity that needs to be integrated into electricity grids. The demand growth rate is in line with the Spanish NECP [24]. The scenario characteristics and their denominations are summarised in Table 1.

Table 1: Scenarios for estimating electricity grid requirements for integrating RES

Scenario	**0%_Non-RES**	**0%_RES**	**2.3%_Non-RES**	**2.3%_RES**
New generation capacity restrictions	Non-RES only	-	Non-RES only	-
Annual load growth	0%	0%	2.3%	2.3%
RES share over electricity generation	42%	80%	27%	81%

The above-mentioned methodology for calculating RES network integration costs is illustrated with an exemplary Spanish-like case study which assesses the 2030 electricity mix. All scenarios incorporate the closure of existing coal power plants. TEP is performed on a synthetic 481-node transmission network, representing a reduction of the Spanish transmission grid [62]. Unit costs for expanding the transmission grid are derived from a cost catalogue for the Spanish transmission system [59]. For the RES scenarios, the amount of DG is derived from historical data of the Spanish electricity system. The data details the capacity of each technology per voltage level. Low, medium and high voltage installations form part of the distribution grid in Spain [63]. Hence, the share of existing G&S capacities installed at these voltage levels is applied to the additional RES capacity connected to the distribution level in this study.

The results of the RES network integration costs are evaluated two-fold. First, the order of magnitude of grid reinforcement costs is assessed for each of the four scenarios. Second, the resulting grid costs of the RES scenarios are analysed in relation to the corresponding non-RES scenario (i.e. 0%_RES is compared to 0%_Non-RES and the same for the 2.3% demand growth scenarios). In this second step, network integration costs are determined incrementally from non-RES pathways to RES, which allows to reduce the impact of other effects, such as load growth. This analysis focuses on the impact of high RES pathways compared to future scenarios with no new RES.

Figure 3 summarises the investment cost results of the case study. The figure shows the staking of G&S investments and costs incurred for electricity transmission (T) and distribution (D) connection and expansion. The analysis confirms that RES-intense electricity systems result in higher CAPEX requirements in terms of G&S capacity and electricity networks. When comparing the corresponding RES and non-RES scenarios, total investment requirements are multiplied by 34 and 4, respectively, in the scenarios without and with load growth. The high increase in the scenarios without load growth is due to the fact that no new G&S capacity is installed. Hence, investment costs are reduced to a small investment into the transmission network to update the synthetic grid to the current G&S capacities and loads. Another finding of this analysis is that the grid-related CAPEX represent below 10% of total CAPEX (i.e. grid-related and G&S capacity investment).

When focusing only on electricity grid expansion requirements, investment costs are multiplied by 2.9 and 2.5, respectively, in the scenarios without and with load growth. The levelised cost for expanding electricity networks to integrate additional PV and wind capacity is 2.41 and 1.58 EUR/MWh for the scenarios without and with demand growth, respectively.

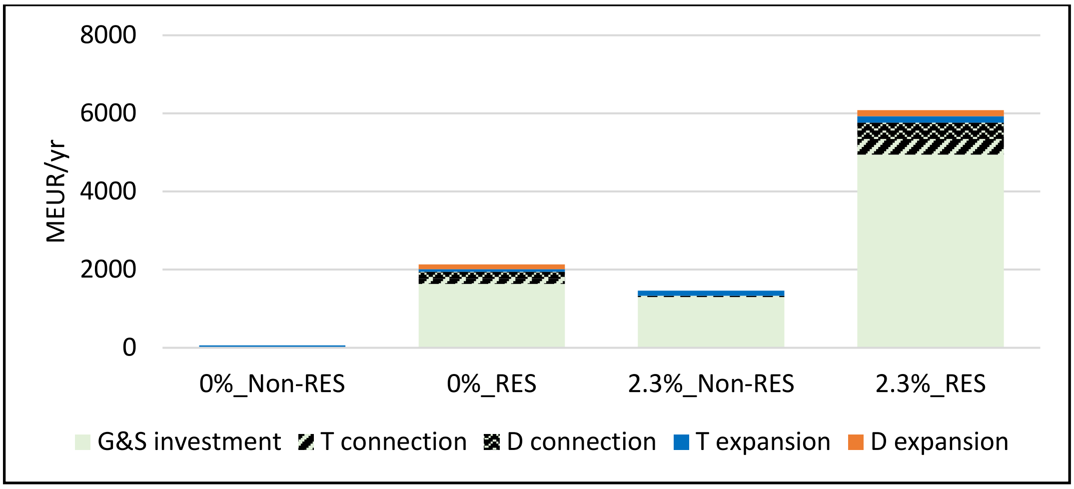

Figure 3: Stacking of all annualised investment cost components

However, the CAPEX increases are more than compensated by reductions in OPEX due to the decrease in fuel use and emissions. Figure 4 summarises this finding. The term avoided operating costs is introduced in this paper to support the analysis. Avoided costs represent the ratio of OPEX reduction and additional RES energy generation in RES scenarios vs the corresponding non-RES scenario. The avoided operating cost is determined at 36.13 and 46.66 EUR/MWh without and with demand growth, respectively. This means that each MWh of RES energy injected into the network reduces operating costs by 36.13 and 46.66 EUR compared to the corresponding non-RES scenario.

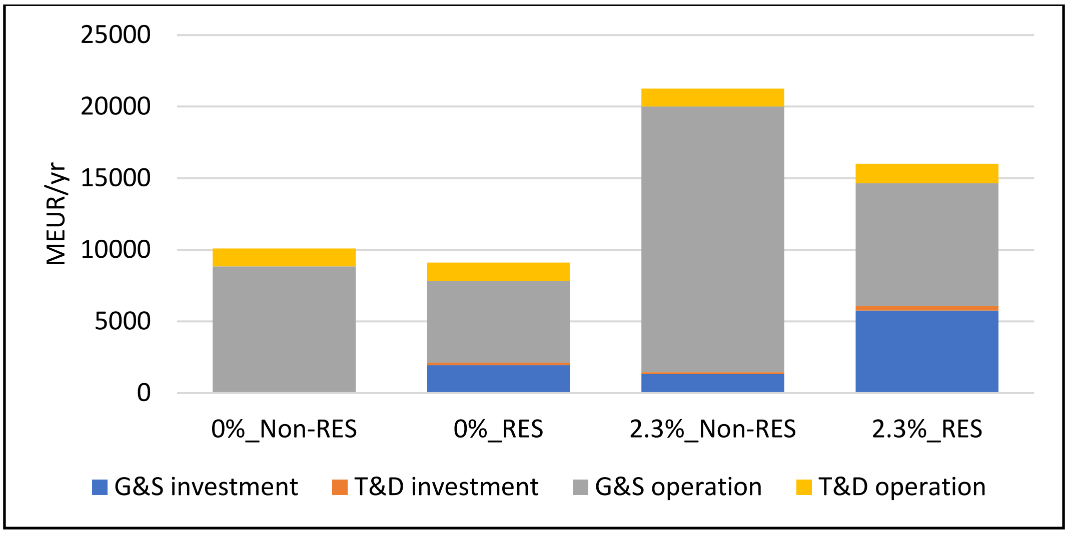

Figure 4: Total annualised investment and operating costs for each scenario (connection costs included in the G&S investment term)

This study quantifies electricity transmission and distribution reinforcement requirements for a Spanish-like electricity system. RES network integration costs are determined in an incremental manner compared to a baseline scenario where no new RES capacity is built. The case study finds that annualised network expansion costs are at least doubled when RES generation is expanded instead of non-RES, translating to 1.58 to 2.41 EUR of additional grid costs per MWh of RES injected into the network. Further, this study demonstrates that the potential of RES generation is in reducing operating costs. Despite the increasing network investment costs, total annual system costs are reduced by 9.7% and 24.7% for the scenarios without and with demand growth, respectively.

This study has established a methodology for determining RES network integration costs and demonstrated the functionality of the methodology in a Spanish-like case study. In the next section, the methodology is applied to another network with notably different RES and demand dispersion to assess the generalisability of the findings of Paper 1.

This work contributes

- A methodology for assessing RES network integration costs accounting for electricity transmission and distribution costs as well as grid connection costs.
- A methodology for the geographical allocation of G&S assets and loads.
- A transmission expansion asset candidate identification methodology.
- The incremental evaluation of high RES G&S capacity mixes over future scenarios with no additional RES capacity.

Associated contributions

The investigation presented in this section is presented in further detail in the research paper **"Assessment of electricity network investment for the integration of high RES shares: A Spanish-like case study"**, published in **Sustainable Energy, Grids and Networks (Q1)**. The paper is annexed in 7.1.

It can be cited as:

> L. Herding, R. Cossent, M. Rivier, J. P. Chaves-Ávila, and T. Gómez, **Assessment of electricity network investment for the integration of high RES shares: A Spanish-like case study**, *Sustainable Energy, Grids and Networks*, vol. 28, pp. 100561-1 - 100561-14, December 2021. [Online: November 2021], doi: 10.1016/j.segan.2021.100561.

Furthermore, additional case studies with the methodology have led to a conference participation, denominated:

> L. Herding, J.P. Chaves, S. Bañales, R. Cossent, M. Rivier, T. Gómez, **'Do network investment costs outweigh the benefits of integrating high shares of renewable generation into electricity networks?'**, 9th International Conference on Integration of Renewable and Distributed Energy Resources - IRED 2022, Adelaide (Australia). 24-26 October 2022.

2.2 Transmission grid requirements for integrating RES and DG

Previous research has allowed to assess RES network integration costs as incremental costs when comparing electricity systems with high RES and systems with low RES participation. The second paper of this thesis takes a more detailed look at transmission grid requirements for integrating RES [51]. This contribution selects two large-scale synthetic transmission grids with notably different geographical distributions of renewable resource availability and load density. The impact of RES on transmission grid reinforcement is determined according to the methodology presented in 2.1. Hence, the four scenarios of Table 1 are assessed on both transmission grids included in this analysis. The TEP expansion framework and its simplifications (i.e. reduction of load levels, continuous investment decision into pre-determined candidate assets) remain the same as in 2.1.

The methodology is refined to evaluate the influence of the dispersion of RES on transmission grid requirements. In that regard, dispersion is interpreted geographically as well as voltage-level related. The sensitivity analysis modifies the allocation criteria of the additional RES capacities to the transmission nodes that has been presented in 2.1. Table 2 presents an overview of the RES dispersion sensitivities and their impact on the allocation of RES throughout the transmission network. The RES concentration sensitivity assesses the geographical concentration of RES capacities in areas with the highest resource availability. As a result of increasing the concentration, the incremental RES capacities are connected to a reduced set of transmission grid nodes.

The DG share sensitivity seeks to assess, for a given total installed RES generation capacity, the impact of increasing share of distributed generation, i.e. the share of that capacity connected at distribution level, on transmission grid reinforcement requirements. Thus, increasing the share of DG participation shift RES capacity from transmission grid nodes with high resource availability to grid nodes closer to demand. In those sensitivities, increasing shares of PV are considered to no longer connect to the transmission system as utility-size generation units but are converted into DG. Those units are allocated within distribution networks. For TEP, this results in an allocation downstream of the transmission grid and changes the net load served via the transmission network. The geographical allocation of the DG capacities is adjusted to the areas with the highest likelihood of investing in PV DG, namely the purchase power of private households and the building density of the different geographical areas of the network. The latter is employed an additional factor to express the fact that, despite similar purchase power in urban and rural areas, rooftop PV can be installed in a greater scale in non-urban areas. As shown in Table 2, shares of up to 100% of future PV capacities connecting to the distribution grid are assessed in the study. Although not realistic, the high DG shares allow to gain further insight into the transmission system under evaluation.

The sensitivities are applied to the RES scenarios only. The base cases for both sensitivities are the results of the 0%_RES and the 2.3%_RES scenario derived according to the methodology presented in 2.1.

Table 2: RES dispersion sensitivities assessed in Paper 2

Sensitivity	Impact on RES allocation
RES concentration	1. Base case (BC): around 25% of transmission nodes with RES 2. RES concentration (RES_Con): up to 10% of transmission nodes with RES
DG share	1. Base case (BC): 0% distributed generation 2. Five sensitivities with increasing shares of DG (20%, 40%, 60%, 80%, 100%)

As mentioned above, this paper contrasts two large-scale synthetic transmission grids with notably different geographical distributions of renewable resource availability and load density, namely the synthetic Spanish network employed in 2.1 and the ERCOT zone in Texas, USA. The Electric Reliability Council of Texas (ERCOT) is the independent SO in charge of the electricity network in Texas [64]. Table 3 provides an overview of the main characteristics of both systems. The ERCOT network is known for existing congestions in the corridor connecting the resource-rich geographical areas with demand centres, i.e. the West-East Interconnection. Again, TEP is linked to GEP via geographical allocation with local data of the Texan and Spanish electricity systems.

Table 3: Main characteristics of the synthetic Spanish and Texan transmission networks

	Spain	Texas
Nodes	479	2,000
Lines and transformers	880	3,206
Total grid length (km)	36,273	48,580
Peak load (GW)	40.23	56.93
Annual system load (TWh)	225.43	325.32
Voltage levels (kV)	220 & 400	115, 161, 230 & 500
Load centres	Dispersed throughout the territory	Concentrated on the coastline in the East
Optimal RES generation sites	Dispersed throughout the territory	Mainly in the West of the territory

In the first step of the analysis, TEP is carried out for the four scenarios introduced in Table 1. Figure 5 shows the results for the two electricity systems under evaluation. Due to the significant difference in system size and the corresponding magnitude of costs, the system costs are normalised with the system's electricity demand to enable comparability. The figure highlights that the system costs are in the same order of magnitude for both systems under evaluation. Still, the synthetic Texan transmission grid observes an investment cost increase. This increase is especially notable in the renewable scenarios. It is caused by the fact that the initial Spanish electricity system already shows a 42% RES penetration, while the initial participation of RES in the Texan electricity system is notably lower (around 12%). Further, the closure of coal power plants is more noticeable in the Texan system. This leads to a significant increase in G&S capacity investments in the cost-optimal RES scenarios, which result in a final RES share of 80%. Those new G&S investments trigger an increased requirement for transmission reinforcements due to the aggravation of the existing bottleneck of the West-East Interconnection in the ERCOT grid.

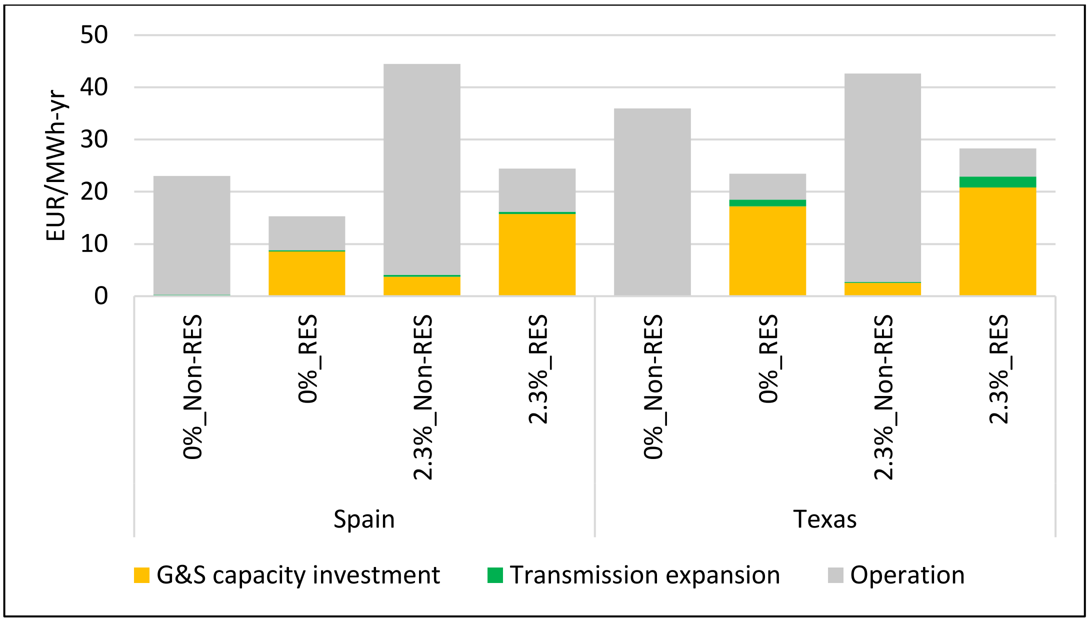

Figure 5: Investment requirements per unit of demand (EUR/MWh-yr)

In the second step of the analysis of the base case, the results of the reinforcement requirements are assessed incrementally between the corresponding non-RES and RES scenarios. The ratio of relative cost reduction (RCR) is introduced in this paper to compare the needs of the two networks. RCR represents the ratio of OPEX reduction divided by additional CAPEX in G&S capacity and transmission expansion. RCR is greater than unity in all scenarios, ranging from around 1.4 in the Texan network without demand growth to 2.2 in the case of the Spanish network with demand growth. It means that the decrease in OPEX via the deployment of RES compensates the required increase in CAPEX. RCR is lower in the Texan network due to i) increased CAPEX requirements in the RES scenarios to compensate for the low initial RES share of the capacity mix and to overcome the West-East Interconnection bottleneck, and ii) lower natural gas prices decreasing the system costs in the non-RES scenarios. Still, the CAPEX increase is compensated by the corresponding OPEX decrease, even in the highly ERCOT transmission congested network. This finding is in line with the results of 2.1 and highlights the outstanding benefits of increasing investment in both generation and transmission capacity to decrease total system costs due to fuel and emission savings.

As introduced in Table 2, a complementary sensitivity analysis to the dispersion of future RES G&S capacities throughout the system is performed on the RES scenarios of both networks. The assessment of both geographical and voltage level-related dispersion of RES over a common base case scenario is a contribution of this work.

The analysis of the first sensitivity shows that a higher concentration of RES capacity in resource-rich network zones is summarised in Figure 6. The figure compares the annualised transmission upgrade costs per unit of RES capacity integrated into the network (EUR/kWyr) for the base case (BC) and the RES concentration (RES_Con) sensitivity. In the Spanish network, the concentration of RES does not significantly impact unit transmission costs due to the geographical dispersion of both load centres and RES resource availability (Table 3). This reduces the effect of the concentration of new RES capacities to a few network nodes in resource-rich areas of the Spanish network. In the Texan network, transmission unit investment costs are more than doubled in the RES_Con sensitivities due to the aggravation of the existing bottleneck of the West-East Interconnection.

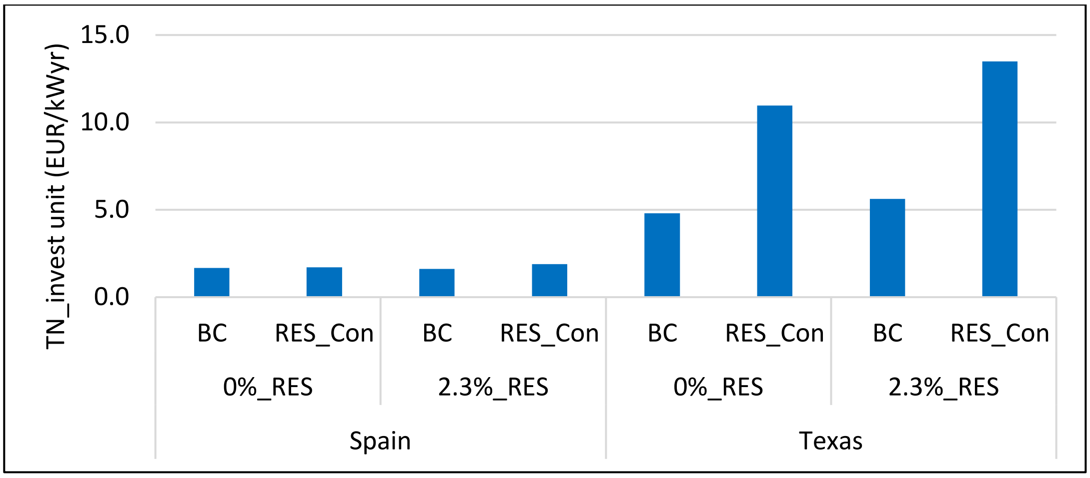

Figure 6: Unit transmission investment costs for the RES concentration sensitivity

In contrast, the implementation of distributed generation leads to allocating generation close to demand centres, resulting in transmission grid savings of up to 30% (Table 2). The findings of the DG sensitivities are summarised in Figure 7. The figure shows the growing share of DG (measured as DG over total PV capacity) for the two RES scenarios in each network under analysis. The increasing DG capacities are presented assessed in comparison to the base case (BC) where no DG is installed. Hence, the transmission grid reinforcement incurred in the BC represents the baseline of 100%. Correspondingly, if a DG sensitivity's relative investment is below 100%, it indicates a reduction of transmission reinforcement needs compared to the base case. Almost all DG sensitivities in both geographical zones and demand growth scenarios allow transmission investment reductions. Only in the Spanish scenario without demand growth do two sensitivities result in minor increases in transmission grid costs: DG_20% leads to a 3% cost increase and DG_100% to a 1.2% increase concerning the BC. These low changes are considered negligible due to the updating requirements of the initial synthetic Spanish network. The Texan synthetic network allows a relative reduction of transmission expansion costs of at least 6% (0% demand growth, DG_20%). The saving potential in the Texan synthetic transmission grid underlines the existing bottlenecks hampering an efficient West-East Interconnection. Higher DG participation locates generation resources closer to the demand centres, thus reducing the requirements for reinforcing the transmission network.

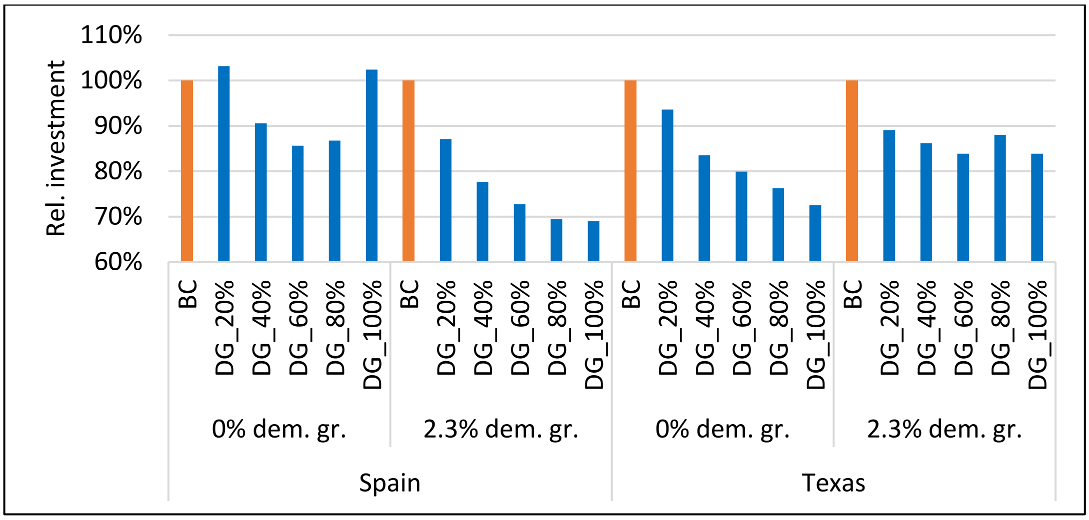

Figure 7: Transmission expansion investment at rising DG penetrations wrt the BC

In general terms, the case studies confirm that decarbonising the electricity system requires a higher investment in RES generation and storage capacity, as well as in grid assets, than the capacity needed in non-RES scenarios. However, the incremental investment costs in renewable generation, storage and grid expansion in the RES scenarios are largely offset by fuel and emission cost reductions compared to non-RES scenarios. This holds true even when significant congestions in the initial transmission system exist, such as the West-East Interconnection in the synthetic ERCOT network.

The two sensitivities on the geographical and voltage level allocation of new RES capacities highlight the trade-off between optimal RES placement according to resource availability and optimal placement to keep grid reinforcement requirements low. A geographical concentration of RES generation capacities aggravates pre-existing grid bottlenecks, more than doubling transmission reinforcement requirements. On the contrary, fostering DG rollout is found to be a helpful tool for reducing transmission grid expansion requirements up to 30%, especially in scenarios with demand growth.

Overall, the results of this paper point out that to meet the 2030 decarbonisation goals, the relevant discussion concerning the decarbonisation of the electricity mix should not be whether grid investment costs may outweigh the benefits of increasing renewable shares. Instead, the debate should focus on ensuring a fast grid connection for the new renewable capacity necessary to achieve the necessary decarbonisation and electrification levels.

This work contributes

- An application of a common methodology for quantifying the impact of high RES shares on two large-scale electricity transmission networks with notably different RES and load dispersions.
- Generalisation of the findings of Paper 1 with a second transmission system with significantly different characteristics.
- A systematic comparison of various RES dispersion factors via a sensitivity analysis with a common baseline scenario.

- A quantification of the impact of increasing participation of DG on transmission systems with different characteristics.

Associated contributions

The investigation associated with the presented methodology is detailed in the research paper **"Assessing the impact of renewable energy penetration and geographical allocation on transmission expansion cost: a comparative analysis of two large-scale systems"**, published in **Sustainable Energy, Grids and Networks (Q1)**. The paper is annexed in 7.2.

It can be cited as:

L. Herding, R. Cossent, M. Rivier, and S. Bañales, **Assessing the impact of renewable energy penetration and geographical allocation on transmission expansion cost: A comparative analysis of two large-scale systems**, *Sustainable Energy, Grids and Networks*, vol. 38, pp. 101349-1 - 101349-13, June 2024. [Online: March 2024], doi: 10.1016/j.segan.2024.101349.

2.3 Large-scale distribution grid cost estimation for integrating DER

The third paper of this research line seeks to enhance the methodology presented in 2.1 by further developing the approach for estimating electricity distribution grid reinforcement costs [52]. 29 billion EUR/yr is projected for connecting new demand to distribution grids in Europe alone [23]. Another 8 billion EUR/yr for connecting new DG capacity to the grid. In this contribution, a model for estimating electricity distribution grid reinforcement requirements for integrating DER throughout the Spanish peninsular territory is developed.

The *DIstribution COst Model for the Energy Transition (DISCOMET)* is a tool to carry out deterministic large-scale estimations of electricity distribution grid investment for the energy transition. The model performs a geographical allocation of future distributed energy resources, including DG, EVs, and HPs to the level of local administrative units (LAU), comprised of over 8,000 municipalities in peninsular Spain. Furthermore, the model accounts for low (LV), medium (MV) and high voltage (HV) distribution grids within each LAU.

The different DER are geographically allocated via individual criteria that express the likelihood of the uptake of a particular technology in a municipality. Figure 8 presents a flowchart of the geographical allocation process performed by the DISCOMET model. Since the drivers for the adoption of each type of DER differ among them, the allocation criteria are different for load electrification via EVs, HPs, and distributed generation. DG allocation differentiates between utility-scale installations and prosumer installations. The former represents installations aiming to maximise profits, and the latter represents electricity consumers seeking to generate their own power. As the flowchart shows, the installations have different voltage levels and allocation criteria. LV installations (i.e. LV DG, EVs and HPs) are allocated via criteria that express the likelihood of private households to invest into these installations. The geographical allocation of future LV load electrification considers the household income as a means to represent purchase power, the Required Thermal Energy

Demand (RTED) for HP allocation, and the substitution rate of EVs to forecast citizens acquiring EVs. RTED is a metric that expresses the theoretical thermal energy demand of a household in function of its size, occupancy and location. The higher RTED, the more profitable for a household to replace an old thermal heating system with an HP. Further, simultaneity factors are included in the model to represent the impact of peak load increase on electricity grid infrastructure requirements. LV prosumer allocation is carried out via a similar approach. The criteria include the household income, the installed capacity, and building density to express the availability of sufficient rooftop surface in a municipality.

Utility-scale DG is allocated according to criteria which allow investors to maximise profits from selling electricity to the grid. Hence, the first allocation criterion is resource availability of PV and wind, respectively. Furthermore, the environmental classification of the terrain is considered. This metric is an indicator published by the Spanish ministry and expresses how likely it is to obtain a favourable environmental evaluation for a RES project [65]. The last criterion for utility scale DG allocation is the available HC of the current distribution network. The Spanish ministry requires DSOs to publish this informative value to drive investment into areas with available grid capacity [66]. The identification of the geographical allocation criteria for future DER is a contribution of this work.

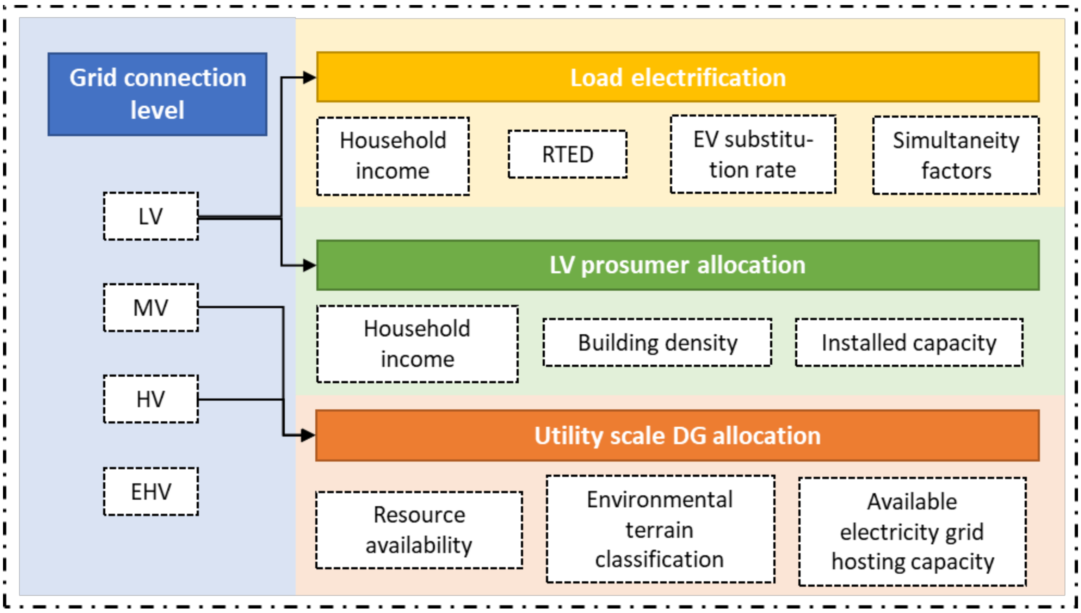

Figure 8: Flowchart of the calculation process of the distribution cost model

In a Spanish case study, distribution grid investment is determined via individualised reinforcement costs for each of the 47 peninsular Spanish provinces (NUTS 2 regions), distinguishing between urban (U), semi-urban (SU), rural concentrated (RC) and rural dispersed distribution (RD) supply zones within the provinces. These reinforcement costs of different types of supply zones are based on historical data for a large set of provinces extracted and extrapolated from the cost database of a Spanish DSO. Figure 9 shows the distributions of the annualised grid costs extracted from the database. The figure represents the difference of the magnitude of costs according to distribution supply zone. The normal distributions are composed by the average unit costs for integrating new grid capacity throughout the Spanish provinces covered by the DSO. These costs are extrapolated to the remaining provinces following the normal distribution observed in the data. The costs are applied to grid upgrades in the MV and HV grid. The unit cost catalogue is a contribution of this work.

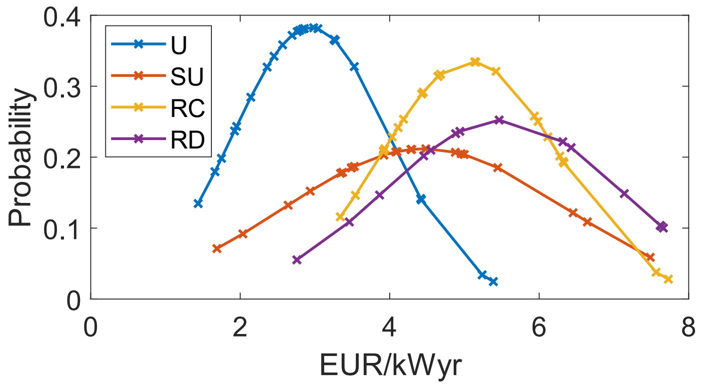

Figure 9: Normal distributions of grid costs observed by a Spanish DSO

The availability of individualised distribution grid expansion unit costs according to service zone type requires classifying all considered municipalities into U, SU, RC or RD. The Spanish municipalities are assigned to a distribution grid service zone according to an estimation of the number of residential supply points in the municipality [67]. The Spanish Statistical Institute publishes the number of households for municipalities with over 2,000 inhabitants [68]. This number is employed as an indicator of the number of residential electricity supply points for urban and semi-urban areas. It cannot be used to distinguish rural concentrated from rural dispersed areas because both consist of less than 2,000 supply points. The number of supply points for rural areas is simplified as the number of inhabitants of a municipality [69]. The supply zone characterisation is contrasted with the characterisation carried out by a Spanish DSO. The methodology correctly identifies 95% of U municipalities and 90% of SU municipalities. The accuracy decreases to 88% in RC and 77% in RD areas. Still, the majority of municipalities is classified correctly and the methodology is applied to all municipalities of the Spanish peninsula. The service zone classification of the municipalities is a contribution of this work.

The required reinforcement in a municipality is calculated with different criteria for LV and for higher voltage levels. Spanish regulation requires DSOs to publish the available HC for new generators for all network nodes above 1 kV [66]. Hence, the network's HC for utility-scale DG is known at MV and HV. No information on HC is available for LV DG connections and load electrification. For the analysis, the LV network's HC is considered zero to obtain a conservative estimation of reinforcement requirements. The model does not account for a detailed representation of the existing electricity grid. The existing grid and its capacity to integrate DER is represented via the available HC.

The model contemplates the effect of a new connection on upstream networks. This means that the capacity installed in an LV network requires available capacity in the corresponding upstream MV and HV grids to guarantee the evacuation of energy generation or load to be served. As indicated in Figure 8, simultaneity factors are employed to address the impact of peak load increase on electricity grid capacity requirements for assessing the upstream effect of load electrification (EVs and HPs) [70]. The simultaneity factors express the likelihood of the contracted capacity to be consumed simultaneously and are employed by DSOs for system planning. The simultaneity factors are 0.4 at the LV level, 0.85 at MV and 0.95 at HV [70].

An exemplary 2030 case study is performed to show the functionality of the model. The additional capacities installed are derived from the Spanish NECP [71]. The amount of DG per voltage level is estimated with historical data of the Spanish electricity system [58]. Table 4 shows the share of PV and wind capacity connected per voltage level resulting from the Spanish NECP and the corresponding voltage level allocation. Additionally, according to the NECP, an additional 3.5 million of private owned EVs and 2,894 ktep of thermal energy demand covered by HPs are expected for 2030. These numbers represent the increases for the target year, i.e. additional capacities that need to be integrated in the distribution network.

Table 4: DG capacity per voltage level in Spain

	LV	MV	HV	EHV
Share of capacity per voltage level				
PV	8%	15%	16%	61%
Wind	1%	4%	35%	60%
Resulting capacity per voltage level (MW)				
PV	2,526	4,552	4,683	18,348
Wind	-	885	8,062	13,353

The analysis finds that reinforcement requirements for integrating DG and for integrating EVs/HPs are geographically misaligned, as shown in the final allocation of capacities in Figure 10. That means that infrastructure built for serving new peak load might not be available for evacuating DG output and vice versa, increasing the total amount of new infrastructure (and the corresponding investment) needed. Also, local consumption of DG energy seems difficult, requiring more grids to transport electricity from one DSO area to another. The misaligned allocation of loaf electrification and DG further highlights that DSOs in different parts of the territory will likely face different challenges for adapting their networks to the requirements faced throughout the energy transition, requiring the regulator to respond accordingly through efficient regulatory design.

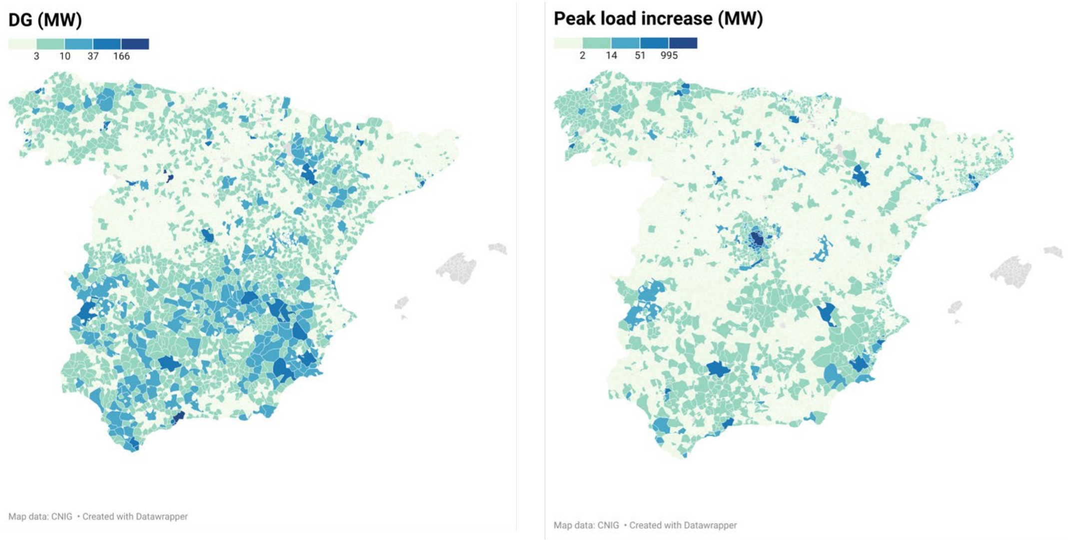

Figure 10: Geographical allocation of DER derived via the distribution cost model

Figure 11 shows the distribution grid reinforcement requirements derived from the geographical allocation presented above. The figure presents the capacity requirements and their economic implications in terms of annualised investment. Further, the figure allows to draw conclusions on the reinforcement requirements per voltage level and per distribution grid service zone type (U, SU, RC, RD). The 2030 Spanish case study requires upgrades of 44 GW of network assets, translating to 197 MEUR/yr of investment costs. The majority of reinforcements are required in HV networks. This is mainly because the 69% of DG is allocated to HV networks (Table 4). Furthermore, upstream network capacity is needed for DER connected at the LV and MV levels. Regarding distribution service zones, most required grid upgrades are located in rural concentrated areas. This is because half of the peninsular municipalities are classified as RC.

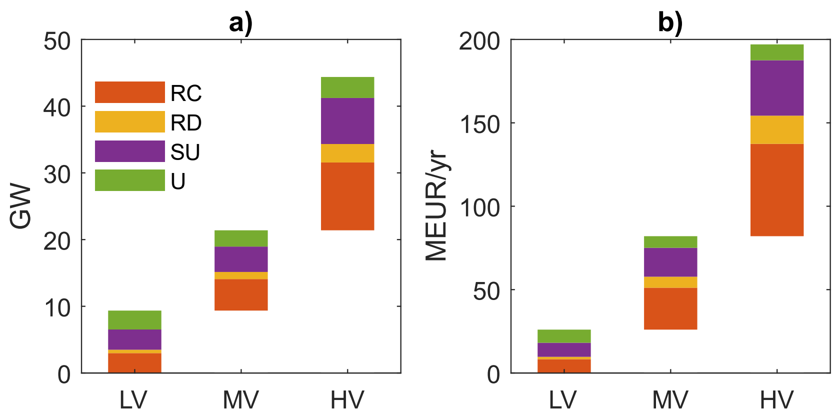

Figure 11: DISCOMET case study results: reinforcement requirements – a) Capacity and b) annualised investment

Figure 12 shows how much of the annualised distribution grid reinforcement requirements are triggered by the grid integration of DG and by the increase of peak load. Several sensitivities on the impact of the LV simultaneity factor on the grid upgrades for load electrification are included in the figure. The sensitivities seek to assess the potential increase of simultaneity, as non-optimal residential load management might increase the simultaneity factor, i.e. due to simultaneous heat demand [72].

The results show that, at the current LV simultaneity factor of 0.4, the required reinforcement costs for load electrification amount to approximately half the cost required for DG integration. As LV load simultaneity factors increase towards 0.8, grid costs approach the magnitude of DG. At LV load simultaneity factors of 0.9 or 1, grid costs for load surpass those for DG. Realistic values of future LV simultaneity factors might be between 0.4 and 0.8, as the coefficient describes the simultaneity of the entire load. The base load will likely follow historical simultaneity factors, while electricity demand for EVs or HPs might show higher simultaneity factors. Consequently, the simultaneity factor of the entirety of the load is not expected to reach 1. In any case, the efficient management of future electricity demand is crucial for maintaining distribution grid costs at a reasonable magnitude.

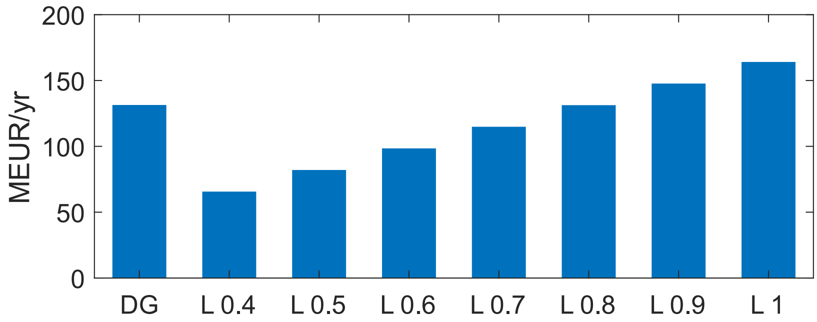

Figure 12: Annualised distribution grid investment for DG integration and load electrification

Overall, the case study demonstrates that the model represents a tool to efficiently assess the impact of the geographical allocation of DG and load electrification on distribution grids of the whole Spanish peninsular territory based on the costs of actual projects in a Spanish DSOs' network. The results show a potential misalignment of the geographical allocation of future DG capacities and the peak load increase due to the electrification of LV loads via EVs and HPs. This finding points out that the DSOs covering different parts of the territory are likely to face a variety of challenges that are not aligned between the territories.

This work contributes

- A methodology for the geographical allocation of DG and demand electrification technologies (EVs and HPs) to all voltage levels classified as distribution-level in Spain (LV, MV, HV) with a resolution of Local Administrative Units (> 8,000 municipalities in the case of Spain).
- The classification of Spanish peninsular municipalities into distribution service zone types (i.e. urban, semi-urban, rural concentrated, rural dispersed) according to Spanish regulation.
- The deployment of a unit expansion cost catalogue extracted from the database of a Spanish DSO, as well as extrapolation methodology to the whole country.

- A tool to efficiently assess the impact of the geographical allocation of DG and load electrification on distribution grids of the whole Spanish peninsular

Associated contributions

The investigation associated with the presented methodology is detailed in the research paper **"Large-scale estimation of electricity distribution grid reinforcement requirements for the energy transition – A 2030 Spanish case study"**, published in **Energy Reports (Q2).** The paper is annexed in 7.3.

It can be cited as:

L. Herding, M. Pérez-Bravo, R. Barrella, R. Cossent, M. Rivier, **Large-scale estimation of electricity distribution grid reinforcement requirements for the energy transition – A 2030 Spanish case study**. *Energy Reports*. Vol. 12, pp. 5432 - 5444, December 2024. [Online: November 2024]

Furthermore, the model *DIstribution COst Model for the Energy Transition* (DISCOMET) was officially registered as intellectual property, register number 16 / 2025 / 995.

3

INCREASING THE USE OF THE EXISTING NETWORK

The first research line, presented in Chapter 2, sought to quantify the costs of RES and DER integration into electricity transmission and distribution networks. The research, presented in the form of three academic papers, has shown that the cost magnitude of electricity grid reinforcement requirements is not prohibitive. Instead, the research has highlighted that the debate should focus on ensuring a fast and efficient grid connection of new RES and DER assets. The second research line, detailed in this chapter, is concerned with increasing the use of existing networks.

The permitting process is one of the main bottlenecks for RES expansion, which is brought up frequently within the sector and is well-known by policymakers [39], [73], [74]. One crucial part of the permitting process is the assignation of electricity grid access. The procurement of electricity grid access for a new RES generator is limited by the electricity network's capacity for connecting additional generation and load without requiring reinforcement is called hosting capacity (HC).

The HC describes how much generation or load can be connected to a network node without degrading the network performance outside the safety limits of operational parameters such as frequency or voltage limits [75]. It is the threshold a DSO passes on to connection-seekers. This threshold of HC needs to be guaranteed by the DSO, which is why it is usually calculated with very conservative assumptions to ensure grid stability. Due to the guaranty of the availability of the assigned network capacity, this kind of connection agreement is denominated firm connection agreement. While *hosting capacity* refers to the availability of the network to integrate new generation capacity or load, *connection agreement* describes the agreement of the customer and the DSO and includes the definition of the *access rights*, i.e. the terms under which the customer can make use of the network connection point.

The terminologies of HC, network access rights and connection agreements are summarised in Table 5. Firm access means that the assigned HC is available at all times, even in the case of network failures [43], [76]. Usually, the threshold of HC is constant throughout the year. Accordingly, it is called static hosting capacity (SHC). DSOs are incentivised to underestimate HC rather than overestimate their networks' capacities, as compensation payments might be enforced if a customer with a firm connection faces curtailment. This is because the connection is granted as a firm connection with uninterruptible access rights.

Contrary to a firm connection, flexible connections allow for a more dynamic definition of the network capacity offered to a network user [77], commonly referred to as non-firm access or flexible connection. It represents the option for the DSO to define the network's HC more dynamically to adjust to the operational reality of the network instead of calculating a conservative static hosting capacity threshold as currently performed by most DSOs [38], [78]. The network access is interruptible to allow the DSO to curtail the connection in case it is required. In some cases, a flexible connection refers to allowing a generator to connect to the network before the required reinforcement has been carried out [79]. In these cases, the connection is non-firm because the DSO cannot yet guarantee the firmness of HC at all times. It is described as a temporary flexible connection as it is expected to convert to a firm connection once the network upgrades are carried out.

Table 5: Terminology of hosting capacity, access rights and connection agreements

	Firm	Flexible
Hosting capacity	Static hosting capacity	Dynamic hosting capacity
Access rights	Uninterruptible	Interruptible
Connection agreement	Firm	Non-firm/Flexible

The research papers of this research line consider the permanent option of non-firm connections by exploring the benefits of increasing the use of the existing electricity grid infrastructure in line with the dynamic nature of operating conditions. The first paper of this chapter (annexed in 7.4) assesses the potential of a dynamic definition of a network node's HC. Further, it introduces the concept of security-aware dynamic hosting capacity to account for the network's N-1 outages and their probabilities [53]. The methodological approach, main findings, and contributions are summarised in Section 3.1.

In the first research paper, HC is defined from the network's perspective. This means HC is a technologically neutral quantification of the maximum injectable energy into a network node within the grid's operating limits. The second paper of this research line (annexed in 7.5) complements those findings by adding a RES investor's perspective to assessing dynamic hosting capacity. It seeks to evaluate whether dynamic HC definitions are of interest from a profit-maximisation point of view and to quantify their impact on optimal generation capacity [55]. The methodological approach, main findings, and contributions are summarised in Section 3.2.

3.1 Considering dynamic operating conditions for defining HC

As described in Chapter 3, distribution grid hosting capacity is currently defined as a conservative static threshold in many regulations [43]. The fourth paper of this thesis evaluates a more dynamic definition of HC [53]. Dynamic hosting capacity (DHC) reflects that the dynamic operating conditions due to RES and load variability allow for the injection of more energy than the conservative definition of a static threshold. In this thesis, HC is defined as the maximum injectable energy into a specific network node.

The network's operational security limits are enforced when calculating the maximum injectable energy for a node. That means that hosting capacity is limited by thermal line loading limits, voltage limits, and the short-circuit ratio which limits the maximum capacity of a single generator that can be installed at the grid connection point. HC is a nodal property and technologically neutral as it depicts the maximum energy injection within the grid's operational limits and does not respond to a specific technology's generation profile.

Several different definitions of HC are assessed in this work. They are denominated *HC concepts*. Table 6 provides an overview of the five different HC concepts under analysis and their characteristics in terms of tine granularity and reliability considerations. Within the concepts of HC, SHC refers to a fixed threshold of HC applied throughout all hours of the year, independent of the variability of RES availability and demand. DHC represents a relaxation of the time granularity restrictions, leading to a time-series definition of HC. As indicated in the table, SHC and DHC are assessed for two different types of reliability considerations. N-1 refers to defining the network configuration according to the asset failure resulting in the lowest value of HC. Optimal network reconfiguration is accounted for in case of N-1 contingencies as a means to guarantee security of supply. For SHC N-1, the assessment is performed over the worst-case hour considered. For DHC N-1, this translates to evaluating all N-1 asset failures over all hours considered for the time-series computation of HC. The lowest threshold is assigned hour by hour. This means that the final DHC N-1 curve is a result of various N-1 failures affecting different points of time throughout the evaluation horizon. In contrast to N-1, SHC N and DHC N consider all network assets operating under normal conditions, hence relaxing the reliability criterion for HC calculation. SHC N-1 is the definition of HC according to the Spanish regulation on HC calculation for generation [76].

Table 6: HC concepts assessed in Paper 4

HC concept	Time granularity	Reliability considerations
SHC N-1	Snapshot	Deterministic worst-case N-1
SHC N	Snapshot	-
DHC N-1	Time-series	Deterministic worst-case N-1
DHC N	Time-series	-
SDHC	Time-series	Probabilistic N-1

Both SHC N-1 and DHC N-1 represent conservative assumptions on the likelihood of asset failures by limiting the maximum injectable energy according to the most limiting N-1 network outage. Security-aware dynamic hosting capacity (SDHC) is proposed in this research paper as a means to account for N-1 asset failures in a non-worst-case manner. Outages and the corresponding network configurations are considered according to their probabilities of occurrence. SDHC is derived by determining the DHC for each N-1 contingency, accounting for the respective probability of occurrence of the N-1 contingency scenario according to the asset's forced outage rate (FOR). While SDHC is represented as an hourly time-series in this case, the time granularity can be adjusted to the requirements of the study. SDHC is calculated according to Eq. 1, where h represents the hour of the year, j represents the number of network assets accounted for SDHC calculation (i.e. all normally closed lines and transformers), and i indexes the network component under N-1 contingency. The definition of SDHC and the systematic comparison of relaxing time granularity restrictions (SHC vs DHC) or reliability constraints (N-1 vs N) with a common baseline based on a regulatory reference (SHC N-1) are contributions of this work.

$$SDHC_h = DHC_h^N \left[\prod_{j=1}^{N} (1 - FOR_j) \right] + \sum_{i \in \Omega_{N-1}} DHC_{h,i}^{N-1} * FOR_i * \left[\prod_{\substack{j=1 \\ j \neq i}}^{N} (1 - FOR_j) \right] \quad \text{Eq. 1}$$

The HC concepts are assessed at three different nodes of the CIGRE benchmark MV network with DER [80], [81], [82]. The nodes are highlighted in yellow in Figure 13. Node 3 is selected due to its proximity to the external grid, node 5 due to its location downstream in feeder 1, and node 14 due to its location in feeder 2. In this case study, the grid's operational limits are defined according to Spanish regulation, which aligns with UNE-EN 50160.

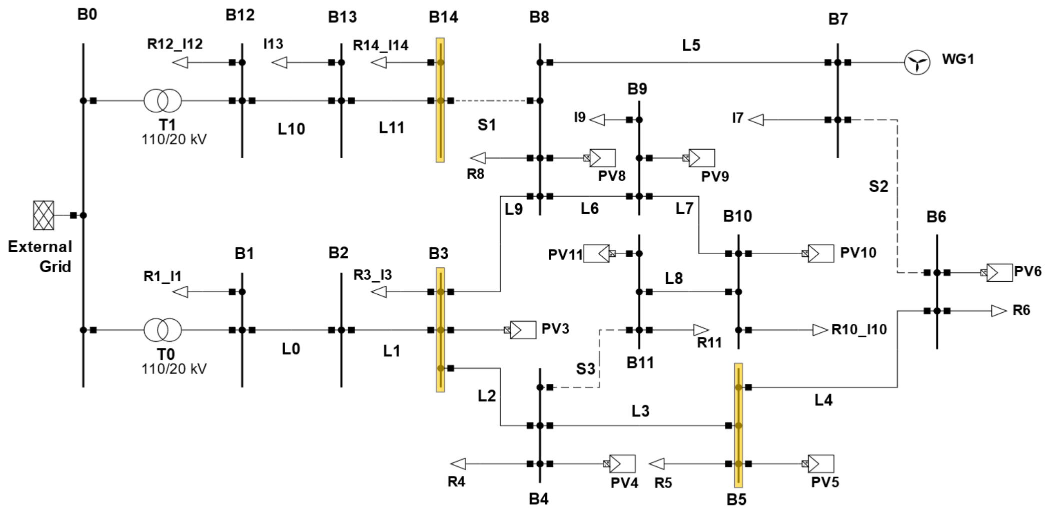

Figure 13: Line diagram of the CIGRE benchmark MV network

For this representative case study, SHC N-1 and SHC N (Table 6) are determined for the reference scenario snapshot defined in Spanish regulation [76]. It requires load to be defined at the minimum observed simultaneous system demand. Pre-existing generators are considered at two different thresholds of their access capacity. Generators at the node under evaluation are considered at 100%, and generators at all other network nodes are considered at 90% of their granted access capacity. This scenario aims to assess a conservative snapshot of network operation to ensure the resulting SHC value is available under all possible operating conditions.

All dynamic definitions of HC are evaluated with time consistency throughout the year. This allows to assess the impact of DHC on RES installations that will be performed in the following section. The HC curves are derived from the variability of load and the output of existing DG, namely wind and PV. Various yearly conditions of PV and wind resource availability are identified and employed combinatorically, i.e. every sample year of PV availability is evaluated against every sample year of wind availability due to often low correlations between PV and wind availability [83], [84], [85]. Additionally, several years of load are considered in the evaluation. The annual curves are selected out of various historical curves. Load curves represent loads observed in the Spanish system [86]. Residential load is assumed to follow the low voltage load curves, while commercial demand is assumed to follow the tariff category 6.1A, representing MV consumers [87]. The RES availability curves are derived for a location in Almería, southern Spain [88], [89]. Selection criteria for the input curves of RES availability consider the correlations between the curves, capacity factors throughout the year, and full load hours, among others. Finally, the representative years account for three years of load, three years of PV availability and six years of wind availability. Wind is represented in more detail due to the randomness of the resource. The combinatorial analysis of dynamic HCs results in 3 load * 3 PV * 6 wind = 54 sample years to assess. This means that DHC N-1, DHC N and SDHC are determined for 54 annual time-series.

The case study results are summarised in Figure 14. The results are presented as an annual injectable energy into the network node under evaluation without violating the grid's operating limits. The energy injection in the SHC N-1 case is used as a baseline (100%). The figure points out the potential of relaxing the N-1 contingency criteria for calculating SHC. SHC N yields a noticeable increase in injectable energy at nodes 5 and 14. The impact of relaxing the reliability criterion (SHC N-1 vs SHC N) is not noticeable at node 3 as optimal reconfiguration allows to cover loads surrounding the node.

Furthermore, the figure points out the significant increase in injectable energy when comparing DHC to SHC. Even the deterministic consideration of hourly worst-case N-1 DHC leads to an increase of annual injectable energy of at least 19%. SDHC does not show a significant variation from DHC N. This is due to the low FORs of the network under analysis. The MV CIGRE benchmark network consists of mainly underground lines of short length (< 5km), decreasing the probability of asset failures. The variation between SDHC and DHC N is below 0.1% at all three HC evaluation nodes. Consequently, compared to the N-1 restricted SHC, SDHC allows for additional injectable energy of 62%, 67%, and 76% at nodes 3, 5 and

14, respectively (i.e. the same values observed for DHC). These values point out that N-1 contingencies do not significantly affect DHC due to low FORs of the network under analysis.

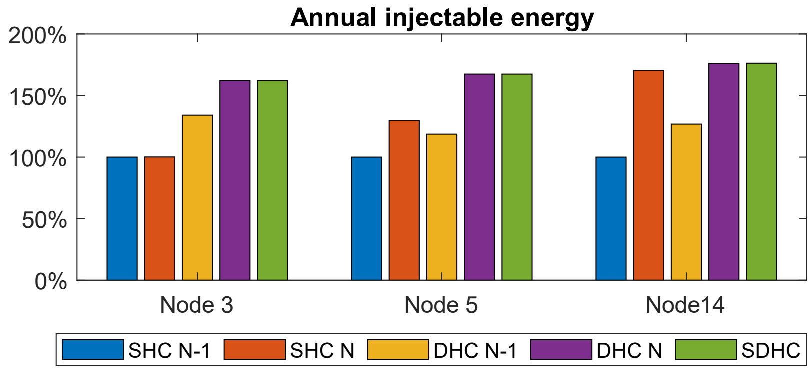

Figure 14: Increase of injectable energy for the different HC concepts

The assessment of alternative HC concepts with a relaxation of the time granularity or the deterministic reliability restrictions has shown the potential hosting capacity available in existing electricity networks without requiring lengthy reinforcement. A HC concept that allows for the probabilistic consideration of N-1 asset failures is proposed.

Relaxing the deterministic worst-case N-1 reliability criteria for HC calculation and moving to SHC N allows for a notable increase of up to 50% of injectable energy. The dynamic definition of HC allows for a further increase in the injectable energy to 62% to 76% compared to the regulatory baseline of SHC N-1. The difference between DHC N and SDHC is insignificant due to the low forced outage rates of the network under analysis.

In the following section, these technologically neutral conclusions on HC from network perspective are complemented with an assessment of employing RES to exploit the additional HC available when relaxing calculation criteria. The approach seeks to maximise a RES investor's worst-case profits by optimising the generation capacity installed at a network node with a given HC.

This work contributes

- The definition of security-aware dynamic hosting capacity to account for network contingencies' probabilities impact on DHC.
- A technologically neutral evaluation of a network node's HC.
- A systematic comparison of static and dynamic HC concepts with a common baseline defined via regulatory criteria.
- A quantification of the potential of relaxing hosting capacity calculation criteria for unlocking significant amounts of existing electricity grid hosting capacity.

Associated contributions

The investigation associated with the presented methodology is detailed in the research paper **"A security-aware dynamic hosting capacity approach to enhance the integration of**

renewable generation in distribution networks", published in the **International Journal of Electrical Power & Energy Systems (Q1)**. The paper is annexed in 7.4.

It can be cited as:

L. Herding, L. Carvalho, R. Cossent, and M. Rivier, **A security-aware dynamic hosting capacity approach to enhance the integration of renewable generation in distribution networks**, *International Journal of Electrical Power & Energy Systems*, vol. 161, pp. 110210-1 - 110210-13, October 2024. [Online: September 2024], doi: 10.1016/j.ijepes.2024.110210.

3.2 Optimal local RES capacity investment decisions under flexible HC definitions

Section 3.1 has shown that significantly more energy could be potentially injected into electricity distribution networks if regulation allowed to relax HC calculation criteria and moving towards flexible connections (Table 5). In the following step, it needs to be determined whether this increase in injectable energy would actually translate into an increase in installed RES capacity and how much of the injectable potential would be materialized in practice. This assessment considers the profit-maximisation perspective of a potential investor in RES capacity [55]. The methodology is denominated “Optimal local RES capacity investment decisions” in reference to the optimisation of RES capacity downstream of the grid connection point

The RES capacity investment planning methodology under uncertainty is composed of several optimisation steps. The methodology is summarised in Figure 15 and will be described in more detail throughout this section. The figure presents a flowchart of the local RES capacity investment planning process and summarises the inputs, calculation steps and results. Further, the number of scenarios managed in each methodology step is included in the figure.

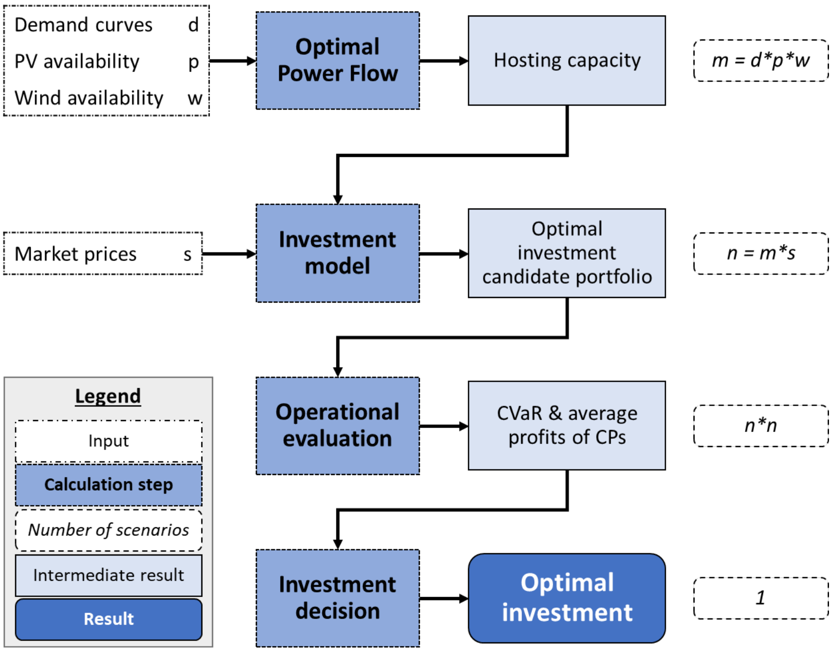

Figure 15: Flowchart of the local RES capacity investment planning process

As a first step, Optimal Power Flow (OPF) is employed to derive a node's HC, as detailed in 3.1. As presented previously, the HC result depends on load and RES variability, represented via input curves. The analysis is combinatorial, leading to $m = d*p*w$ HC results. The OPF analysis is carried out for four of the five different concepts of HC introduced in 3.1. SDHC is not explicitly modelled due to the insignificance of the variations from DHC N.

The HC output from the OPF assessment is input to an investment model that optimises the renewable capacity installed for each HC definition [54]. At this stage, the number of scenarios is enhanced to n scenarios due to the consideration of additional input representing market prices. As an output, the model provides one investment candidate portfolio (ICP) for each of the n scenarios. In this work, the term portfolio describes the generation capacity installed downstream of the grid interconnection point. A portfolio may consist of a technology mix of PV, wind and battery capacity if deemed optimal by the investment model. The n different ICPs describe the portfolios that make the optimal decision for each of the n scenarios and the corresponding RES availability, HC, and market prices.

The investment model considers both investments and operation and maintenance (O&M) costs. Eq. 2 provides the profit maximisation objective function of the resulting model for generation capacity optimisation. The optimal capacity is a result of the hourly (indexed with h) energy injection E_inj_h and its remuneration Rem_h, as well as the investment (Inv) and $O\&M$ costs for the capacity P of each technology, indexed with t. The investment model is a contribution of this thesis.

$$max\left[\sum_h (E\_inj_h * Rem_h) - \sum_t (P_t * Inv_t) - \sum_t (P_t * O\&M_t)\right] \quad \text{Eq. 2}$$

The restriction under analysis in this work is the hourly energy injection, which is limited by *HC* (Eq. 3). In the case of DHC, HC takes on the corresponding hourly values. In the case of SHC, the threshold is fixed by a static value throughout all hours of the year.

$$E\_inj_h \leq HC_h \quad \text{Eq. 3}$$

Hourly energy injection depends not only on HC but also on the energy available *E_inj*, as shown in Eq. 4. The latter is a direct result of the PV and wind capacity installed, their respective availability curves, and the use of the 4h batteries if the model opts for them. Available energy may be subject to curtailment (*E_curt*) to ensure that injected energy does not surpass HC.

$$E\_inj_h = \sum_t E\_avail_{t,h} - E\_curt_h \quad \text{Eq. 4}$$

The hourly remuneration Rem_h per unit of injected energy (EUR/MWh) is modelled according to the remuneration method used in RES auction schemes (Eq. 5), given that a significant part of renewables is remunerated via that scheme [90]. The remuneration is determined as a combination of the RES auction clearing price *CP* and the hourly market price MP_h. Those two values are coupled via a coupling coefficient *CC*, as employed in the Spanish auction design [91]. This adjustment allows for limited exposure to market volatility while providing certainty for the portfolio's remuneration.

$$Rem_h = CP + CC * (MP_h - CP) \quad \text{Eq. 5}$$

For an optimal investment decision, each of the *n* ICPs needs to be assessed throughout different scenarios of changing operating conditions, i.e. RES and HC availability and market prices. Each ICP is assessed throughout the remaining scenarios in this evaluation. As shown in Figure 15, the operational assessment provides the ICPs' profits throughout all *n* scenarios, allowing to determine the average profits and CVaR of each ICP. These outputs represent the ICPs' performances in various scenarios of grid and market conditions.

Table 7 shows the scheme of the operational evaluation. The second line shows that a total of *n* ICPs are derived with the investment model. Those ICPs are subject to the input curves of RES and HC availability and remuneration considered for the annual computation of the investment model and represent the optimal investment decision for those inputs. Each ICP's operational performance is assessed throughout all other years of RES and HC availability and remuneration to determine the optimal ICP. This can be read column-wise from the table. For example, the first column shows that the ICP obtained from the first combination of input curves is fixed (ICP_1), and profits are assessed with all other combinations of input curves ($Op_{1,1}$ to $Op_{1,n}$). The evaluation is repeated for each of the *n* ICPs to determine which yields the best performance throughout the variety of input years.

Table 7: Operational evaluation scheme for comparing capacity investment candidate portfolios

	Candidate portfolio				
	ICP_1	...	...	...	ICP_n
Operational evaluation	$Op_{1,1}$	...	...	...	$Op_{n,1}$
	...	...	...	...	...
	...	...	...	...	...
	$Op_{1,n}$	...	...	...	$Op_{n,n}$

The results of the operational evaluation allow to determine the optimal ICP for local RES capacity investment. The investment decision is made with the help of Conditional Value-at-Risk (CVaR) [92]. CVaR is often employed to determine an optimal portfolio with minimum worst-case losses. It is an evolution of Value-at-Risk (VaR). Contrary to VaR, CVaR does not just refer to one specific point at the probability distribution function (PDF) of losses but describes the interval of all loss values observed below the threshold of VaR. It allows to provide a more risk-aware representation of the worst-case losses of a portfolio. In this work, CVaR is applied to the profits of the candidate portfolios. Consequently, the optimal ICP is the one that yields the maximum value of CVaR since CVaR presents worst-case profits. Identifying the optimal combination of RES generation technologies to respond to uncertainty regarding resource availability, HC, and remuneration is a contribution of this work.

The local RES capacity investment planning methodology under uncertainty is carried out independently for the HC concepts proposed in Table 6, except for SDHC, as mentioned previously. Further, the optimal generation capacity is determined once for non-hybrid and once for hybrid RES capacity mixes. The HC curve input is represented by the 54 sample years of DHC N-1 and DHC N derived from the combinatorial analysis of PV, wind and load curves presented in 3.1. Each DHC is assessed with the corresponding availability curve of PV and wind to guarantee the coherence of the observed HC throughout a year and the availability of the DG unit to be optimised in this step. Additionally, a total of five different years of hourly market prices are assessed to analyse the impact of uncertain market prices on optimal RES generation capacity mixes. The last five years ($s = 5$) of Spanish SPOT market prices are evaluated in this analysis [86]. The clearing price is set to 60 EUR/MWh according to historical results throughout Europe [93], and the coupling coefficient is set to 5% according to previous Spanish auctions [94]. A sensitivity analysis is performed to assess a lower clearing price (*CP = 40 EUR/MWh*), as Spanish auction results have been reported to be below 37 EUR/MWh. Additionally, sensitivities assess and coupling coefficients of 25%, 50%, 75% and 100%. A CC

The investment model is run year by year, resulting in $n = 54 * 5 = 270$ different ICPs, each one the optimal result for one sample year. The profits of the 270 operational results for each ICP offer sufficient data points for CVaR analysis. CVaR is determined for the worst-case profits at the 5% cut-off of the profit PDF.

Local RES capacity investment planning is carried out for the three nodes of the CIGRE MV benchmark network which were assessed in the HC study in 3.1. Figure 16 shows the results of the operational valuation of the four HC concepts under assessment for node 5. NH and H represent the results for the non-hybrid and the hybrid capacity expansions, respectively. The figure plots the CVaR results over the average profits for the 270 candidate portfolios within each case of HC and hybridisation. The relation between CVaR and average profits is linear. This means that the ICP which yields maximum CVaR is the same which leads to maximum average profits. This linearity is due to the low exposure to volatile market prices as the coupling coefficient is 5%. The CC sensitivities show that the ICP resulting in maximum CVaR is no longer the same as the ICP resulting in maximum average profits at increasing exposure to market volatilities. At CCs > 25%, the optimal investment decision is impacted by the risk-aversion or risk-prone attitude of the investor.

Furthermore, Figure 16 shows that the impact of moving from N-1 to N reliability criteria for HC calculation on CVaR and average profits is more pronounced than the impact of hybridisation. Combining hybridisation and DHC (i.e. DHC N H) allows for a significant increase in CVaR and average profits compared to SHC N-1 NH.

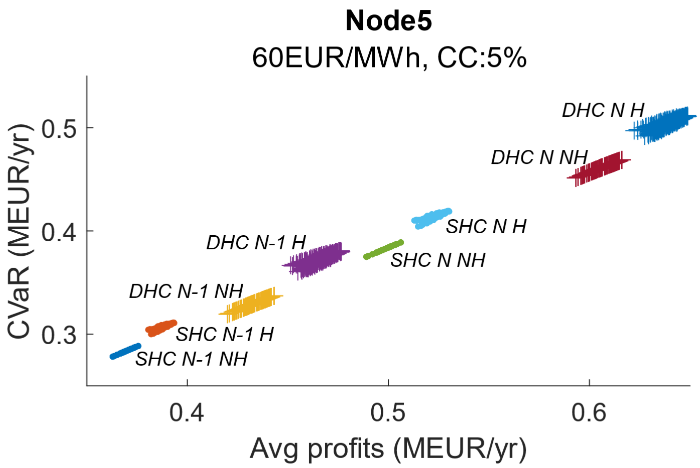

Figure 16: Operational evaluation of HC concepts and hybridisation

The assessment shown in Figure 16 allows to determine the optimal ICP for each HC and hybridisation case according to maximum CVaR and average profits. The results of the investment decision are summarised in Figure 17. No battery capacity is installed due to the magnitude of CAPEX. The relaxation of HC calculation criteria significantly impacts installed capacities and energy injection, increasing profits and CVaR, as observed in Figure 16. DHC N NH leads to a 65% increase in installed capacity and energy injection compared to SHC N-1 NH. CVaR and average annual profits are increased by 62% and 64%, respectively. Relaxing only the reliability constraint but not the time granularity constraint (i.e. SHC N NH) increases all indicators under evaluation by 35%. These increases from SHC N-1 align with the increases in injectable energy derived from the node's HC (Figure 14).

When accounting for hybridisation, the previous findings are amplified due to the complementarity of PV and wind profiles to maximise the use of available network hosting capacity. DHC N H leads to a 127% increase in installed capacity compared to SHC N-1 NH. The average annual energy injection increases by 86%, and CVaR and average annual profits increased by 77% and 73%, respectively. Even without relaxing the time constraint, the increase is notable. SHC N H shows an 81% increase in installed capacity and 51% additional average annual energy injection compared to SHC N-1 NH. CVaR and average profits are increased by 45% and 41%, respectively.

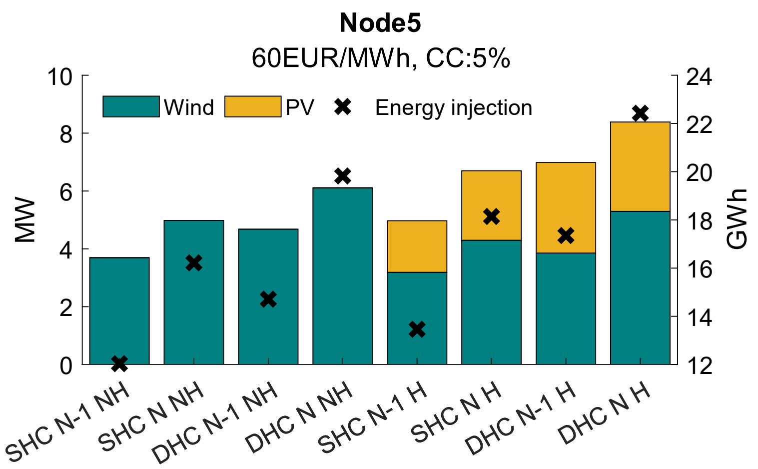

Figure 17: Optimal generation portfolio investment decisions for the HC concepts and hybridisation

The analysis and conclusions are enhanced by several sensitivity analyses regarding the network node, the clearing price, and the coupling coefficient. Detailed results can be found in the paper. The sensitivities to the network node and the clearing price show that the increases in profits from SHC N-1 to alternative HC concepts are in the order of magnitude of the increases of injectable energy observed in the HC assessment (Figure 14). The CC sensitivity assessment shows that, for sensitivities at CC ≥ 50%, CVaR and average profits are no longer in a linear relationship. In these cases, the ICP with the maximum CVaR is no longer the same ICP yielding maximum average profits. Figure 18 shows that observation for the sensitivity of a CC of 75%. The figure shows the operational evaluation of the ICPs derived for DHC N H.

The results of the sensitivity indicate the existence of a Pareto front that supports the identification of the optimal investment decision. The ICPs on the Pareto front are characterised by the fact that there is no other ICP which shows higher CVaR and average profits. Of the 270 ICPs subject to the operational evaluation, 54 ICPs form the Pareto front. CVaR of the ICPs on the Pareto front ranges from 0.064 MEUR/yr to 0.162 MEUR/yr (+157% from the minimum CVaR), and average profits range from 0.983 MEUR/yr to 1.132 MEUR/yr (+15% from the minimum average profits). Further, the ICPs on the Pareto front can be grouped into three groups similar in CVaR and average profits, as supported by the visualisation in Figure 18.

In cases such as the one at hand, the final investment decision depends on the risk-aversion or risk-prone attitude of the investor. A more risk-averse investor would opt for an ICP of group 1, as the ICPs have the highest CVaR and the lowest investment requirements, i.e. capital at risk. Installing more capacity means moving towards ICP group 3, which reduces CVaR, but maximises average profits. A more risk-prone investor might opt for an investment decision in ICP group 2. This group is characterised by intermediate values of CVaR and average profits. The average profits of group 3 almost reach the maximum average profits of the ICPs on the Pareto front while maintaining CVaR at a higher level.

The analysis of the CC sensitivity highlights the contribution of the CVaR method for determining an optimal local RES capacity investment decision while accounting for risk. Investment decisions based on average profits alone would have resulted in a higher total investment.

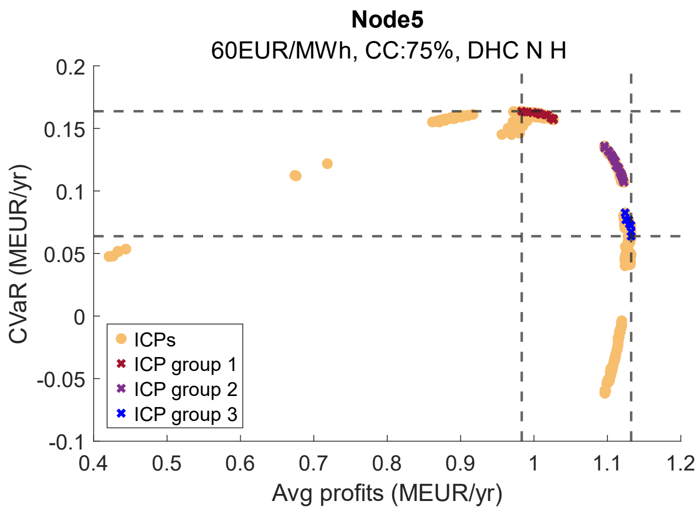

Figure 18: Operational evaluation at CC = 75%

This paper proposes a methodology to account for a RES generation capacity investor's perspective on the ongoing discussion of a more efficient use of existing electricity distribution networks required for a successful energy transition. A cascade methodology is employed to point out how a more flexible definition of hosting capacity and the hybridisation of PV and wind energy can help increase the use of existing network capacity. This work shows that, despite increased uncertainty, DHC is of interest to RES investors. All proposed HC concepts show an increase in installed capacity and profits from the regulatory HC criterion. The corresponding increase in injected energy underlines the relevance of the HC concepts in speeding up the energy transition by enhancing the use of existing electricity distribution grids without endangering a safe network operation. Further, a sensitivity analysis highlights the strengths of the CVaR method for determining the optimal RES capacity investment under uncertainty.

This work contributes

- A methodology for local RES generation capacity portfolio optimisation under uncertainty of RES and HC availability and market prices which allows to adjust to different levels of risk adversity from a RES investor perspective.
- The development of a RES capacity investment optimisation model specifically adapted to the context of the analyses of the different HC concepts carried out in this thesis.
- An impact quantification of measures to increase the use of existing electricity distribution network capacity, namely hybridisation and HC calculation relaxation.
- A sensitivity analysis to enhance the robustness of the conclusions.

Associated contributions

The investigation associated with the presented methodology is detailed in the research paper **"Local renewable capacity investment planning under distribution grid hosting capacity uncertainty via Conditional Value-at-Risk"**, currently available as working paper here. The paper is annexed in 7.5.

Furthermore, part of this work was presented at the **2023 IEEE Belgrade PowerTech** under the title **"Enhancing RES Grid Connection via Dynamic Hosting Capacity and Hybridization"**. The paper is annexed in 7.6.

It can be cited as:

L. Herding, R. Cossent, and M. Rivier, 'Enhancing RES Grid Connection via Dynamic Hosting Capacity and Hybridization', presented at the 2023 IEEE Belgrade PowerTech, Belgrade, Serbia: IEEE, 2023. doi: 10.1109/PowerTech55446.2023.10202726

4

RECOMMENDATIONS FOR SPEEDING UP RES ELECTRICITY GRID INTEGRATION

The research presented in this thesis is highly relevant in the current regulatory context of preparing electricity grids for the energy transition, highlighted in 1.1. Hence, the lessons learned throughout the research allow to draw high-level conclusions on mechanisms that can help foster a rapid and efficient electricity grid integration of RES and DER. These recommendations are presented throughout the remainder of this section.

The contributions of the first research line (Chapter 2) highlight the economic benefits of fostering the development of electricity systems with high shares of RES to decrease the system costs to be borne by society. The results presented in sections 2.1 and 2.2 show that the reduction of operating costs of thermal generation plants compensates for the increase of electricity grid reinforcement requirements even in electricity systems with noticeable pre-existing bottlenecks, making high-RES electricity systems an economically attractive option for society.

These findings show that the increased investment in electricity grids is required for a future energy system with lower annual costs. The availability of electricity grids is crucial to harvest the benefits of RES. SOs should be encouraged to prepare their grid for integrating future RES and DER. For this, they should be allowed to recur to anticipatory investments required for an efficient connection of future resources, as recommended by the European Commission [39]. Preparing the grid ahead of time allows to reduce the denials of future connection requests triggered by a lack of available grid capacity and can help mitigate connection queues at grid nodes where grid reinforcement is ongoing.

Further, SOs investment plans should account for the uncertainty of the geographical allocation of future RES capacity as well as account for the fact that not all installations that request electricity grid access will finally enter operation. This requires a shift from traditional investment planning involving a single scenario of future RES and loads [95], towards considering several possible geographical allocation scenarios and their probabilities. The work presented in Section 2.2 has shown the impact of different geographical allocation scenarios on the resulting reinforcement requirements of electricity networks.

The combination of multiple-scenario-based investment planning and anticipatory investments represents a means to prepare electricity grids for significant capacity additions ahead of time at a reasonable cost. Introducing multiple-scenario-based electricity grid planning in the context of anticipatory investment reduces the probability and magnitude of misinvestment due to scenario errors. Misinvestments are still likely to occur but to a reduced degree. However, this work has highlighted that the available OPEX reduction more than compensates for the increase of CAPEX in high-RES systems. Minor increases in investment costs are still expected to be outweighed by the operating cost reduction. Further, the magnitudes of CAPEX requirements in Chapter 2 are based on conservative assumptions and likely overestimate CAPEX requirements, further increasing the saving potential of high-RES systems.

Apart from allowing SOs to anticipate the investment requirements, regulators should address the guidelines on how available grid capacity is calculated. Chapter 3 of this work shows the potential of unlocking distribution system hosting capacity by relaxing the time granularity and reliability considerations. The findings support EU Directive 2019/944 on the potential of flexible electricity grid connection agreements [46]. The Directive calls for the implementation of temporary flexible connections. The results of Section 3.2 highlight the potential of flexible HC to increase local RES capacity investments. The availability of flexible connections increases the capacity installed with a profit-maximisation approach. This finding highlights the potential of flexible connections, even in permanent schemes in areas where grid reinforcement is not an option.

The analyses presented in sections 3.1 and 3.2 contribute to the understanding of flexible distribution grid connections. National Regulatory Authorities need to update the regulatory HC calculation criteria to move away from restrictive firm electricity grid access. In the process, DSOs will require regulatory security to ensure that no penalisations will result from the implementation of interruptible connections. Currently, customers might be eligible for compensation when facing curtailments. Further, the metrics of security of supply need to account for the difference of curtailments of customers with flexible connections and those with firm connections.

Implementing flexible connections could occur as a capacity assigned with non-firm access complementing a firm capacity. Spanish regulation foresees the co-existence of both concepts [96]. Besides the co-existence of firm and non-firm network access, a flexible connection is always voluntary for the connection-seeker. The optionality is important for connection-seekers to understand the benefits of flexible connections. Small customers, especially, might prefer a firm access scheme due to the enhanced certainty of grid access availability. DSOs should be required to respond to a connection request with information on the different grid access options available at the connection node. This allows connection-seekers to understand the difference in connection costs and time of firm and flexible connections. In the case of temporary flexible connections, as required by EU Directive 2019/944 [46], the connection-seeker needs to be made aware of the estimated time to complete the necessary reinforcements.

The research on the second research line has further quantified the potential of the local hybridisation of RES. The case study in Section 3.2 shows that the hybridisation behind the grid connection point can significantly increase the use of the existing electricity network. The impact is amplified in combination with the relaxation of HC calculation criteria. From a system perspective, maximising energy injection does not represent a risk to the safe network operation as long as the maximum injectable energy is not surpassed at the grid connection point.

The combination of the research lines selected for this thesis allows to develop meaningful recommendations on preparing electricity grids for the energy transition. The regulatory recommendations are summarised below:

- R1. Allow SOs to perform anticipatory electricity grid investments.
- R2. Require SOs to perform investments based on an analysis of different scenarios rather than on one deterministic assessment. The scenarios should tackle different placements of future RES assets.
- R3. Implement flexible electricity grid connections, optional for the connection-seeker.
- R4. Provide regulatory security to DSOs regarding the current considerations of security of supply which do not allow for interruptible connections without penalisations.
- R5. In the absence of sufficient firm access capacity, require DSOs to respond to connection requests with the different connection options (i.e. firm and flexible) and the involved connection costs and time.
- R6. Eliminate regulatory barriers limiting the local hybridisation of different RES generation technologies downstream of the grid connection point, as long as the energy injection does not surpass HC.

.

5

CONCLUSIONS, CONTRIBUTIONS AND FUTURE RESEARCH

5.1 Conclusions

This thesis aims to contribute to the global ambition of decarbonising the energy system. It focuses on the electricity grid of the future as a backbone to integrate vast quantities of renewable energy sources and transport the generated electricity to load centres which are growing due to electrification. With the definition of two research lines, this thesis has quantified the electricity grid reinforcement costs for integrating high RES and DER shares into electricity transmission and distribution grids. It has quantified the potential of enhancing the usage of existing electricity networks via the relaxation of hosting capacity calculation criteria and hybridisation of RES. By doing so, this thesis has raised research questions which have been presented in 1.2 and are addressed in the following. Answering those research questions has allowed to address the objectives of both research lines. They will be pointed out in the course of this section.

A) Do RES-driven electricity grid investment requirements outweigh the benefits of high RES future pathways?

This thesis has assessed RES network integration on the electricity transmission and the distribution level (Obj. 1). A methodology for assessing the incremental impact of high RES pathways compared to those where no new RES capacity is installed is developed. Papers 1 and 2 of this thesis employ this methodology on two different electricity grids and show that the CAPEX-intensity of high-RES pathways due to increased generation capacity and electricity grid investment requirements is outweighed by the OPEX reduction due to decreased fuel usage and emissions. By doing so, energy systems with high RES participation represent a more economical alternative despite an initial increase in investment costs. Even in transmission systems with significant existing bottlenecks, the OPEX reduction in the high RES scenarios represents 140% of the CAPEX increase. Furthermore, electricity grid reinforcement costs represent less than 10% of the total CAPEX requirements for decarbonising the energy sector. This finding holds even in strongly congested networks with high needs for new transmission assets to connect resource-rich areas with load centres.

B) How do different RES dispersions within the grid influence the magnitude of electricity transmission grid reinforcement requirements for integrating RES?

This thesis has further assessed the impact of RES dispersion on the reinforcement requirements of two large-scale electricity transmission networks with a notably different geographical distribution of resource availability and load (Obj. 2). In Paper 2, RES dispersion is assessed independently in terms of geographical allocation of new resources and the voltage level they connect to. The analysis shows that large distances between resource availability and load centres aggravate existing grid bottlenecks and more than double transmission grid reinforcement requirements. The work further shows that increasing the participation of DG in the electricity mix is a measure that moves RES generation capacity from remote, resource-rich areas towards existing distribution networks that are closer to demand. This shift reduces the need for more transmission assets, especially in networks with pre-existing bottlenecks. The avoided transmission grid reinforcement via DG is quantified at up to 30% compared to the base case without DG.

C) What are the distribution grid reinforcements for a nationwide integration of DER?

This thesis has contributed to the understanding of challenges faced by the distribution grid when integrating DER by proposing a large-scale model for estimating reinforcement requirements with a geographical resolution of LAU (Obj. 3). A Spanish case study in Paper 3 shows that distribution grids may face a geographical misalignment between DG and load electrification, highlighting the need for regulatory design that accommodates the challenges faced in both cases. The case study shows that existing electricity grid hosting capacity cannot be efficiently used due to a geographical misalignment of available grid capacity and the allocation of future utility-scale DG. Furthermore, a sensitivity on load simultaneity factors shows that distribution grid reinforcement need might more than double at increasing simultaneity factors, thus pointing out the importance of the efficient management of future loads for maintaining distribution grid costs at a reasonable magnitude.

D) Can flexible connections and RES hybridisation help maximise the use of existing electricity grids?

This thesis evaluates two mechanisms for increasing the use of existing electricity grids: flexible connections and hybridising different renewable generation technologies to exploit the complementarity of PV and wind resource availability. An investment model is developed to assess the optimal capacity installed under various definitions of a network node's hosting capacity. The model allows to contrast hybridised generation capacity expansion with non-hybridised expansion for the same hosting capacity and is presented as a conference contribution (Obj. 5).

E) How much electricity network hosting capacity can be unlocked via the relaxation of calculation criteria?

Flexible connections are first evaluated from a network perspective, showing the additional energy that can be injected into the grid's nodes when allowing for a relaxation of HC calculation criteria (Obj. 4). The analysis is presented in Paper 4. The evaluation of injectable energy expresses the maximum energy a node can absorb without violating the grid's operating limits and is technologically neutral. Static hosting capacity is calculated according to the Spanish regulatory requirements. Those requirements limit SHC to the most restrictive N-1 asset outage, applied to a scenario of minimum load and maximum output of existing generation. In contrast, dynamic hosting capacity is derived from the hourly operation of the network and is subject to the variability of load and the output of existing DG. The injectable energy is found to increase by 50% under dynamic definitions of hosting capacity.

Additionally, this thesis proposes the concept of security-aware dynamic hosting capacity, which allows DHC to account for electricity network asset failures. For SDHC, the N-1 outages of all existing network assets are considered according to their probability. SDHC does not yield significant variations of injectable energy when compared to DHC. This is due to the low probabilities of N-1 outages and highlights how severely the conservative regulatory requirements for calculating a node's HC limit the usage of the existing networks.

F) How do flexible connections and hybridisation affect the investment decisions regarding new RES capacity?

The aforementioned investment model is enhanced to perform RES capacity investment optimisation from an investor's point of view of profit maximisation (Obj. 6). The various definitions of HC are assessed once for a single technology and once when allowing for hybridisation. The optimal generation capacity is determined with the help of Conditional Value-at-Risk of the profits of several candidate portfolios in Paper 5. The results show that both CVaR and expected average profits are increased under dynamic definitions of hosting capacity as well as via hybridisation, making them attractive from a RES investor's point of view. This leads to an increase of installed capacity and, consequently, of energy injection into the electricity grid. The relaxation of HC calculation criteria increases installed capacity by up to 65%. When combined with the hybridisation of PV and wind, installed capacity is increased by up to 127%.

At low exposures to market prices, the relation between CVaR and average profits is linear. However, at increasing coupling coefficients to volatile market prices, CVaR and average profits are no longer in a linear relationship, which complicates the optimal investment decision depending on the investor's risk-aversion or risk-prone attitude. Still, installed capacities and energy injection are significantly increased with the help of the relaxation of HC calculation criteria and hybridisation, underlining the relevance of both measures for enhancing the use of existing electricity networks. This work further presents an approach for selecting the most suitable candidate portfolio depending on the risk-adversity of an investor, as demonstrated via a sensitivity analysis.

This thesis contributes to the field of electricity network connection of renewable energy generation. It has demonstrated that the economic order of magnitude of required grid reinforcement does not represent an impediment to the energy transition. Even though the costs do not seem to jeopardise the energy transition, grid expansion and connection times have been identified to represent a bottleneck to the efficient connection of new generation assets and loads. Flexible connections and the hybridisation of renewable technologies behind the grid connection point are identified as two different ways to enhance the usage of existing networks. The contributions of this thesis quantify the potential of both for increasing the hosting capacity of the existing networks and for improving the attractiveness of investing in renewable generation assets, seeking to speed up the energy transition through a rapid rollout of renewable energy sources. A detailed list of contributions to both research lines is provided in 5.2.

5.2 Contributions

Based on the objectives presented in 1.2, this thesis has contributed to the two research lines of assessing electricity grid reinforcement costs and evaluating the enhancement of the use of the existing network. The contributions to each of the research lines are listed in the following:

I. <u>Assessment of electricity grid reinforcement costs</u>

C1. Development of a methodology to assess the incremental transmission, distribution and connection costs for high-RES future pathways compared to low-RES futures (Paper 1).

C2. Application of the methodology to two large-scale realistic systems with notably different RES and load dispersion (Paper 2).

C3. Demonstration that the CAPEX intensity of high-RES pathways is more than compensated by the reduction of OPEX compared to low-RES pathways on two large-scale systems (Paper 1, Paper 2).

C4. Systematic comparison of the impact of various RES dispersion factors on transmission grid reinforcement via sensitivity analysis with a common base case scenario (Paper 1, Paper 2).

C5. Development of a large-scale distribution grid cost estimation model to assess the grid requirements for integrating DER with a geographical resolution of LAU (Paper 3).

C6. Demonstration that the geographical allocation of future DG capacities might be misaligned with the allocation of load growth due to household electrification (Paper 3).

II. <u>Increasing the use of the existing electricity network</u>

C7. Development of the concept of security-aware dynamic hosting capacity to account for RES and load variability as well as network asset failures when computing a network node's HC (Paper 4).

C8. Quantifying additional injectable energy at dynamic definitions of hosting capacity, compared to static hosting capacity derived via regulatory criteria (Paper 4).
C9. Development of an investment model to determine the optimal DG capacity to be installed for the different definitions of HC (Conference Paper, Paper 5).
C10. Assessment of the impact of hybridisation on efficiently using available HC under the intermittent nature of RES (Conference Paper, Paper 5).
C11. Quantification of the impact of the different HC concepts and hybridisation on optimal RES capacity investments from a profit-maximisation point of view (Paper 5).
C12. Demonstration that dynamic definitions of HC are desirable from both network and profit-maximising RES promoter perspectives (Paper 4, Paper 5).

Further, the joint assessment of both research lines presented in this thesis has allowed to formulate regulatory recommendations in response to the current situation of preparing electricity networks for the energy transition.

5.3 Future research

This thesis has shown that future energy systems with high RES participation are of interest not just from an environmental point of view but that, as of today, they already offer a cheaper alternative to fossil-fuel-based energy systems. This work has contributed to the matter of RES electricity grid connection, showing that the connection time rather than the costs represent a bottleneck for the energy transition and quantifying the impact of HC enhancement via the relaxation of calculation criteria and hybridisation.

Still, some topics of interest for future research can be identified for both research lines. A non-exhaustive list of future research topics includes:

I. <u>Assessment of electricity grid reinforcement costs</u>
   - Transmission grid modelling has been carried out on isolated synthetic transmission networks. As stated in this thesis, large-distance interconnection is a means to help smooth out the effect of RES variability. Hence, the implementation of interconnections into the modelling methodology is of interest for future research.
   - The distribution cost estimation model presented in Paper 3 addresses the impact of DER integration into distribution networks. There are other new demand sectors which have not been included in neither the transmission nor the distribution modelling. Some examples are: a large-scale rollout of storage, the ramp-up of the hydrogen sector, and the electrification of industrial energy consumption.
   - The DISCOMET proposed in this thesis addresses DER and prosumer installations at the LV level. Topics such as industrial electrification, industrial or commercial self-consumption, and the impact of EV charging infrastructure have been out of the scope of the model development. However, the effect of

these new energy vectors on electricity distribution grids needs to be assessed to provide a holistic view of distribution grid reinforcement requirements for the energy transition.

- The distribution expansion unit cost catalogue employed in DISCOMET has a high geographical resolution to express that costs cannot be expected to be the same in the different distribution networks throughout the territory. However, a simplification in terms of voltage levels needed to be performed to ensure sufficient data availability for the extrapolation to the rest of the territory. A disaggregation of costs for MV and HV should be performed in future research to efficiently capture the difference in costs incurred for reinforcing electricity grid assets at different voltage levels.

II. Evaluate the enhancement of the use of existing electricity grids

- The HC study performed for Paper 4 has shown that network contingencies have such a low probability of occurrence that the security-aware dynamic hosting capacity does not deviate from the DHC which does not account for any asset failures. An interesting piece of future work should assess the replicability of these findings and the generalisability of the results. Networks with a meshed topology as well as grids with higher FORs (i.e. more overhead lines and longer lines) are of interest.
- All HC concepts are assessed as nodal HC for one network node at a time. The implementation of flexible connections, however, would lead to generators being connected under a flexible access scheme throughout the whole network. The question of assessing several nodes' flexible HC, i.e. how to calculate HC with pre-existing flexible connections, needs to be addressed prior to a regulatory implementation of the relaxation of HC calculation criteria.
- The DHC study is performed on a radially operated MV system with 15 nodes. The scalability of the methodology to bigger networks and networks with meshed operation is of interest for future research.
- This same DHC study employs 54 sample years to assess hosting capacity under the influence of the variability of RES output and load. The modelling process involved the detailed modelling of all sample years with hourly resolution. A systematic application of this method to all nodes of an electricity distribution grid requires a feasible scalability of the methodology. A comparison of the hosting capacity results with those obtained via other methods, such as Monte Carlo Simulation (MCS) study could be of interest. MCS is often used in studies that involve time series subject to uncertainty.
- The last paper of this thesis evaluates optimal RES capacity investments under different definitions of a network node's hosting capacity. Future work should tackle the regulatory aspects of introducing flexible connections. Connection-seekers could be presented with the choice of a firm connection with a low hosting capacity (SHC N-1) or a higher hosting capacity subject to uncertainty (DHC N). Paying for the reinforcement could also be an option. Hence,

connection-seekers could be presented with a menu of contracts from the DSO when requesting access to a network node (see 4). This would allow for individual choices based on aspects such as risk-adversity.

- Papers 4 & 5 have assessed flexible connections and hybridisation to enhance RES's integration into existing electricity grids. However, there are other HC enhancement techniques which have been out of scope for this thesis. Those mechanisms include, among others, voltage control, dynamic line rating and demand-side-management. The impact of different methods on enhancing hosting capacity is an interesting field of future research. The role of storage for HC enhancement is another promising line of research.

6

REFERENCES

[1] O. Hoegh-Guldberg *et al.*, 'Chapter 3 — Global Warming of 1.5 ^{o}C'. in Global Warming of 1.5°C. An IPCC Special Report on the impacts of global warming of 1.5°C above pre-industrial levels and related global greenhouse gas emission pathways, in the context of strengthening the global response to the threat of climate change, sustainable development, and efforts to eradicate poverty. Cambridge University Press, Cambridge, UK and New York, NY, USA, pp. 175–312, 2018. Accessed: Sep. 04, 2024. [Online]. Available: 10.1017/9781009157940.005

[2] UNFCCC, 'The Paris Agreement'. Accessed: Sep. 06, 2024. [Online]. Available: https://unfccc.int/process-and-meetings/the-paris-agreement

[3] European Environment Agency, 'carbon dioxide equivalent', European Environment Agency - Glossary. Accessed: Sep. 10, 2024. [Online]. Available: https://www.eea.europa.eu/help/glossary/eea-glossary/carbon-dioxide-equivalent

[4] United Nations, 'What Is Climate Change?', United Nations. Accessed: Sep. 04, 2024. [Online]. Available: https://www.un.org/en/climatechange/what-is-climate-change

[5] M. Crippa *et al.*, *GHG emissions of all world countries*. Luxembourg: Publications Office of the European Union, 2024. Accessed: Apr. 10, 2025. [Online]. Available: doi:10.2760/4002897

[6] IEA, 'CO2 Emissions in 2022'. Accessed: Sep. 09, 2024. [Online]. Available: https://www.iea.org/reports/co2-emissions-in-2022

[7] United Nations, 'Renewable energy – powering a safer future', United Nations. Accessed: Sep. 04, 2024. [Online]. Available: https://www.un.org/en/climatechange/raising-ambition/renewable-energy

[8] F. Gutiérrez-Martín, R. A. Da Silva-Álvarez, and P. Montoro-Pintado, 'Effects of wind intermittency on reduction of CO2 emissions: The case of the Spanish power system', *Energy*, vol. 61, pp. 108–117, Nov. 2013, doi: 10.1016/j.energy.2013.01.057.

[9] A. J. Chapman, B. C. McLellan, and T. Tezuka, 'Prioritizing mitigation efforts considering co-benefits, equity and energy justice: Fossil fuel to renewable energy transition pathways', *Applied Energy*, vol. 219, pp. 187–198, Jun. 2018, doi: 10.1016/j.apenergy.2018.03.054.

[10] B. N. Stram, 'Key challenges to expanding renewable energy', *Energy Policy*, vol. 96, pp. 728–734, Sep. 2016, doi: 10.1016/j.enpol.2016.05.034.

[11] S. Sen and S. Ganguly, 'Opportunities, barriers and issues with renewable energy development – A discussion', *Renewable and Sustainable Energy Reviews*, vol. 69, pp. 1170–1181, Mar. 2017, doi: 10.1016/j.rser.2016.09.137.

[12] BNEF, '2H 2023 LCOE Update: An Uneven Recovery', BloombergNEF. Accessed: Dec. 20, 2023. [Online]. Available: https://about.bnef.com/blog/2h-2023-lcoe-update-an-uneven-recovery/

[13] UNFCCC, 'Renewable Power Remains Cost-Competitive amid Fossil Fuel Crisis'. Accessed: Sep. 10, 2024. [Online]. Available: https://unfccc.int/news/renewable-power-remains-cost-competitive-amid-fossil-fuel-crisis

[14] IEA, 'Electricity 2024 - Analysis and forecast to 2026', IEA. Accessed: Sep. 10, 2024. [Online]. Available: https://www.iea.org/reports/electricity-2024

[15] United Nations, 'UN Climate Change Conferences', United Nations. Accessed: Sep. 10, 2024. [Online]. Available: https://www.un.org/en/climatechange/un-climate-conferences

[16] United Nations and COP28 UAE, 'COP28: Global Renewables And Energy Efficiency Pledge'. Accessed: Sep. 10, 2024. [Online]. Available: https://www.cop28.com/en/global-renewables-and-energy-efficiency-pledge

[17] H.R.5376 - 117th Congress (2021-2022), 'Inflation Reduction Act of 2022'. Accessed: Sep. 09, 2024. [Online]. Available: https://www.congress.gov/bill/117th-congress/house-bill/5376

[18] J. Badlam, J. Cox, A. Kumar, N. Mehta, S. O'Rourke, and J. Silvis, 'The Inflation Reduction Act: Here's what's in it - McKinsey & Company'. Accessed: Sep. 10, 2024. [Online]. Available: https://www.mckinsey.com/industries/public-sector/our-insights/the-inflation-reduction-act-heres-whats-in-it

[19] Council of the EU and European Council, 'European Green Deal', Consilium. Accessed: Sep. 12, 2024. [Online]. Available: https://www.consilium.europa.eu/en/policies/green-deal/

[20] Council of the EU and European Council, 'Fit for 55'. Accessed: Sep. 09, 2024. [Online]. Available: https://www.consilium.europa.eu/en/policies/green-deal/fit-for-55/

[21] European Commission, 'Renewable Energy Directive'. Accessed: Sep. 12, 2024. [Online]. Available: https://energy.ec.europa.eu/topics/renewable-energy/renewable-energy-directive-targets-and-rules/renewable-energy-directive_en

[22] Council of the EU, ‘Renewable energy: Council adopts new rules’, Consilium. Accessed: Sep. 09, 2024. [Online]. Available: https://www.consilium.europa.eu/en/press/press-releases/2023/10/09/renewable-energy-council-adopts-new-rules/

[23] Eurelectric, ‘Grids for speed - Eurelectric Power Summit 2024’. Accessed: May 23, 2024. [Online]. Available: https://powersummit2024.eurelectric.org/grids-for-speed/

[24] European Commission, ‘National energy and climate plans’. Accessed: May 04, 2022. [Online]. Available: https://commission.europa.eu/energy-climate-change-environment/implementation-eu-countries/energy-and-climate-governance-and-reporting/national-energy-and-climate-plans_en

[25] ACER and CEER, ‘Challenges of the Future Electricity System’, CEER. Accessed: Jul. 11, 2024. [Online]. Available: https://www.ceer.eu/publication/acer-ceer-paper-on-challenges-of-the-future-electricity-system/

[26] I. J. Perez-Arriaga, J. D. Jenkins, and C. Batlle, ‘A regulatory framework for an evolving electricity sector: Highlights of the MIT utility of the future study’, *ECONOMICS OF ENERGY & ENVIRONMENTAL POLICY*, vol. 6, no. 1, pp. 71–92, März 2017, doi: 10.5547/2160-5890.6.1.iper.

[27] TenneT, ‘SuedLink’, TenneT. Accessed: Apr. 04, 2025. [Online]. Available: https://www.tennet.eu/de/projekte/suedlink

[28] TransnetBW, ‘SuedLink’. Accessed: Apr. 04, 2025. [Online]. Available: https://suedlink.com/s-a

[29] U.S. DOE, ‘National Transmission Needs Study’. Oct. 2023. [Online]. Available: https://www.energy.gov/gdo/national-transmission-needs-study

[30] U.S. DOE, ‘National Transmission Planning Study’. U.S. Department of Energy, Oct. 2024. Accessed: Oct. 07, 2024. [Online]. Available: https://www.energy.gov/gdo/national-transmission-planning-study

[31] European Commission, ‘Electricity interconnection targets’. Accessed: Sep. 12, 2024. [Online]. Available: https://energy.ec.europa.eu/topics/infrastructure/electricity-interconnection-targets_en

[32] E. Cremona, ‘Breaking borders: The future of Europe’s electricity is in interconnectors’, Ember. Accessed: Sep. 12, 2024. [Online]. Available: https://ember-climate.org/insights/research/breaking-borders-europe-electricity-interconnectors/

[33] ENTSO-E, ‘What are the concrete benefits for Europe of investing in its cross-border transmission grid and storage infrastructure?’ Accessed: Sep. 12, 2024. [Online]. Available: https://tyndp.entsoe.eu/

[34] O. US EPA, ‘Distributed Generation of Electricity and its Environmental Impacts’. Accessed: Sep. 12, 2024. [Online]. Available: https://www.epa.gov/energy/distributed-generation-electricity-and-its-environmental-impacts

[35] IEA, 'Unlocking the Potential of Distributed Energy Resources', IEA. Accessed: May 01, 2024. [Online]. Available: https://www.iea.org/reports/unlocking-the-potential-of-distributed-energy-resources

[36] K. A. Horowitz *et al.*, 'An Overview of Distributed Energy Resource (DER) Interconnection: Current Practices and Emerging Solutions', NREL/TP--6A20-72102, 1508510, Apr. 2019. doi: 10.2172/1508510.

[37] G. Plimmer, 'Renewables projects face 10-year wait to connect to electricity grid', *Financial Times*, May 08, 2022. Accessed: Sep. 27, 2024. [Online]. Available: https://www.ft.com/content/7c674f56-9028-48a3-8cbf-c1c8b10868ba

[38] CEER, 'CEER Paper on Alternative Connection Agreements'. Accessed: Dec. 11, 2023. [Online]. Available: https://www.ceer.eu/documents/104400/-/-/e473b6de-03c9-61aa-2c6a-86f2e3aa8f08

[39] European Commission, *COMMISSION RECOMMENDATION on speeding up permit-granting procedures for renewable energy projects and facilitating Power Purchase Agreements*. 2022. Accessed: Sep. 13, 2023. [Online]. Available: https://eur-lex.europa.eu/legal-content/EN/TXT/?uri=PI_COM%3AC%282022%293219&qid=1653033569832

[40] European Commission, 'Recommendation and guidance on speeding up permit-granting for renewable energy and related infrastructure projects'. Accessed: May 20, 2024. [Online]. Available: https://energy.ec.europa.eu/publications/recommendation-and-guidance-speeding-permit-granting-renewable-energy-and-related-infrastructure_en

[41] J. Rand *et al.*, 'Queued Up: Characteristics of Power Plants Seeking Transmission Interconnection | Energy Markets & Policy'. Accessed: May 16, 2024. [Online]. Available: https://emp.lbl.gov/queues

[42] FERC, 'Explainer on the Interconnection Final Rule | Federal Energy Regulatory Commission'. Accessed: May 16, 2024. [Online]. Available: https://www.ferc.gov/explainer-interconnection-final-rule

[43] J. P. Chaves Avila *et al.*, 'EUniversal D5.1 - Identification of relevant market mechanisms for the procurement of flexibility needs and grid services', Jan. 2021, doi: https://euniversal.eu/wp-content/uploads/2021/02/EUniversal_D5.1.pdf.

[44] Eurelectric, 'Electrification Action Plan'. Accessed: Sep. 24, 2024. [Online]. Available: https://www.eurelectric.org/wp-content/uploads/2024/06/electrification-action-plan-final.pdf

[45] European Commission, 'Directive (EU) 2024/1711 of the European Parliament and of the Council of 13 June 2024 amending Directives (EU) 2018/2001 and (EU) 2019/944 as regards improving the Union's electricity market design'. Accessed: Jan. 13, 2025. [Online]. Available: https://eur-lex.europa.eu/eli/dir/2024/1711/oj/eng

[46] European Commission, 'Directive (EU) 2019/944', vol. 158. Jul. 16, 2024. Accessed: Dec. 14, 2020. [Online]. Available: https://eur-lex.europa.eu/legal-content/EN/TXT/?uri=CELEX%3A02019L0944-20240716

[47] L. Meeus, T. Jamasb, and C. Smidt, 'Danish Utility Regulator's Anthology Project Series on Better Regulation in the Energy Sector Vol. 2 - INCENTIVES AND DIGITALIZATION FOR FLEXIBILITY IN THE GREEN TRANSITION', 2024, doi: 10.51138/julk8455.

[48] Enedis, 'Flexibilities to enhance the Energy Transition and the performance of the Distribution Network'. Accessed: Sep. 14, 2023. [Online]. Available: https://www.enedis.fr/sites/default/files/documents/pdf/flexibilities-enhance-energy-transition-performance-distribution-network.pdf

[49] C. Murphy, D. Harrison-Atlas, N. Grue, T. Mosier, J. Gallego-Calderon, and S. Elliott, 'Complementarity of Renewable Energy-Based Hybrid Systems', NREL/TP--6A20-81901, 1972008, MainId:82674, Apr. 2023. doi: 10.2172/1972008.

[50] L. Herding, R. Cossent, M. Rivier, J. P. Chaves-Ávila, and T. Gómez, 'Assessment of electricity network investment for the integration of high RES shares: A Spanish-like case study', *Sustainable Energy, Grids and Networks*, vol. 28, p. 100561, Dec. 2021, doi: 10.1016/j.segan.2021.100561.

[51] L. Herding, R. Cossent, M. Rivier, and S. Bañales, 'Assessing the impact of renewable energy penetration and geographical allocation on transmission expansion cost: A comparative analysis of two large-scale systems', *Sustainable Energy, Grids and Networks*, vol. 38, p. 101349, Jun. 2024, doi: 10.1016/j.segan.2024.101349.

[52] L. Herding, M. Pérez-Bravo, R. Barrella, R. Cossent, and M. Rivier, 'Large-scale estimation of electricity distribution grid reinforcement requirements for the energy transition – A 2030 Spanish case study', *Energy Reports*, vol. 12, pp. 5432–5444, Dec. 2024, doi: 10.1016/j.egyr.2024.11.026.

[53] L. Herding, L. Carvalho, R. Cossent, and M. Rivier, 'A security-aware dynamic hosting capacity approach to enhance the integration of renewable generation in distribution networks', *International Journal of Electrical Power & Energy Systems*, vol. 161, p. 110210, Oct. 2024, doi: 10.1016/j.ijepes.2024.110210.

[54] L. Herding, R. Cossent, and M. Rivier, 'Enhancing RES Grid Connection via Dynamic Hosting Capacity and Hybridization', presented at the 2023 IEEE Belgrade PowerTech, Belgrade, Serbia: IEEE, 2023. doi: 10.1109/PowerTech55446.2023.10202726.

[55] L. Herding, L. Carvalho, R. Cossent, and M. Rivier, 'Renewable capacity investment planning under distribution grid hosting capacity uncertainty via Conditional Value-at-Risk', 2025.

[56] ENTSO-E, 'Planning the future grid - TYNDP'. Accessed: Feb. 03, 2025. [Online]. Available: https://tyndp.entsoe.eu/

[57] A. Shokri Gazafroudi, F. Neumann, and T. Brown, 'Topology-based approximations for N-1 contingency constraints in power transmission networks', *International Journal of*

Electrical Power & Energy Systems, vol. 137, p. 107702, May 2022, doi: 10.1016/j.ijepes.2021.107702.

[58] CNMC, 'Información mensual de estadísticas sobre las ventas de régimen especial'. Accessed: Oct. 07, 2022. [Online]. Available: https://www.cnmc.es/estadistica/informacion-mensual-de-estadisticas-sobre-produccion-de-energia-electrica-partir-de-8

[59] MINETUR, 'Orden IET/2659/2015'. [Online]. Available: https://www.boe.es/buscar/pdf/2015/BOE-A-2015-13487-consolidado.pdf

[60] MINETUR, 'Orden IET/2660/2015'. Accessed: Feb. 11, 2021. [Online]. Available: https://www.boe.es/boe/dias/2015/12/12/pdfs/BOE-A-2015-13488.pdf

[61] T. Freire-Barceló *et al.*, 'Storage and demand response contribution to firm capacity: Analysis of the Spanish electricity system', *Energy Reports*, vol. 8, pp. 10546–10560, Nov. 2022, doi: 10.1016/j.egyr.2022.08.014.

[62] P. Frías *et al.*, 'Assessment report on the impacts of RES policy design options on future electricity markets'. Accessed: Jun. 02, 2021. [Online]. Available: https://res-policy-beyond2020.eu/pdffinal/Assessment%20report%20on%20the%20impacts%20on%20future%20electricity%20markets%20(beyond2020%20-%20D5-2).pdf

[63] Jefatura del Estado, 'Ley 24/2013'. Accessed: Apr. 04, 2025. [Online]. Available: https://www.boe.es/buscar/act.php?id=BOE-A-2013-13645

[64] FERC, 'ERCOT'. Accessed: Sep. 19, 2024. [Online]. Available: https://www.ferc.gov/industries-data/electric/electric-power-markets/ercot

[65] MITECO, 'Zonificación ambiental para energías renovables: Eólica y Fotovoltaica', Ministerio para la Transición Ecológica y el Reto Demográfico. Accessed: Apr. 08, 2025. [Online]. Available: https://www.miteco.gob.es/es/calidad-y-evaluacion-ambiental/temas/evaluacion-ambiental/zonificacion_ambiental_energias_renovables.html

[66] CNMC, 'Circular 1/2021'. Accessed: Sep. 19, 2021. [Online]. Available: https://www.boe.es/eli/es/cir/2021/01/20/1/con

[67] Ministerio de Economía, 'Real Decreto 1955/2000'. [Online]. Available: https://boe.es/buscar/act.php?id=BOE-A-2000-24019

[68] INE, 'Viviendas por municipios (con más de 2.000 habitantes) y tipo de vivienda', INE. Accessed: May 11, 2023. [Online]. Available: https://www.ine.es/jaxiT3/Tabla.htm?t=3456

[69] INE, 'Censos de Población y Viviendas 2011. Resultados Municipales'. Accessed: Feb. 13, 2023. [Online]. Available: https://www.ine.es/jaxi/Tabla.htm?path=/t20/e244/avance/p02/l0/&file=1mun00.px

[70] L. Pieltain Fernandez, T. Gomez San Roman, R. Cossent, C. Mateo Domingo, and P. Frias, 'Assessment of the Impact of Plug-in Electric Vehicles on Distribution Networks', *IEEE*

TRANSACTIONS ON POWER SYSTEMS, vol. 26, no. 1, pp. 206–213, Feb. 2011, doi: 10.1109/TPWRS.2010.2049133.

[71] European Commission, 'Spain - Final updated NECP 2021-2030 (submitted 2024)'. Accessed: Apr. 08, 2025. [Online]. Available: https://commission.europa.eu/publications/spain-final-updated-necp-2021-2030-submitted-2024_en

[72] J. Röder, B. Meyer, U. Krien, J. Zimmermann, T. Stührmann, and E. Zondervan, 'Optimal Design of District Heating Networks with Distributed Thermal Energy Storages – Method and Case Study', *International Journal of Sustainable Energy Planning and Management*, vol. 31, pp. 5–22, May 2021, doi: 10.5278/ijsepm.6248.

[73] European Commission, *Proposal for a COUNCIL REGULATION laying down a framework to accelerate the deployment of renewable energy*. 2022. Accessed: Sep. 13, 2023. [Online]. Available: https://eur-lex.europa.eu/legal-content/EN/TXT/?uri=CELEX%3A52022PC0591&qid=1669020920010

[74] Deloitte, 'La planificación y la tramitación de las infraestructuras eléctricas para la Transición Energética', Deloitte Spain. Accessed: Oct. 21, 2022. [Online]. Available: https://www2.deloitte.com/es/es/pages/energy-and-resources/articles/planificacion-y-tramitacion-infraestructuras-electricas.html

[75] M. H. J. Bollen and N. Etherden, 'Overload and overvoltage in low-voltage and medium-voltage networks due to renewable energy — Some illustrative case studies', in *2011 2nd IEEE PES International Conference and Exhibition on Innovative Smart Grid Technologies*, Dec. 2011, pp. 1–8. doi: 10.1109/ISGTEurope.2011.6162645.

[76] CNMC, 'Resolución de 20 de mayo de 2021, de la Comisión Nacional de los Mercados y la Competencia, por la que se establecen las especificaciones de detalle para la determinación de la capacidad de acceso de generación a la red de transporte y a las redes de distribución'. Accessed: Sep. 13, 2021. [Online]. Available: https://www.boe.es/eli/es/res/2021/05/20/(4)

[77] European Commission, 'COM(2023) 757 final'. Accessed: Nov. 29, 2023. [Online]. Available: https://eur-lex.europa.eu/legal-content/EN/TXT/PDF/?uri=COM:2023:757:FIN

[78] Ofgem, 'Access and Forward-Looking Charges Significant Code Review – Summer 2019 working paper', Access and Forward-Looking Charges Significant Code Review – Summer 2019 working paper. Accessed: Aug. 07, 2020. [Online]. Available: https://www.ofgem.gov.uk/publications-and-updates/access-and-forward-looking-charges-significant-code-review-summer-2019-working-paper

[79] European Commission, '(EU) 2024/1711'. Accessed: Sep. 27, 2024. [Online]. Available: https://eur-lex.europa.eu/legal-content/EN/TXT/HTML/?uri=OJ%3AL_202401711

[80] CIGRE, 'Benchmark Systems for Network Integration of Renewable and Distributed Energy Resources', e-cigre. Accessed: Oct. 26, 2023. [Online]. Available: https://e-

cigre.org/publication/ELT_273_8-benchmark-systems-for-network-integration-of-renewable-and-distributed-energy-resources

[81] K. Rudion, A. Orths, Z. A. Styczynski, and K. Strunz, 'Design of benchmark of medium voltage distribution network for investigation of DG integration', in *2006 IEEE Power Engineering Society General Meeting*, Jun. 2006, p. 6 pp.-. doi: 10.1109/PES.2006.1709447.

[82] University of Kassel and Fraunhofer IEE, 'CIGRE Networks — pandapower 2.4.0 documentation'. Accessed: Oct. 26, 2023. [Online]. Available: https://pandapower.readthedocs.io/en/v2.13.1/networks/cigre.html

[83] J. Widen, 'Correlations Between Large-Scale Solar and Wind Power in a Future Scenario for Sweden', *IEEE Transactions on Sustainable Energy*, vol. 2, no. 2, pp. 177–184, Apr. 2011, doi: 10.1109/TSTE.2010.2101620.

[84] A. Couto and A. Estanqueiro, 'Assessment of wind and solar PV local complementarity for the hybridization of the wind power plants installed in Portugal', *Journal of Cleaner Production*, vol. 319, p. 128728, Oct. 2021, doi: 10.1016/j.jclepro.2021.128728.

[85] D. Harrison-Atlas, C. Murphy, A. Schleifer, and N. Grue, 'Temporal complementarity and value of wind-PV hybrid systems across the United States', *Renewable Energy*, vol. 201, pp. 111–123, Dec. 2022, doi: 10.1016/j.renene.2022.10.060.

[86] REE, 'Bienvenido | ESIOS electricidad · datos · transparencia'. Accessed: Oct. 23, 2023. [Online]. Available: https://www.esios.ree.es/es

[87] CNMC, *Resolución de 18 de marzo de 2021, de la Comisión Nacional de los Mercados y la Competencia, por la que se establecen los valores de los peajes de acceso a las redes de transporte y distribución de electricidad de aplicación a partir del 1 de junio de 2021*, vol. BOE-A-2021-4565. 2021, pp. 33575–33593. Accessed: Oct. 23, 2023. [Online]. Available: https://www.boe.es/eli/es/res/2021/03/18/(3)

[88] S. Pfenninger and I. Staffell, 'Long-term patterns of European PV output using 30 years of validated hourly reanalysis and satellite data', *Energy*, vol. 114, pp. 1251–1265, Nov. 2016, doi: 10.1016/j.energy.2016.08.060.

[89] I. Staffell and S. Pfenninger, 'Using bias-corrected reanalysis to simulate current and future wind power output', *Energy*, vol. 114, pp. 1224–1239, Nov. 2016, doi: 10.1016/j.energy.2016.08.068.

[90] IEA, 'Renewable electricity capacity remuneration policy types, 2020-2025 – Charts – Data & Statistics', IEA. Accessed: Oct. 10, 2024. [Online]. Available: https://www.iea.org/data-and-statistics/charts/renewable-electricity-capacity-remuneration-policy-types-2020-2025-2

[91] MITECO, 'Real Decreto 960/2020'. Accessed: Dec. 09, 2020. [Online]. Available: https://boe.es/buscar/doc.php?id=BOE-A-2020-13591

[92] M. Zhang, Y. Tang, L. Liu, and D. Zhou, ‘Optimal investment portfolio strategies for power enterprises under multi-policy scenarios of renewable energy’, *Renewable and Sustainable Energy Reviews*, vol. 154, p. 111879, Feb. 2022, doi: 10.1016/j.rser.2021.111879.

[93] IEA, ‘Renewable electricity – Renewable Energy Market Update - May 2022 – Analysis’, IEA. Accessed: Oct. 23, 2024. [Online]. Available: https://www.iea.org/reports/renewable-energy-market-update-may-2022/renewable-electricity

[94] MITECO, ‘Subastas del Régimen Económico de Energías Renovables’, Ministerio para la Transición Ecológica y el Reto Demográfico. Accessed: Nov. 08, 2024. [Online]. Available: https://www.miteco.gob.es/content/miteco/es/es/energia/renovables/regimen-economico.html

[95] MITECO and REE, ‘Plan de desarrollo de la Red de Transporte de Energía Eléctrica Período 2021-2026’. 2024. Accessed: Oct. 14, 2024. [Online]. Available: https://www.planificacionelectrica.es/sites/default/files/2024-04/REE_PLAN_DESARROLLO_MAP.pdf

[96] CNMC, *Circular 1/2024*, vol. BOE-A-2024-20760. 2024, pp. 129888–129917. Accessed: Apr. 22, 2025. [Online]. Available: https://www.boe.es/eli/es/cir/2024/09/27/1

7

ANNEX

7.1 Paper 1

- We quantify the grid investments needed to integrate high amounts of RES
- Results show that RES drive significant grid expansion and connection costs
- However, incremental grid investments represent only 6-10% of RES investment costs
- RES-driven reduction in operating costs compensate for incremental grid costs
- High RES penetration is found to reduce total system costs (investment + operation)

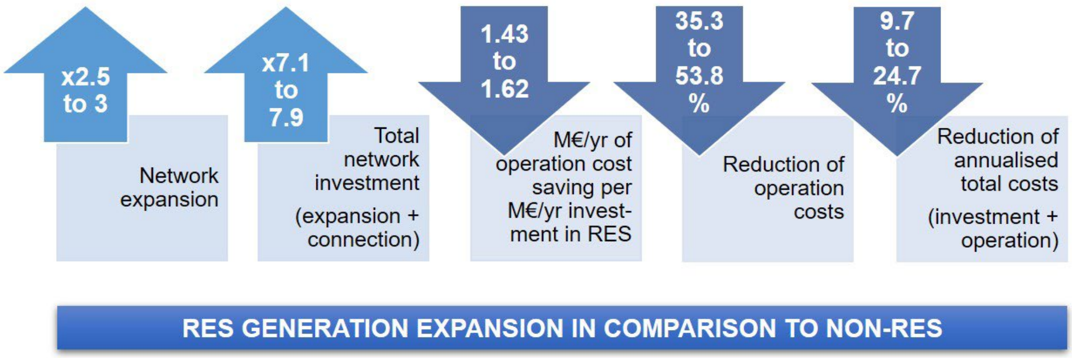

Assessment of electricity network investment for the integration of high RES shares: A Spanish-like case study

Leslie Herding*, Rafael Cossent, Michel Rivier, José Pablo Chaves-Ávila, Tomás Gómez

Institute for Research in Technology (IIT), ICAI School of Engineering, Universidad Pontificia Comillas, C/Santa Cruz de Marcenado 26, 28015 Madrid, Spain

*) Corresponding author: lherding@comillas.edu

Abstract

In the course of the energy transition, the EU member states' National Energy and Climate Plans seek to install significant amounts of intermittent renewable generation capacity over this decade. Previous studies underline the social, political, and economic benefits of the electricity sector decarbonisation. The economic analysis of renewable energy sources (RES) integration is commonly performed with single-bus generation expansion models that seek the cost-optimal expansion of RES generation capacity to reduce operational expenses. However, electricity grids will require investments to adapt to the integration of high amounts of RES capacity. This paper contrasts the cost-optimal generation capacity mix obtained from a single-bus expansion model with a conservative estimation of electricity network investment requirements for an exemplary Spanish-like case study. RES network investment costs are put in context with an alternative non-RES generation expansion pathway. Network investment costs considered include expansion costs for both transmission and distribution grids. Electricity network expansion costs represent 6 to 10% of the corresponding generation capacity investment. Despite increasing network investment costs, the integration of high RES shares into electricity grids reduces operating costs when compared to non-RES pathways. Fuel and emission savings exceed total investments (generation capacity, network expansion, and connection costs).

Keywords

Power sector decarbonisation; electricity network costs; renewable energy sources

1 Introduction

The electricity sector is bound to play a central role in the ongoing energy transition, as reflected in the ambitious energy policy measures put in place worldwide. In the European context, the European Green Deal not only aims at decarbonising electricity generation but includes further electrification of demand. To meet this growing electricity demand while ensuring the targeted reductions in greenhouse gas emissions, new generation facilities included in the member states' National Energy and Climate Plans (NECP) primarily consist of photovoltaic (PV) and wind power plants. In the Spanish NECP, the integration of renewable energy sources (RES) for the year 2030 requires the installation of around 60 GW of these technologies [1]. The government expects this development to require massive investments to expand both RES generation capacity and electricity grids needed to transport electricity from the new generation sites to the demand centres.

The benefits of investing in RES are numerous and largely covered in the literature. Direct advantages for the population include local job creation and health benefits via reducing emissions [2]–[4]. The authors of [5] point out political benefits such as an increase in energy security due to the reduction of dependency from fuel imports and improvements in energy access with the help of distributed energy resources (DER). The potential of economic benefits of system operating cost reduction with renewables is analysed in [6] . The authors state that the employment of RES permits to decrease the generation from fossil fuels which in consequence reduces emissions. This decrease leads to monetary savings of fuel costs and CO_2 emission expenses. These findings are supported by [7]. Furthermore, the authors state that a 100% renewable electricity sector leads to decreased levelised cost of electricity (LCOE) in Europe. According to the authors, the LCOE is reduced from 80 €/MWh in 2015 to 56 €/MWh in the study's target year 2050.

However, the adaption of electricity grids to high shares of renewable energy generation is not analysed in detail by the studies listed above. The integration of intermittent generation capacity is a challenge for the operation of electricity networks by introducing significant up- and downwards ramps of RES generation that need to be met by other generators [8]. Additional generation capacity of both dispatchable and intermittent nature is required to compensate for the low full-load hours of PV and wind generators, leading to a significant increase of total installed generation capacity [9]. Scenarios with high RES shares lead to the requirement of overcapacities to meet different generation and demand levels throughout the year [10]. The authors find that transmission grid expansions are a tool to support the integration of higher RES shares at a lower system-wide LCOE. Both national grid reinforcements and interconnections are crucial for accommodating high shares of RES generation in European electricity grids: reinforcement for the connection of relatively remote areas with high RES potential and interconnections to smoothen the effect of intermittency throughout Europe by connecting areas with different generation patterns [11]. The authors perform a transmission grid interconnection study to analyse the integration of high shares of variable renewable energy (PV and wind). Transmission grid extensions are a suitable tool for the least-cost integration of RES capacity into the European power grid. In line with the findings of [10], both renewable overproduction and backup capacity requirements decrease in systems with interconnections. Interconnection investment for an optimal grid is quantified at significant magnitudes of up to 44 % of the generation capacity investment [11]. Although the key messages of both studies underline the importance of electricity grids for the integration of RES, the expansion of national transmission grids is not the focus. Furthermore, distribution grids are not part of the analysis.

This paper seeks to evaluate both transmission and distribution grid costs in the context of generation capacity expansion costs. It aims at assessing the monetary order of magnitude of the requirements of electricity grid adaption for the integration of high RES shares. The case study at hand analyses a Spanish-like electricity system with the target year of 2030, the same time horizon considered by the NECPs mentioned above. For an adequate evaluation of the electricity network requirements for the integration of renewable energy, grid expansion costs are computed for a total of four scenarios: two scenarios with high RES shares and two scenarios in which no additional RES capacity is installed. This allows identifying whether the integration of high RES shares into electricity grids represents an economic burden compared to a system without RES. Therefore, two different kinds of scenarios are addressed throughout the paper, namely RES and Non-RES scenarios. The case study aims at a general evaluation of whether RES leads to an increase in electricity grid costs and jeopardises the economic benefits of operating cost savings rather than at a detailed electricity grid expansion planning. Grid connection costs are considered as an additional cost component to express the connection of new generation facilities to the closest grid node. The different scenarios' electricity network investment costs are put in context with the investment costs for the expansion of generation and storage capacities as performed previously in [11]. Similar to [6], the benefits of RES integration are evaluated based on operating cost reductions. The main contribution of this work is the evaluation of whether the economic conclusions drawn with single-bus generation expansion models are reversed when considering electricity grid expansion and connection costs. As a result, this paper also contributes to computing the relative weight of all network costs in relation to generation and storage investment and operating costs. Finally, the results show the network costs of connecting ambitious renewable generation targets. All of the beforementioned contributions are performed as a realistic case study for Spanish-like electricity grids.

The remainder of this paper is organised as follows. Section 2 describes the methodology applied throughout the different stages of the modelling process. Section 3 provides details on the data used for the Spanish-like case study. Section 4 summarises the results of the main cost components. Section 5 presents the main conclusions and policy implications.

2 Methodology

In the course of the decarbonisation of the electricity sector, thermal generation units are progressively replaced by new, renewable generation capacity. Apart from the investment related to the installation of this additional capacity, these new units cause an impact in electricity grids which are addressed as three different components shown in Figure 1: i) reinforcements to the existing transmission grid, ii) reinforcement of the existing distribution grid (if applicable), and ii) connection costs.

In this work, the required reinforcements of the existing grid triggered by the connection of new generation capacity are computed separately for transmission and distribution networks. It is relevant to note that distribution costs are only applicable to the RES capacity connected to this system, whereas all additional RES capacity has a potential impact on the transmission grid. Therefore, distribution grid costs are only relevant for scenarios with additional RES capacity, as bigger thermal generation units connect directly to the transmission grid [12]. The connection of the generating units to the existing electricity grid is referred to separately as grid connection costs. This term is limited to the physical connection from the power plant to the nearest substation of the energy harvesting network, i.e. the cost of the connection line and new switchbay. A conceptual overview of the data flow of the investment cost calculation process is provided in Figure 11 in Appendix B.

Figure 1: Cost components involved in the network expansion

The summation of the additional generation (and storage) investment costs with the three grid cost components described above results in the total RES integration costs calculated in this paper. In the following, the methodology followed to estimate each one of these costs components is described.

2.1 Generation and storage expansion

Different scenario pathways are contrasted to evaluate the impact of the integration of RES into electricity network expansion costs under different conditions. First, it is necessary to determine what the initially installed generation capacities are so as to serve as a common initial starting point. In this study, the capacity expected to be still operative in 2030 is determined based on the operating lifetime of each generation technology, the year of commissioning of existing plants, and currently declared policies on coal and nuclear power decommissioning.

The additional generation and storage investments required are obtained for different future scenarios with the same methodology and modelling tools used in [13] and are taken as an external input to this work. Generation and storage capacity expansion is modelled separately from transmission grid expansion. Recent investigation shows the benefits of joint generation and transmission expansion planning [14]. However, generation and network investment decisions are made independently in the current regulatory framework in many deregulated electricity systems. Moreover, current regulation concerning grid investments and network access presents some asymmetries between transmission and distribution, which drive actual investment decisions by RES promoters away from the global optimum.

Scenarios of the generation expansion model consist of four representative weeks with hourly generation and demand data. Storage facilities are operated weekly. The generation and demand profiles allow comparing the results obtained for several scenario pathways. This is a common methodology to derive conclusions on different hypotheses on the rollout of RES. Usually, different renewable scenarios in line with international decarbonisation efforts are compared to each other [6], [7]. In contrast to that, the scenario pathways for this study seek to point out the electricity grid expansion costs triggered by renewable energy integration. Therefore, as will be presented in section 3, two pathways for 2030 are compared; a system where significant RES investments are made and a scenario where generation expansion alternatives were limited to non-RES technologies.

2.2 Electricity grid expansion

2.2.1 Transmission grid expansion

Several projects analyse the impact of different renewable energy integration scenarios in the European transmission grid. Particular focus is set on comparing different pathways of RES development [11], [15]–[17]. The typical top-down modelling approach of transmission grids leads to analyses based on specific scenarios of renewable capacity installed, obtaining a total grid cost depending on the scenario. As pointed out in the previous section, this work aims to evaluate the costs of RES grid integration and a comparison to a non-RES pathway. The different generation capacity expansion scenarios obtained in the previous step are implemented in a transmission expansion planning (TEP) model[1]. Generation and demand profiles from the generation expansion model are distributed in the transmission network according to the following criteria:

- Existing capacity: existing demand and thermal generation capacity of the initial transmission grid are scaled according to the scenario requirements. For RES capacity, the existing capacity in the Spanish autonomous communities is considered as one parameter for the allocation of power plants within the transmission network [18].
- Resource availability: a second criterion for allocating RES capacity within the network is the availability of natural resources (wind speed and solar irradiation).
- For the computation of the different scenarios, the capacity is scaled at the same nodes. This method is considered a conservative estimation due to the concentration of capacity within the same zones, leading to reinforcement requirements of the connecting network corridors.

Due to the complexity of the TEP computation, the model is allowed to opt for continuous network investment decisions to maintain computation time at a reasonable threshold. These investment decisions serve as an approximate indicator of actual system investment needs. A detailed TEP performance is out of the scope of this work. Furthermore, generation and load data are modelled with representative load levels to reduce the computational complexity of the optimisation problem. Hourly generation and load values are clustered into 144 representative load levels derived from the clustering process summarised in Figure 2.

[1] https://www.iit.comillas.edu/technology-offer/tepes

Hourly storage profiles are provided as an output of the generation expansion model via weekly operation. The profiles are treated separately according to the generation and demand periods to guarantee the contemplation of the different functionalities of storage facilities.

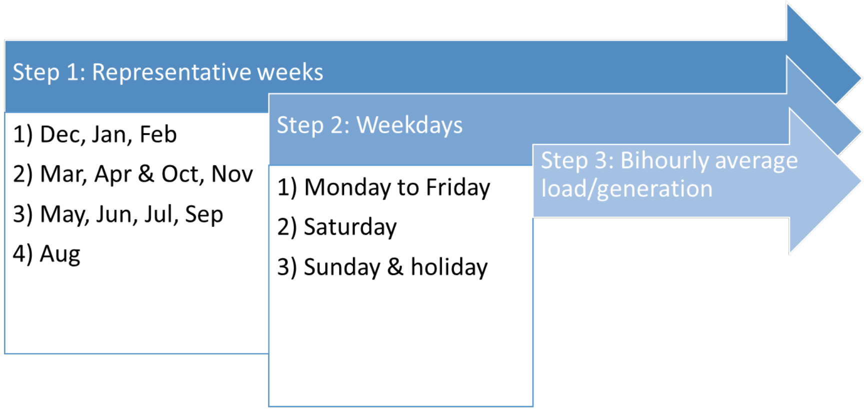

Figure 2: Clustering process of representative generation and load profiles for transmission grid modelling

As indicated in section 2, the total additional capacity is considered in the transmission modelling process, i.e. transmission and distribution connected generators. Distributed generation (DG) connected at distribution grids can potentially be consumed locally, especially when met with demand growth. In this case, no transmission reinforcement is required for the integration of this generation capacity. However, DG might exceed local demand, especially at high RES shares. Including the DG capacity at the distribution substations included in the transmission network model leaves the optimisation model to account for the impact of the DG in the wider transmission grid. If no evacuation capacity is required, no reinforcement need is detected.

2.2.2 Distribution grid expansion

As pointed out in the description of the different investment cost components, distribution grid costs are only relevant for scenarios with new renewable capacity. Thermal generation capacity traditionally connects to the transmission grid and does not cause downstream reinforcement. For the renewable scenarios, distribution grid expansion costs are determined as shown in Figure 3.

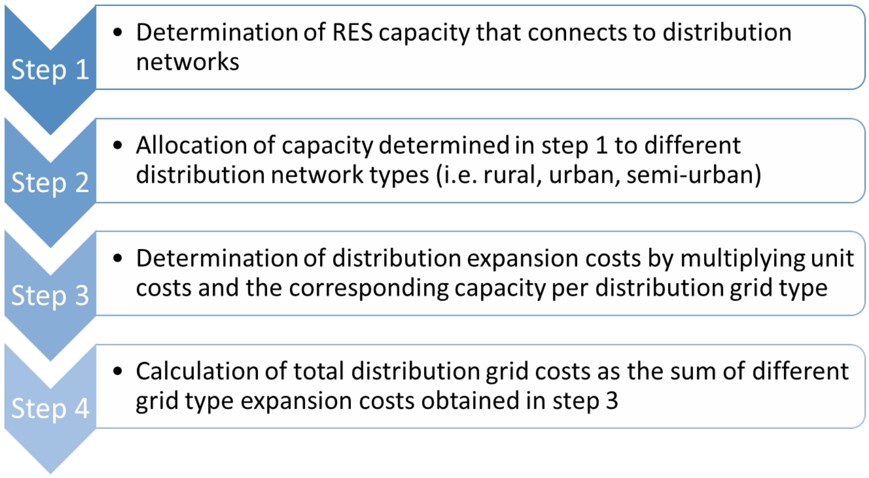

Figure 3: Distribution grid cost calculation methodology

Several studies have assessed incremental distributed generation (DG) grid costs via distribution network expansion models. Although countries and generation technologies differ, annual unit costs are found mainly below 15 €/kW-yr [19]–[23]. The studies explain costs above 15€/kW-yr with costly upgrades of network components caused by integrating a small DG unit [23], resulting in very high unit costs due to economies of scale in network investments. This analysis disregards them for not been considered representative of an average value.

In general, distribution grid unit costs are found higher in rural zones [19], [22], [24]. The authors of [19] find distribution grid unit costs below 2 €/kW-yr in urban Spanish distribution networks, below 5 €/kW-yr in semi-urban and around 10 €/kW-yr in rural network zones. This trend is depicted in the unit cost assumptions applied in this study. The unit costs considered for the calculation of the scenarios are presented in Table 1. Furthermore, the cost of the network integration of high DG shares is found lower when combined with demand growth as more distributed energy is consumed locally [22]. In the equal-cost assumption, scenarios without and with demand growth are computed with the same unit cost. The trend mentioned in [22] is implemented as a separate assumption where annualised distribution grid unit costs are higher without demand growth. This tendency is expressed as a specific cost assumption in Table 1. Rural distribution grid costs are increased compared to the equal-cost assumption to represent the results found in [24]. The authors find distribution grid costs for integrating PV into rural distribution networks of approximately 15 €/kW-yr.

Table 1: Annualised distribution grid unit costs employed for computation [19]–[24]

Annualised distribution grid unit costs (EUR/kW)	Rural	Semi-urban	Urban

Equal costs			
No demand growth	10	5	2
Demand growth	10	5	2
Specific costs			
No demand growth	15	6	2.5
Demand growth	12	4	2

2.3 Electricity grid connection

Literature on grid connection costs of renewables is abundant [25]–[30]. However, as stated in [30], grid connection costs in different countries vary according to the charging approach implemented in regulation. Deep connection charges require the generator seeking connection to pay all necessary reinforcement on the existing network. Shallow connection charges represent the contrary where the network operator pays for the required works to reinforce the existing grid and recovers the costs through the network charges paid by all ratepayers [31]. The charging approach varies from country to country [32]. In this work, connection costs are computed as the physical connection from the new generator's location to the corresponding existing electricity grid node. This case study includes a general estimation of the order of magnitude of unit connection costs for new generation capacity. A detailed computation of grid connection costs is out of the scope of this work. Connection costs are estimated as detailed in Figure 4.

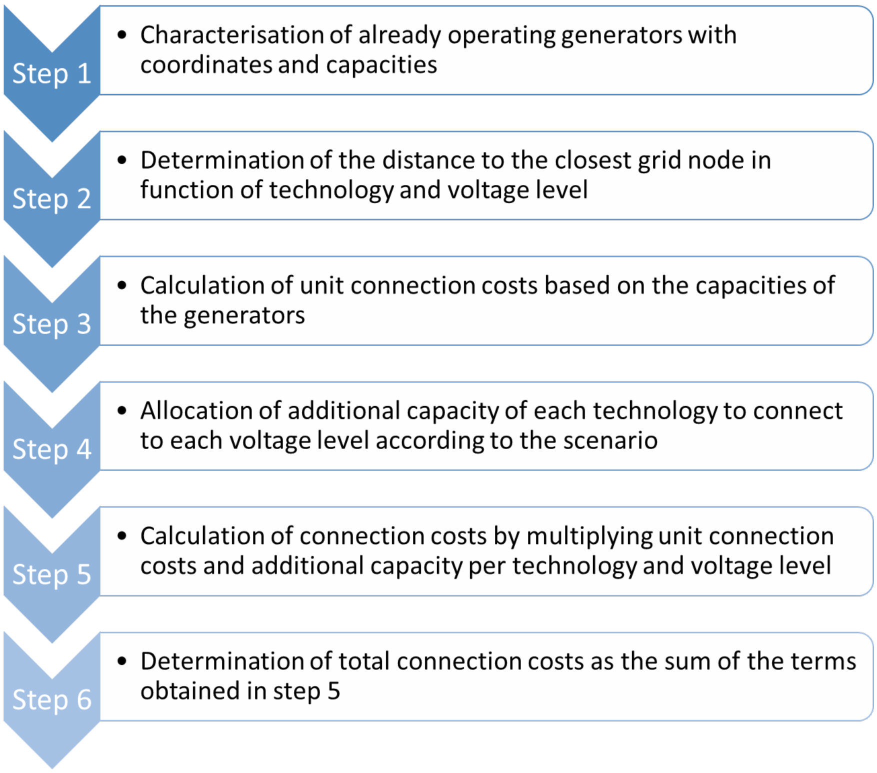

Figure 4: Connection cost estimation methodology

All reinforcements required on the existing network are included in the grid expansion costs described above.

2.4 System operating cost savings

The economic benefit of integrating renewable energy generation capacity into electricity grids is reducing total system costs, expressed as operating cost reduction. This reduction results mainly from a decrease in thermal generation, leading to fuel cost savings. Also, by reducing the output of thermal generators, emission costs are reduced [5], [6]. The reduction of system costs is the objective of the generation expansion model used in [33]. However, this model assesses the costs for a single-bus system expansion. Consequently, it does not consider how transmission network constraints can affect the generation economic dispatch, thus increasing operating costs. In order to incorporate this effect, the operating costs used to evaluate the benefits of RES integration into electricity grids in this case study are based on the generation dispatch calculated by the transmission expansion model. The operating costs considered by the transmission model include costs for fuel, CO_2 and variable O&M. For the comparison of the scenarios, fixed O&M costs are included in the operating cost term. The reduction of operating costs is contrasted to the different investment cost components described above. With this methodology step, conclusions on whether the scenarios obtained from the generation expansion model are still beneficial when considering electricity grid costs can be drawn.

3 Case study

The methodology for evaluating electricity grid investment costs for high RES shares in comparison to Non-RES systems, described in the previous section, is applied to a Spanish-like electricity system. The methodology of this case study employs exemplary data of a Spanish-like electricity system for the sake of illustration and coherence. Data of the Spanish transmission and distribution networks are not publicly available. The case study works with approximations of the system that are described in the following. Hence, the results should not be interpreted as an exact depiction of the Spanish electricity system. The case-specific assumptions for the determination of the different investment cost components are presented in the following sections.

3.1 Future generation and storage capacity

The baseline of each scenario is the mid-2019 generation capacity and demand of Spain. Both scenario pathways (Non-RES and RES capacity expansion) are computed without demand growth and with 2.3% annual demand growth. Table 2 provides an overview of the features characterising each scenario: their denomination, the demand growth considered and whether the generation expansion plan is based or not on RES capacity[2]. The four scenarios have been selected to analyse the research question of whether electricity grid investment represents an economic burden for the integration of high RES shares. In the scenarios without demand growth (0%_Non-RES and 0%_RES), the impact of the technological change of the generation capacity mix towards renewables is analysed. The scenarios with demand growth (2.3%_Non-RES and 2.3%_RES) have been chosen for this case study to increase the generation capacity that needs to be integrated into electricity grids. Electricity grid investment for integrating high RES shares is analysed as incremental costs. That is, the RES and the non-RES scenarios of the corresponding demand growth are compared to each other. Furthermore, the generation expansion model allows accounting for demand flexibility. Heating and cooling, domestic hot water, refrigeration and EVs are considered controllable loads by the generation expansion model. The provision of demand response by these sources is modelled as in [34]. To account for the availability of flexibility provision in the short term (2030), 25% of the controllable load is considered available to shift during the day

[2] https://www.iit.comillas.edu/technology-offer/sploder

in this case study, maintaining the comfortable limits. An overview of operating cost input parameters for the modelling process is provided in Appendix A. CO_2 is priced at 84.84 €/ton [35].

Table 2: Demand growth and generation expansion hypothesis

Scenario	**0%_Non-RES**	**0%_RES**	**2.3%_Non-RES**	**2.3%_RES**
Annual demand growth (%)	0	0	2.3	2.3
New generation capacity	Non-RES	RES	Non-RES	RES

Letting the generation expansion model freely select the more profitable investments for 2030 and the assumptions described above lead to a massive investment in utility PV and onshore wind capacity, backed by the existing installed thermal and hydro capacity. RES scenarios are therefore built using the expansion model without any technology-based expansion constraint. Non-RES scenarios, on the other hand, are built by explicitly removing RES generation from the generation technology expansion candidates. Installed capacities in each of the scenarios are detailed in Table 3. The scenario without demand growth and with non-renewable generation expansion restrictions (0%_Non-RES) does not require any additional generation capacity. The 2019 capacity remaining in place until 2030 provides sufficient capacity to operate the system safely without investing in new power plants. In the scenario without restrictions for the future capacity mix (0%_RES), the model invests in utility PV and onshore wind capacity due to the potential of operating cost savings via RES. At an annual demand increase of 2.3% and the restriction of generation investment employed (2.3%_Non-RES), the generation expansion model invests mainly in combined cycle gas turbine (CCGT) power plants to meet growing demand cost-efficiently. Additionally, pumped hydro storage capacity is included. When eliminating the generation investment restriction (2.3%_RES), the model mainly invests in utility PV and onshore wind. This new capacity is complemented with open cycle gas turbines (OCGT) and pumped storage to compensate for the low firm capacity coefficients of RES generation[3]. Total additional capacity is significantly higher in the 2.3%_RES scenario.

Table 3: Existing and additional generation and storage capacity for each scenario

Technology	Existing still operational (MW)	*0%_Non-RES additional (MW)*	*0%_RES additional (MW)*	*2.3%_Non-RES additional (MW)*	*2.3%_RES additional (MW)*
Nuclear	3,050	0	0	0	0
CCGT	24,560	0	0	17,422	0
OCGT	0	0	0	0	12,288
PV (utility)	8,372	0	27,710	0	43,438
Wind (on-shore)	25,553	0	9,895	0	41,030
Hydro	15,614	0	0	0	0
Pumped storage	7,890	0	0	1,657	3,800
Others	8,826	0	0	0	0

Figure 5 shows the hourly profiles of demand and RES generation. The profiles represent the seasonal clusters introduced in the first step of Figure 2. For demonstrability, the 0%_RES scenario is represented. However, the generation expansion model works with the sample profile shapes. This means that the other scenarios show the same profiles with a scaling according to the difference of demand growth and installed RES capacity. Electricity demand shows a noticeable change in shape during the month of August. The requirement of air-conditioning increases demand. The seasonal character of RES can be observed in the figure. PV peaks are higher during the summer months, while the wind profile indicates less resource availability during the afternoon hours in the summer months.

[3] Firm capacity requirements are included in the generation expansion model as proposed in [13]. The sum of the capacity of each technology multiplied by its firm capacity coefficient is required to cover 110% of peak demand. The firm capacity coefficients per technology are included in Table 9 of Appendix A.

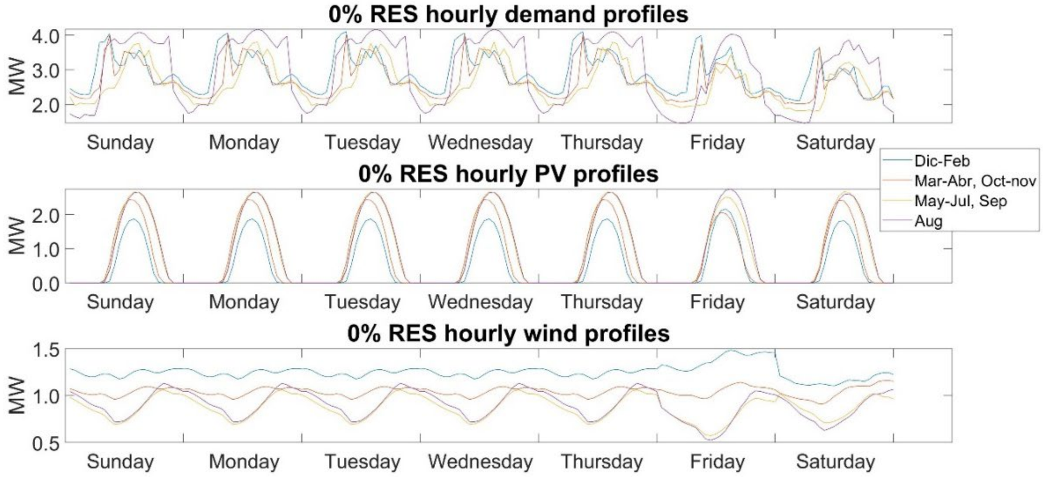

Figure 5: Hourly demand and RES generation profiles of the representative weeks of 0%_RES example scenario

3.2 Electricity grid expansion

3.2.1 Transmission grid

An approximation of the Spanish transmission network is used as a starting point for this part of the analysis. The grid is based on the transmission system used in [36] and characterised by 479 nodes connected via 880 branches at 220 or 400 kV. The transmission system is considered an island, without any interconnections to neighbouring countries to singularise the effect of the national generation mix on electricity grid expansion costs. The transmission expansion model is connected to the generation expansion model via a geographical allocation of the generation capacity throughout the transmission network.

1. Existing generation capacity per technology as provided by [37]: considering the geographical distribution of existing generation capacity allows to identify interesting locations already used by an increased number of generators. Also, the current regulatory framework might incentivise certain provinces more than others.

2. Availability of natural resources for RES (i.e. solar irradiation and wind speed): the potential of a location for RES generation depends strongly on the availability of natural resources. Hence, this aspect is considered as a second capacity allocation factor.

3.2.2 Distribution grid

The distribution expansion cost is only relevant for those DG units that connect at low (LV) or medium (MV) voltage up to 36 kV. Table 4 shows the PV and wind capacity share currently connected at each voltage level in the Spanish electricity system. Although the high voltage (HV) level[4] is considered part of the distribution grid in Spain, units for that range in Table 4 mainly represent units connected to the transmission grid via dedicated HV evacuation lines. Hence, these units do not cause any reinforcement in the distribution grid, and they are considered via connection lines assessed as grid connection costs (see section 3.3). Thus, around 42.9% of PV and 5.5% of wind installations are connected to MV and LV distribution networks in Spain. These shares are assumed to stand also for the additional capacity of the generation expansion scenarios. As only PV and wind might connect to distribution voltage levels, the non-RES scenarios are not included in this part of the analysis.

Table 4: Installed solar PV and wind capacity per voltage level in Spain [12]

Technology	**0 kV to 1 kV**	**1 kV to 36 kV**	**36 kV to 72,5 kV**	**72,5 kV to 145 kV**	**145 kV to 400 kV**
Solar PV (%)	17.33	25.58	9.51	7.17	40.41
Wind (%)	1.23	4.31	12.27	27.32	54.87

Once the capacity to connect to distribution grids is known, the RES installations need to be assigned to the distribution grid types urban, rural and semi-urban to compute the different unit costs presented in Table 1. Based on the different unit cost assumptions, total distribution grid expansion costs are calculated according to the methodology described in the following.

- The studies found in the literature analyse distribution grid reinforcement costs due to different DG technologies in representative networks. Due to the complex size of distribution grids, the common methodology uses representative grids. These representative networks depict a small part of the distribution system.
- For the allocation of the total additional RES capacity according to distribution grid type (i.e. urban, semi-urban and rural), scaling is necessary. It allows splitting the

[4] Above 36 kV and up to 132 kV

national additional generation capacity into the different distribution network types. In contrast to unit costs, scaling the representative distribution grid costs to system scale does depend on the country characteristics.

- The authors of [19] employ a scaling of representative distribution grids to the Spanish distribution system. Their scaling approach is based on the transformation capacity per voltage level. It comprises the contracted capacity at MV level and the MV/LV transformation capacity installed at the corresponding feeders. This methodology finds that almost half of the transformation capacity of Spanish distribution grids is located in distribution grids of urban configuration, below 20% in grids of rural configuration and the rest in semi-urban grids. The high share of urban distribution networks resulting from this calculation methodology is due to the consideration of contracted demand. Big cities, i.e. demand centres, are of urban network configuration. This allocation approach can be considered a suitable approximation for prosumer installations expected to expand proportionally to existing demand.

- As a second hypothesis, prosumer installations are considered to represent the LV installations. Consequently, LV DG is expected to install in proportion to existing electricity demand to compute distribution grid expansion costs.

- The amount of DG is determined according to Table 4 and allocated in the different distribution grid types according to the shares of the LV assumption presented in Table 5.

MV installations are assumed to be of utility-scale size. The location of these installations is expected to take place outside the demand centres. Hence, no MV installation is considered to connect to urban distribution grids. The assumption gives higher weight to rural zones, where RES rollout is expected to occur due to the higher availability of terrain. It is considered a conservative cost assumption due to higher distribution grid unit costs in rural zones (Table 1). However, the exact share of utility-scale RES to connect to rural and semi-urban distribution networks is unknown. Sensitivities of the rural grid share from 60 to 80% are performed as three different MV assumptions presented in Table 5.

Table 5: Allocation of RES capacity according to distribution network type

Network type	**LV assumption [19]**	**MV1 assumption**	**MV2 assumption**	**MV3 assumption**

Urban	47%	0%	0%	0%
Semi-urban	35%	40%	30%	20%
Rural	18%	60%	70%	80%

Figure 6 shows the allocation of capacity into electricity grids of the three scenarios with additional capacity resulting from the methodology introduced in section 2.2 and the data presented throughout this section. CCGT, OCGT and hydropower plants connect to the transmission grid directly. Wind and PV are allocated to the grids according to Table 4. Additionally, the distribution grid is separated into the three network types discussed above. The capacity connected to distribution grids is allocated to urban, rural and semi-urban networks as shown in Table 5. For the allocation of MV capacity, the MV2 assumption is employed to create this diagram. Capacity connecting to the subtransmission grid is directly connected to the energy harvesting network, as explained at the beginning of this section.

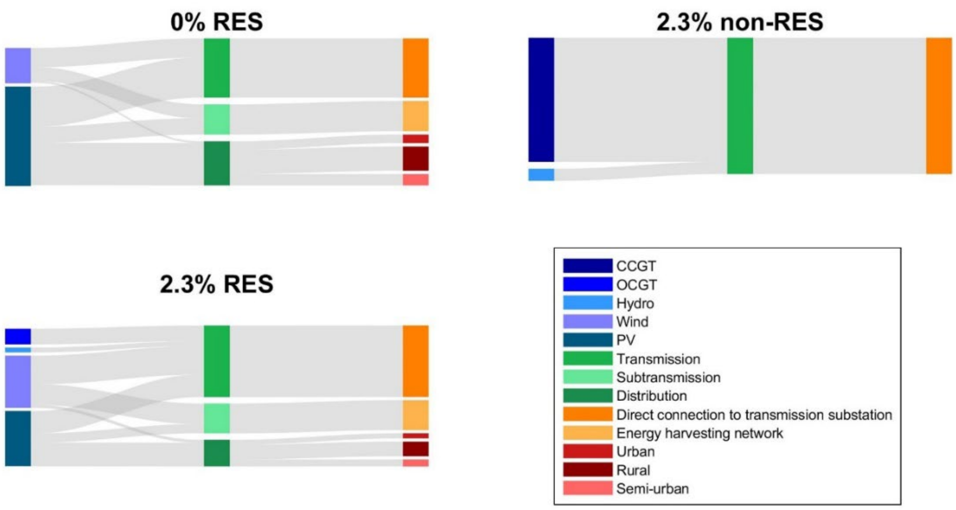

Figure 6: Sankey diagrams of capacity allocation per technology

3.3 Electricity grid connection

Approximate coordinates of the locations of Spanish generators represent the starting point of this approach [38]–[40]. The distance from the grid of generators connected to the HV and extra-high voltage (EHV) network is obtained with representative data of the Spanish transmission system applied for the TEP analysis, considering the generators to connect to the closest transmission node in the database of the Spanish-like transmission grid described in section 3.2.1. Generators connected to the LV and the MV distribution network are considered to be located at 10 km of the distribution grid connection point, based on the maximum feeder length in rural distribution networks [41]. The installations of LV and MV voltage levels are considered within the same connection cost term. The electrical components are considered aerial single circuit lines and switchbay with air-insulated switchgear with costs according to the Spanish Ministry [42], [43]. Total annualised costs of the connecting power lines are determined with the following categorisation based on statistics from the Spanish regulator [12]: PV and hydro generators below 10 MW connect at MV level, generators between 10 and 25 MW at HV level, generators with a capacity of over 25 MW connect at EHV level. For wind energy, these limits are slightly higher as found in the data (MV < 15 MW; 15MW ≤ HV < 30 MW, EHV ≤ 30MW) [12]. Connection costs are annualised with a discount rate of 7% and a lifespan of 40 years. As the last step, annualised connection costs are converted into unit costs with the respective capacities for each generator in the database.

The annual unit connection costs obtained for each of the generation technologies are summarised in Figure 7. For PV and wind generators, minor unit connection cost differences are found at the different voltage levels, based on similar distances to the point of connection. For HV and EHV, the distances obtained from the second approach are between 15 and 17 km for PV and wind and even lower for thermal power plants (12 km). Maximum distances are obtained for hydropower plants due to remote locations with optimum generation conditions (30 km). Hence, the hydro connection shows increased unit connection costs compared to the other EHV unit connection costs. Real generators are likely to find a new node at a shorter distance. This estimation is considered a conservative approach for a worst-case estimation of connection costs.

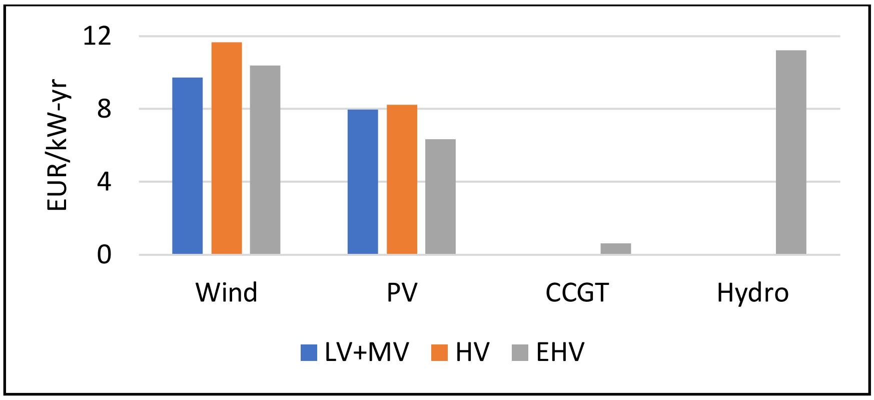

Figure 7: Annualised unit connection costs according to technology and voltage level

4 Results: System investment costs and benefits

In this section, the different components of the investment costs are presented for the Spanish case study. Annualised costs are obtained with a rate of return of 7% over the lifetime of the installation[5]. Benefits of the investments in the form of operating cost reductions are discussed in section 4.4; an analysis of results is provided in 4.5. All monetary results are given in 2019 Euros.

4.1 Generation and storage expansion costs

The total additional capacity of the technologies for each scenario is contrasted with the annual generation expansion costs in Table 6. Both renewable scenarios result in higher generation expansion investments than the non-renewable scenario with additional thermal generation capacity (2.3%_Non-RES). This increment in costs is explained by the significant increase of additional generation and storage capacity for the renewable scenarios, as shown in the literature [10], [11]. An indicator to make easier comparisons among scenarios is the annual generation unit costs (EUR/kW-yr). The unit costs are the ratio of annual generation investment and the additional capacity, resulting in lower values for both renewable scenarios.

Table 6: Total additional capacity and annualised generation and storage investment per scenario

		0%_ Non-RES	**0%_ RES**	**2.3%_ Non-RES**	**2.3%_ RES**
RES share of generation	%	42	80	27	81
Additional capacity	(MW)	0	37,605	19,079	100,556
Annualised generation investment	(MEUR/yr)	-	1,946	1,331	5,764
Annualised generation unit investment	(EUR/kW-yr)	-	51.8	69.7	57.3

4.2 Electricity grid expansion costs

4.2.1 Transmission grid expansion costs

Both scenarios without demand growth (0%) result in the same magnitude of annualised transmission grid costs: 63 M€/yr. This means that the adjustment of the initial transmission

[5] The same rate is applied to all generators and grid investments. Lifetime of electricity grid assets is considered 40 years, details on the lifetime assumptions of the different generation technologies is provided in Appendix A

network results in the same costs as the integration of over 37.5 GW of renewable generation capacity. The analysis of the scenarios with demand growth (2.3%) shows that the integration of renewable generation capacity leads to increased transmission investment to serve the increased demand. The outcome of the TEP model results in an annualised transmission grid investment of 130 M€/yr in the non-RES scenario and 162 M€/yr in the renewable scenario. This represents an increase of around 25% in the renewable scenario, while the new generation capacity in the RES scenario is over five times the additional capacity in the non-RES scenario.

4.2.2 Distribution grid expansion costs

For the calculation of distribution grid expansion costs, a suitable approach for the allocation of MV installations in rural and semi-urban grids needs to be determined first. Table 7 shows the annualised distribution grid costs of the three MV allocation assumptions presented previously in Table 5. As the deviation between the assumptions is minor, distribution grid costs are computed with 70% of MV connections in rural grids to represent an average approximation.

Table 7: Evaluation of MV distribution grid allocation assumptions

		0%_RES			**2.3%_RES**		
MV capacity allocation assumption		**MV1**	**MV2**	**MV3**	**MV1**	**MV2**	**MV3**
Capacity at semi-urban/rural distribution grids	%	40/60	30/70	20/80	40/60	30/70	20/80
Total additional capacity	MW	37,605			100,556		
Additional capacity connected at distribution grids	MW	12,439			20,912		
Capacity per distribution grid type							
Urban	MW	2,314	2,314	2,314	3,775	3,775	3,775
Semi-urban	MW	5,320	4,569	3,817	8,927	7,639	6,351
Rural	MW	6,823	7,574	8,326	11,503	12,791	14,079
Distribution grid expansion costs							
Equal cost assumption	MEUR	82	86	90	139	146	152
Specific cost assumption	MEUR	115	122	129	150	160	170

The employment of specific costs results in higher magnitudes of distribution grid reinforcement because almost all unit costs are elevated compared to the equal-cost assumption. This development is more noticeable in the scenario without demand growth (0%_RES) because unit grid costs are considered higher without demand growth due to the compensation effect of local DG and demand growth described above. Final distribution network expansion costs are considered according to the specific unit cost assumption to consider the more conservative magnitude of distribution grid costs. This methodology results in 122 M€/yr and 160 M€/yr for the scenarios 0%_RES and 2.3%_RES, respectively.

4.2.3 Total grid expansion costs

The final results of transmission and distribution expansion costs for each of the four scenarios are summarised in Table 8. As explained above, transmission grid costs are the same in the scenarios without demand growth (0%) and similar in the scenarios with demand growth (2.3%). The distribution grid term is applied to renewable scenarios only. This factor is the primary driver of the increase of electricity grid expansion costs in the RES scenarios compared to the respective non-RES scenarios. Installations that connect at the distribution grid level trigger reinforcement needs in both networks, transmission and distribution. Electricity network reinforcement needs are tripled (0%_RES) and doubled (2.3%_RES) by the PV and wind installations that connect at distribution level.

Although the renewable scenarios at least double the network expansion costs by connecting partly to the distribution grid, they represent a small share when contrasted with the generation and storage capacity investment costs presented above (Table 6).

Table 8 includes an indicator of the ratio of network expansion costs (transmission and distribution) and generation and storage investment. Grid expansion costs of all scenarios are below 10% of the corresponding generation and storage investments. In the renewable scenarios without and with demand growth, electricity network expansion investment is 9.5 and 5.6% of generation investment, respectively. When the additional generation capacity is non-RES, electricity grid expansion costs reach 9.8% of the expenses for generation expansion.

Table 8: Annualised transmission and distribution expansion costs of the four scenarios considered

		0%_ Non-RES	**0%_ RES**	**2.3%_ Non-RES**	**2.3%_ RES**
Transmission expansion	(MEUR/yr)	63	63	130	162
Distribution expansion	(MEUR/yr)	0	122	0	160

Electricity grid expansion/ Generation investment	%	-	9.5	9.8	5.6

4.3 Electricity grid connection costs

An overview of all annualised electricity grid investment costs is presented in Figure 8, comparing connection costs for transmission (T) and distribution (D) grids with the grid expansion costs presented above. Connection costs represent 63 (0%_RES) to 72% (2.3%_RES) of the costs in the renewable scenarios and 19% in the 2.3%_Non-RES scenario. The 0%_Non-RES scenario does not include a connection cost term as no additional generation or storage capacity is installed. Although these connection cost investments are likely to represent an overestimation, they do provide information about the approximate order of magnitude of costs to expect for connecting new power plants to the electricity grids. The results further support the hypothesis that network expansion costs do not represent the critical part of RES investment costs.

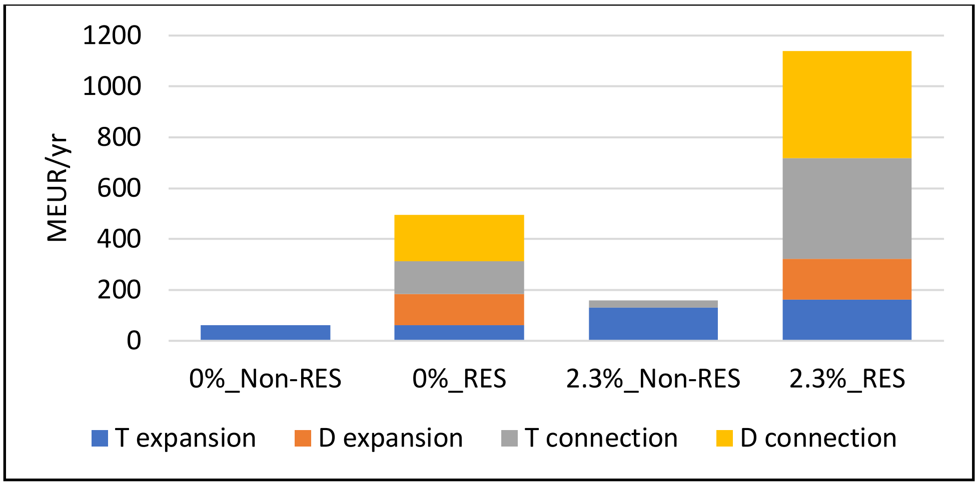

Figure 8: Stacking of grid expansion and connection costs for each scenario

Commonly, connection costs are borne by the generator wishing to connect to the electricity grid. These costs are included in the unit capacity expansion costs alongside the costs for the procurement and installation of the generation units. It is therefore contemplated for the calculation of the generation and storage expansion costs presented in section 4.1. Hence, the connection cost term is not included separately in the cost balances to avoid double counting.

Figure 9 shows the stacking of all annualised investment cost components. Significant increases can be observed from the non-RES to the corresponding RES scenario. Without demand growth, annualised investment requirements are multiplied by four. With demand growth, the multiplier increases to 37. However, the figure also points out that the electricity grid expansion represents a minor share of investment costs.

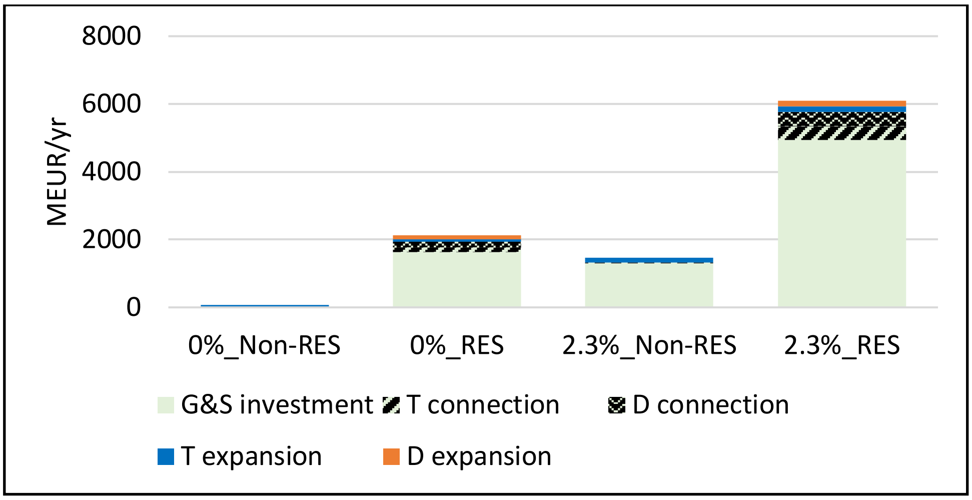

Figure 9: Stacking of all annualised investment cost components

4.4 System operating cost savings

The total investment costs are found higher for renewable generation and storage capacity expansion scenarios than for non-renewable scenarios. However, replacing thermal generation capacity with RES allows reducing system operating costs [5]–[7]. Figure 10 underlines the monetary benefits obtained from operating an electricity system with around 80% RES share[6]. In both cases, without and with demand growth, generation and storage (G&S) operating costs are reduced when employing renewable energies. The saving potential of G&S operating costs is given through the reduction of fossil fuel costs and emissions (priced at 84.84 €/ton [35]). Generation and storage operating costs are reduced by 35 and 54% for the scenarios without and with demand growth, respectively. This reduction is influenced by the CO_2 price employed. However, a sensitivity with a reduction to 30 €/ton did not result in a significant variation in the percentual reduction of operating costs[7].

[6] Including PV, wind, hydro and other RES such as biomass.
[7] Additional sensitivities of the four scenarios have been computed. The analysis showed no variation of the conclusions drawn from the four scenarios presented in the main body of the paper. A brief exemplary description is included in Appendix C.

This reduction of operating costs leads to a decrease in total annualised system costs, which are the sum of annualised investment and operating costs. With investment in additional RES generation and storage capacity, annual system costs are reduced by 9.7% in the scenarios without demand growth. This finding is especially striking because no additional generation and storage capacity is built in the scenario 0%_Non-RES. Investing in RES capacity results in a system cost reduction, even when compared with a scenario with no investment in generation and storage capacity at all. For each €/yr invested in the 0%_RES scenario, annual operating costs are reduced by 1.43 € in comparison to the 0%_Non-RES scenario. When considering an annual demand growth of 2.3%, both scenarios require additional generation and storage capacity. The alternative of additional thermal generation capacity increases the saving potential that is provided through RES. The 2.3%_RES scenario results in 24.7% lower total annualised system costs than the 2.3%_Non-RES scenario, even though investment costs are quadruplicated. Annual operating costs are reduced by 1.62 € for each € of annualised investment in the 2.3%_RES scenario.

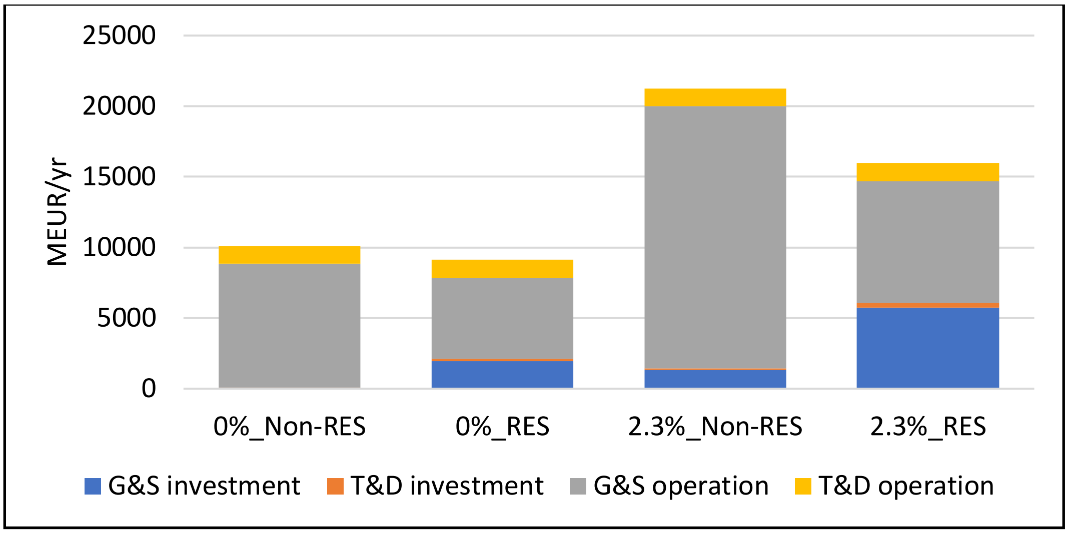

Figure 10: Total annualised investment and operating costs for each scenario (connection costs included in the G&S investment term)

The concept of avoided costs is employed to evaluate the operating cost savings due to additional PV and wind capacity. This concept is derived from [44], [45], where this indicator is used to express the expected revenues of renewable energy generators based on the replacement of more costly generators. In this work, the concept of avoided cost is adapted as a performance indicator and determined as operating cost savings due to the employment of RES technologies (Tech), as indicated in Eq. 1. The RES and Non-RES label in the terms of the equation refers to the RES and Non-RES scenarios addressed in the study.

$$Avoided\ costs = \frac{(Operation\ cost_{Non-RES} - Operation\ cost_{RES})}{\sum_{Tech}(Generation_{Tech,RES} - Generation_{Tech,Non-RES})} \qquad \text{Eq. 1}$$

The avoided operating cost is determined at 36.13 and 46.66 €/MWh without and with demand growth, respectively.

4.5 Analysis of results

The expansion of RES generation capacity significantly increases the required installed generation and storage capacity compared to thermal generation to comply with firm capacity requirements and compensate for low full-load hours. In the non-RES scenario without demand growth, no additional generation capacity is required, while 37 GW of additional capacity are installed in the RES scenario without demand growth. In the scenarios with demand growth, the expansion of RES generation and storage capacity requires around five times the additional generation capacity of a non-RES expansion.

Annualised transmission and distribution network expansion costs are more than doubled when RES generation is expanded instead of non-RES. This increase is due to the integration of around 43% of PV and 6% of wind capacity in distribution grids, while non-RES capacity is directly connected to the transmission grid. When considering grid connection costs, network investment costs are up to six times higher when RES generation is expanded instead of non-RES. In RES scenarios, 63 to 72% of total grid investment costs corresponds to the worst-case estimation of the grid connection cost term. Annualised unit grid investment costs (expansion and connection) per additional RES generation capacity sums up to slightly over 13 and 11 €/kW-yr without and with demand growth, respectively: 4.9 and 3.2 €/kW-yr for network expansion costs and 8.3 and 8.1 €/kW-yr for grid connection costs. In the non-RES scenario with generation expansion, this term is reduced to 8.4 €/kW-yr, of which 1.6 €/kW-yr correspond to the connection cost term.

Despite the increasing network investment costs, the potential of RES generation in the operating cost reduction is still significant. Adding network costs to the economic consideration of the scenarios does not revise the least-cost options determined by the single-bus generation expansion model. By investing in RES, annualised total system costs are reduced 9.7 and 24.7% in the scenarios without and with demand growth, respectively.

5 Conclusions and policy implications

This work presents a case study to evaluate whether the consideration of generation-driven electricity grid expansion and connection costs has a significant impact on the economic viability of integrating high RES shares into the electricity system. A realistic Spanish-like case study is used to quantify the different network investment cost components. Four distinct 2030 scenarios are assessed and compared. These scenarios were obtained from a single-bus generation expansion model by combining two different generation and storage expansion scenarios and two demand growth rates.

Generation and storage installation costs are found to significantly increase in renewable scenarios compared to non-renewable pathways (i.e. additional load is met with investments in thermal generation). Transmission grid expansion costs are of the same magnitude in the RES and the Non-RES scenarios without demand growth, regardless of the generation expansion pathway, and increase 25% in the RES scenario when demand growth is considered. In the 0%_RES scenario, distribution grid expansion costs were estimated to be twice as much as transmission expansion costs, while in the 2.3%_RES scenario, both grid expansion terms are of approximately the same magnitude. Grid connection costs represent the expenses for installing power lines to connect the new power plants to the closest grid node. The pessimist estimation of connection costs results in significantly higher expenses in the renewable scenarios than in the respective non-renewable scenarios.

The additional investment requirements in the renewable scenarios are triggered by the significant increase in additional generation and storage capacity. The additional capacity is significantly higher in the RES scenarios when compared to the corresponding Non-RES scenario. In consequence, all investment cost components are higher in the renewable scenarios. However, compared to the generation and storage capacity investment, transmission and distribution grid costs represent a minor share of total investment costs. Electricity grid expansion costs represent 9.5 and 5.6% of the total investment costs in the RES scenarios and 9.8% in the non-RES scenario. The increase of total investment costs is contrasted by a significant reduction in operating costs due to reducing fuel and emission costs in the renewable scenarios. After including electricity grid expansion costs, the employment of RES technologies still allows reducing annual operating costs 1.43 and 1.62 € per each € of annualised investment for the scenarios without and with demand growth, respectively.

The results of this case study confirm that the needed decarbonisation of the electricity sector can be achieved even at lower costs than other non-RES alternative futures. Comparing the scenarios without demand growth underlines that investing in new renewable generation capacity allows decreasing overall system costs, even though no generation or distribution grid investment is made in the non-renewable scenario.

This paper shows that electricity grid expansion is not the crucial investment component (compared to generation and storage investment) in a realistic case study. Furthermore, despite increasing electricity network investment requirements in both renewable scenarios, operating cost reductions outweigh the investment in renewables, comprising both generation and network costs. Therefore, electricity grid investment costs should not be seen as an economic barrier for integrating high RES shares and complying with the 2030 decarbonisation goals.

This conclusion may be reinforced by the fact that the results presented in this paper were obtained under pessimistic assumptions, especially in the case of grid connection costs, which are difficult to estimate due to limited data availability. Furthermore, the Spanish-like electricity system has been modelled as an island without any interconnections. As pointed out in [11], large-scale interconnections represent a valuable tool to smoothen the effect of RES variability by connecting zones with different RES generation profiles. Although this factor may have a limited impact in the case of Spain due to its low interconnection capacity with central Europe, it can be very significant in highly interconnected systems. On the other hand, the upwards pressure of large shares of intermittent RES on some system operation costs, most notable balancing costs, has not been assessed in this paper.

Future research should also seek to include flexibility measures from demand, generation and storage units to further decrease network investment costs by optimising grid usage during critical hours. The ongoing electrification of demand applications is expected to change the load profile, especially towards 2050. Thus, additional research should analyse electricity grid costs of integrating high RES shares in the light of changing demand profiles. Lastly, even though, as discussed above, incremental network costs should not hamper the achievement of decarbonisation goals, regulation related to grid connection and expansion may in practice hamper RES integration, e.g. e.g. outdated or excessively conservative hosting capacity calculation criteria, or via inefficient and inflexible grid capacity allocation mechanisms. Hence, suitable regulatory frameworks enabling an efficient and rapid integration of RES capacity into electricity networks should be set in place.

6 Acknowledgements

The authors would like to thank Teresa Freire Barceló and Francisco Martín Martínez for the provision of scenario input data and Andrés Ramos Galán for the patience and support throughout the modelling process.

This research has been carried out thanks to the Iberdrola Chair on Energy and Innovation and the funding of the RETOS COLABORACIÓN programme of the Spanish Ministry of Science and Innovation and the Spanish State Research Agency (project "Platform of innovative models to accelerate the energy decarbonisation of the economy (MODESC)", with reference number RTC2019- 007315-3).

7 References

[1] Spanish Government, 'Spanish National Energy and Climate Plan', Jan. 20, 2020. https://ec.europa.eu/energy/sites/ener/files/documents/es_final_necp_main_es.pdf (accessed Jul. 15, 2020).

[2] F. Gutiérrez-Martín, R. A. Da Silva-Álvarez, and P. Montoro-Pintado, 'Effects of wind intermittency on reduction of CO2 emissions: The case of the Spanish power system', *Energy*, vol. 61, pp. 108–117, Nov. 2013, doi: 10.1016/j.energy.2013.01.057.

[3] A. J. Chapman, B. C. McLellan, and T. Tezuka, 'Prioritising mitigation efforts considering co-benefits, equity and energy justice: Fossil fuel to renewable energy transition pathways', *Appl. Energy*, vol. 219, pp. 187–198, Jun. 2018, doi: 10.1016/j.apenergy.2018.03.054.

[4] B. N. Stram, 'Key challenges to expanding renewable energy', *Energy Policy*, vol. 96, pp. 728–734, Sep. 2016, doi: 10.1016/j.enpol.2016.05.034.

[5] S. Sen and S. Ganguly, 'Opportunities, barriers and issues with renewable energy development – A discussion', *Renew. Sustain. Energy Rev.*, vol. 69, pp. 1170–1181, Mar. 2017, doi: 10.1016/j.rser.2016.09.137.

[6] M. Ortega-Izquierdo and P. del Río, 'Benefits and costs of renewable electricity in Europe', *Renew. Sustain. Energy Rev.*, vol. 61, pp. 372–383, Aug. 2016, doi: 10.1016/j.rser.2016.03.044.

[7] M. Ram *et al.*, 'Global Energy System based on 100% Renewable Energy – Power, Heat, Transport and Desalination Sectors', 2019. http://energywatchgroup.org/wp-content/uploads/EWG_LUT_100RE_All_Sectors_Global_Report_2019.pdf (accessed Mar. 10, 2021).

[8] A. S. Brouwer, M. van den Broek, A. Seebregts, and A. Faaij, 'Impacts of large-scale Intermittent Renewable Energy Sources on electricity systems, and how these can be modeled', *Renew. Sustain. Energy Rev.*, vol. 33, pp. 443–466, May 2014, doi: 10.1016/j.rser.2014.01.076.

[9] G. Notton *et al.*, 'Intermittent and stochastic character of renewable energy sources: Consequences, cost of intermittence and benefit of forecasting', *Renew. Sustain. Energy Rev.*, vol. 87, pp. 96–105, May 2018, doi: 10.1016/j.rser.2018.02.007.

[10] S. Pfenninger and J. Keirstead, 'Renewables, nuclear, or fossil fuels? Scenarios for Great Britain's power system considering costs, emissions and energy security', *Appl. Energy*, vol. 152, pp. 83–93, Aug. 2015, doi: 10.1016/j.apenergy.2015.04.102.

[11] K. Schaber, F. Steinke, P. Mühlich, and T. Hamacher, 'Parametric study of variable renewable energy integration in Europe: Advantages and costs of transmission grid extensions', *Energy Policy*, vol. 42, pp. 498–508, Mar. 2012, doi: 10.1016/j.enpol.2011.12.016.

[12] CNMC, 'Información mensual de estadísticas sobre las ventas de régimen especial', Sep. 2020. https://www.cnmc.es/estadistica/informacion-mensual-de-estadisticas-sobre-las-ventas-de-regimen-especial-contiene-49 (accessed Feb. 10, 2021).

[13] T. Gerres, J. P. Chaves Avila, F. Martin Martinez, M. Rivier Abbad, R. Cossent Arin, and A. Sanchez Miralles, 'Rethinking the electricity market design: Remuneration mechanisms to reach high RES shares. Results from a Spanish case study', *ENERGY POLICY*, vol. 129, pp. 1320–1330, Jun. 2019, doi: 10.1016/j.enpol.2019.03.034.

[14] C. Matamala, R. Moreno, E. Sauma, J. Calabrese, and P. Osses, 'Why reducing socio-environmental externalities of electricity system expansions can boost the development of solar power generation: The case of Chile', *Sol. Energy*, vol. 217, pp. 58–69, Mar. 2021, doi: 10.1016/j.solener.2021.01.034.

[15] S. Lumbreras *et al.*, 'Centralized vs. Decentralised development of the electricity sector', Mar. 2018. https://www.set-nav.eu/sites/default/files/common_files/deliverables/WP6/D6.4%20Case%20study%20report%20on%20decentralised%20vs%20centralised%20RES%20developments%20in%20the%20electricity%20sector.pdf

[16] A. Held *et al.*, 'How can the renewables targets be reached cost-effectively? Policy options for the development of renewables and the transmission grid', *Energy Policy*, vol. 116, pp. 112–126, May 2018, doi: 10.1016/j.enpol.2018.01.025.

[17] ECF, 'A practical guide to a prosperous, low-carbon Europe', 2010, doi: http://www.roadmap2050.eu/attachments/files/Volume1_fullreport_PressPack.pdf.

[18] REE, 'Consulta el estado de las solicitudes', Apr. 10, 2021. https://www.ree.es/es/clientes/generador/acceso-conexion/conoce-la-capacidad-de-acceso (accessed Dec. 14, 2020).

[19] Greenpeace, 'Estudio técnico de viabilidad de escenarios de generación eléctrica en el medio plazo en España', p. 62, Mar. 2018, doi: https://es.greenpeace.org/es/wp-content/uploads/sites/3/2018/03/Generacion-Electrica_baja_5-03-2018.pdf.

[20] J. D. Jenkins and I. J. Perez-Arriaga, 'Improved Regulatory Approaches for the Remuneration of Electricity Distribution Utilities with High Penetrations of Distributed Energy Resources', *ENERGY J.*, vol. 38, no. 3, pp. 63–91, Mai 2017, doi: 10.5547/01956574.38.3.jjen.

[21] C. Mateo, P. Frias, and K. Tapia-Ahumada, 'A comprehensive techno-economic assessment of the impact of natural gas-fueled distributed generation in European electricity distribution networks', *ENERGY*, vol. 192, Feb. 2020, doi: 10.1016/j.energy.2019.116523.

[22] L. Olmos, R. Cossent, T. Gómez, and C. Mateo, 'Case studies of system costs of distribution areas', Sep. 04, 2009.

[23] MIT, 'The Future of Solar Energy', 2015. http://energy.mit.edu/wp-content/uploads/2015/05/MITEI-The-Future-of-Solar-Energy.pdf (accessed Apr. 06, 2020).

[24] R. Gupta *et al.*, 'Spatial analysis of distribution grid capacity and costs to enable massive deployment of PV, electric mobility and electric heating', *Appl. Energy*, vol. 287, p. 116504, Apr. 2021, doi: 10.1016/j.apenergy.2021.116504.

[25] IRENA, 'Renewable energy technologies: cost analysis series - Solar Photovoltaics', Jun. 2012. https://www.solar-united.org/wp-content/uploads/2017/02/RE_Technologies_Cost_Analysis-SOLAR_PV.pdf (accessed Feb. 02, 2021).

[26] IRENA, 'Renewable energy technologies: cost analysis series - Wind Power', Jun. 2012. https://www.irena.org/-/media/Files/IRENA/Agency/Publication/2012/RE_Technologies_Cost_Analysis-WIND_POWER.pdf (accessed Feb. 02, 2021).

[27] M. I. Blanco, 'The economics of wind energy', *Renew. Sustain. Energy Rev.*, vol. 13, no. 6, pp. 1372–1382, Aug. 2009, doi: 10.1016/j.rser.2008.09.004.

[28] C. Mone, T. Stehly, B. Maples, and E. Settle, '2014 Cost of Wind Energy Review', Oct. 2015. https://www.nrel.gov/docs/fy16osti/64281.pdf (accessed Feb. 10, 2021).

[29] C. Mone, M. Hand, M. Bolinger, J. Rand, D. Heimiller, and J. Ho, '2015 Cost of Wind Energy Review', May 2017. https://www.nrel.gov/docs/fy17osti/66861.pdf (accessed Feb. 10, 2021).

[30] IRENA, 'Renewable power generation costs in 2019', 2020. https://www.irena.org/-/media/Files/IRENA/Agency/Publication/2020/Jun/IRENA_Power_Generation_Costs_2019.pdf (accessed Feb. 02, 2021).

[31] R. C. Knight, J. P. Montez, F. Knecht, and T. Bouquet, 'Distributed generation connection charging within the European Union', Sep. 2005. https://www.ceer.eu/documents/104400/-/-/cacc41c3-7177-7652-71f7-b2b2ef3472a9 (accessed Jul. 09, 2020).

[32] J. P. Chaves Avila *et al.*, 'EUniversal D5.1 - Identification of relevant market mechanisms for the procurement of flexibility needs and grid services', Jan. 2021, doi: https://euniversal.eu/wp-content/uploads/2021/02/EUniversal_D5.1.pdf.

[33] F. Martin-Martinez, A. Sanchez-Miralles, M. Rivier, and C. F. Calvillo, 'Centralised vs distributed generation. A model to assess the relevance of some thermal and electric factors. Application to the Spanish case study', *ENERGY*, vol. 134, pp. 850–863, Sep. 2017, doi: 10.1016/j.energy.2017.06.055.

[34] T. Freire-Barceló *et al.*, 'Storage and demand response contribution to firm capacity: analysis of the Spanish electricity system', *IIT Work. Pap.*, vol. IIT-21-096WP, Jun. 2021, doi: https://www.iit.comillas.edu/publicacion/working_paper/es/434/Storage_and_demand_response_contribution_to_firm_capacity:_analysis_of_the_Spanish_electricity_system.

[35] IEA, 'World Energy Outlook 2019 – Analysis', *IEA*, Nov. 2019. https://www.iea.org/reports/world-energy-outlook-2019 (accessed Feb. 10, 2021).

[36] P. Frías *et al.*, 'Assessment report on the impacts of RES policy design options on future electricity markets', Oct. 2013. https://res-policy-beyond2020.eu/pdffinal/Assessment%20report%20on%20the%20impacts%20on%20future%20electricity%20markets%20(beyond2020%20-%20D5-2).pdf (accessed Jun. 02, 2021).

[37] REE, 'Estado de las solicitudes', Apr. 30, 2021. https://www.ree.es/es/clientes/generador/acceso-conexion/conoce-el-estado-de-las-solicitudes (accessed Jul. 29, 2020).

[38] AEE, 'Mapa de parques eólicos'. https://www.aeeolica.org/sobre-la-eolica/la-eolica-espana/mapa-de-parques-eolicos (accessed Feb. 10, 2021).

[39] REE, 'Mapas de interés'. https://ree.carto.com/u/liquidaciones/builder/732be485-f2d6-4215-8653-3de62f3c9509/embed (accessed Feb. 10, 2021).

[40] MITECO, 'Registro de instalaciones'. https://energia.gob.es/electricidad/Regimenordinario/Paginas/RegInstalaciones.aspx (accessed Feb. 10, 2021).

[41] S. Allard, V. Debusschere, S. Mima, T. T. Quoc, N. Hadjsaid, and P. Criqui, 'Considering distribution grids and local flexibilities in the prospective development of the European power system by 2050', *Appl. Energy*, vol. 270, p. 114958, Jul. 2020, doi: 10.1016/j.apenergy.2020.114958.

[42] MINETUR, 'Orden IET/2659/2015', Dec. 12, 2015. https://www.boe.es/buscar/pdf/2015/BOE-A-2015-13487-consolidado.pdf

[43] MINETUR, 'Orden IET/2660/2015', Dec. 12, 2015. https://www.boe.es/boe/dias/2015/12/12/pdfs/BOE-A-2015-13488.pdf (accessed Feb. 11, 2021).

[44] C. Namovicz, 'Assessing the Economic Value of New Utility-Scale Renewable Generation Projects', Jun. 17, 2013. https://www.eia.gov/conference/2013/pdf/presentations/namovicz.pdf (accessed Mar. 10, 2021).

[45] A. Brown *et al.*, 'Estimating Renewable Energy Economic Potential in the United States: Methodology and Initial Results', *Renew. Energy*, p. 154, 2016, doi: https://www.nrel.gov/docs/fy15osti/64503.pdf.

8 Appendix

8.1 Appendix A

Table 9: Modelling cost input parameter

	CO2emis-sions [EUR/MWh]	Fuel [Eur/MWh]	O&M [Eur/MWh]	Lifetime of new genera-tors [years]	Firmness coefficient [-]
Nuclear	0	8.72	0	-	0.97
CCGT	28	32.58	2	25	0.96
OCGT	42.42	48.88	11	25	0.96
Hydro	0	0	3	80	0.44
Pumped hydro	0	0	3	80	0.96
Wind	0	0	0.01	30	0.07
PV	0	0	0	25	0
ENS	0	0	1000	-	-

8.2 Appendix B

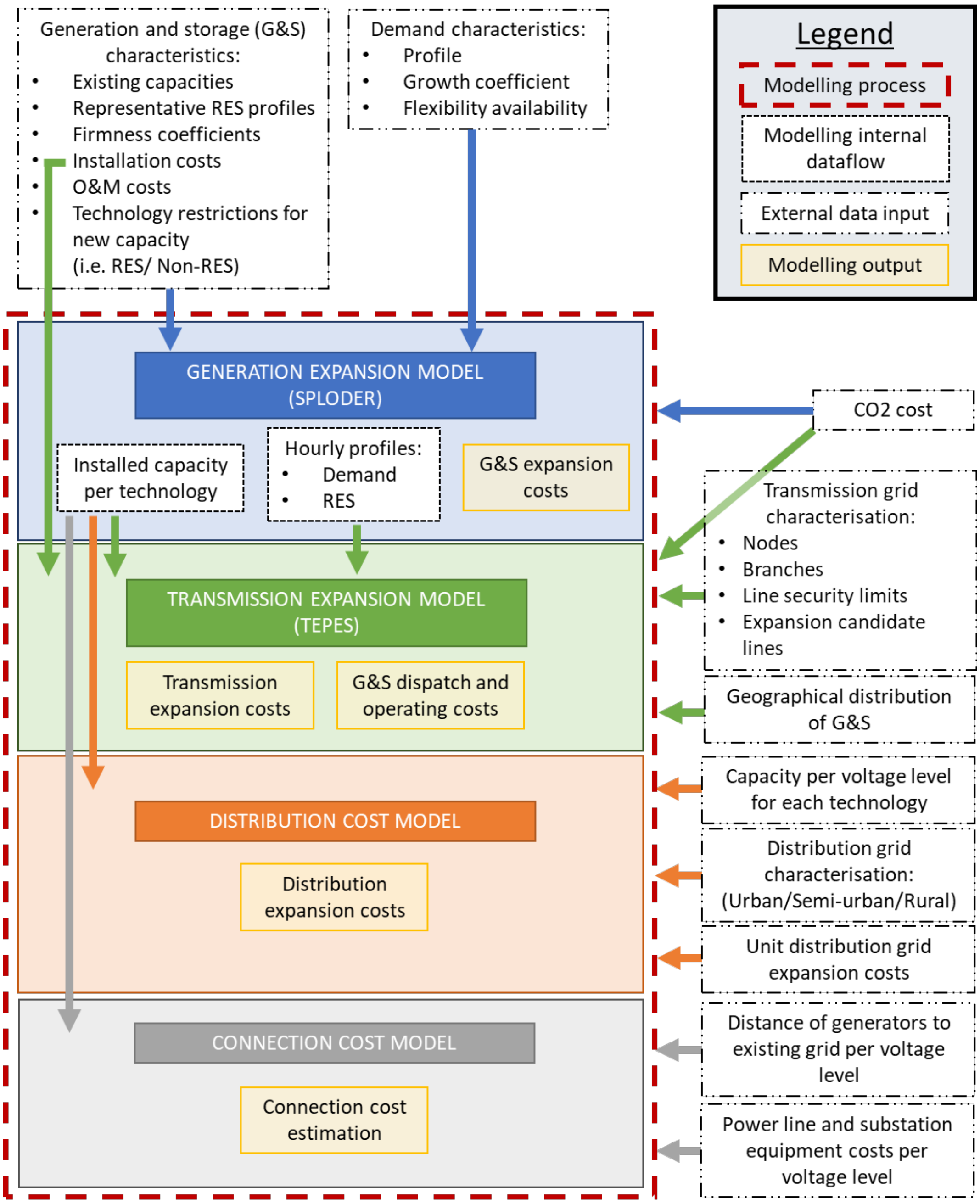

Figure 11: Conceptual dataflow of the investment cost determination process

8.3 Appendix C

Apart from the four scenarios described previously, several sensitivities have been studied in the transmission expansion model to analyse their impact on the order of magnitude of electricity grid investment requirements. The sensitivities that have been analysed include:

a) A reduction of the CO_2 price to 30 €/ton

b) A variation of transmission grid power line security factors (the standard security factor applied to the existing network as well as to expansion candidate lines is 0.66, variations to 0.5 and 0.7 have been analysed)

c) The concentration of RES locations in the transmission network to a maximum of 5 nodes to zones with high availability of solar irradiation and wind, respectively. This reallocation is applied to the incremental invested capacity only.

Although the sensitivities show a minor change in transmission expansion and operation costs, the order of magnitudes and the corresponding conclusions do not vary. These sensitivities have not been included in the paper for the sake of brevity. In Table 10, the sensitivity of CO_2 cost is presented compared to the base case for the scenarios with demand growth. The base case represents the numbers included in the paper. The sensitivity is implemented in the transmission expansion model, which is used to obtain the generation dispatch. Hence, transmission investment and the generation and storage operation costs vary. The reduction of the CO_2 price from 84.84 to 30 €/ton decreases the generation operating costs in both cases, as a thermal generation can operate at a lower cost. However, when comparing the Non-RES and the RES scenarios, the reduction of operating costs (Non-RES: 11,139 MEUR/yr; RES: 2,190 MEUR/yr; difference: 8,940 MEUR/yr) still more than compensates the increase of transmission investment (Non-RES: 125 MEUR/yr; RES: 152 MEUR/yr; difference: 27 MEUR/yr) and the distribution investment of 160 MEUR. The same observations have been made for the scenarios without demand growth and the other sensitivities.

Table 10: CO2 scenario sensitivity results for the 2,3% demand growth scenarios

	2.3%_Non-RES		**2.3%_RES**	
	Base case	**CO2 sensitivity**	**Base case**	**CO2 sensitivity**
Annualised distribution investment (MEUR/yr)	-	-	160	160
Annualised transmission investment (MEUR/yr)	130	125	162	152
Annual generation and storage operation costs (MEUR/yr)	14,546	11,139	3,028	2,190
Transmission investment decrease (MEUR/yr)	5		6	
Operating cost decrease (MEUR/yr)	3,407		837	

7.2 Paper 2

- We assess the impact of transmission grid characteristics on RES integration costs.
- Two sensitivities evaluate the impact of RES localisation on transmission costs.
- High distances between generation sites and demand increase investments.
- High geographical concentration can more than double transmission investment.
- Integrating distributed generation allows to decrease transmission reinforcement.

Assessing the impact of renewable energy penetration and geographical allocation on transmission expansion cost: a comparative analysis of two large-scale systems

Leslie Herding[a,*], Rafael Cossent[a], Michel Rivier[a], Santiago Bañales[b]

[a] Institute for Research in Technology (IIT), ICAI School of Engineering, Universidad Pontificia Comillas, C/Santa Cruz de Marcenado 26, 28015 Madrid, Spain

[b] Iberdrola Innovation Middle East, Qatar Science & Technology Park, Doha, Qatar

[*] Corresponding author: lherding@comillas.edu

Abstract

Ambitious renewable energy development plans require an efficient electricity grid connection of massive generation capacity. Significant transmission network investments are considered necessary to support the energy transition. This paper analyses the transmission grid reinforcement requirements of two large-scale electricity systems with notably different geographical distributions of renewable resource availability and load density. The results indicate that optimal transmission expansion accounts for less than 10% of total annualised system investment (generation capacity + transmission grid). This is true even in transmission systems with significant existing bottlenecks. The study includes a sensitivity analysis of the location of renewable energy source (RES) capacity. The sensitivities examine the impact of varying the concentration of RES in resource-rich areas, as well as the proportion of RES capacity connected at the distribution level. Both sensitivities are evaluated over a common base case scenario. The results show that a higher concentration of RES capacity in resource-rich network zones can more than double the optimal transmission expansion requirements. In contrast, the implementation of distributed generation (DG) leads to the allocation of generation closer to demand centres, resulting in transmission grid savings of up to 30%. These effects are more pronounced in networks where RES capacity is located further away from major demand centres. This is because existing bottlenecks are exacerbated by higher RES concentration and relieved as the share of DG increases.

Keywords

Energy transition; power system decarbonisation; distributed generation; transmission expansion planning; power system planning

1 Introduction

To achieve the decarbonisation of the electricity sector, a significant amount of renewable energy sources (RES) generation capacity is required to replace the phased-out fossil base load capacities. This process involves electrifying other energy sectors (e.g. transport), which will further increase the electricity demand to be covered by RES. As a result, governments have ambitious plans to accelerate the installation of new RES capacity. In the case of Spain, the National Energy and Climate Plan (NECP) aims to add around 6 GW/yr of photovoltaic (PV) and wind capacity by 2030 [1]. This rapidly increasing generation capacity needs to be accommodated in the electricity grid to efficiently connect the most suitable generation sites with growing demand centres. The transmission grid is expected to play a significant role in connecting demand centres to future renewable energy generation sites, often located in remote areas [2].

This raises the question of whether the costs and time required to expand the electricity grid may hinder the necessary energy transition. Previous work, based on the analysis of a large-scale system representative of Spain, has shown that transmission investment costs per se should not be a major barrier to the energy transition, as they represent a small share of total investment needs once generation and storage costs are accounted for [3]. However, further analyses can shed light on to what extent this conclusion can be generalised to transmission systems with different characteristics or locations of new RES capacity. This work analyses transmission expansion requirements for integrating high RES shares into two electricity networks with notably different renewable availability and load density. The study mentioned above for the Spanish system [3] is complemented with a case study in the geographical zone of Texas to evaluate the generalisability of the findings. The synthetic transmission network in Texas exhibits significantly different demand density and geographical distribution of RES potential compared to the synthetic Spanish network.

In addition to inherent system characteristics, different RES allocation factors will impact the investment needs of the transmission grid. A criterion that has been found to influence transmission grid reinforcement requirements in the literature is the development of distributed generation (DG), i.e. generation directly connected at the distribution level or behind the end-user meter. The installation of DG is gaining popularity in the current context of high electricity prices [4]. The authors of [5] state that DG can help to reduce transmission congestion by reducing local demand. [6] states that connecting RES in the form of DG represents a more economical solution than connecting utility-size RES in areas far away from the existing grid and demand.

A 100% renewable European energy system is analysed in [7]. The study includes the modelling of prosumers to evaluate the impact of increased interconnections on a future renewable Europe. The results show that prosumer installations have the potential to reduce the consumption from the grid by 17% and peak load served by the grid by 6%, reducing the use of the transmission grid. According to [8], placing RES closer to demand instead of at optimal generation sites with the highest capacity factors helps to alleviate transmission congestion. This was observed in a German case study on a 41-node transmission system. [9] proposes a model for the co-planning of DG allocation and transmission expansion. The study demonstrates that the rollout of DG is a tool to lower transmission investment and total planning costs compared to a system without DG. This is shown through a case study based on the IEEE 24-bus test system. The authors of [10] analyse the impact of DG on transmission grids using an 11-node Queensland network. The study compares 20% and 40% DG penetration of wind and solar PV scenarios to a base case without DG. It finds that distributed PV can significantly defer transmission investment, while the DG wind scenarios point out the influence of the DG's location in the grid on transmission requirements. [11] analyses the integration of RES into the Chinese electricity system with a transmission network representing one node per Chinese province. Large distances between optimal RES generation sites and demand centres characterise the case study. The authors analyse various scenarios, from RES located at demand centres to RES located according to optimal resource availability, and find lower transmission costs in scenarios where RES are placed closer to demand. However, according to [12], high DG penetrations can reverse this effect by causing congestions through reverse power flows at high penetration levels, which in turn trigger transmission reinforcement requirements..

A second criterion affecting transmission costs for integrating high RES shares is the spatial allocation of utility-scale installations among the grid. Concentrating utility-scale RES in areas with the highest resource availability represents the contrary extreme to the rollout of high DG shares. The study in [11] includes scenarios where RES are placed based on resource availability. The study finds that placing RES away from demand increases grid costs compared to placing them closer to demand. [13] confirms that considering transmission expansion costs shifts the optimal spatial distribution of PV and wind capacity to be more decentralised than when only natural resource availability is considered. This is based on a case study of the 16 German federal states.

Based on the abovementioned literature, the main contributions of this paper can be summarised as follows:

1) **Modelling the impact of RES integration into large-scale transmission systems:**

   The transmission systems simulated in the literature presented before rarely exceed the size of a few tens of buses. This is in contrast to national transmission systems, which typically consist of hundreds or thousands of buses [14], [15], [16], [17]. Both synthetic transmission grids employed in the case studies presented in this paper represent large-scale networks of 480 (Spain) and 2000 (Texas) nodes, respectively. The use of large-scale networks enables a more detailed geographical location of future renewable energy generation plants. As for new transmission lines, the increased granularity allows for a more robust evaluation of transmission expansion requirements related to different scenarios of RES placements.

2) **Systematic comparison of various RES dispersion factors via sensitivity analysis with a common base case scenario:**

   The literature review shows that RES-driven transmission investment requirements can be generally mitigated when new RES capacity is either connected at transmission level closer to demand-rich areas and/or connected in the form of DG, i.e. injecting electricity in the same voltage levels where it is consumed. However, these studies typically analyse only one system and one factor affecting the dispersion of RES, such as concentration or share of DG. They do not systematically compare the impact of different system characteristics or RES dispersion factors using the same methodology.

   After evaluating the impact of the geographical distance of zones with high RES potential and demand centres on transmission expansion requirements for integrating high RES shares, two additional sensitivities are analysed in this paper to address this issue. The Spanish and Texan synthetic large-scale transmission networks are evaluated for both sensitivities. The objective of this study is to improve the analysis of transmission grid reinforcement requirements under different hypotheses of the connection of future RES capacities: i) the concentration of RES capacities in resource-rich zones of the network, and ii) the increasing share of additional RES capacity connected as distributed generation (DG). A multi-criteria approach was developed for the placement of DG installations. The sensitivity ranges were selected to compare two extremes of the location of future RES capacity throughout the transmission grid: according to the highest resource availability or at the same locations and voltage levels of electricity demand in the form of DG. The analysis improves upon the literature findings by providing a comparative analysis of sensitivities using a consistent methodology. This is achieved by applying the same modelling methodology, with a common base case scenario, to two large-scale synthetic electricity networks.

The paper is structured as follows: section 2 summarises the modelling methodology, and section 3 presents the Spanish and Texan test cases. The results from the base case studies and the sensitivities are presented in section 3.3.1. Section 5 concludes the study.

2 Methodology

The impact of high RES shares on transmission grid expansion requirements is analysed with different scenarios of generation capacity and electricity demand for 2030. First, the optimal generation and storage (G&S) capacities for each scenario are determined with a single node generation expansion model (GEP). The scenarios and the GEP model are described in section 2.1. In a second step, the impact of these G&S capacities on electricity transmission grid reinforcement is analysed with a detailed transmission expansion planning (TEP) model, presented in section 2.2. GEP is modelled separately from TEP, and the GEP model is linked to the TEP model via the geographical distribution of G&S capacities. Recent investigation shows the benefits of joint generation and transmission expansion planning [18]. However, generation and network investment decisions are made independently in the current regulatory framework in many deregulated electricity systems. Moreover, current regulation concerning grid investments and network access presents some asymmetries between transmission and distribution, which drive actual investment decisions by RES promoters away from the global optimum.

Figure 1 summarises the modelling methodology of GEP and TEP. This case study employs two validated optimisation models in cascade for generation[1] and transmission[2] expansion modelling. Although there is no joint optimisation, RES capacity is allocated with realistic

[1] https://www.iit.comillas.edu/oferta-tecnologica/sploder
[2] https://www.iit.comillas.edu/oferta-tecnologica/tepes

generation site selection criteria throughout the transmission network. The allocation criteria are presented in section 2.2. Additional sensitivities are evaluated by repeating the geographical allocation of RES capacity ((4), Figure 1) in the transmission grid under different hypotheses. Details about the sensitivities will be described in 2.3.

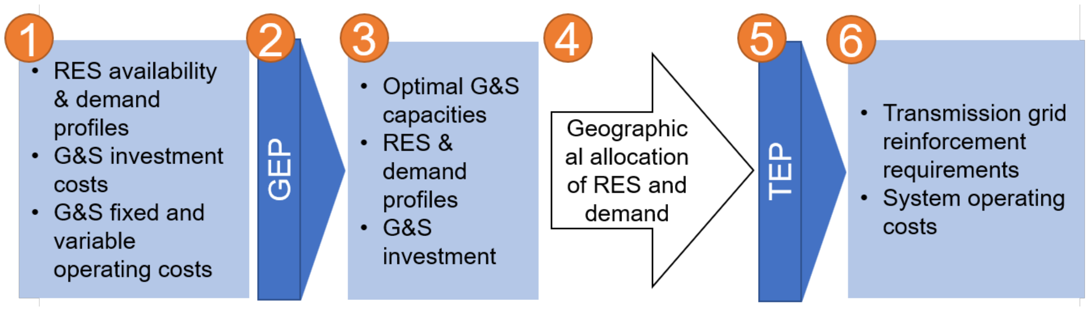

Figure 1: Overview of modelling methodology

2.1 Generation and storage capacity expansion

Future generation and storage (G&S) capacity scenarios are designed to analyse the incremental impact of renewable energies on transmission grid expansion requirements. GEP (step (2), Figure 1) is carried out with the *Smart Planning and Operation of Distributed Energy Resources (SPLODER)*[3] model from the Institute for Research in Technology [19], [20]. The model is suitable for great-scale generation expansion planning, including utility-scale size generation installations.

G&S capacity expansion is based on the input included in step (1) of the modelling flowchart (Figure 1):

- Hourly profiles of demand that needs to be covered and availability of RES resources
- Economic input per generation technology: G&S capacity investment costs and fixed and variable operating costs (O&M, fuel, emissions)

Following the same approach as in [3], four generation capacity expansion scenarios are considered for each power system evaluated. These four scenarios are obtained by combining two load growth rates, i.e. 0% and 2.3% per year, and two generation technology options: a fully non-renewable pathway (i.e. no new PV or wind capacity is permitted) and a cost-minimising technology mix. This allows evaluating the impact of economically optimal high-RES shares on electricity grid costs compared to a pathway with traditional thermal generation

[3] https://www.iit.comillas.edu/technology-offer/sploder

capacities. The resulting scenarios are named according to the corresponding annual demand growth rate and the technology pathway (0%_Non-RES, 0%_RES, 2.3%_Non-RES, 2.3%_RES). In the scenarios without demand growth (0%_Non-RES and 0%_RES), the impact of the technological change of the generation capacity mix towards renewables is analysed. The scenarios with demand growth (2.3%_Non-RES and 2.3%_RES) have been chosen for this case study to increase the generation capacity that needs to be integrated into electricity grids. Furthermore, it is a scenario selected to represent the expected demand growth due to the electrification of demand via heat pumps and electric vehicles.

2.2 Transmission grid modelling

The GEP model is a single-node electricity sector model. Hence, future generation and storage capacity needs to be geographically allocated to serve as an input to the TEP model ((4), Figure 1). Utility-sized renewable generation facilities are assigned to the generation nodes according to weighted scaling factors compounded by:

i. Pre-existing capacities [21], [22],
ii. Availability of natural resources (irradiation, wind) [23],
iii. Suitability of the different network zones for future RES deployment [24].

A more detailed description of the geographical allocation of RES generation capacity is provided in the case study presentation due to some case-specific variations. Pumped hydro storage installations are allocated according to the geographical characteristics of the terrain, i.e. height differences and availability of water reservoirs. Battery storage capacity is allocated proportionally to PV and wind capacity to account for the possibility of peak shaving with storage plants. Non-RES generation is allocated in relation to already existing thermal electricity generation plants. This assumption is based on the hypothesis of the suitability of existing generation sites and pre-existing fuel acquisition infrastructure.

Electricity transmission grid modelling ((5), Figure 1) is carried out with the *Long-Term Transmission Expansion Planning Model for an Electric System (TEPES)*[4] model from the Institute for Research in Technology. The TEPES model optimises the transmission grid expansion, minimising total system costs compounded by investment and operating costs.

[4] https://www.iit.comillas.edu/technology-offer/tepes

To maintain the computational burden of TEP of large-scale electricity networks as manageable as possible, the time resolution of the transmission expansion problem is expressed by 144 representative load levels, derived as in [3]. Additionally, the expansion candidate lines are pre-selected according to congestions and nodal price differences in the electricity system without expansion. For this step, future generation and demand are allocated at the corresponding transmission nodes, and a first iteration without expansion is run. TEP is then carried out in an additional iteration step. In the expansion iteration, the TEPES model is allowed to opt into continuous investment decisions. Continuous investment decisions are opposed to binary decisions where the model can only either build (1) or not (0) the candidate line. In the continuous decision framework, investment decisions can be of any magnitude between 0 and 1, indicating a tendency for reinforcement requirements rather than the final detailed transmission expansion plan. This is deemed suitable for the scope of this study as the objective is to evaluate the order of magnitude of reinforcement requirements rather than carrying out a detailed TEP. The continuous investment decisions enable the evaluation of the order of magnitude of transmission network investments required to integrate high RES shares while permitting the computation of large-scale electricity networks at reasonable time thresholds. Additionally, TEP is carried out via lossless power-flow calculations to maintain the computational complexity of the large-scale system at a reasonable limit.

2.3 Sensitivity analysis

Different sensitivity analyses are evaluated for further conclusions on the similarities and differences of the reinforcement requirements of the selected large-scale synthetic transmission networks. In this paper, *scenarios* describe the expansion of G&S capacities for the future power system (demand growth coefficients, technology restrictions for additional capacity), and *sensitivities* refer to variations in the allocation of these capacities within the grid. Hence, different *scenario* assumptions act at step (1) of the modelling process (Figure 1), while *sensitivity* assumptions act at step (4).

The sensitivities analyse i) the impact of the concentration of new RES capacities in the zones with the highest potential and ii) the impact of distributed generation on transmission grid expansion requirements. Consequently, the sensitivities are limited to the renewable scenarios without (0%_RES) and with demand growth (2.3%_RES), as the Non-RES scenarios remain unchanged. The sensitivities aim to evaluate the impact of different geographical dispersions of RES on transmission grid reinforcement requirements. The total PV capacity (rooftop +

utility-scale) is the same for all sensitivities. The sensitivities are evaluated based on their impact on the transmission grid costs compared to the common base case scenario.

Table 1 provides an overview of the different sensitivities and the change performed in step (4) of the modelling process. The six sensitivities, namely RES_Con and five different DG shares, are evaluated for each case study and each demand growth scenario and are compared to the TEP results of the corresponding base case. The base case represents the results from the initial modelling process as described in 2.1 and 2.2. The sensitivity assumptions are described in more detail in 2.3.1 and 2.3.2.

Table 1: Overview of sensitivities applied to the RES scenarios

Parameter	Sensitivities
RES concentration	1. Base case (BC): around 25% of transmission nodes with RES 2. RES concentration (RES_Con): up to 10% of transmission nodes with RES
DG share	1. Base case (BC): 0% distributed generation 2. Five sensitivities with increasing shares of DG (20%, 40%, 60%, 80%, 100%)

2.3.1 Concentrated RES allocation

The sensitivity on RES concentration is assessed by placing a higher share of the additional capacity in those grid areas with higher availability of natural resources. This leads to the concentration of significant RES capacities in limited geographical zones. Thus, the total additional capacity of PV and wind is located in the zones with the highest irradiation and wind, respectively.

2.3.2 Increasing the share of distributed generation

Although part of the high voltage (HV) grid is considered part of the distribution network in some countries, this work focuses on the rollout of smaller installations located close to demand. HV is not considered in this analysis because, although it is technically part of the distribution grid in countries such as Spain, it is, in fact, usually referred to as sub-transmission. Consequently, the assumption of HV-connecting generation capacity representing smaller DG units close to demand does not hold. Hence, the definition of DG is limited to low voltage (LV)- and medium voltage (MV)- connecting installations. Furthermore, wind capacity is not assigned as DG due to a lack of applications for domestic wind installations. Hence, the deployment of different levels of distributed generation (DG) is evaluated by allocating increasing amounts of PV capacity closer to demand centres. High shares of DG are expected to decrease transmission grid reinforcement requirements for two reasons:

1. The total amount of RES capacity remains unchanged when DG participation increases. This results in the new capacity being increasingly located in distribution grids, closer to the demand. As the participation of utility-sized RES decreases, the need for power lines to transport electricity from remote areas to the cities decreases accordingly.
2. As generation capacity connected to distribution grids increases, the transmission grid's net electricity demand (gross demand minus DG production) decreases. This effect might reduce transmission expansion requirements, especially in scenarios with demand growth.

Overall, five different sensitivities to DG are analysed. Sensitivities start at 20% DG and increase in intervals of 20% up to 100% DG. These shares are applied to the additional PV capacity installed in each RES scenario (0%_RES, 2.3%_RES) resulting from the generation expansion planning (section 2.1). This analysis does not consider distributed wind as expected magnitudes of DG wind capacities are small. DG availability is included in TEP as a reduction of demand allocated in step (4) of Figure 1.

Several assumptions are required for evaluating increasing DG shares. The geographical allocation of DG varies from utility-scale RES installations. DG installations are located at demand nodes, while utility-scale RES is located at generation nodes (i.e. with no demand). The geographical allocation criteria are different for LV- and MV-connecting installations. Hence, in the first step, the composition of DG needs to be determined. This allows to classify DG capacity according to the voltage level of connection (i.e. LV and MV). The composition of DG according to voltage level is determined via historical information on grid connections in the corresponding network area.

MV installations are allocated according to the same criteria as utility-scale RES (section 2.2): resource availability, already installed capacity and suitability factors. However, unlike utility-sized installations, MV DG is located at demand nodes instead of generation nodes. The allocation criteria are based on the hypothesis that MV installations are of greater scale and expected to be installed by promoters seeking a maximisation of profits. LV-connecting DG is considered to represent rooftop PV prosumer installations. These installations are allocated according to different criteria, as private households seeking to become prosumers do not optimise their location for maximising potential benefits but connect DG to lower their electricity bill. The new allocation criteria modify step (4) of the modelling process of the base case (Figure 1). LV prosumer installations are allocated among the territory according to the following criteria with equal weight:

1. Household income: Currently, rooftop PV installations require private investment. The potential of people willing to undertake such an investment is considered more likely in areas with higher household incomes. Each transmission network node is assigned to an income area to consider the geographical distribution of average household incomes.
2. Building density: The household income criterion might lead to a similar evaluation of an urban and a rural geographical zone. However, in reality, urban zones offer fewer rooftop areas available for the installation of PV as people tend to live in flats rather than in separate houses. Hence, the building density of an area is considered an additional factor to express that, independent of household income, rooftop PV can be installed in a greater scale in non-urban areas.

2.4 Normalised ratios

Due to the different sizes of the synthetic networks, transmission grid reinforcement results are compared via normalised ratios. Table 2 presents an overview of the normalised ratios employed in the analysis, their purpose, and their units. The ratios are described in more detail in the following.

Table 2: Overview of normalised ratios for evaluating grid costs for integrating high RES shares

Normalised ratio	**Purpose**	**Unit**
Unit transmission network investment (TN_invest_{unit})	Evaluation of annualised transmission grid investment per unit of additional generation capacity integrated into the grid for each scenario.	EUR/kWyr
Relative cost reduction (RCR)	Operating cost reduction per additional investment in G&S capacity and the transmission grid. This ratio is incremental from the Non-RES to the corresponding RES scenario.	MEUR /MEUR

Grid integration cost (GIC)	Increase of transmission grid investment per additional unit of energy injected into the grid. This ratio is incremental from the Non-RES to the corresponding RES scenario.	EUR/MWh
Unit transmission savings	Decrease of transmission grid investment per DG capacity integrated into the net-work. This ratio is an incremental ratio from the base case (BC) with 0% DG to the corresponding DG scenario.	EUR/kWyr

Annualised unit transmission network (TN) investment (invest) costs express the transmission investment per additional generation capacity (P_add) of all technologies (Tech) as in Eq. 1. The normalised ratio is based on the metric of incremental unit grid investment cost commonly seen in distribution grid expansion studies [25], [26].

$$TN\_invest_{unit} = \frac{TN\_invest}{\sum_{Tech} P\_add_{Tech}} \left[\frac{EUR}{kWyr}\right] \quad \text{Eq. 1}$$

The relative cost reduction (RCR) via the use of RES is put into context with the incremental annual investment costs for both G&S capacity and electricity grids in RES scenarios. The parameter is based on the system operating cost savings presented in [3] and calculated according to Eq. 2 for each demand growth pathway.

$$RCR = -\frac{OPEX_{RES} - OPEX_{Non-RES}}{CAPEX\ (G\&S + grid)_{RES} - CAPEX\ (G\&S + grid)_{Non-RES}} \left[\frac{MEUR}{MEUR}\right] \quad \text{Eq. 2}$$

The grid integration cost (GIC) of RES generation is based on the network development costs presented by [27]. In this paper, the analysis is carried out in incremental terms between Non-RES and RES scenarios as in Eq. 3. For this ratio, the incremental annualised transmission network (TN) investment (invest) is divided by the additional PV and wind energy injection into electricity grids (E_inj).

$$GIC = \frac{TN\_invest_{RES} - TN\_invest_{Non-RES}}{E\_inj(PV + Wind)_{RES} - E\_inj(PV + Wind)_{Non-RES}} \left[\frac{EUR}{MWh}\right] \quad \text{Eq. 3}$$

For an evaluation of transmission grid cost savings via integrating distributed generation, distributed PV capacity and transmission cost savings with respect to the base case (BC) are analysed according to Eq. 4. Based on the transmission grid cost savings with respect to 0%

DG (BC), so-called unit transmission grid savings are determined. The evaluation is based on unit transmission savings (UTS) and considers the annualised transmission network (TN) investments (invest) and the DG capacity installed (install) in each sensitivity Si with respect to sensitivity S1.

$$UTS_{DG\_i} = -\frac{TN\_invest_{DG\_i} - TN\_invest_{BC}}{DG\_install_{DG\_Si} - DG\_install_{BC}} \quad \left[\frac{EUR}{kWyr}\right] \qquad \text{Eq. 4}$$

3 Case study input

The methodology for assessing transmission grid reinforcement requirements at high RES shares has been applied to a Spanish-like electricity grid before [3]. In this work, a second large-scale electricity network is studied to evaluate the replicability of the methodology and analyse the factors that influence the magnitude of required transmission grid reinforcement costs in different electricity networks. The European electricity network is contrasted with a synthetic transmission network in the US: the ERCOT zone in Texas. The ERCOT zone represents an interesting test case for evaluating the impact of high RES shares on transmission grid costs as renewable potential (irradiation, wind speed) is located far off the demand centres. This configuration requires a robust transmission grid to ensure the connection of future renewable generation sites in the Northwest of the network zone with the big cities located in the coastal area. This section introduces the generation capacity mix (3.1) that is input for the two great-scale transmission grids (3.2). Input for the sensitivities is provided in 3.3.

3.1 Generation capacity mix

The optimal GEP is determined for each of the four scenarios described in section 2.1 (0%_Non-RES, 0%_RES, 2.3%_Non-RES, 2.3%_RES). All scenarios represent a time horizon of 2030. Total G&S capacities resulting from GEP (step (3) of Figure 1) are summarised in Table 3 for each scenario. Additionally, the incremental capacity with respect to the initial capacity mix is included. Available technologies for GEP are detailed in the Appendix. In the Non-RES scenarios, no new solar or wind capacity can be installed. The initial Spanish capacities are derived from [3], representing the 2019 installed capacities with the closure of coal and the reduction of nuclear capacity as foreseen by the government. The initial capacity mix of the Texan system is considered as in [22] with the closure of existing coal capacities to account for the decarbonisation of the electricity sector. Technology cost input is summarised in the

Appendix. Gas prices are considered according to 2030 scenarios prior to the gas crisis. CO_2 is priced at 84.84 EUR/ton [28].

In the non-renewable scenarios without demand growth, no additional generation capacity is required to serve the existing demand in both systems. That means that the current available generation capacity is sufficient to back up the closure of coal power plants without endangering the electricity system's reliability.

Table 3: Total G&S capacity per scenario *(and increase wrt the initial scenario)* (GW)

	Initial	**0% demand growth**		**2.3% demand growth**	
	-	**Non-RES**	**RES**	**Non-RES**	**RES**
Spain (GW)	101	101 *(+0)*	139 *(+38)*	120 *(+19)*	202 *(+101)*
Texas (GW)	86	86 *(+0)*	189 *(+103)*	110 *(+24)*	265 *(+179)*

Figure 2 shows the technological composition of the capacity mixes. RES generation technologies show quite a high initial participation in the Spanish capacity mix. This is not the case for the capacity mix connected to the ERCOT grid. In Spain, storage consists of pumped hydropower plants, while four-hour batteries are employed as storage in Texas. Battery storage is not installed in Spain by the GEP model due to their high investment costs. The pumped storage considered for the Spanish system represents a more efficient option.

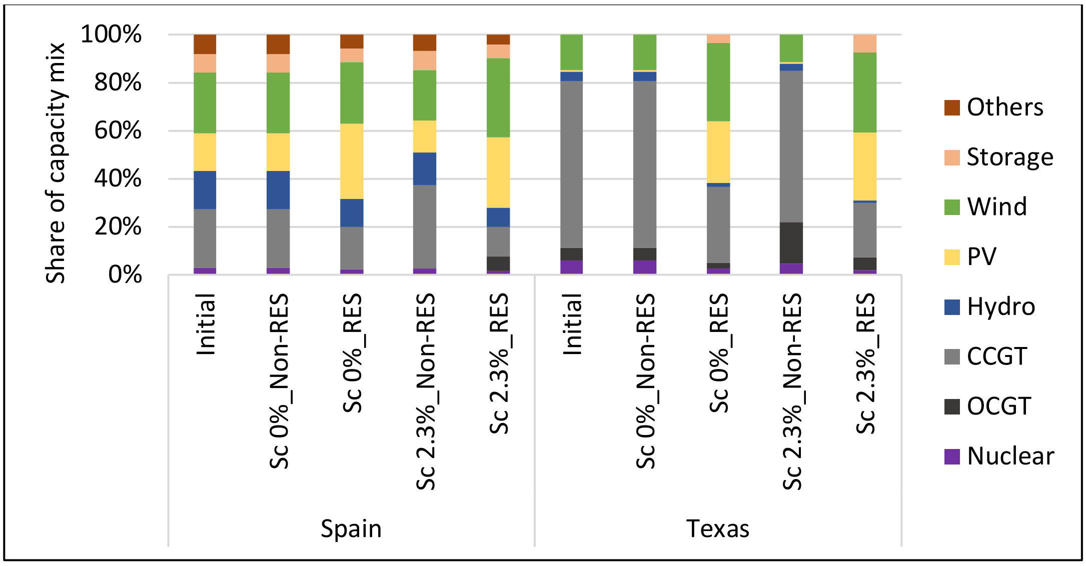

Figure 2: Pre-existing generation and storage capacities

The 0%_RES scenario points out the economic efficiency of renewable generation technologies. The installed capacities result from the optimisation of electricity generation capacities without technological restrictions. This means that the GEP model considers it economically optimal to install 38 GW RES in Spain and over 100 GW in Texas to switch from existing thermal generation to new renewable generation, even though existing generation capacity can serve demand without additional investments (as seen in the 0%_Non-RES scenarios without additional generation capacity). The reduction of operating costs of the existing generation mix compensates for the investment in significant amounts of renewable generation technologies, even though no demand growth needs to be met.

3.2 Transmission expansion

3.2.1 Initial transmission network

The impact of high RES shares on transmission grid requirements is analysed with synthetic networks of the two geographical zones under consideration:

- Europe: An approximation of the peninsular Spanish transmission network is used as a starting point for this part of the analysis. The synthetic grid is based on the transmission system used in [3]. The synthetic network comprises 479 nodes and 880 lines and transmission transformers, summing up to 36,273 km of electrical lines.
- United States: The ERCOT zone of the Texan transmission network is modelled with the synthetic network data published in [22]. The synthetic network comprises 2,000 nodes and 3,206 lines and transmission transformers, summing up to 48,580 km of grid lines. Although ERCOT does not cover the entirety of Texas, the terms ERCOT and Texas are used interchangeably in this analysis.

The synthetic power grid of the ERCOT zone is chosen due to its different geographical characteristics in comparison to the synthetic Spanish network. While renewable energy and electricity demand are distributed throughout the whole national territory in Spain, Texas represents a case where the areas with the highest RES potential (North and West) are far away from the demand centres on the coast. Figure 3 and Figure 4 provide an overview of both electricity grids. Figure 4 also shows the lack of corridors from the Northwest of the network to the demand centres further in the East. In the further course of this paper, the lack of connection from the resource-rich zones to the demand centres in Texas is referred to as *West-East interconnection*.

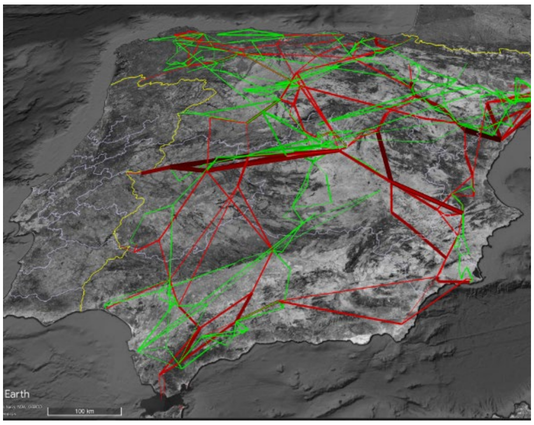

Figure 3: Synthetic Spanish transmission grid (green: 220 kV, red: 400 kV)

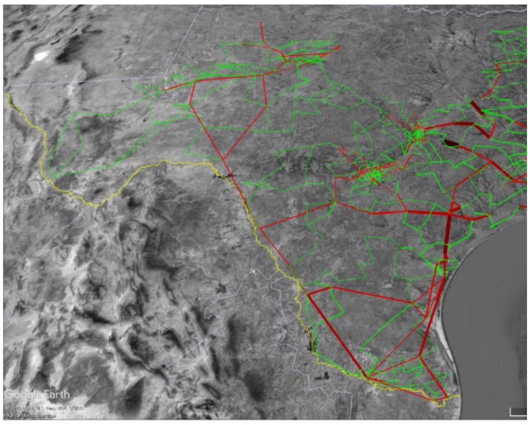

Figure 4: Synthetic Texan transmission grid (green: 115 & 161 kV, red: 230 & 500 kV)

For a more detailed understanding of the synthetic ERCOT network, demand, resource availability, and the capacity of the existing network are presented. The analysis is based on the eight weather zones introduced by ERCOT and shown in Figure 5.

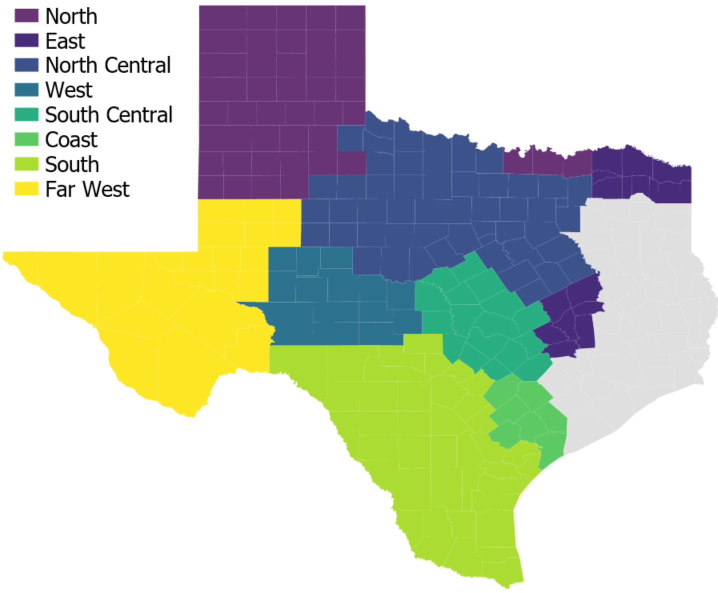

Figure 5: ERCOT weather zones, based on [24], [29]

Table 4 provides an overview of the relative distribution of electricity demand, transmission grid capacity (measured in GW-km of the initial grid before expansion), and RES availability by resource (PV and wind). The latter is computed as the share of the total RES electricity available per zone in the base case of the 0%_RES scenario, which is taken as a reference due to the lack of RES in the initial network. This available electricity is determined as the RES installed capacity, resulting from the GEP model, allocated to each weather zone (following the methodology in section 2.2) times the corresponding capacity factors.

The relative distribution of demand and grid capacity is aligned throughout the zones. 87% of electricity demand and 75% of the existing network capacity is located in the grid zones around the metropolitan areas (North Central, South Central, South and Coast). While 45% of available PV energy is located in these zones, the share drops to 30% for wind energy. Following the allocation criteria, 70% of available wind energy is located in the zones North, Far West and West. This allocation points out the importance of the interconnection of the western RES-dominated zones of the network with the demand-dominated eastern zones.

Table 4: Mapping of the geographical distribution of the synthetic ERCOT network

	Coast	**East**	**Far West**	**North**	**North Central**	**South**	**South Central**	**West**
Demand	28%	5%	3%	2%	32%	10%	17%	3%
Grid capacity	23%	9%	3%	8%	29%	6%	17%	6%
RES availability (based on 0%_RES)								
PV	8%	13%	14%	14%	15%	9%	13%	14%
Wind	8%	0%	24%	25%	7%	15%	0%	20%

Interconnections with neighbouring grids can lead to additional reinforcement requirements in well interconnected transmission systems, as power exchanges of neighbouring countries can increase the power flows throughout the national transmission system [30]. However, this is not the case for the synthetic networks under considerations. According to the Spanish transmission system operator, the degree of the Iberian peninsula's electric interconnection with the rest of Europe via France is still low [31]. The lack of interconnection recently allowed the Spanish and Portuguese governments to intervene temporarily in the electricity market, denominated as the Iberian exception. The European Commission authorised the intervention due to the low degree of interconnection of the Iberian peninsula [32]. Portugal is excluded from the analysis as the case study aims to evaluate national (local in the case of Texas) transmission expansion requirements for increasing RES penetration of the network. This simplification is justified by the size disparity between Portugal and Spain. In consequence, the influence of cross-border flows is not considered to lead to a significant cost difference in the Spanish network's reinforcement requirements. The degree of interconnection of the ERCOT network is very limited [33]. Given these particularities of the electricity systems of Spain and the ERCOT zone, the transmission modelling focuses on the detailed modelling of each synthetic network rather than on a depiction of interconnections. Consequently, both networks are modelled without interconnections to neighbouring power grids.

This approach allows focusing on the differences of the networks, i.e. geographical distribution of RES potential and load density.

3.2.2 Geographical allocation of RES generation units

As mentioned in 2.2, generation capacity must be allocated geographically when moving from single-node GEP to TEP. In the case of utility-scale PV and wind, this allocation is performed differently for Spain and Texas. In the case of Texas, the nodal suitability for utility-scale RES is based on the weather zone in which the node is located (Figure 5). The system operator, ERCOT, publishes estimations of the suitability of weather zones for RES in the network development plan [24]. In the development, ERCOT evaluates the weather zones according to resource availability. Additionally, urban density is considered for wind evaluation, expressing that future wind generation sites will not coincide with densely populated urban areas.

For the synthetic Spanish transmission network, RES generation units are allocated according to resource availability (i.e., wind speed and irradiation) [23] and already installed capacities as published by the system operator [21]. Both indicators are considered to have equal weight. Pre-existing capacities are included as an allocation factor due to the nature of the synthetic network. The initial network characteristics do not represent the actual system characteristics. Due to this, the allocation criteria are applied to the total amount of RES capacity and not just the additional capacity in each scenario. Hence, the pre-installed capacity criterion ensures that a part of the existing RES capacity is allocated according to the real geographical allocation of generators.

3.3 Sensitivity analysis

3.3.1 Concentrated RES allocation

For evaluating the impact of RES concentration on transmission reinforcement requirements, the location of new RES capacities (step (4). Figure 1) is modified to the most resource-rich zones of the network.

In the Spanish electricity system, additional PV and wind installations are concentrated in the provinces with the highest potential of natural resources:

- Wind: Cádiz, Lugo, Navarra and Tarragona, resulting in a concentration of the total capacity in only five transmission network nodes located mainly in the north of the country and one zone in the southern zone close to the Portuguese border [34]. This represents a much higher concentration than the base case, where additional wind capacity is distributed among 35 nodes.

- PV: Almería, Badajoz, Granada and Huelva, resulting in a concentration of the total capacity to seven transmission nodes located in the south of the country [35]. This represents a much higher concentration than the base case, where additional PV capacity is distributed among 110 nodes.

For the ERCOT zone, new renewable generation installations are allocated according to the highest potentials assigned in the 2020 Long-Term System Assessment of the system operator ERCOT [24]. The highest potentials are found in the Northern and Western zones of the network. Additional PV capacity is concentrated to 189 nodes (compared to 485 nodes in the base case), and wind capacity is concentrated to 73 nodes (373 in the base case).

Table 5 provides an overview of each system's capacity concentration per node (MW/node) and demand growth scenario, comparing the base case (BC) to the RES concentration (RES_Con) sensitivity. Capacity per node is multiplied by 16 (PV) and 7 (wind) in the Spanish system and by 3 (PV) and 5 (wind) in the Texan system.

Table 5: Capacity per node in the base case and the RES concentration sensitivity

	Spain		**Texas**	
	0%_RES	**2.3%_RES**	**0%_RES**	**2.3%_RES**
PV				
Base case (MW/node)	252	395	97	152
RES concentration (MW/node)	3959	6205	250	389
Concentration ratio (RES_Con/BC)	16	16	3	3
Wind				
Base case (MW/node)	283	1172	131	204
RES concentration (MW/node)	1979	8206	671	1040
Concentration ratio (RES_Con/BC)	7	7	5	5

3.3.2 Determination of DG composition

The share of PV capacity expected to connect at the different voltage levels of the Spanish electricity network is derived from historical data published by the Spanish regulator, Comisión Nacional de los Mercados y la Competencia (CNMC) [36]. 39% of distributed PV capacity is connected at LV, while 61% is connected to MV. Furthermore, the data underlines that DG wind in Spain is negligible at LV and MV levels. Future connections of new RES capacity are considered to connect in line with the historical statistics of voltage levels of RES connections.

For the ERCOT grid, the share of RES connected to distribution grids is determined according to the U.S. Energy Information Administration's (eia) 2019 annual electric power industry report and generator-specific information [37], [38]. According to the datasets, 48% of distributed PV installations connect to LV grids and the remaining 52% to MV grids. As in Spain, the share of wind that can be considered DG in Texas is negligible.

3.3.3 Geographical allocation of LV- and MV-connected distributed generation units

In Spain, household income [39] and building density [40] are derived from the Spanish statistics institute INE. In Texas, average household income is considered according to the U.S. Census Bureau's Small Area Income and Poverty Estimates [41]. The suitability of the different grid zones for the installation of PV is derived from ERCOT planning scenarios [24].

In Spain, the information is provided for each of the 15 peninsular autonomous communities. Average annual household income levels in 2019 ranged from 21,611 to 37,552 Euros. The highest income levels are in the country's centre and along the north coast, namely in Madrid, the Basque Country and Navarre. The U.S. Census Bureau provides information on a higher resolution for Texas. 2019 average household income is available for 254 counties and shows a much broader income range, from US$ 24,732 to US$ 151,806 (22,011 to 135,107 Euros). The highest incomes are around the metropolitan areas of San Antonio, Austin, Houston, and Dallas. Additionally, a few rural areas in the West around Midland County show high income levels.

Figure 6 shows the load duration curves of DG assigned per node in Spain and Texas. The representation is limited to the 2.3%_RES scenarios of both systems for brevity. The resulting assignation of the 0%_RES scenarios is proportional to the displayed curves by the ratio of installed PV capacity in the 0%_RES and the 2.3%_RES scenarios. The maximum DG assigned in Spain is 291 MW per node in the DG_100% sensitivity. In Texas, this value ascends to 100 MW per node. The 100%_DG sensitivity yields an average assignation of 191 MW/node in Spain and 65 MW/node in Texas. The different magnitudes in the Spanish and the Texan systems directly result from the different amount of demand nodes in each grid (228 in Spain and 1125 in Texas).

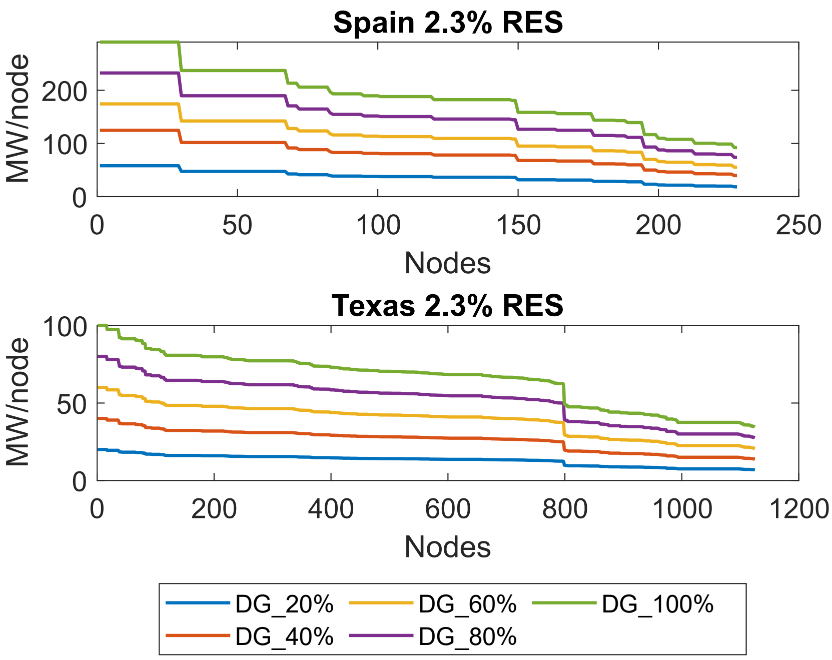

Figure 6: Magnitude of DG assigned per node in Spain and Texas 2.3%_RES

4 Transmission expansion results

In this section, the case studies are presented in detail. Annualised costs are obtained with a rate of return of 7% over the installation's lifetime. The same rate is applied to all G&S and grid investments. The lifetime of electricity grid assets is considered 40 years. Details on the lifetime assumptions of the different generation technologies are provided in the Appendix. Refurbishment of assets is not considered in this case study. The result evaluation is carried out via the annualised costs to facilitate the comparison of assets with different lifetimes. All monetary results are given in 2019 Euros (EUR). After the analysis of the base case (section 4.1), the sensitivities RES concentration (section 4.2) and distributed generation (section 4.3) are presented.

4.1 Base case

In this section, the results of applying the methodology described in section 2 to the synthetic ERCOT network are compared to the results of the synthetic Spanish network presented in [3]. First, the investment cost requirements in G&S capacity and transmission network expansion are compared for the four scenarios of each electricity system. After that, normalised ratios presented in 2.4 of both synthetic networks (Spain and Texas) are compared to each other to derive conclusions on the generalisation of the findings of the Spanish-like case study presented in [3].

The annualised investment requirements for the four scenarios for both electricity systems are contrasted in Table 6. Non-RES scenarios without demand growth require no additional generation capacity (Table 3). The demand growth scenarios show that RES pathways require significantly more investments in G&S capacity than Non-RES pathways to compensate for low full-load hours of renewable technologies.

For Spain, transmission grid requirements are the same in both scenarios without demand growth. Expansion requirements in the 0%_Non-RES scenario are explained by increased requirements of updating the initial synthetic network to the 2019 generation capacity and demand, adjusting to the closure of coal power plants, and reducing operative nuclear power plants according to governmental targets. Adjusting the network to a high-RES system does not result in extra costs. In the scenarios with demand growth, Spanish transmission grid requirements increase by 25% from the Non-RES to the RES scenario.

Transmission grid investment costs show significantly higher increases for the synthetic ERCOT grid. The 0%_Non-RES scenario only requires minor grid updates to adjust the grid to the closure of coal power plants. The transition to high RES shares multiplies the transmission expansion costs by 47. Network adaption requirements of the West-East interconnection (section 3.2) of generation sites with demand centres drive high investment costs. The same is observed in the scenarios with demand growth where transmission expansion requirements are multiplied by eleven from the Non-RES to the RES scenario.

However, the synthetic Texan grid does not lead to significant variations throughout the scenarios when analysing the participation of transmission investment costs over total investment costs. The Spanish renewable scenarios lead to the lowest values, with around 3% of the total annualised investment assigned to the transmission grid. All other scenarios, RES and Non-RES, result in 7.0% to 9.5%. Transmission grid costs account for a greater share of total investment costs in the RES scenarios in the Texan system due to the increased reinforcement requirements of the West-East interconnection required for integrating RES.

Table 6: G&S capacity and transmission grid investment requirements

	0%_Non-RES	0%_RES	2.3%_Non-RES	2.3%_RES
Annualised G&S capacity investment (MEUR/yr)				
Spain	-	1,946	1,331	5,764
Texas	-	5,609	1,180	9,612
Annualised transmission grid investment (MEUR/yr)				
Spain	63	63	130	162
Texas	10	494	88	1009
Grid expansion / total investment costs (G&S + transmission)				
Spain	-	3.1%	8.9%	2.7%
Texas	-	8.1%	7.0%	9.5%

Figure 7 shows the annualised unit transmission grid costs for all scenarios with additional capacity (i.e. no value is provided for the 0%_Non-RES scenarios as no new capacity is installed, Table 3). The ratios are derived via Eq. 1 (section 2.4). The highest unit cost is attributed to the Spanish 2.3%_Non-RES scenario, while the Spanish RES scenarios result in the lowest annualised unit costs of below 1.7 EUR/kWyr. RES integration leads to lower unit transmission costs in a grid where demand and RES generation sites are distributed geographically, as is the case for Spain. Integrating thermal generation capacity in the 2.3%_Non-RES scenario requires the connection of concentrated generation sites with a geographically distributed demand, increasing transmission unit costs.

Annualised unit transmission grid costs for the Texan transmission system range from 3.7 to 5.6 EUR/kWyr and show no significant variation from RES to Non-RES scenarios. RES scenarios require slightly higher unit investment costs in Texas than the Non-RES scenario due to the West-East interconnection investment requirements.

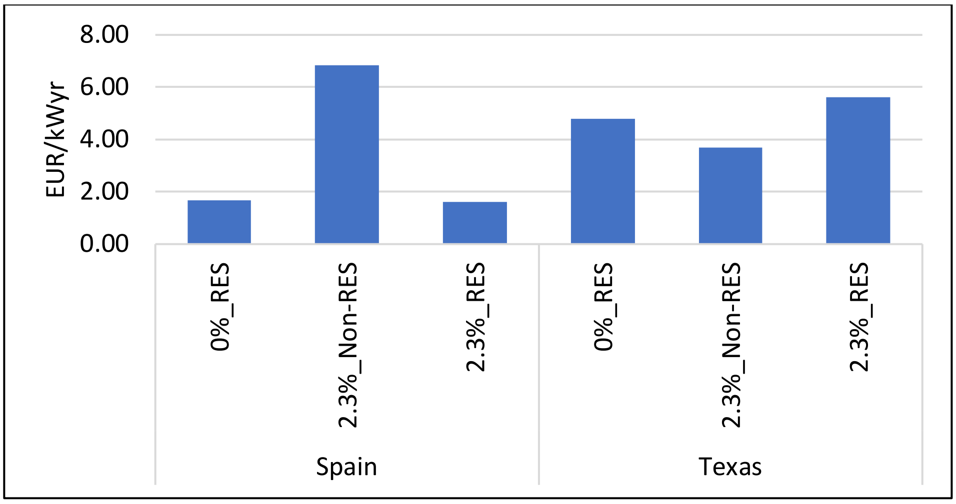

Figure 7: Base case annualised unit transmission grid costs (TN_invest_{unit})

The incremental normalised ratios from Eq. 2 and Eq. 3 (section 2.4) are summarised in Table 7. The relative cost reduction is greater than unity in all cases, indicating that the investment in RES allows a reduction of operating costs greater than the incremental investment required. No significant variation is observed throughout the zones. The same amount of investment yields the highest operating cost reduction potential in Spain. The reduction potential is 1.59 MEUR/MEUR incremental annual investment in the 0% demand growth scenarios and reaches 2.23 MEUR/MEUR in the 2.3% demand growth scenarios. Higher fuel costs for gas generators and lower CAPEX (G&S and transmission) in Spain explain the higher saving potential.

The grid integration cost (GIC) for RES generation is less aligned throughout the case studies. The case of Texas shows higher GIC due to the increased reinforcement requirements in the West-East interconnection, reaching 2.61 EUR/MWh in the scenario with demand growth. In Spain, the integration of additional RES generation results in less than 0.20 EUR/MWh in the scenario with demand growth. In the Spanish scenario without demand growth, transmission investment is of the same magnitude in the Non-RES and the RES pathways. The GIC is better understood in context with the LCOE of PV and wind generation. The LCOE of PV is reported at a median value of 54 EUR/MWh, and the median LCOE of onshore wind is 48 EUR/MWh [42]. Hence, grid integration costs are below 5.5% of generation LCOE. Summing the grid integration costs to the G&S LCOE of PV and wind, respectively, still results in values below the LCOE of thermal generation capacity, i.e. CCGT at 87 EUR/MWh [42], [43].

Table 7: Incremental normalised ratios for the base cases

		RCR [MEUR/MEUR]	GIC [EUR/MWh]
No demand growth	**Spain**	1.59	-
	Texas	1.41	2.15
Demand growth	**Spain**	2.23	0.16
	Texas	1.47	2.61

Overall, the results presented in this section show the generalisability of the findings presented in the Spanish-like case study [3]. Despite the increase of transmission expansion requirements in the synthetic ERCOT network due to the West-East interconnection bottleneck, normalised ratios of the expansion costs of the Texan and the Spanish synthetic networks are of the same order of magnitude. Transmission grid reinforcement costs are below 10% of total investment costs (G&S + grid), and transmission grid integration costs of high RES shares are below 5.5% of the LCOE of RES generation capacity provided in the literature.

4.2 Impact of RES capacity concentration on transmission expansion costs

This section analyses the impact of geographical RES concentration in resource-rich network zones. The results of the sensitivity (section 2.3) are compared to the corresponding base case scenario (section 4.1). The resulting transmission expansion costs are presented in this section.

The unit transmission investment costs (TN_invest_{unit}, Table 2) and the RES curtailment levels are selected as parameters to evaluate the effects of RES concentration. The sensitivity results (RES_Con) are compared to the corresponding base cases (BC, section 4.1) in Figure 8. As the capacity installed is the same in the BC and RES_Con sensitivities and only the location varies, the percental increase of unit transmission investment from the BC to RES_Con is the same as the increase of total transmission investment. Transmission grid costs are normalised with installed capacity for the sake of presentability.

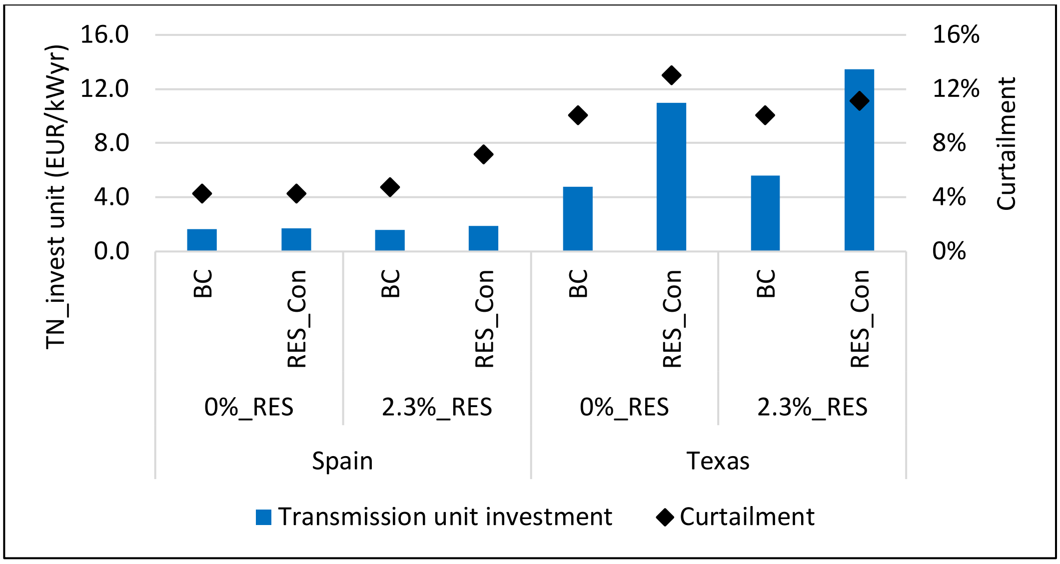

Figure 8: Unit transmission investment costs and RES curtailment levels increase in RES concentration sensitivities and base cases

The results indicate that the synthetic Spanish transmission network, where RES potential and electricity demand are more distributed among the grid (Figure 3), is better prepared to deal with a scenario of RES concentration without significantly impacting unit transmission costs and RES curtailment. In the 0%_RES scenario, the RES_Con sensitivity shows no significant increase in these two parameters. In the 2.3%_RES scenario, the concentration of additional capacity increases transmission investment by 17% and RES curtailment by 50%. This means that 7.15% of available PV and wind energy object to curtailment.

In the synthetic ERCOT network, the existing West-East bottleneck (section 3.2) increases the impact of RES concentration in zones with high RES potential, away from demand centres. Compared to the base case, transmission investment requirements are multiplied by 2.3 and 2.4 when RES capacity is concentrated in zones with high resource potential. For the 0%_RES scenario, this increase in investment costs is accompanied by a rise of the curtailment rate, increasing from 10% to 13% of available PV and wind energy. In the 2.3%_RES scenario, curtailment is only slightly increased from 10% in the base case to 11% of available PV and wind energy in the RES concentration sensitivity. Significantly higher investment is required for the Texan concentration sensitivities to reach similar curtailment levels to the base case.

The findings of the Texan network point out the trade-off between optimal dispersion of RES capacity among the grid and optimal availability of resources. Large distances between the demand centres and areas with optimal RES availability significantly increase the impact of geographical RES concentration on transmission reinforcement requirements.

4.3 Impact of high DG shares on transmission expansion costs

This section evaluates the impact of the deployment of different shares of DG on transmission grid costs. The effect of DG on electricity grid expansion requirements in the two electricity systems is evaluated in comparison with the base case in which no DG is installed. This work focuses on the transmission network by analysing large-scale electricity grids. DG integration into distribution networks is covered broadly within existing literature [25], [26], [44], [45], [46], [47]. Transmission investment is put in context with the base case (BC) (section 4.3.1), and transmission grid cost savings via DG integration are evaluated (section 4.3.2).

4.3.1 Transmission expansion investment

Results show that transmission expansion requirements vary according to location, demand growth scenario, and DG sensitivity. In general terms, transmission reinforcement costs are higher in Texas than in Spain due to the high adaption requirements of the synthetic ERCOT transmission system to accommodate renewable generation capacity in the resource-rich West. At the same time, the demand is mainly located in the coastal area (section 4.1). Figure 9 focuses on the relative transmission investment requirements when moving from the base case to increasing shares of DG. For each electricity system (Spain, Texas) and each scenario (0% demand growth, 2.3% demand growth), the base case serves as a respective baseline for transmission investments. Hence, the BC always provides the baseline at 100% relative investment.

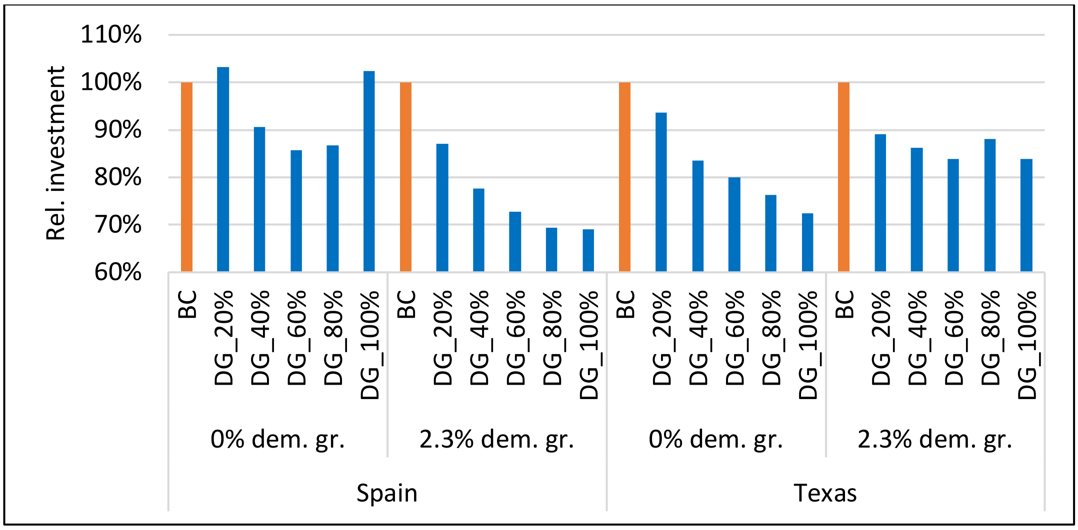

Figure 9: Transmission expansion investment wrt the BC per scenario and sensitivity

Almost all DG sensitivities in both geographical zones and demand growth scenarios allow transmission investment savings. Only in the Spanish scenario without demand growth do two sensitivities result in minor increases in transmission grid costs: DG_20% leads to a 3% cost increase and DG_100% to a 1.2% increase concerning the BC. These low changes are considered negligible due to the updating requirements of the initial synthetic Spanish network described in section 4.1. Consequently, the Spanish 0% demand growth scenario allows less potential transmission grid savings with DG employment. The 2.3% demand growth scenario underlines the transmission expansion saving potential via DG deployment. The integration of RES capacity into the transmission network is a stronger reinforcement driver than the grid update requirements at such significant amounts of RES capacity (Table 3).

The Texan synthetic network allows a relative reduction of transmission expansion costs of at least 6% (0% demand growth, DG_20%). The saving potential in the Texan synthetic transmission grid underlines the existing bottlenecks hampering an efficient West-East interconnection (section 3.2). Higher DG participation locates generation resources closer to the demand centres, thus reducing the requirements for reinforcing the transmission network. The sensitivities of increasing DG shares in scenarios with a 2.3% annual demand increase, the 80% DG sensitivity results in higher transmission grid requirements than both the 60% and the 100% sensitivities. The DG allocation criteria (see 2.3.2) lead to a geographical allocation that is not always aligned with the geographical dispersion of demand. Hence, available local generation capacity surpasses load in some network zones. This leads to reverse power flows between the load centres in the network's East and centre areas at 80% DG penetration. At 100% DG, these inter-zonal power flows are reduced due to more DG availability in all zones. Consequently, transmission grid costs are reduced in the 100% DG sensitivity. Furthermore, the peak in transmission investment is compensated by reduced operating costs due to a decrease in CCGT participation in the energy mix. Hence, total system costs (operation + transmission investment) are lower in the 60% DG sensitivity than in the 80% sensitivity.

As observed above, in the Spanish synthetic network, the highest relative cost reductions are yielded in the scenario with demand growth due to the incorporation of higher amounts of RES capacity impacting the transmission grid. In the Texan synthetic network, the reverse effect is observed. The demand growth scenario incorporates such a significant amount of RES that the location of DG PV has less influence on the transmission grid reinforcement requirements. Wind capacity is still located in the Western zone of the network (Table 4), creating bottlenecks that need to be solved by investing in the West-East interconnection.

4.3.2 DG-induced transmission expansion savings

Figure 10 contrasts the DG capacity installed and unit transmission savings (Eq. 4, section 2.4) for each sensitivity. Unit transmission savings range from slightly negative values in two Spain 0% demand growth sensitivities (20% and 100% DG, in line with the observations in Figure 9) to over 7.5 EUR/kWyr for the Texan 2.3% demand growth DG_20%. Unit transmission saving potential is generally higher in the Texan synthetic network. This finding points out the influence of the West-East congestion that is being reduced by placing PV capacities close to demand centres, even though DG availability surpasses demand.

Low DG shares in demand growth scenarios allow the highest unit transmission savings in both grids. Although relative reductions of transmission grid costs are lower at sensitivities with low DG shares (Figure 9), the installed PV DG capacity, i.e. the denominator of Eq. 4, is also smaller, increasing unit transmission savings. Contrarily, reverse power flows are more likely to occur in hours with negative net demand at high DG penetrations. In these sensitivities, transmission grid reinforcement is necessary to evacuate corresponding energy to the wider network, reducing the unit transmission savings, especially in sensitivities DG_80% and DG_100%.

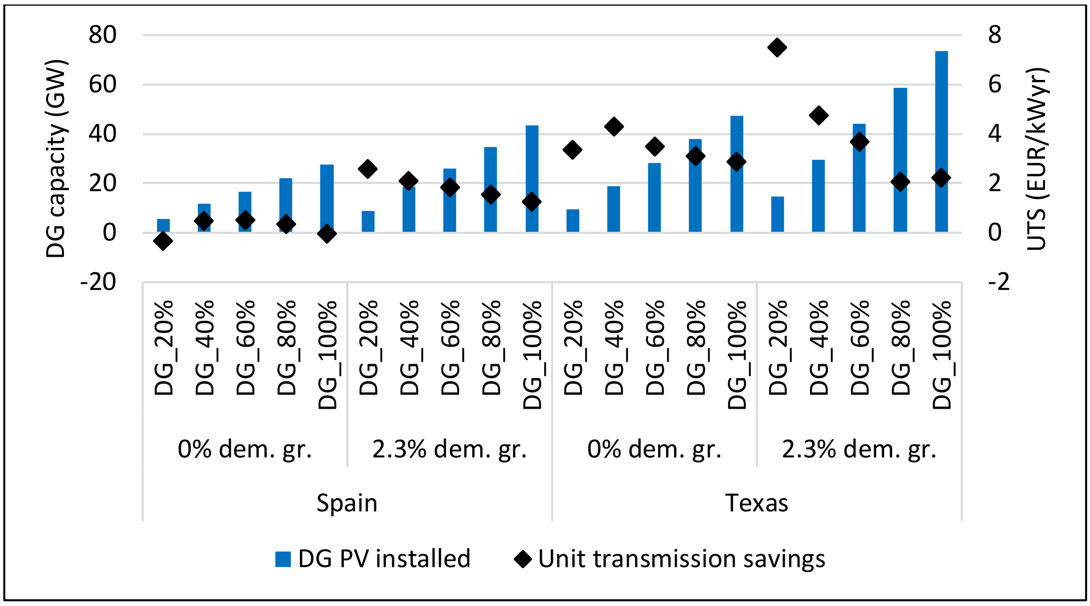

Figure 10: Distributed PV capacity and unit transmission savings per scenario and sensitivity (with respect to the BC with 0% DG)

5 Conclusions

This paper investigates electricity transmission grid reinforcement requirements for future scenarios with high RES penetrations. A pre-existing study about the effects on transmission grid expansion requirements when investing in RES instead of Non-RES generation capacity is complemented by contemplating a second large-scale electricity transmission network with notably different RES availability and load density. The analysis considers two pathways: one with no growth in electricity demand and one with an annual growth of 2.3%. Electricity systems with high RES shares have been contrasted with systems without additional RES capacity for both demand growth pathways. The scenarios were evaluated with a common methodology, employing synthetic transmission networks of two different geographical zones: Spain and Texas. The Spanish synthetic transmission network represents a 479-node network where RES generation sites and load are distributed throughout the territory. In the synthetic 2000-node network of the ERCOT zone in Texas, the highest RES potential is found in network zones far away from demand, driving bottlenecks in the connection of RES generation sites and demand centres.

In general terms, the case studies confirm that decarbonising the electricity system requires a higher investment in RES generation and storage capacity, as well as in grid assets, than the capacity needed in Non-RES scenarios. Transmission grid investment costs for integrating high RES shares account for 21 to 75 EUR/kW of new RES capacity, depending on the conditions of the initial transmission system. Compared to Non-RES G&S expansion pathways, incremental electricity grid costs for injecting additional PV and wind energy account for up to 2.61 EUR/MWh incremental transmission grid costs in systems with pronounced bottlenecks in the initial system aggravated by RES, representing up to 5.5% of PV and wind LCOE.

Furthermore, the incremental investment costs in renewable generation, storage and grid expansion in the RES scenarios are largely offset by fuel and emission cost reductions compared to Non-RES scenarios. Comparing the Spanish and Texan RES and Non-RES scenarios without demand growth underlines that investment in new renewable generation capacity decreases overall system costs, even though no additional G&S capacity is required in the non-renewable scenarios. Even significant congestions in the initial transmission system, such as the West-East interconnection in the synthetic ERCOT grid, do not jeopardise the savings from RES. Despite higher transmission reinforcement requirements in the synthetic Texan electricity grid due to greater distances between RES generation sites and demand centres, the reduction in annual operating costs outweighs the additional investment costs in all scenarios. Operating costs are reduced by up to 2.23 MEUR per MEUR of incremental investment cost when moving from Non-RES to RES.

The results confirm that grid investment costs should not be seen as an economic barrier to integrating high shares of RES and meeting the 2030 decarbonisation targets, regardless of the grid configuration. Furthermore, the case studies confirm that the required decarbonisation of the power sector can be achieved at lower costs than in other Non-RES alternative futures.

In addition to assessing the generalisability of the findings on transmission costs for integrating high shares of renewable energy into large electricity grids of different types, this paper contributes further sensitivities on the impact of the geographical dispersion of renewable generation capacity on transmission costs. The sensitivities are systematically evaluated with the base case as a common baseline, following a consistent methodology for evaluating different geographical dispersions. As seen from the ERCOT sensitivities, the concentration of RES in zones with the highest resource availability can significantly increase transmission investment requirements and curtailment levels. In the synthetic Spanish network, a network with more dispersed demand and resource availability (geographically speaking), the effect of RES concentration on transmission investment and curtailment levels ranges from almost none (0%_RES) to some (2.3%_RES). The results of the Texas case study underline the trade-off between optimal RES placement according to resource availability and optimal placement to keep grid reinforcement requirements low.

Increasing participation of distributed generation in future high RES scenarios can alleviate the burden from the transmission grid. The sensitivities provide a large-scale electricity grid perspective to prior smaller-scale studies in the literature. DG is located directly at demand centres, hence representing electricity that does not need to be transported through the transmission grid to reach consumption sites. Fostering DG rollout is found to be a helpful tool for reducing transmission grid expansion requirements, especially in scenarios with demand growth. In the synthetic Spanish transmission system, the benefits of 100% DG are reduced as local production exceeds demand. The resulting reverse power flows again require transmission grid reinforcement. This effect is not observed in the synthetic ERCOT grid due to the lack of interconnection between RES generation sites and demand centres. Thus, high DG shares reduce the need for reinforcing the West-East interconnection, resulting in higher transmission savings. These results highlight the importance of prosumer installations, not only from a citizen participation point of view but also for an efficient use of the transmission system.

Despite the simplifications applied throughout the case study, mainly due to computational issues, the results of the TEP allow for an assessment of the impact of different RES dispersion factors on the transmission system. The base case results highlight the outstanding benefits of increasing investment in both generation and transmission capacity to decrease total system costs due to fuel and emission savings. This conclusion holds even in highly congested networks such as the ERCOT transmission network with the existing West-East interconnection issue. Overall, the results point out that to meet the 2030 decarbonisation goals, the relevant discussion concerning the decarbonisation of the electricity mix should not be whether grid investment costs may outweigh the benefits of increasing renewable shares. Instead, the debate should focus on ensuring a fast grid connection for the new renewable capacity necessary to achieve the decarbonisation and electrification levels that are needed.

6 Acknowledgements

The authors would like to thank Teresa Freire Barceló and Francisco Martín Martínez for the provision of scenario input data and Andrés Ramos Galán for the patience and support throughout the modelling process.

This research has been carried out thanks to the Iberdrola Chair on Energy and Innovation and the funding of the RETOS COLABORACIÓN programme of the Spanish Ministry of Science and Innovation and the Spanish State Research Agency (project "Platform of innovative models to accelerate the energy decarbonisation of the economy (MODESC)", with reference number RTC2019- 007315-3).

7 References

[1] Spanish Government, 'Spanish National Energy and Climate Plan'. Accessed: Oct. 26, 2023. [Online]. Available: https://commission.europa.eu/energy-climate-change-environment/implementation-eu-countries/energy-and-climate-governance-and-reporting/national-energy-and-climate-plans_en

[2] K. Schaber, F. Steinke, P. Mühlich, and T. Hamacher, 'Parametric study of variable renewable energy integration in Europe: Advantages and costs of transmission grid extensions', *Energy Policy*, vol. 42, pp. 498–508, Mar. 2012, doi: 10.1016/j.enpol.2011.12.016.

[3] L. Herding, R. Cossent, M. Rivier, J. P. Chaves-Ávila, and T. Gómez, 'Assessment of electricity network investment for the integration of high RES shares: A Spanish-like case study', *Sustainable Energy, Grids and Networks*, vol. 28, p. 100561, Dec. 2021, doi: 10.1016/j.segan.2021.100561.

[4] UNEF, 'El autoconsumo fotovoltaico instalado en España creció un 108% respecto a 2021', UNEF. Accessed: Jan. 30, 2023. [Online]. Available: https://www.unef.es/es/comunicacion/comunicacion-post/

[5] P. V. Gomes and J. T. Saraiva, 'State-of-the-art of transmission expansion planning: A survey from restructuring to renewable and distributed electricity markets', *International Journal of Electrical Power & Energy Systems*, vol. 111, pp. 411–424, Oct. 2019, doi: 10.1016/j.ijepes.2019.04.035.

[6] S. Ullah, A. M. A. Haidar, P. Hoole, H. Zen, and T. Ahfock, 'The current state of Distributed Renewable Generation, challenges of interconnection and opportunities for energy conversion based DC microgrids', *Journal of Cleaner Production*, vol. 273, p. 122777, Nov. 2020, doi: 10.1016/j.jclepro.2020.122777.

[7] M. Child, C. Kemfert, D. Bogdanov, and C. Breyer, 'Flexible electricity generation, grid exchange and storage for the transition to a 100% renewable energy system in Europe', *Renewable Energy*, vol. 139, pp. 80–101, Aug. 2019, doi: 10.1016/j.renene.2019.02.077.

[8] A. Schroeder, P.-Y. Oei, A. Sander, L. Hankel, and L. C. Laurisch, 'The integration of renewable energies into the German transmission grid—A scenario comparison', *Energy Policy*, vol. 61, pp. 140–150, Oct. 2013, doi: 10.1016/j.enpol.2013.06.006.

[9] H. Ranjbar, S. H. Hosseini, and H. Zareipour, 'A robust optimization method for co-planning of transmission systems and merchant distributed energy resources', *International Journal of Electrical Power & Energy Systems*, vol. 118, p. 105845, Jun. 2020, doi: 10.1016/j.ijepes.2020.105845.

[10] F. Luo, J. Zhao, J. Qiu, J. Foster, Y. Peng, and Z. Dong, 'Assessing the Transmission Expansion Cost With Distributed Generation: An Australian Case Study', *IEEE Transactions on Smart Grid*, vol. 5, no. 4, pp. 1892–1904, Jul. 2014, doi: 10.1109/TSG.2014.2314451.

[11] H. Liu, G. B. Andresen, and M. Greiner, 'Cost-optimal design of a simplified highly renewable Chinese electricity network', *Energy*, vol. 147, pp. 534–546, Mar. 2018, doi: 10.1016/j.energy.2018.01.070.

[12] J. H. Zhao, J. Foster, Z. Y. Dong, and K. P. Wong, 'Flexible Transmission Network Planning Considering Distributed Generation Impacts', *IEEE Transactions on Power Systems*, vol. 26, no. 3, pp. 1434–1443, Aug. 2011, doi: 10.1109/TPWRS.2010.2089994.

[13] M. Drechsler, J. Egerer, M. Lange, F. Masurowski, J. Meyerhoff, and M. Oehlmann, 'Efficient and equitable spatial allocation of renewable power plants at the country scale', *Nat Energy*, vol. 2, no. 9, Art. no. 9, Jul. 2017, doi: 10.1038/nenergy.2017.124.

[14] REE, 'Gestor de la red y transportista'. Accessed: Jan. 30, 2023. [Online]. Available: https://www.ree.es/es/actividades/gestor-de-la-red-y-transportista

[15] ERCOT, 'Electrical Bus to Hub List'. Accessed: Jan. 30, 2023. [Online]. Available: https://www.ercot.com/mp/data-products/data-product-details?id=NP3-220-SG

[16] RTE, 'Maintaining and making adjustments to the grid'. Accessed: Jan. 30, 2023. [Online]. Available: https://www.rte-france.com/en/uninterrupted-flow-current/maintaining-and-making-to-the-grid

[17] National Grid, 'Network and infrastructure | National Grid ET'. Accessed: Jan. 30, 2023. [Online]. Available: https://www.nationalgrid.com/electricity-transmission/network-and-infrastructure

[18] C. Matamala, R. Moreno, E. Sauma, J. Calabrese, and P. Osses, 'Why reducing socio-environmental externalities of electricity system expansions can boost the development of

solar power generation: The case of Chile', *Solar Energy*, vol. 217, pp. 58–69, Mar. 2021, doi: 10.1016/j.solener.2021.01.034.

[19] F. Martin-Martinez, A. Sanchez-Miralles, M. Rivier, and C. F. Calvillo, 'Centralized vs distributed generation. A model to assess the relevance of some thermal and electric factors. Application to the Spanish case study', *ENERGY*, vol. 134, pp. 850–863, Sep. 2017, doi: 10.1016/j.energy.2017.06.055.

[20] C. F. Calvillo, A. Sanchez-Miralles, J. Villar, and F. Martin, 'Optimal planning and operation of aggregated distributed energy resources with market participation', *APPLIED ENERGY*, vol. 182, pp. 340–357, Nov. 2016, doi: 10.1016/j.apenergy.2016.08.117.

[21] REE, 'Consulta el estado de las solicitudes'. Accessed: Dec. 14, 2020. [Online]. Available: https://www.ree.es/es/clientes/generador/acceso-conexion/conoce-el-estado-de-las-solicitudes

[22] A. B. Birchfield, T. Xu, K. M. Gegner, K. S. Shetye, and T. J. Overbye, 'Electric Grid Test Cases'. Accessed: Aug. 08, 2020. [Online]. Available: https://electricgrids.engr.tamu.edu/electric-grid-test-cases/

[23] NREL, 'System Advisor Model (SAM)'. Accessed: Mar. 22, 2022. [Online]. Available: https://sam.nrel.gov/

[24] ERCOT, 'Planning'. [Online]. Available: https://www.ercot.com/gridinfo/planning

[25] R. Gupta *et al.*, 'Spatial analysis of distribution grid capacity and costs to enable massive deployment of PV, electric mobility and electric heating', *Applied Energy*, vol. 287, p. 116504, Apr. 2021, doi: 10.1016/j.apenergy.2021.116504.

[26] Greenpeace, 'Estudio técnico de viabilidad de escenarios de generación eléctrica en el medio plazo en España', p. 62, Mar. 2018, doi: https://es.greenpeace.org/es/wp-content/uploads/sites/3/2018/03/Generacion-Electrica_baja_5-03-2018.pdf.

[27] A. Held *et al.*, 'How can the renewables targets be reached cost-effectively? Policy options for the development of renewables and the transmission grid', *Energy Policy*, vol. 116, pp. 112–126, May 2018, doi: 10.1016/j.enpol.2018.01.025.

[28] IEA, 'World Energy Outlook 2019 – Analysis', IEA. Accessed: Feb. 10, 2021. [Online]. Available: https://www.iea.org/reports/world-energy-outlook-2019

[29] State of Texas, 'Texas Counties Map | Open Data Portal'. Accessed: Feb. 14, 2024. [Online]. Available: https://data.texas.gov/dataset/Texas-Counties-Map/48ag-x9aa

[30] ACER, 'ACER Market Monitoring Report 2020 – Electricity Wholesale Market Volume'. Accessed: Mar. 15, 2024. [Online]. Available: https://www.ceer.eu/documents/104400/7244444/ACER-MMR2020-EWMV/8dfe6055-7849-b888-7285-a126b94c7041

[31] 'El sistema eléctrico español. Sistema eléctrico 2021', p. 55, Jun. 2022.

[32] European Commission, 'Press release: Commission approves Spanish and Portuguese measures', European Commission - European Commission. Accessed: Nov. 18, 2022. [Online]. Available: https://ec.europa.eu/commission/presscorner/detail/en/IP_22_3550

[33] FERC, '147 FERC ¶ 61,113'. May 15, 2014.

[34] NEWA Consortium, ‘Welcome to the New European Wind Atlas’, New European Wind Atlas. Accessed: Sep. 08, 2022. [Online]. Available: https://map.neweuropeanwindatlas.eu/

[35] Solargis, ‘Global Solar Atlas’. Accessed: Sep. 08, 2022. [Online]. Available: https://globalsolaratlas.info/map

[36] CNMC, ‘Información mensual de estadísticas sobre las ventas de régimen especial’. Accessed: Oct. 07, 2022. [Online]. Available: https://www.cnmc.es/estadistica/informacion-mensual-de-estadisticas-sobre-produccion-de-energia-electrica-partir-de-8

[37] eia, ‘Form EIA-860 detailed data with previous form data’. Accessed: Mar. 23, 2022. [Online]. Available: https://www.eia.gov/electricity/data/eia860/

[38] eia, ‘Annual Electric Power Industry Report, Form EIA-861 detailed data files’. Accessed: Mar. 23, 2022. [Online]. Available: https://www.eia.gov/electricity/data/eia861/

[39] INE, ‘Renta por hogar por comunidades autónomas’, INE. Accessed: May 16, 2022. [Online]. Available: https://www.ine.es/jaxiT3/Tabla.htm?t=9949

[40] INE, ‘Edificios según tipo de edificio por tamaño del municipio y nº de inmuebles’, INE. Accessed: Jul. 27, 2022. [Online]. Available: https://www.ine.es/jaxi/Tabla.htm?path=/t20/e244/edificios/p03/l0/&file=01001.px&L=0

[41] U.S. Census Bureau, ‘Small Area Income and Poverty Estimates (SAIPE)’. Accessed: Jul. 27, 2022. [Online]. Available: https://www.census.gov/data-tools/demo/saipe/#/?map_geoSelector=mhi_c&s_state=48&s_year=2020&s_measures=mhi_snc

[42] IEA, ‘Projected Costs of Generating Electricity 2020’. Dec. 2020. Accessed: Apr. 07, 2022. [Online]. Available: https://www.iea.org/reports/projected-costs-of-generating-electricity-2020

[43] C. Kost, S. Shammugam, V. Jülch, H.-T. Nguyen, and T. Schlegl, ‘Levelized Cost of Electricity- Renewable Energy Technologies’, p. 42, Mar. 2018, doi: https://www.ise.fraunhofer.de/content/dam/ise/en/documents/publications/studies/EN2018_Fraunhofer-ISE_LCOE_Renewable_Energy_Technologies.pdf.

[44] J. D. Jenkins and I. J. Perez-Arriaga, ‘Improved Regulatory Approaches for the Remuneration of Electricity Distribution Utilities with High Penetrations of Distributed Energy Resources’, *The Energy Journal*, vol. 38, no. 3, pp. 63–91, May 2017, doi: 10.5547/01956574.38.3.jjen.

[45] C. Mateo, P. Frias, and K. Tapia-Ahumada, ‘A comprehensive techno-economic assessment of the impact of natural gas-fueled distributed generation in European electricity distribution networks’, *ENERGY*, vol. 192, Feb. 2020, doi: 10.1016/j.energy.2019.116523.

[46] MIT, ‘The Future of Solar Energy’. Accessed: Apr. 06, 2020. [Online]. Available: http://energy.mit.edu/wp-content/uploads/2015/05/MITEI-The-Future-of-Solar-Energy.pdf

[47] L. Olmos *et al.*, ‘Case studies of system costs of distribution areas’. [Online]. Available: https://www.iit.comillas.edu/publicacion/informe/es/11/Case_studies_of_system_costs_of_distribution_areas

[48] T. Freire-Barceló *et al.*, ‘Storage and demand response contribution to firm capacity: analysis of the Spanish electricity system’, *IIT working paper*, vol. IIT-21-096WP, Jun. 2021,

doi: https://www.iit.comillas.edu/publicacion/working_paper/es/434/Storage_and_demand_response_contribution_to_firm_capacity:_analysis_of_the_Spanish_electricity_system.

[49] NREL, 'Annual Technology Baseline (ATB)'. Accessed: Mar. 22, 2022. [Online]. Available: https://atb.nrel.gov/

8 Appendix

Table 8: Modelling cost input parameter; ES costs are computed according to [48]; US costs according to NREL 2019 ATB [49]

	CO2 emissions (EUR/MWh)	Firmness (-)	Investment cost (EUR/kW)		Fuel (EUR/MWh)		O&M (EUR/MWh)		Lifetime (years)		Round-trip efficiency
			Spain	**US**	**Spain**	**US**	**Spain**	**US**	**Spain**	**US**	
Nuclear	0	0.97	-	-	8.72	7.3	0	0	-	-	-
CCGT	28	0.96	845.1	776.8	32.58	19.1	2	2.7	25	55	-
OCGT	42.42	0.96	544.1	776.8	48.88	28.3	11	6.4	25	55	-
Hydro	0	0.44	-	-	0	0	3	0	80	100	-
4h Battery	0	0.69	961	443.1	0	0	0.00025	0	10	15	0.9
Pumped hydro storage*	0	0.96	600 to 1000	N/A	0	-	3	-	80	-	0.75
PV	0	0.07	500	515.1	0	0	0	0	30	30	-
Wind	0	0	950	1026	0	0	0.01	0	25	30	-
ENS	0	-	-	-	0	0	1000	1000	-	-	-

*) The assumptions for pumped hydro storage available to the GEP model for the Spanish electricity system are based on the extension of existing generation sites. Hence, installation costs might be lower than in other references.

7.3 Paper 3

- A parametric model to estimate DER-driven distribution reinforcements is proposed.
- The model considers four types of DER, allocated per municipality and voltage level.
- The model is applied to a policy-based 2030 scenario for Spain.
- Results show a geographical misalignment of DG and load electrification.
- Total reinforcement requirements sum up to 130% of the annual investment limit.

Energy Reports 12 (2024) 5432–5444

Contents lists available at ScienceDirect

Energy Reports

journal homepage: www.elsevier.com/locate/egyr

Review article

Large-scale estimation of electricity distribution grid reinforcement requirements for the energy transition – A 2030 Spanish case study

Leslie Herding *, Manuel Pérez-Bravo, Roberto Barrella, Rafael Cossent, Michel Rivier

Institute for Research in Technology (IIT), ICAI School of Engineering, Universidad Pontificia Comillas, C/Santa Cruz de Marcenado 26, Madrid 28015, Spain

A R T I C L E I N F O

Keywords:
Distribution grids
Distributed generation
Electric vehicles
Heat pumps

A B S T R A C T

The increasing interest in distributed energy resources (DER) challenges electricity distribution grids to host the required distributed generation (DG) capacities and the expected load increase from electrification. However, a large-scale estimation of costs for integrating DER into low, medium, and high voltage distribution networks has yet to be addressed. This paper contributes a model for the large-scale estimation of the impact of distributed generation, electric vehicles and heat pumps on network reinforcement requirements. The model allocates future DER geographically to 8000 Spanish peninsular municipalities. The large-scale model considers low, medium and high voltage distribution grids. The resulting distribution grid investment is determined via individualised reinforcement costs for each of the 47 peninsular Spanish provinces, distinguishing between urban, semi-urban, rural concentrated and rural dispersed configurations of distribution networks. A 2030 case study shows that the geographical allocation of DG is not aligned with the allocation of load electrification, leading to total investment requirements of 2627 MEUR. This finding points out that distribution system operators covering different parts of the territory are likely to face a variety of challenges that are not aligned across the territories, requiring regulation to account for a variation of distribution grid expansion requirements for the energy transition.

1. Introduction

Distribution system operators (DSOs) face growing distributed energy resources (DERs) penetrations. These comprise utility-scale generation units connecting to distribution grids and low voltage (LV) customers seeking to generate their own electricity. Decarbonising the heat and transport sectors also leads to further demand electrification and additional DER penetration. Ambitious decarbonisation targets are expected to impact electricity grids (IEA, 2024a), and its evaluation requires certain assumptions on the geographical allocation of future DER capacities to be made first.

Some authors have proposed methods for the large-scale allocation of Renewable Energy Resources (RES) generation throughout predefined regions of a given country based on general data and simplified grid representation. In these cases, only transmission grids are considered. The authors of (Sun et al., 2022) employ a data envelopment analysis to allocate Chinese RES targets optimally among the 30 Chinese provinces. Renewable portfolio standards are assigned according to indicators related to electricity consumption so that each province might cover a share of domestic electricity consumption via RES. An approach for allocating RES capacity throughout Chinese provinces by minimising the levelised cost of electricity (LCOE) and transmission costs is presented in (Xu et al., 2021). In (Drechsler et al., 2017), the authors propose an approach for the efficient and equitable spatial allocation of photovoltaic (PV) and wind resources throughout Germany. The approach searches for the social optimum of "the evenness of burdens from renewable electricity production across the German population", accounting for transmission expansion requirements between different zones of the country.

Other studies focus on the DER allocation within a specific distribution grid, considering the electrical characteristics of the network. The allocation of DER within the distribution grid is also the subject of literature (Pesaran H.A.A et al., 2017; Ehsan and Yang, 2018). An algorithm for the optimal allocation of wind, PV, gas turbines and storage devices on a 69-bus distribution system case study is proposed in (Home-Ortiz et al., 2019). The optimal location and size of multiple distributed generation (DG) units for minimising losses are evaluated in (Lee and Park, 2009). The methodology is demonstrated on the 30-bus IEEE medium voltage (MV) test system. In (Lee and Park, 2013), the work of the previously mentioned paper is improved by enhancing the

* Corresponding author.
E-mail address: lherding@comillas.edu (L. Herding).

https://doi.org/10.1016/j.egyr.2024.11.026
Received 9 September 2024; Received in revised form 21 October 2024; Accepted 6 November 2024
Available online 16 November 2024

representation of RES sizes. The study works with the MV IEEE 31-bus benchmark system. The integration of PV, electric vehicles (EVs) and heat pumps (HPs) into a low voltage (LV) system with 170k households in Switzerland is analysed in (Gupta et al., 2021). The authors work with a DSO to define network reinforcement requirements. Network reinforcement costs from the DSO area are assumed to apply to the rest of the country.

Due to the size and complexity of distribution grid feeders, literature on RES allocation in distribution networks commonly focuses on the location within one selected feeder of one voltage level. Extrapolation to a national scale is not a frequent part of the analysis. The authors of (Gupta et al., 2021) estimate nationwide grid costs for integrating DER into LV grids. The analysis does not include MV and high voltage (HV) distribution networks. Grid reinforcement requirements are assessed on a national level for German low, medium and high voltage networks in (Vu, 2018). In various scenarios, the authors assess the reinforcement required for integrating DG (i.e. PV, wind and biomass) and EVs into 238 different regions. A method for assessing distribution reinforcement requirements for integrating EV chargers is proposed in (Ferreira et al., 2020). The large-scale study considers 25,000 low voltage networks. The impact of residential load electrification and EV integration into Californian electricity grids is evaluated in (Elmallah et al., 2022). The authors consider temporal and spatial aspects of future loads. Costs are computed according to a catalogue, and the available capacity of the circuits is considered to determine reinforcement needs. To the best of the authors' knowledge, there is no large-scale study to assess the costs of integrating DER into low, medium and high voltage distribution networks, contemplating distributed generation, electric vehicles, and heat pumps.

This paper contributes a model to estimate large-scale distribution electricity grid reinforcement requirements for accommodating distributed energy resources throughout the Spanish peninsular territory. The model considers electricity distribution systems at low, medium and high voltage. DER technologies comprise multiple technologies for distributed generation and load electrification. DG is represented via PV and wind generation; load electrification is carried out via residential EVs and HPs. The spatial distribution of the new resources is determined via deterministic input parameters rather than via optimisation to depict that promoters do not always follow the economically optimal allocation. The allocation is carried out via so-called scaling factors. Scaling factors are comprised of attributes that describe the likelihood of a technology being installed in a given area, such as the availability of natural resources (i.e. wind speed, irradiation) or a household's purchase power. Grid expansion costs are individualised for each of the 47 peninsular Spanish provinces and distinguish between urban, semi-urban, rural concentrated and rural dispersed distribution areas. Provincial unit expansion costs are extrapolated from the cost database of a Spanish DSO. The contributions can be summarised as follows:

- Methodology for the geographical allocation of DG and demand electrification technologies (EVs and HPs) with a resolution of Local Administrative Units (> 8000 municipalities in the case of Spain).
- Consideration of all voltage levels classified as distribution-level in Spain, i.e. from low to high voltage.
- Deployment of unit expansion costs extracted from the database of a Spanish DSO, as well as extrapolation methodology to the whole country.

The remainder of this paper is organised as follows: Section 2 illustrates the criteria employed for the geographical DER allocation. The approach for calculating grid reinforcements is presented in Section 3. Section 4 presents the case study. Section 5 concludes the paper.

Fig. 1. Peninsular autonomous communities (NUTS 2).

2. Geographical allocation methodology

The Spanish peninsular territory comprises 15 autonomous communities (CA, Fig. 1), 47 provinces (Fig. 2) and over 8000 municipalities (Fig. 3). Autonomous communities represent the regional classification at the NUTS[1] 2 level, provinces at NUTS 3, and the municipalities are Spanish Local Administrative Units (LAU).[2] The allocation of DG, EVs and HPs is carried out at the municipality level. However, the other territorial classifications are relevant for data processing and will be referenced throughout the document.

The allocation of DER to municipalities is made via scaling factors (SFs). The criteria for calculating the SFs differ for DG and demand electrification technologies. Fig. 4 provides a generalised representation of the SF calculation methodology. Mixed SFs are employed. They allow the definition of scaling factors that consider several criteria. The mixed SFs, SF_m^{mix}, of each municipality m are calculated from n individual SFs, SF_m^{ind}, and their weights w. Individual scaling factors allow considering different criteria C deemed relevant for allocating future DG, EVs and HPs. Examples of these criteria are resource availability and household income. An overview of the criteria employed is shown in Table 1; further details are described in Section 2.1 for DG and 2.2 for load electrification.

It must be noted that, due to the large scale of the model, regional differences in the uptake of DER are captured via the criteria employed for the SFs only. Other differences, such as regional policies to foster certain technologies, are not considered explicitly in the model. Hence, the geographical allocation of future DER carried out by the model might deviate from the actual conditions. However, individual scaling factors, such as the geographical distribution of the population, allow for a reasonable estimation of load electrification trends. Furthermore, the criteria employed for utility-scale DG represent the most relevant criteria for selecting optimal generation sites (MITECO and REE, 2024). All data for the geographical allocation is employed with a geographical granularity level of municipalities (LAUs), enhancing the level of detail observed in previous studies. The scaling factors will be described in more detail throughout this section.

The sum of the weights of all the criteria for determining the mixed SF is unity (Eq. 1). Consequently, the sum of all municipalities' mixed SFs is unity, meaning that SF_m^{mix} represents the share of DER allocated to each municipality. Hence, the final capacity of each of the DG technologies (i.e. PV and wind), number of EVs or demand via HPs of a particular municipality can be obtained by multiplying the total amount by its SF_m^{mix}.

[1] Nomenclature of Territorial Units for Statistics (NUTS) is a classification of countries' regions for statistical purposes, deployed in the European Union. It is used for harmonising European regional statistics and allows to carry out socio-economic analyses of the regions (Eurostat, 2024a).

[2] Local administrative units (LAU) represent a subdivision of NUTS 3 regions and comprise municipalities and communes in the European Union (Eurostat, 2024b).

Fig. 2. Peninsular provinces (NUTS 3).

Fig. 3. Peninsular municipalities (LAU).

$$SF^{ind}_{1,m} = \frac{C_{1,m}}{\sum_m C_{1,m}}$$

$$SF^{ind}_{2,m} = \frac{C_{2,m}}{\sum_m C_{2,m}}$$

$$\vdots$$

$$SF^{ind}_{n,m} = \frac{C_{n,m}}{\sum_m C_{n,m}}$$

$$SF^{mix}_{m} = \sum_{i=1}^{n} \left(SF^{ind}_{i,m} * w_i\right)$$

Fig. 4. Scaling factor calculation for the geographical allocation.

$$\sum\nolimits_{i=1}^{n} w_i = 1 \qquad (1)$$

It is relevant to consider whether the capacity is installed in urban or rural areas, as network expansion costs vary according to grid characteristics (Prettico et al., 2016). Table 2 indicates the four categories established in Spanish regulation, their number of supply points (Ferreira et al., 2020), and the abbreviated denomination of each distribution zone type used in this paper. Municipalities are assigned a supply zone type according to an estimation of the number of supply points obtained through the methodology presented in Appendix A.

2.1. Geographical allocation of distributed generation

The methodology differentiates between small prosumer installations and utility-size installations. Prosumer installations are allocated according to criteria expressing the likelihood of a household investing in a rooftop PV installation. Utility-scale installations are expected to seek profit maximisation or, as a proxy, the maximisation of electricity generation. Fig. 5 summarises the generation capacity allocation process. Prosumer installations comprise those connected to low voltage (LV), whereas utility-size DG connects to medium voltage (MV) and high voltage (HV). The extra high voltage level (EHV) is part of the transmission system and, hence, is excluded from this analysis. The allocation criteria for prosumer and utility-scale installations are detailed in Sections 2.1.1 and 2.1.2, respectively.

Table 1
Summary of criteria used for the determination of mixed SFs.

	DG		Electrification	
	Prosumer	Utility-scale	EVs	HPs
Household income	X			X
Contracted power	X			
Building amount	X			
Resource availability		X		
Environmental sensitivity (ES)		X		
Hosting capacity (HC)		X		
EV substitution rate			X	
Required thermal energy demand (RTED)				X

2.1.1. Prosumer allocation

Prosumer is a denomination for grid users that are producers and consumers, commonly referring to LV customers opting to install DG capacity. Hence, LV connecting generation capacity is considered for prosumer allocation. Wind energy connected to LV grids is assumed to be negligible, and the prosumer analysis is limited to residential behind-the-meter PV systems. Three indicators are considered for prosumer deployment: their contracted capacity, the average household income, and the building density (Table 1).

Reducing the electricity consumed from the grid is one of the main drivers for prosumer installations (UNEF, 2023). Consequently, the contracted capacity of grid consumers is one indicator to estimate the geographical distribution of future prosumer development. The Spanish ministry publishes the contracted capacity of secondary substations (MV and below) for each province in the continuity of supply statistics (MITECO, 2023a). The database contains the contracted capacity and the number of supply points for each type of electricity supply zone (Table 2) within each province (Fig. 2). This data allows to determine the installed capacity per supply point for each province according to the supply zone. Total contracted capacity S for municipality m, subject to their electricity supply zone sz, is obtained with Eq. 2, where SP represents the number of supply points determined via the methodology described in Appendix A, and pr indicates the provinces.

$$S_{m(sz)} = \left(\frac{S}{SP}\right)_{pr(m),sz} * SP_m \qquad (2)$$

However, a household's decision to purchase a PV system is not solely based on the size of its electricity demand but also on the purchasing power of the household. Thus, the average household income of the municipalities is also considered (INE, 2022a).

Furthermore, the building density of the territory is included as a third indicator (INE, 2022b). This indicator expresses that, although households may have similar electricity demand and purchase power levels, urban areas have less available surface per supply point for installing PV panels than rural areas. As people are more likely to live in apartment buildings in urban areas, not every household disposes of an

Table 2
Classification of electricity distribution grid types according to supply points (Ministerio de Economía, 2000).

	Denomination	Number of supply points
Urban	U	$>$ 20k
Semi-urban	SU	2k to 20k
Rural concentrated	RC	200 to 2k
Rural dispersed	RD	$<$ 200

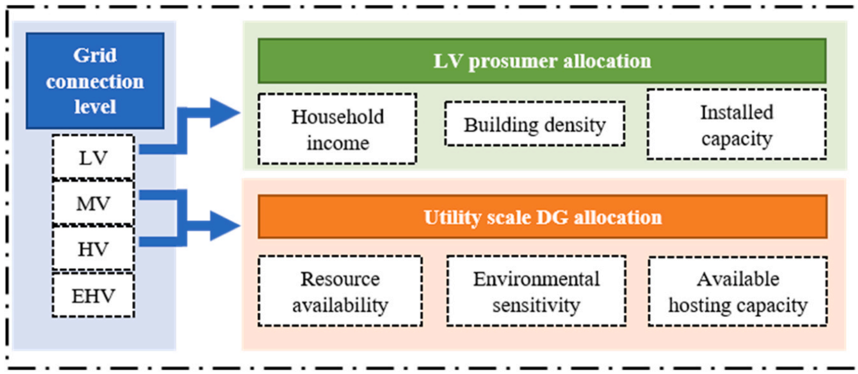

Fig. 5. Flowchart of the generation capacity allocation process.

individual rooftop for PV. On the contrary, people are more likely to live in separate houses in rural communities, disposing of surfaces for PV installations for individual households.

The individual scaling factors of contracted capacity, household income, and building density are computed for the prosumer allocation mixed SF according to Fig. 4 with equal weight of every individual SF.

2.1.2. Utility-scale allocation

The geographical allocation of utility-scale generation connected to MV and HV grids is split into two steps to account for the considerations of DG promoters when deciding the location of a new plant, as shown in Fig. 6.

Firstly, the most suitable region (NUTS2) for RES deployment is selected using resource availability as a primary indicator. Additionally, the Spanish ministry's environmental sensitivity (ES) classification (MITECO, 2023b) is considered. The surface of the Spanish territory is classified according to its environmental suitability for developing PV and wind energy, respectively. It expresses the likelihood of a favourable environmental evaluation of the project. Next, the capacity is assigned to the municipalities of each region. The available hosting capacity (HC) is considered an additional indicator. Spanish DSOs are required to publish the available HC for distribution voltage levels (i.e. from 1 kV up to 132 kV). For the sake of simplicity, the methodology considers the HC published by the five biggest DSOs in Spain, supplying over 75 % of total electricity consumers (e-distribución, 2023; E-REDES, 2023; i-DE, 2023; UFD, 2023; Viesgo, 2023; CNMC, 2020).

The scaling factors for both steps are calculated as shown in Fig. 4. Resource availability and ES are computed as equivalent areas ($km^{2eq}_{t,m}$), derived via Eq. 3. Both criteria are different for the technologies t, i.e. PV and wind. The terrain of each municipality is classified into groups g. In the case of resource availability, the groups rank the terrain's potential for RES production. For ES, the groups express the likelihood of a positive environmental evaluation of a generation installation.

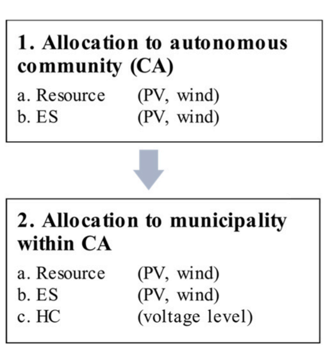

Fig. 6. Two-step utility-scale DG allocation process.

Table 3
Weighting criteria for the determination of equivalent km^2.

Group	1	2	3	4	5
Weight	0	0.1	0.3	0.7	1

$$km^{2eq}_{t,m} = \sum_{g} \left(w_g * km^2_{g,t,m} \right) \quad (3)$$

Five groups are employed for both criteria, ranging from no suitability (i.e., very low resource availability/very low probability of a successful environmental evaluation) to high suitability. The weights of the five groups for the computation of Eq. 3, w_g, are presented in Table 3.

The units of the criteria and the weights for the computation of the mixed SF for utility-scale DG allocation are provided in Table 4. Step 2 indicates two different weight options for the criteria. This approach is introduced because some CAs have no available HC. Consequently, this factor is only accounted for when capacity is available to guarantee that the Step 2 mixed SF of the municipalities within each CA sums to unity.

2.2. Mapping of demand electrification technologies

2.2.1. Electric vehicles

Spanish EV adoption has been more measured compared to other European nations, with a fleet electrification rate below 1.5 % in 2023 (European Commission, 2024a). The Spanish National Energy and Climate Plan[3] (NECP) aims at 5.5 million EVs by 2030, encompassing various vehicle categories such as cars, motorbikes, vans, and buses (Spanish Government, 2023). Private cars are anticipated to constitute 3.5 million of these vehicles, representing 14 % of the existing fleet. This analysis only addresses the implications of the private charging infrastructure (home and workplace) on the distribution grid, which is expected to account for approximately 70 % of the total amount of EVs anticipated for 2030 (LaMonaca and Ryan, 2022; Transport and Environment, 2020).

Given the varying reliance on private cars across regions within the country and the disparate rates of infrastructure development, it is unrealistic to assume a uniform EV penetration across municipalities. This study extrapolates from historical EV registration data from 2015–2022 for each municipality to project the distribution of the EV fleet in 2030

[3] As mandated by the Energy Union Strategy, EU Member States publish their mid-term decarbonisation targets in the form of National Energy and Climate Plans (NECPs) (European Commission, 2024b). In those plans, the Member States describe their ambitions for 2030, covering decarbonisation, energy efficiency, energy security, internal energy market, and research, innovation and competitiveness (European Commission, 2022). The NECPs are updated every two years.

Table 4
Criteria units and weights for two-step DG allocation SF.

Criterion	Unit	Weight Step 1 CA	Weight Step 2 Municipality
Resource availability	km^{2eq}	0.6	0.33 / 0.5
ES	km^{2eq}	0.4	0.33 / 0.5
HC	MW	-	0.33 / 0

(Dirección General de Carreteras, 2024). The country is segmented into 89 categories, each estimated to have different EV ownership rates. These categories include non-urban and urban municipalities with populations ranging from 5000 - 20,000 to 20,000 - 50,000 and 86 distinct Urban Areas (UA). Note that the municipality classification for allocating future EVs differs from the power distribution service zones presented in Table 2. The reason is that the electricity grid classification is based purely on the number of electricity supply points within the municipality, which is deemed insufficient to capture all factors relevant to the adoption of EVs accurately. Instead, municipalities are classified based on the *Statistical Atlas of Urban Areas* published by the Spanish Government, which considers additional indicators such as population density, demographics, housing characteristics, price indices, and existing and planned transport infrastructure (Ministerio de Vivienda y Agenda Urbana, 2023). This approach is considered better suited for EV allocation.

Fig. 7 shows that, by the end of 2022, the rate of EV ownership in municipalities ranged from 0.9 to 1.6 EVs per 1000 residents. However, to achieve the target of 3.5 million EVs by 2030, the rate of EV ownership must escalate to between 66 and 115 EVs per 1000 residents, contingent on the specific region.

Under these growth assumptions, the projected number of EVs per municipality can be determined based on their territory type. The distribution capacity needed to accommodate the home charging infrastructure for the expected fleet of every municipality is calculated under the assumption that every new EV is expected to increase the contracted capacity on the customer side by up to 3.6 kW (Hall and Lutsey, 2024).

2.2.2. Heat pumps

The mixed SF for HP allocation shows similarities to the prosumer PV allocation: average household income represents purchase power. Furthermore, the Required Thermal Energy Expenditure (RTEE) model is employed.[4] The model provides theoretical expenses for each municipality and considers factors such as the building type, the climate zone of the municipality (Barrella and Blas-Álvarez, 2024), and the average household size. This paper estimates the required thermal energy demand (RTED) by using the RTEE model, given in kWh/(household*yr), scaled to each municipality via the number of supply points (Appendix A). This is a proxy of the number of households in each municipality. The RTED per municipality indicates the relative distribution of heat demand throughout municipalities. The mixed SF is calculated according to Fig. 4, with equal weight of average household income (EUR) and RTED per municipality (MWh/yr) (see Table 1). The former has been demonstrated to be a key barrier to heat pumps' adoption (Barrella et al., 2020; Sunderland and Gibb, 2024; Duarte et al., 2021), while the latter is a crucial variable in a diverse climate such as the Spanish one (Barrella and Blas-Álvarez, 2024).

With that, HPs' thermal energy demand is allocated to each municipality. Then, the corresponding electricity demand is calculated according to Eqs. 4–8, following the assumption that a household covers all its annual thermal energy requirements (heating and cooling) via the installed HP. First, Eq. 4 determines the number of HPs, *n°HP*, per municipality *m* as the ratio of thermal energy assigned via the mixed SF, E^{th},

[4] The RTEE models the annual theoretical expenses of a household for heating and cooling (Barrella et al., 2023), (Barrella et al., 2021)

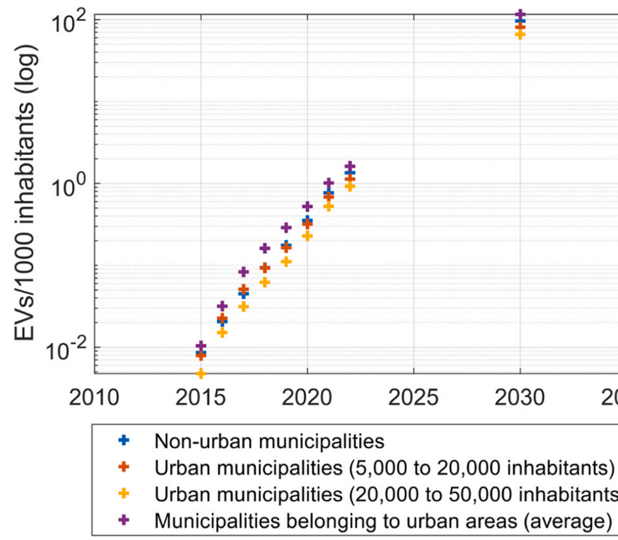

Fig. 7. Evolution of the EV ownership rate by type of territory (2015–2030) (Dirección General de Carreteras, 2024).

and the annual thermal energy demand *RTED* of a dwelling *d* in the municipality *m*. This allocation is subject to the restriction in Eq. 5 to avoid that small municipalities with high per-capita RTED and high average household incomes being assigned thermal energy above their total RTED. The peak thermal energy requirement of a dwelling in each municipality, $\overline{E^{th}_{d,m}}$, is determined via Eq. 6. The unit peak thermal energy requirement per square meter is an input to the model, derived from the methodology of (Barrella et al., 2020). The average dwelling size within a municipality, $m^2{}_{d,m}$, is derived from the same input dataset. The peak electrical energy requirement of a dwelling, $\overline{E^{el}_{d,m}}$, is determined by dividing the peak thermal energy demand by the performance factor *PF*, which is the Coefficient Of Performance (COP) in the case of the heating peak and the Energy Efficiency Ratio (EER) in the case of the cooling peak (Eq. 7). The COP and EER vary by municipality according to the climate zone. Finally, the electric capacity of installed HPs for each municipality, P^{el}_m, is derived as the product of maximum electrical energy to be supplied per dwelling and the number of dwellings expected to install a HP in the municipality.

$$n^{o}HP_m = \frac{E^{th}_m}{RTED_{d,m}} \tag{4}$$

$$E^{th}_m \leq RTED_{d,m} * SP_m \tag{5}$$

$$\overline{E^{th}_{d,m}} = \frac{\overline{E^{th}_m}}{m^2} * m^2{}_{d,m} \tag{6}$$

$$\overline{E^{el}_{d,m}} = \frac{\overline{E^{th}_{d,m}}}{PF_m} \tag{7}$$

$$P^{el}_m = \overline{E^{el}_{d,m}} * n^{o}HP_m \tag{8}$$

3. Distribution grid reinforcement

3.1. Unit grid expansion costs

DER-driven distribution reinforcement costs depend on several factors, such as whether the feeder is an urban or a rural network feeder (Herding et al., 2021). For example, rural networks commonly show longer lines to serve fewer customers (Prettico et al., 2016), as areas are less densely populated than urban zones.

The unit costs applied in this study are actual costs based on the database of a Spanish DSO. Costs considered refer to grid expansion works for connecting third-party installations. The cost database details construction works over the last few years, including the size of the installation, the related cost, and the municipality. The costs are classified into the electricity grid service zones according to the municipality (Table 2). Only those provinces with sufficient data are considered for determining an average expansion cost. Table 5 shows the provinces with data availability on average unit costs per distribution grid zone. RD areas show significantly lower data availability.

The data is analysed to identify the most fitting extrapolation for covering the 47 provinces of the peninsular territory. Fig. 8 shows the annualised costs converted into normal distributions considering each grid type's average cost and standard deviation. For the annualisation of electricity grid asset costs carried out throughout this document, the asset lifetime is assumed to be 40 years, and the discount rate is set at 7 % (Herding et al., 2021).

For statistical analysis of the distributions, the p-value test is carried out and confirms the 3rd-degree normal distribution. Extrapolation to the remaining provinces is carried out by randomly assigning a probability value to each province, allowing for assigning costs based on the distribution function. These costs are applied to MV and HV grids. LV costs are determined via two cost terms charged to customers of Spanish distribution networks. These costs must be paid for new connections and increasing the contracted capacity (Villasur, 2023). They represent access and extension rights (Table 6).

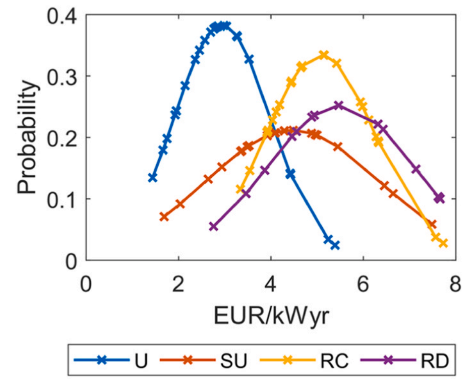

Fig. 8. Normal distributions of unit grid costs per grid type extracted from the database.

Table 6
Regulated costs for increasing contracted LV capacity (Villasur, 2023).

Term	Cost
Access rights	19.70 EUR/kW
Extension rights	17.37 EUR/kW

3.2. Determining grid reinforcement requirements

Distribution grid reinforcement is calculated for each municipality based on the allocation performed via the criteria presented in Section 2. DER integration might trigger reinforcements for various reasons, such as voltage and frequency deviations or thermal line loading limits. The maximum capacity that can be connected to a network node without causing any threat to the safe network operation is denominated hosting capacity. The proposed model employs HC as a threshold of DER that can be connected without requiring new network assets, as will be specified in the following subsections.

The municipality-specific reinforcement is then aggregated for MV and HV according to the province and grid type. Reinforcement costs can then be calculated via the cost catalogue described in 3.1. For LV, costs are assigned according to Table 6. The reinforcement requirements are determined differently for DG (3.2.1) and demand electrification (3.2.2).

3.2.1. Distributed generation

Network reinforcement for connecting DG is calculated via the existing nodal HC. DG connections are contrasted to the HC of the connection voltage level and the available HC in the upstream networks. The MV network must accommodate both MV and LV connecting DG capacities. Correspondingly, the HV network must accommodate HV, MV and LV capacities. Available HC published by the five biggest Spanish DSOs is considered (e-distribución, 2023; E-REDES, 2023; i-DE, 2023; UFD, 2023; Viesgo, 2023). Spanish regulation requires DSOs to publish HC for all network nodes above 1 kV (CNMC, 2021a). HC is subject to regulatory requirements to ensure the safe operation of distribution grids. DSOs are required to consider aspects such as thermal line loadings, bus voltage levels, and the node's short-circuit power. HC is further limited by pre-existing generation and load facilities and their output/withdrawal (CNMC, 2021b). Hence, this data can only be applied to MV and HV DG installations. Network upgrades are necessary in municipalities where the allocated capacity surpasses available HC. In those municipalities m, the magnitude of the required additional capacity P_add for each voltage level kV is determined via Eq. 9, where DG expresses the total capacity assigned to the municipality at the voltage level under consideration and downstream of it, and HC the available HC.

$$P\_add_{m,kV} = \quad DG_m - HC_{m,kV} \tag{9}$$

However, the data of available HC published by DSOs might show HC across nodes within a limited geographical zone when the HC is only available at one node. Requesting access to one node eliminates the HC at the remaining nodes. This may happen due to upstream network congestion. Consequently, the HC of a municipality cannot be considered the sum of all nodes' HC. Hence, the approach of Eq. 9 represents an upper limit of available HC. A sensitivity will be calculated in which the HC is considered zero.

Due to the lack of HC data for LV grids, the entire LV PV is expected to require reinforcement to avoid underestimating costs.

3.2.2. Demand electrification

The impact of demand electrification is determined via the increase in peak demand. The base load for each municipality is determined via the contracted capacity and a representative LV load profile (MITECO, 2023a; REE, 2023). The municipalities' contracted capacity is obtained from Eq. 2. The municipality's base load profile provides the base load peak. The EV load profile is extracted from (REE, 2023), and the HP load profile from (Barrella et al., 2020). The impact of the peak demand increase on grid reinforcement depends on simultaneity factors (Fig. 9). They are employed by DSOs for system planning and vary per voltage level. They represent hypotheses on the coincidence of peak load. The simultaneity factors employed are provided in Table 7 (Pieltain Fernandez et al., 2011). An LV simultaneity factor of 0.4 is found in the literature. However, non-optimal residential load management might increase the simultaneity factor, i.e. due to simultaneous heat demand (Röder et al., 2021). Hence, a sensitivity evaluation with increasing LV simultaneity factors from 0.4 to 1 in steps of 0.1 is included in the result discussion. Distribution grid HC for connecting new loads is not published by Spanish DSOs. A conservative approach is chosen, which considers the entirety of the peak load increase after applying the simultaneity factor to trigger reinforcement. This is depicted in Fig. 9.

Table 5
Number of provinces with sufficient data available per grid type.

	U	SU	RC	RD
Nº	23	24	24	14

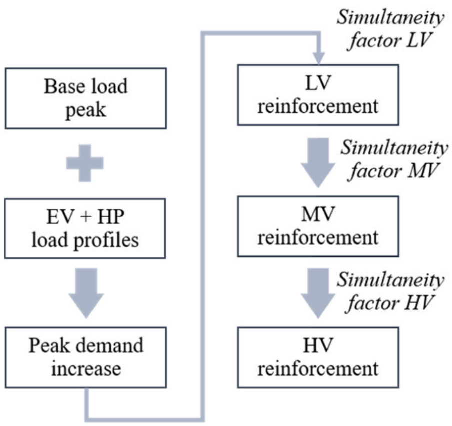

Fig. 9. Determination of reinforcement requirements from demand electrification.

Table 7
Load simultaneity factors (Pieltain Fernandez et al., 2011).

	LV	MV	HV
Simultaneity factor	0.4	0.85	0.95

4. Case study

4.1. Case study input

A case study is carried out to evaluate the model's functionality. The scope is the target scenario of the 2019 Spanish NECP (Spanish Government, 2023). Table 8 provides an overview of the capacities to be added for 2030.

First, the classification according to voltage level is carried out (Fig. 5). The amount of DG per voltage level is estimated with historical data (CNMC, 2022). Table 9 shows the share of PV and wind capacity connected per voltage level as of September 2023. It underlines that wind installations at the LV level are neglectable. Additionally, the table presents the DG capacity installed per voltage level for the case study.

Maps of the input data for the mixed SFs are presented in the following figures. All data is provided at the municipality level (Fig. 3). Fig. 10 presents the average household income. In general terms, income is highest in the country's capital, the northeast of the country, and in other bigger cities such as Murcia (southeast). Fig. 11 presents the annual RTED employed for HP thermal demand allocation. As RTED is expressed as a sum of heating and cooling demand, coastal areas with milder winters have lower RTED. Fig. 12 presents the number of buildings in each municipality for rooftop PV potential evaluation. The geographical distribution of the 2030 EV fleet derived from 2.2.1 is presented in Fig. 13. Fig. 14 and Fig. 15 present the equivalent surface according to the ES of PV and wind, respectively. The highest values are found around the coast in the country's southeast and in the centre of Andalusia. The geographical distribution of terrain suitability of both technologies shows high similarities due to impeding factors (i.e. natural protected areas) applying to both. Fig. 16 and Fig. 17 show the equivalent surface according to resource availability for PV and wind, respectively. PV shows high potential in the South. The map of wind resource availability indicates only a few hotspots throughout the territory.

Table 8
Case study input – added capacities (Spanish Government, 2023).

Technology	PV (MW)	Wind (MW)	EV (num)	HP (ktep)
Capacity	30,110	22,300	3500,00	2894

Table 9
DG capacity per voltage level in Spain (CNMC, 2022).

	LV	MV	HV	EHV
Share of capacity per voltage level				
PV	8 %	15 %	16 %	61 %
Wind	1 %	4 %	35 %	60 %
Resulting capacity per voltage level (MW)				
PV	2526	4552	4683	18,348
Wind	-	885	8062	13,353

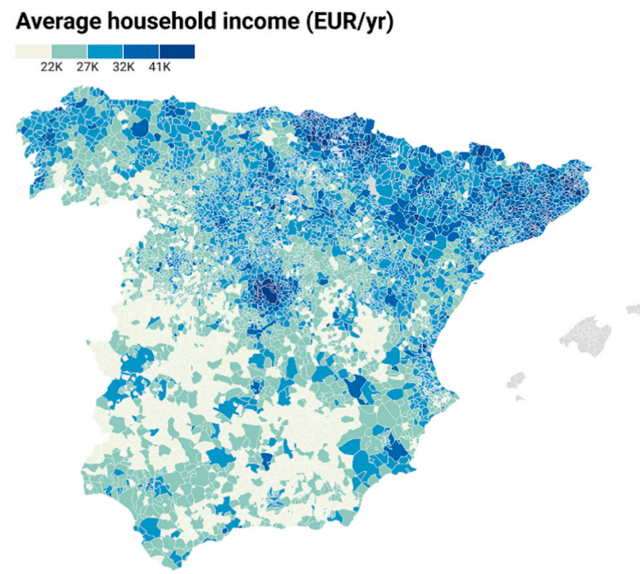

Fig. 10. Average household income (EUR/yr).

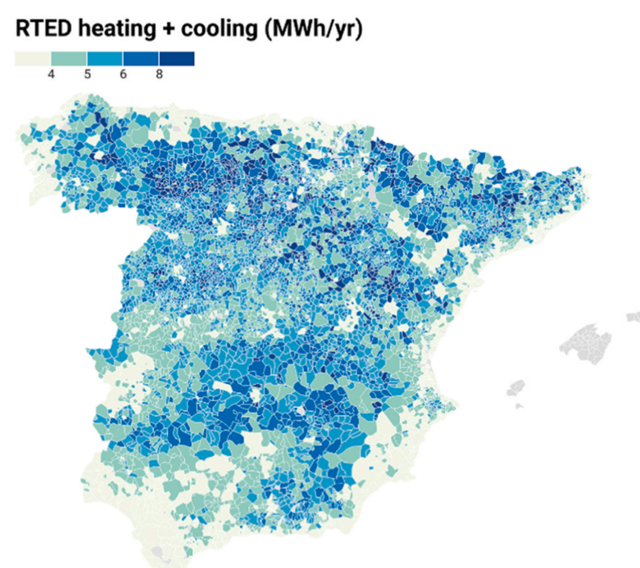

Fig. 11. Annual required thermal energy demand (MWh/yr).

4.2. Case study results

4.2.1. Technological allocation

Fig. 18 presents the resulting geographical distribution of DG capacity and peak load increase. Fig. 18 a) shows that DG capacities are installed predominantly in the South due to the favourable ES (Fig. 14 and Fig. 15) as well as the resource availability for PV installations (Fig. 17). Fig. 18 b) points out that the load increase is concentrated in

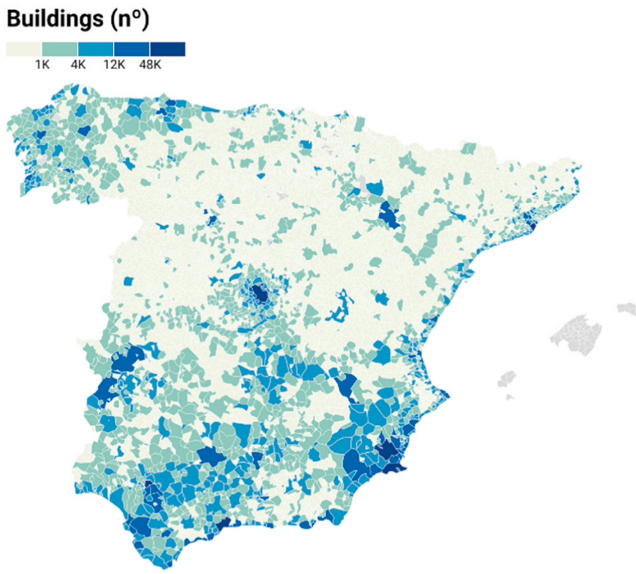

Fig. 12. Number of buildings.

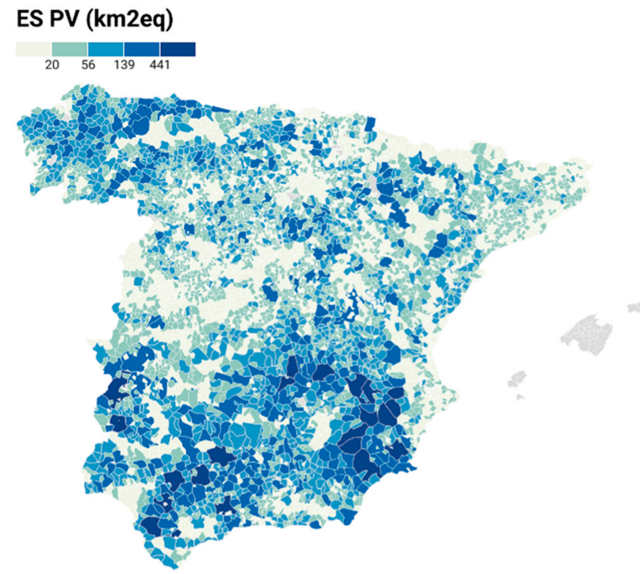

Fig. 14. Environmental sensitivity (km2eq) – PV.

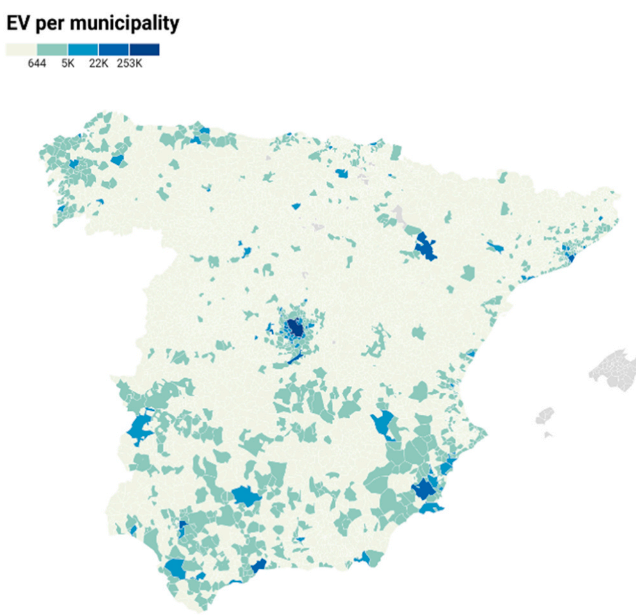

Fig. 13. Geographical distribution of the 2030 EV fleet.

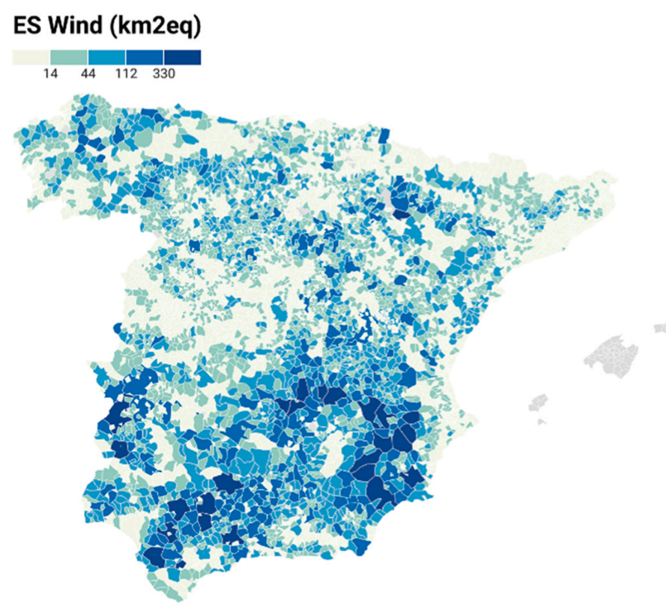

Fig. 15. Environmental sensitivity (km2eq) – Wind.

bigger cities. The cities' population density increases the number of EVs assigned and the total RTED due to more dwellings per municipality. Future electricity demand will not be located in the same municipalities as DG capacities. Consequently, DSOs cannot largely profit from possible synergies between DG availability and load to reduce electricity grid requirements. The correlation between the assignation of DG and the peak load increase is 0.25.

Fig. 19 shows the allocation of DG to the different distribution supply zones. The majority is assigned to SU and RC municipalities. A total of 8.8 GW is assigned to RC municipalities. SU municipalities account for 6.3 GW. U and RD municipalities are assigned below 5 GW of DG due to the low weight of those zone types in the municipalities with the highest DG potential. Figs. 14–17 show that both criteria of equivalent km2 are higher in the South, where most municipalities are classified as SU or RC (Fig. 26).

The allocation of EVs and HPs increases peak electricity demand by 17,078 MW. Applying the simultaneity factors (Table 7) results in required capacities of 6831 MW at LV, 5807 MW at MV and 5516 MW at HV. Fig. 20 shows the peak demand increase per grid zone. It shows an even distribution in all grid zones except RD zones. This result is in line with the geographical distributions of the allocation criteria. Population density increases the RTED of urban municipalities, driving HP allocation. SU and RC municipalities represent 70 % of the Spanish peninsular municipalities (Table 11), leading to a high representation of these zones.

4.2.2. Distribution grid reinforcement requirements

Fig. 21 shows maps of the annualised reinforcement costs per municipality. Fig. 21 a) shows the costs for integrating DG, and Fig. 21 b) shows the costs triggered by the peak load increase. The distribution of costs aligns with the allocation of capacities presented in Fig. 18.

Fig. 22 shows the total reinforcement requirements derived from the geographical allocation. Network upgrades are quantified in capacity as well as in annualised investment costs. Upgrades amount to 44 GW of

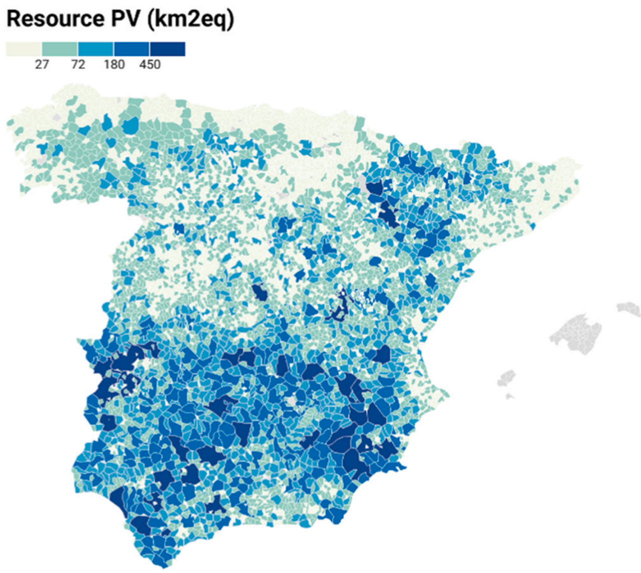

Fig. 16. Resource availability (km2eq) – PV.

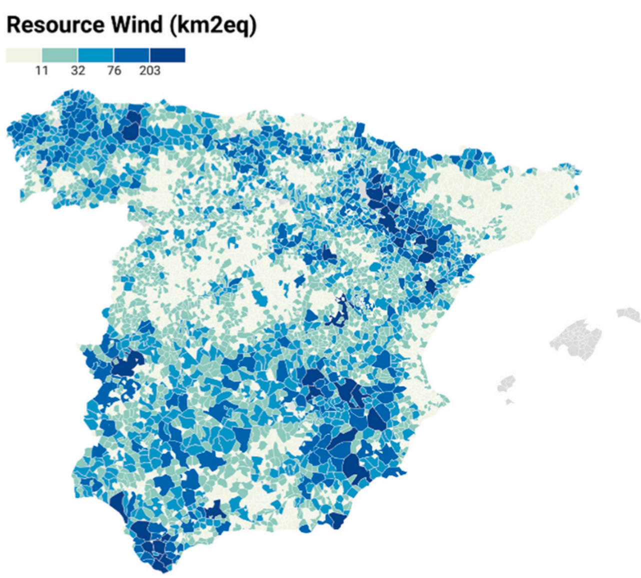

Fig. 17. Resource availability (km2eq) -Wind.

network assets, translating to 197 MEUR/yr of investment. The current regulated investment into the Spanish electricity distribution system is 2012 MEUR (CNMC, 2024). The investment presented in Fig. 22 represents a total of 2627 MEUR, amounting to 130 % of Spain's annual distribution grid investment limit, to be realised by 2030. However, it must be considered that those updates do not include any investment into digitalisation or replacement of assets due to end-of-life, which are expected to require significant investments (IEA, 2024b; Eurelectric, 2024). Furthermore, the upgrades for EV integration are limited to private charging infrastructure and do not account for commercial EV fleets or public charging infrastructure.

Fig. 23 shows the sensitivity results over available HC (3.2.1). Fig. 23 a) represents the stacking of investment requirements for integrating DG when accounting for the municipalities' HC as the sum of the nodes' HC. The magnitude is lower than the costs presented in Fig. 22 b) because the figure is limited to the costs induced for integrating DG; load is not included. Fig. 23 b) shows the investment in case no HC was available. The total costs amount to 131 MEUR/yr in a) and 149 MEUR/yr in b), representing a 14 % increase in the latter. This relatively small increase indicates that the geographical allocation of DG does not optimally exploit HC. Only 5.4 % and 7.6 % of HC are exploited at MV and HV level, respectively. Fig. 24 provides further insight into the issue by showing the total available HC (MV+HV) according to the distribution zone. It shows that most HC is in U and SU municipalities. However, DG capacity is assigned mainly to RC municipalities (Fig. 19). Although this is not an optimal result in terms of exploiting existing grid capacity, factors such as resource availability and environmental sensitivity play a significant role in site selection, driving DG away from municipalities with available HC.

Fig. 25 presents a disaggregation of the distribution grid reinforcement costs triggered by DG (Fig. 21a) and those triggered by load electrification L (Fig. 21b). The different columns for load represent the costs associated with the sensitivities according to the different LV load simultaneity factors described in 3.2.2. The figure shows that, at the LV simultaneity factor of 0.4 (Table 7), the network upgrade costs for load electrification are half the DG integration costs. Grid expansion for integrating DG cannot offset the requirements for load increase due to the different geographical allocations of DG and load (Fig. 18). As LV load simultaneity factors increase towards 0.8, grid costs approach the magnitude of DG. At LV load simultaneity factors of 0.9 or 1, grid costs for load surpass those for DG. Realistic values of future LV simultaneity factors might be between 0.4 and 0.8, as the coefficient describes the simultaneity of the entire load. The base load will likely follow historical simultaneity factors, while electricity demand for EVs or HPs might show higher simultaneity factors. Consequently, the simultaneity factor of the entirety of the load is not expected to reach 1. In any case, the efficient management of future electricity demand is crucial for maintaining distribution grid costs at a reasonable magnitude.

5. Conclusions

This paper presents a deterministic model for calculating distribution grid reinforcement requirements for integrating distributed generation (DG), electric vehicles (EVs) and heat pumps (HPs) throughout Spain. DG covers PV and wind installations. The assessment is carried out for the over 8000 peninsular municipalities and includes LV, MV and HV grids. Electricity distribution expansion costs for MV and HV networks are extracted from the project database of a Spanish DSO and extrapolated to the rest of the territory.

All municipalities are first classified into urban (U), semi-urban (SU), rural concentrated (RC), and rural dispersed (RD) distribution zones according to the Spanish regulation. DG, EVs and HPs are then geographically allocated to the municipalities via individual criteria. DG is allocated differently for prosumer and utility-scale installations.

Distribution grid reinforcement requirements are determined differently for DG and load electrification. The network's nodal HC for accommodating DG is publicly available for voltage levels above 1 kV. Due to the lack of information below 1 kV, zero available HC is assumed for LV PV integration. For load, reinforcement is determined via the peak load increase associated with EV and HP allocation. The resulting reinforcement for each voltage level is determined via simultaneity factors, considering zero available HC for load.

The model's functionality is demonstrated by implementing a 2030 NECP case study. The case study shows that future DG installations are allocated to networks in semi-urban and rural concentrated municipalities. Both resource availability and environmental sensitivity are favourable in SU and RC municipalities. The main part of DG capacity is assigned to HV networks due to the employment of historical data for allocating DG to voltage levels. Despite the availability of HC, a significant part of DG triggers reinforcement due to the location in mainly RC municipalities, while HC availability is dominant in U and SU municipalities.

The peak load increase is allocated equally to all grid zone types except RD due to the low population density of RD municipalities. The

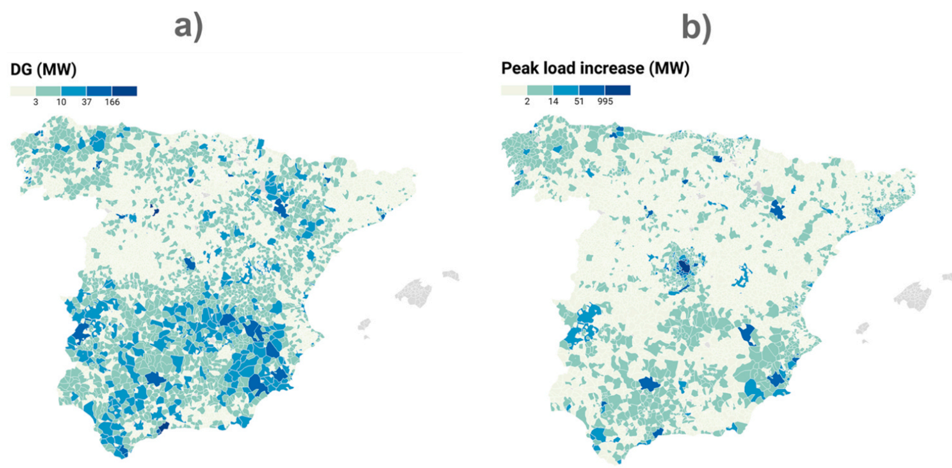

Fig. 18. Geographical allocation of a) peak load increase, b) DG capacity.

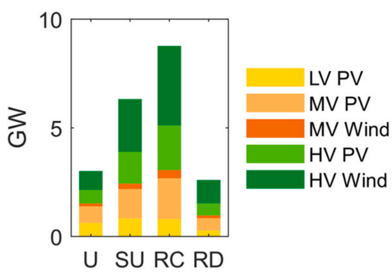

Fig. 19. Stacking of relative DG allocation to distribution supply zone type.

reinforcement due to load increase is around half the costs for integrating DG. However, a sensitivity analysis of the LV load simultaneity factor indicates that increasing simultaneity due to electrification may lead to load-induced costs surpassing DG-induced costs at an LV simultaneity factor of 0.8 and above. This highlights the importance of the efficient management of EVs and HPs so as not to aggravate their impact on distribution grid reinforcement.

The allocation maps of DG and load increase throughout the territory show that future DG capacities are not geographically aligned with the peak load increase. This finding points out that the DSOs covering different parts of the territory are likely to face a variety of challenges

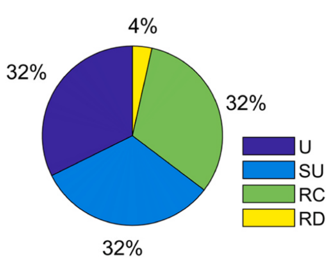

Fig. 20. LV peak demand increase per grid zone.

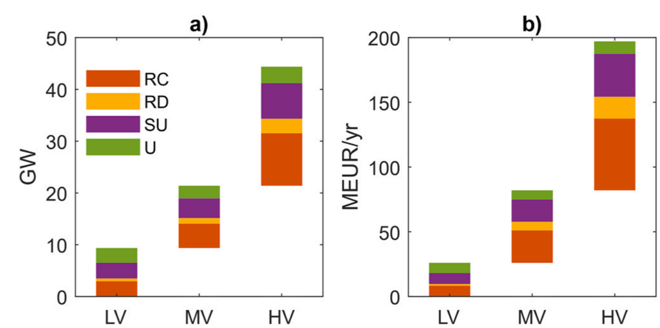

Fig. 22. Reinforcement requirements – a) Capacity and b) annualised investment.

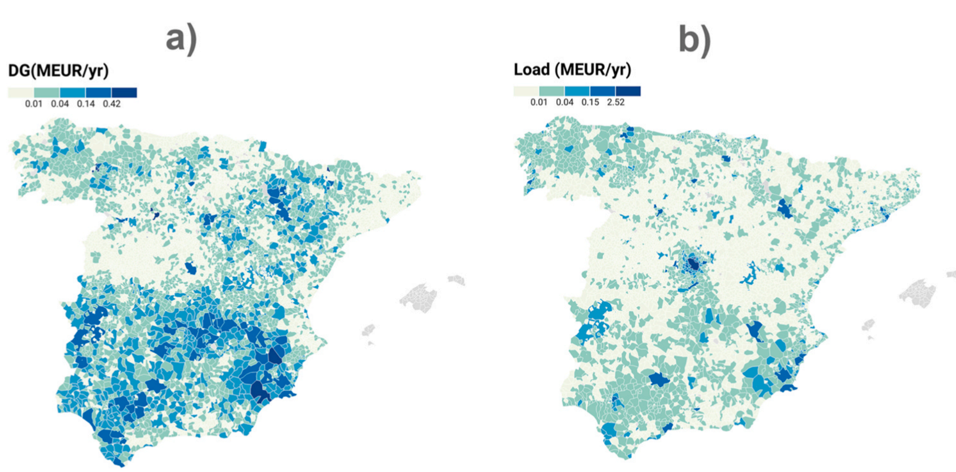

Fig. 21. Map of reinforcement cost triggered by a) DG integration, b) peak load increase.

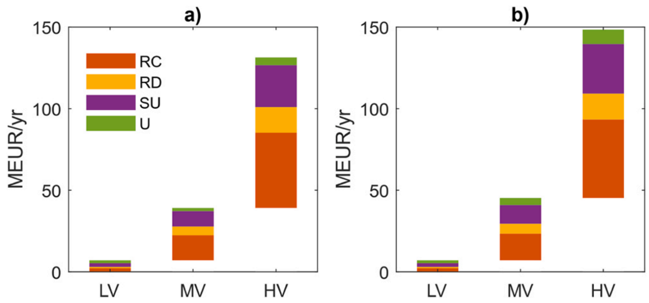

Fig. 23. DG-related investment requirements considering a) available HC and b) 0 available HC.

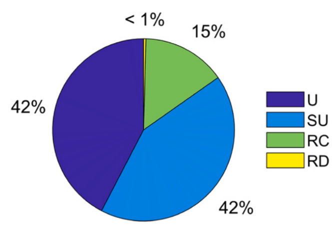

Fig. 24. HC according to grid supply zone.

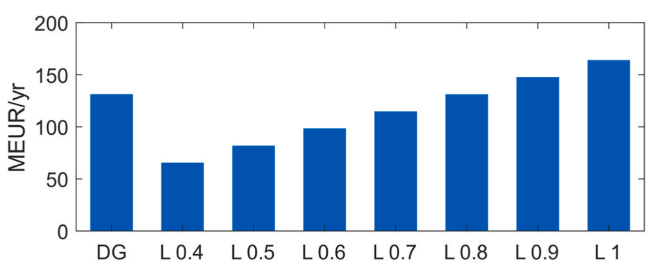

Fig. 25. Annualised investment for DG integration and load electrification sensitivities.

that are not aligned between the territories. The total required investment is 2627 MEUR, representing 130 % of Spain's annual electricity distribution investment limit.

The model represents a tool to efficiently assess the impact of the geographical allocation of DG and load electrification on distribution grids of the whole Spanish peninsular territory based on the costs of actual projects in a Spanish DSOs' network. The model can be employed for other non-Spanish electricity systems when the corresponding input data is provided. Future work should focus on further disaggregating the cost catalogue to contemplate different costs for MV and HV grids and consider the asymmetric nature of costs for integrating generation and load. Furthermore, adding other aspects of electrification, such as public charging infrastructure, electrolysers or the electrification of industrial energy demand, can help further deepen the understanding of the impact of electrification on distribution networks.

CRediT authorship contribution statement

Leslie Herding: Writing – original draft, Visualization, Methodology, Investigation. **Manuel Pérez-Bravo:** Writing – original draft, Visualization, Methodology, Conceptualization. **Michel Rivier:** Writing – review & editing, Supervision, Methodology, Investigation, Funding acquisition, Conceptualization. **Roberto Barrella:** Writing – review & editing, Methodology, Conceptualization. **Rafael Cossent:** Writing – review & editing, Supervision, Methodology, Investigation.

Declaration of Competing Interest

The authors declare the following financial interests/personal relationships which may be considered as potential competing interests: Leslie Herding reports financial support was provided by Ministry of Science ˆfand Innovation and the Spanish State Research Agency. If there are other authors, they declare that they have no known competing financial interests or personal relationships that could have appeared to influence the work reported in this paper.

Acknowledgements

The authors would like to thank Santiago Serna for helping process input data. This research has been supported by the funding of the RETOS COLABORACIÓN programme by the Spanish Ministry of Science and Innovation and the Spanish State Research Agency (MODESC Project, with reference number RTC2019- 007315-3).

Appendix A. : Classification of Spanish municipalities according to distribution grid type

The Spanish municipalities are assigned to a distribution grid service zone according to an estimation of the number of residential supply points in the municipality. The Spanish Statistical Institute publishes the number of households for municipalities with over 2,000 inhabitants (INE, 2023a). This number is employed as an indicator of the number of residential electricity supply points for urban and semi-urban areas. It cannot be used to distinguish rural concentrated from rural dispersed areas because both consist of less than 2,000 supply points. The number of supply points for rural areas is simplified as the inhabitants (INE, 2023b).

The methodology is evaluated on the municipalities in the cooperating DSO's service territory. Table 10 shows the comparison. In the first step, the number of municipalities for each service zone is presented for both, the DSO data and the classification from the algorithm. The results from the algorithm are reduced to the municipalities of the DSO's service territory. The right side evaluates the correct assignations by the algorithm. Results show that urban and semi-urban areas are approximated closely to the DSO's classification of municipalities. The approach for the total zones leads to a shift from RC zones towards RD zones. Still, the majority of municipalities are classified correctly. Applying this approach to the entirety of the Spanish peninsular territory results in the identification of 24,796,759 residential service points. This amounts to 84% of the total registered Spanish service points in 2020 (CNMC, 2020). The final assignation of supply points to the peninsular municipalities is shown in Fig. 26.

Table 10
Verification of municipal grid type estimation via mixed criteria with the DSO's data

	Municipality classification		Correctly identified by the algorithm	
	DSO data	Algorithm	Total	Relative (of algorithm)
U	99	86	82	95%
SU	554	520	469	90%
RC	1957	1879	1649	88%
RD	1136	1264	977	77%

Table 11 evaluates the assignation regarding the number of municipalities and share of surface assigned to each service zone. The table points out that, in terms of the number of municipalities and surface, the majority of the peninsular territory is classified as a rural concentrated distribution grid service zone, while urban zones represent only a minor part of the territory. Rural dispersed areas represent only 13% of the surface despite accounting for 29% of the municipalities.

Table 11
Analysis of municipality service zone assignation

	Share of peninsular municipalities	Share of peninsular surface
U	2%	6%
SU	17%	30%
RC	52%	51%
RD	29%	13%

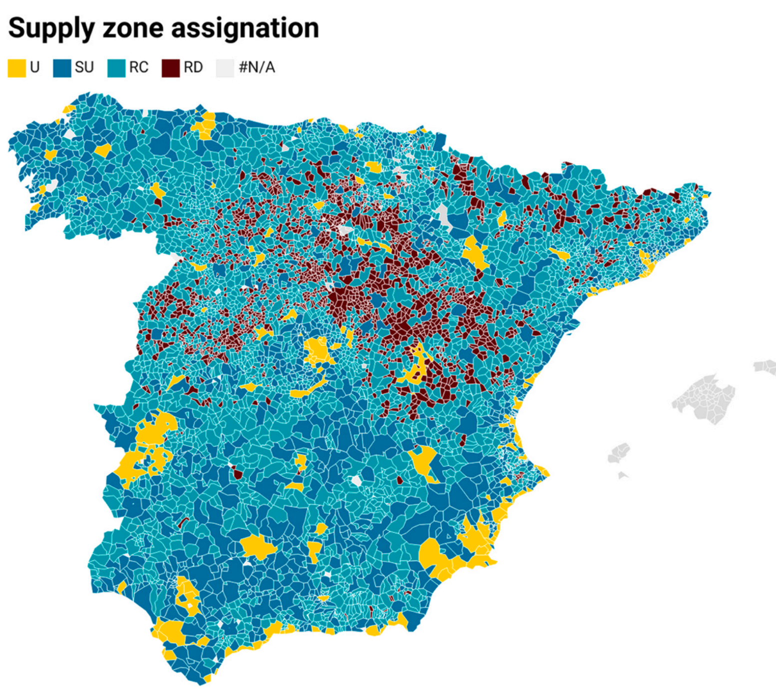

Fig. 26. Supply point assignation of Spanish municipalities.

Data Availability

Data will be made available on request.

References

Barrella, R., Blas-Álvarez, L., 2024. Unpacking the energy crisis impact with a multidimensional vulnerability index: a granular analysis of the Spanish case. GeoJournal. In press.

Barrella, R., Priego, I., Linares, J.I., Arenas, E., Romero, J.C., Centeno, E., 2020. Feasibility study of a centralised electrically driven air source heat pump water heater to face energy poverty in block dwellings in Madrid (Spain). Energies 13 (11). https://doi.org/10.3390/en13112723.

Barrella, R., Linares, J.I., Romero, J.C., Arenas, E., Centeno, E., 2021. Does cash money solve energy poverty? Assessing the impact of household heating allowances in Spain. Energy Res. Soc. Sci. 80, 102216. https://doi.org/10.1016/j.erss.2021.102216.

Barrella, R., Linares, J.I., Romero, J.C., Arenas, E., 2023. Evaluating the impact of energy efficiency strategies on households' energy affordability: a Spanish case study. Energy Build. 295. https://doi.org/10.1016/j.enbuild.2023.113289.

CNMC, 'Los cuatro comercializadores con mayores cuotas en el sector eléctrico redujeron en más de ocho puntos porcentuales la cuota de clientes del mercado libre entre 2017 y 2020'. Accessed: Oct. 02, 2023. [Online]. Available: ⟨https://www.cnmc.es/prensa/informe-supervision-cambios-comercializador-2020t4⟩.
CNMC, 'Circular 1/2021'. Accessed: Sep. 19, 2021a. [Online]. Available: ⟨https://www.boe.es/eli/es/cir/2021/01/20/1/con⟩.
CNMC, 'Resolución de 20 de mayo de 2021b, de la Comisión Nacional de los Mercados y la Competencia, por la que se establecen las especificaciones de detalle para la determinación de la capacidad de acceso de generación a la red de transporte y a las redes de distribución'. Accessed: Sep. 13, 2021. [Online]. Available: ⟨https://www.boe.es/eli/es/res/2021/05/20/(4)⟩.
CNMC, 'Información mensual de estadísticas sobre las ventas de régimen especial'. Accessed: Oct. 07, 2022. [Online]. Available: ⟨https://www.cnmc.es/estadistica/informacion-mensual-de-estadisticas-sobre-produccion-de-energia-electrica-partir-de-8⟩.
CNMC, 'INF/DE/007/22 - PLANES DE INVERSIÓN DISTRIBUCIÓN -2022-2024'. Accessed: May 23, 2024. [Online]. Available: ⟨https://www.cnmc.es/expedientes/infde00722⟩.
Dirección General de Carreteras, 'Portal estadístico'. Accessed: May 02, 2024. [Online]. Available: ⟨https://sedeapl.dgt.gob.es/WEB_IEST_CONSULTA/subcategoria.faces⟩.
Drechsler, M., Egerer, J., Lange, M., Masurowski, F., Meyerhoff, J., Oehlmann, M., 2017. Efficient and equitable spatial allocation of renewable power plants at the country scale. Nat. Energy 2 (9). https://doi.org/10.1038/nenergy.2017.124.
Duarte, R., Miranda-Buetas, S., Sarasa, C., 2021. Household consumption patterns and income inequality in EU countries: scenario analysis for a fair transition towards low-carbon economies. Energy Econ. 104, 105614. https://doi.org/10.1016/j.eneco.2021.105614.
e-distribución, 'Nodos de capacidad acceso'. Accessed: Feb. 13, 2023. [Online]. Available: ⟨https://www.edistribucion.com/content/edistribucion/es/red-electrica/Nodos_capacidad_acceso.html⟩.
Ehsan, A., Yang, Q., 2018. Optimal integration and planning of renewable distributed generation in the power distribution networks: a review of analytical techniques. Appl. Energy 210, 44–59. https://doi.org/10.1016/j.apenergy.2017.10.106.
Elmallah, S., Brockway, A.M., Callaway, D., 2022. Can distribution grid infrastructure accommodate residential electrification and electric vehicle adoption in Northern California? Environ. Res.: Infrastruct. Sustain. 2 (4), 045005. https://doi.org/10.1088/2634-4505/ac949c.
E-REDES, 'Información sobre la Capacidad de la red E-REDES'. Accessed: Feb. 13, 2023. [Online]. Available: ⟨https://www.eredesdistribucion.es/instalaciones/informacion-sobre-la-capacidad-de-la-red⟩.
Eurelectric, 'Grids for speed - Eurelectric Power Summit 2024'. Accessed: May 23, 2024. [Online]. Available: ⟨https://powersummit2024.eurelectric.org/grids-for-speed/⟩.
European Commission, 'National energy and climate plans'. Accessed: May 04, 2022. [Online]. Available: ⟨https://commission.europa.eu/energy-climate-change-environment/implementation-eu-countries/energy-and-climate-governance-and-reporting/national-energy-and-climate-plans_en⟩.
European Commission, 'Homepage | European Alternative Fuels Observatory'. Accessed: May 02, 2024a. [Online]. Available: ⟨https://alternative-fuels-observatory.ec.europa.eu/⟩.
European Commission, 'Energy union'. Accessed: Oct. 15, 2024b. [Online]. Available: ⟨https://energy.ec.europa.eu/topics/energy-strategy/energy-union_en⟩.
Eurostat, 'NUTS - Nomenclature of territorial units for statistics'. Accessed: Oct. 07, 2024a. [Online]. Available: ⟨https://ec.europa.eu/eurostat/web/nuts⟩.
Eurostat, 'Local administrative units (LAU)'. Accessed: Oct. 07, 2024b. [Online]. Available: ⟨https://ec.europa.eu/eurostat/web/nuts/local-administrative-units⟩.
Ferreira, T.S.D., Trindade, F.C.L., Pinto, Y.G., Freitas, W., 2020. New analytical method for analysing the effectiveness of infrastructure reinforcement in electric power distribution systems. Electr. Power Syst. Res. 182, 106250. https://doi.org/10.1016/j.epsr.2020.106250.
Gupta, R., et al., 2021. Spatial analysis of distribution grid capacity and costs to enable massive deployment of PV, electric mobility and electric heating. Appl. Energy 287, 116504. https://doi.org/10.1016/j.apenergy.2021.116504.
D. Hall and N. Lutsey, 'Electric vehicle charging guide for cities'.
Herding, L., Cossent, R., Rivier, M., Chaves-Ávila, J.P., Gómez, T., 2021. Assessment of electricity network investment for the integration of high RES shares: a Spanish-like case study. Sustain. Energy, Grids Netw. 28, 100561. https://doi.org/10.1016/j.segan.2021.100561.
Home-Ortiz, J.M., Pourakbari-Kasmaei, M., Lehtonen, M., Sanches Mantovani, J.R., 2019. Optimal location-allocation of storage devices and renewable-based DG in distribution systems. Electr. Power Syst. Res. 172, 11–21. https://doi.org/10.1016/j.epsr.2019.02.013.
i-DE, 'Mapa de Capacidad'. Accessed: Feb. 13, 2023. [Online]. Available: ⟨https://www.i-de.es/conexion-red-electrica/produccion-energia/mapa-capacidad-acceso⟩.
IEA, 'Unlocking the Potential of Distributed Energy Resources', IEA. Accessed: May 01, 2024a. [Online]. Available: ⟨https://www.iea.org/reports/unlocking-the-potential-of-distributed-energy-resources⟩.
IEA, 'Annual investment in electricity networks 2019-2030 in the Stated Policies Scenario – Charts – Data & Statistics', IEA. Accessed: May 23, 2024b. [Online]. Available: ⟨https://www.iea.org/data-and-statistics/charts/annual-investment-in-electricity-networks-2019-2030-in-the-stated-policies-scenario⟩.
INE, 'Renta por hogar por comunidades autónomas', INE. Accessed: May 16, 2022a. [Online]. Available: ⟨https://www.ine.es/jaxiT3/Tabla.htm?t=9949⟩.
INE, 'Edificios según tipo de edificio por tamaño del municipio y no de inmuebles', INE. Accessed: Jul. 27, 2022b. [Online]. Available: ⟨https://www.ine.es/jaxi/Tabla.htm?path=/t20/e244/edificios/p03/l0/&file=01001.px&L=0⟩.
INE, 'Viviendas por municipios (con más de 2.000 habitantes) y tipo de vivienda', INE. Accessed: May 11, 2023a. [Online]. Available: ⟨https://www.ine.es/jaxiT3/Tabla.htm?t=3456⟩.
INE, 'Censos de Población y Viviendas 2011. Resultados Municipales'. Accessed: Feb. 13, 2023b. [Online]. Available: ⟨https://www.ine.es/jaxi/Tabla.htm?path=/t20/e244/avance/p02/l0/&file=1mun00.px⟩.
LaMonaca, S., Ryan, L., 2022. The state of play in electric vehicle charging services – a review of infrastructure provision, players, and policies. Renew. Sustain. Energy Rev. 154, 111733. https://doi.org/10.1016/j.rser.2021.111733.
Lee, S.H., Park, J.-W., 2013. Optimal placement and sizing of multiple DGs in a practical distribution system by considering power loss. IEEE Trans. Ind. Appl. 49 (5), 2262–2270. https://doi.org/10.1109/TIA.2013.2260117.
Lee, S.-H., Park, J.-W., 2009. Selection of optimal location and size of multiple distributed generations by using Kalman filter algorithm. IEEE Trans. Power Syst. 24 (3), 1393–1400. https://doi.org/10.1109/TPWRS.2009.2016540.
Ministerio de Economía, 'Real Decreto 1955/2000'. [Online]. Available: ⟨https://boe.es/buscar/act.php?id=BOE-A-2000-24019⟩.
Ministerio de Vivienda y Agenda Urbana, DG de Vivienda y Suelo, 'Áreas urbanas en España, 2023', 2023. [Online]. Available: ⟨https://www.mivau.gob.es/urbanismo-y-suelo/suelo/atlas-estadistico-de-las-areas-urbanas⟩.
MITECO, 'Calidad del servicio - Índices zonales agregados'. Accessed: Feb. 13, 2023a. [Online]. Available: ⟨https://energia.serviciosmin.gob.es/Gecos/DatosPublicos/IndicesAgregados⟩.
MITECO, 'GeoPortal'. Accessed: Feb. 13, 2023b. [Online]. Available: ⟨https://sig.mapama.gob.es/geoportal/⟩.
MITECO and REE, 'Plan de desarrollo de la Red de Transporte de Energía Eléctrica Período 2021-2026'. 2024. Accessed: Oct. 14, 2024. [Online]. Available: ⟨https://www.planificacionelectrica.es/sites/default/files/2024-04/REE_PLAN_DESARROLLO_MAP.pdf⟩.
Pesaran H.A, M., Huy, P.D., Ramachandaramurthy, V.K., 2017. A review of the optimal allocation of distributed generation: objectives, constraints, methods, and algorithms. Renew. Sustain. Energy Rev. 75, 293–312. https://doi.org/10.1016/j.rser.2016.10.071.
Pieltain Fernandez, L., Gomez San Roman, T., Cossent, R., Mateo Domingo, C., Frias, P., 2011. Assessment of the impact of plug-in electric vehicles on distribution networks. IEEE Trans. POWER Syst. 26 (1), 206–213. https://doi.org/10.1109/TPWRS.2010.2049133.
G. Prettico, F. Gangale, A. Mengolini, A. Lucas, and G. Fulli, 'Distribution System Operators Observatory: From European Electricity Distribution Systems to Representative Distribution Networks'. EUR 27927 EN; ⟨10.2790/701791⟩, 2016. [Online]. Available: ⟨https://publications.jrc.ec.europa.eu/repository/bitstream/JRC101680/ldna27927enn.pdf⟩.
REE, 'Bienvenido | ESIOS electricidad · datos · transparencia'. Accessed: Oct. 23, 2023. [Online]. Available: ⟨https://www.esios.ree.es/es⟩.
Röder, J., Meyer, B., Krien, U., Zimmermann, J., Stührmann, T., Zondervan, E., 2021. Optimal design of district heating networks with distributed thermal energy storages – method and case study. Int. J. Sustain. Energy Plan. Manag. 31, 5–22. https://doi.org/10.5278/ijsepm.6248.
Spanish Government, 'Spanish National Energy and Climate Plan - 2020 version'. Accessed: Oct. 26, 2023. [Online]. Available: ⟨https://commission.europa.eu/energy-climate-change-environment/implementation-eu-countries/energy-and-climate-governance-and-reporting/national-energy-and-climate-plans_en⟩.
Sun, J., Wen, W., Wang, M., Zhou, P., 2022. Optimizing the provincial target allocation scheme of renewable portfolio standards in China. Energy 250, 123699. https://doi.org/10.1016/j.energy.2022.123699.
L. Sunderland and D. Gibb, 'Taking the burn out of heating for low-income households', Regulatory Assistance Project. Accessed: Jun. 10, 2024. [Online]. Available: ⟨https://www.raponline.org/knowledge-center/taking-burn-out-of-heating-low-income-households/⟩.
Transport and Environment, 'Recharge EU: How many charge points will EU countries need by 2030', Jan. 2020. Accessed: May 02, 2024. [Online]. Available: ⟨https://www.transportenvironment.org/discover/recharge-eu-how-many-charge-points-will-eu-countries-need-2030/⟩.
UFD, 'Capacidad de acceso para la conexión de generación en nuestras subestaciones', Distribuidora de electricidad del Grupo Naturgy. Accessed: Feb. 13, 2023. [Online]. Available: ⟨https://www.ufd.es/capacidad-de-acceso-de-generacion/⟩.
UNEF, 'El autoconsumo fotovoltaico instalado en España creció un 108% respecto a 2021', UNEF. Accessed: Jan. 30, 2023. [Online]. Available: ⟨https://www.unef.es/es/comunicacion/comunicacion-post/⟩.
Viesgo, 'Capacidades de la red - Viesgo Distribución'. Accessed: Feb. 13, 2023. [Online]. Available: ⟨https://www.viesgodistribucion.com/capacidades-de-la-red⟩.
S. Villasur, 'Derechos de acometida: definición y precios', Roams. Accessed: Mar. 17, 2023. [Online]. Available: ⟨https://energia.roams.es/luz/derechos-acometida⟩.
Vu, T., 2018. A Stochastic methodology to determine reinforcement cost of power distribution grid for integrating increasing share of renewable energies and electric vehicles. 2018 15th Int. Conf. Eur. Energy Mark. (EEM) 1–5. https://doi.org/10.1109/EEM.2018.8469890.
Xu, J., Lv, T., Hou, X., Deng, X., Liu, F., 2021. Provincial allocation of renewable portfolio standard in China based on efficiency and fairness principles. Renew. Energy 179, 1233–1245. https://doi.org/10.1016/j.renene.2021.07.101.

7.4 Paper 4

- We assess a relaxation of the calculation criteria for nodal hosting capacity.
- Dynamic HC (DHC) accounts for RES output stochasticity, enhancing grid flexibility.
- Security-aware DHC (SDHC) contemplates the probability N-1 contingencies.
- Security-aware DHC minimises risks, ensuring reliable energy integration.
- DHC and SDHC allow to inject significantly more energy compared to static HC.

A security-aware dynamic hosting capacity approach to enhance the integration of renewable generation in distribution networks

Leslie Herding , Leonel Carvalho, Rafael Cossent, Michel Rivier

Commonly, a network nodes' HC is calculated via conservative criteria to ensure network reliability. This paper evaluates the hourly additional energy that can be safely injected at the network when accounting for different concepts of HC. HC is evaluated as technologically neutral nodal HC.

1 Hosting capacity concepts

HC concept	Time granularity	Reliability considerations
SHC N-1	Static (1 hour)	Deterministic worst-case N-1
SHC N	Static (1 hour)	-
DHC N-1	Dynamic (hourly)	Deterministic worst-case N-1
DHC N	Dynamic (hourly)	-
SDHC	Dynamic (hourly)	Probabilistic N-1

2 Case study

All HC concepts are evaluated for three nodes of a MV network. Hourly HC concepts are evaluated hourly over various sample years.

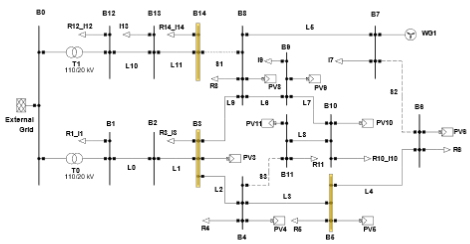

CIGRE MV network with DER

3 Impact of N-1 contingencies on HC

SHC N and DHC N allow for significant additional energy injections compared to SHC N-1.

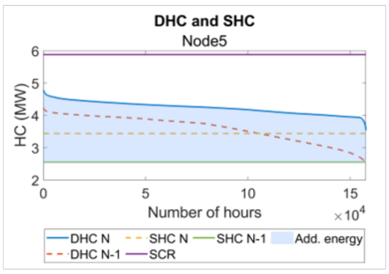

Despite being lower than SHC, worst-case DHC (DHC N-1) still offers at least 20% of additional injectable energy compared to SHC N-1. SDHC does not vary significantly from DHC. Both DHC and SDHC offer an increase of up to 69% of annual injectable energy.

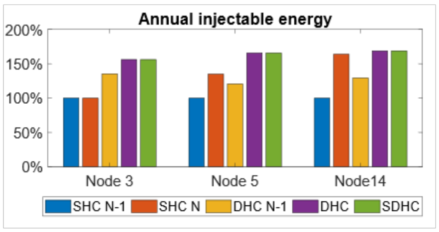

The security-aware DHC allows to minimise risks by contemplating for DHC in the case of asset failures according to probabilities. Due to the low probabilities of asset failures, SDHC does not vary significantly from DHC. The dynamic definition of HC allows to significantly increase the nodes' injectable energy without network reinforcement.

Electrical Power and Energy Systems 161 (2024) 110210

Contents lists available at ScienceDirect

International Journal of Electrical Power and Energy Systems

journal homepage: www.elsevier.com/locate/ijepes

A security-aware dynamic hosting capacity approach to enhance the integration of renewable generation in distribution networks

Leslie Herding [a,*], Leonel Carvalho [b], Rafael Cossent [a], Michel Rivier [a]

[a] Institute for Research in Technology (IIT), ICAI School of Engineering, Universidad Pontificia Comillas, C/Santa Cruz de Marcenado 26, 28015 Madrid, Spain
[b] INESC TEC, Rua Dr. Roberto Frias #378, 4200-465 Porto, Portugal

ARTICLE INFO

Keywords:
Flexible connections
Dynamic hosting capacity
Probabilistic analysis
N-1 contingencies
Distributed generation
Distribution grids

ABSTRACT

Hosting capacity (HC) describes the electricity network's ability to accommodate distributed generation (DG) without deteriorating electrical performance indicators. Distribution system operators typically express their networks' HC as a single threshold, called static hosting capacity (SHC). SHC is determined via conservative regulatory criteria, increasing connection costs and time. This paper explores the potential for additional energy injection into the network via dynamic hosting capacity (DHC). A network node's DHC is derived from the hourly operation of the network, accounting for the time variability of existing distributed generation (DG) output and demand. The methodology considers the network assets' N-1 contingencies and their probabilities, defining the security-aware DHC (SDHC). The SDHC definition is technologically neutral. Through a case study of a radial medium voltage distribution network, the paper highlights the significant limitations of SHC due to conservative calculation criteria mandated by regulators. Annual injectable energy is increased by 62% to 76% when comparing DHC to SHC. Variations between average DHC and SDHC are below 0.01% due to low N-1 probabilities. This finding points out the potential of dynamic hosting capacity definitions, allowing more efficient use of the existing network and facilitating the integration of new DG capacity with reduced connection costs and time.

1. Introduction

Significant additions of renewable energy sources (RES) into the distribution networks are expected over the following decades. The permitting process is one of the main bottlenecks for RES expansion, which is brought up frequently within the sector and is well-known by policymakers [1,2,3]. The electricity grid plays a significant role in integrating new RES generation [4]. Network congestion due to the increasing integration of distributed generation (DG) is already prevalent in European distribution networks [5]. The grid's capacity to integrate further generation or demand is denominated hosting capacity (HC). For the determination of a network node's available HC, the impact of connecting a new unit on performance indicators such as power quality is considered [6]. The capacity of RES that can be connected to the node without exceeding the limit of the performance index is the HC [7].

The European Commission encourages the publication of available network HC to provide transparency to RES promoters and direct connection requests to areas with available grid capacity [8]. Several distribution system operators (DSOs) already provide this information in the form of lookup tables or interactive maps [9,10,11,12,13]. These available HCs commonly represent a static threshold determined via regulatory criteria. However, due to the conservative criteria for calculating the network's HC, reinforcement requirements are often determined for assets that might only be used for a few hours per year [14]. This poses an unnecessary economic burden on connection seekers and increases connection times due to time-consuming network expansion works [8,15]. Flexibility mechanisms can be a valuable tool to reduce distribution network infrastructure investments [14]. One of those tools is flexible network access. Opposed to firm access, flexible network access allows for a more dynamic definition of the network capacity offered to a network user [8]. It represents the option for the DSO to define the network's HC more dynamically to adjust to the operational reality of demand and RES generation fluctuations instead of calculating a static hosting capacity (SHC) threshold as currently performed by most DSOs [5,16]. Increasing advances in digitalisation already performed or foreseen for the near future allow for more monitorisation and a more dynamic operation of electricity distribution grids

* Corresponding author.
E-mail address: lherding@comillas.edu (L. Herding).

https://doi.org/10.1016/j.ijepes.2024.110210
Received 29 February 2024; Received in revised form 2 July 2024; Accepted 27 August 2024
Available online 4 September 2024

[17]. A dynamic control of power injection according to the instantaneous performance of the grid may be expected, enhancing the viability of applying a dynamic HC approach.

Distribution grid HC for integrating RES has been subject to studies for years [6,7,18]. The literature can be categorised according to two dimensions: i) how HC is defined, and ii) the quantification methodology.

The definitions of HC uncertainty, stochastic HC, and locational HC have been reviewed in [19]. However, the HC of modern power systems is of a dynamic nature due to changing load patterns and variable RES availability. Stochastic HC contemplates uncertainties influencing the network's HC. Still, many stochastic HC evaluations define HC as a single threshold applied throughout the whole year [20]. A dynamic definition of HC can speed up the integration of RES into existing electricity networks [21]. A typical Scottish network's HC is evaluated for integrating wind energy via a deterministic and a dynamic probabilistic approach in [22]. The authors focus on determining the HC of the network as a whole rather than exploring the benefits of dynamic hosting capacity (DHC) over SHC. A weekly definition of DHC for integrating PV at a university building in Morocco is evaluated in [23]. The network node's DHC is calculated in the first step, and the optimal PV generator's size in the second step.

The HC of 17 real utility distribution feeders to integrate increasing penetrations of PV is evaluated via a genetic algorithm in [24]. HC is assessed via the Monte Carlo (MC) method based on maximum and minimum daytime load to express extreme operating scenarios. Final HC is determined via a conservative approach as the minimum of detected thresholds. A linear power flow algorithm for maximising a distribution network's HC is proposed in [6]. HC is considered a static threshold for different sets of nodes of the IEEE 33-bus network with no existing DG. A computationally efficient methodology to determine a network's SHC for integrating PV is proposed in [25]. The authors of [26] show via thermal models that implementing dynamic thermal transformer rating allows to connect PV capacity surpassing the rated transformer capacity. The benefits of a dynamic definition of HC for PV that allows for temporary violations of the network's operational limits are evaluated via quasi-static time-series analysis in [27]. In the dynamic evaluation, HC is 60 % to 200 % higher than SHC for the worst-case moment of maximum PV-to-load ratio. However, the final HC results obtained from the dynamic evaluation are presented as a static threshold of PV capacity.

Based on the limitations defined on the literature review, this work contributes the following:

1. **Evaluation of DHC over SHC:** Literature focuses on different HC definitions for integrating a specific technology, i.e. PV or wind power. This work employs an approach similar to the results presented in [23]. HC is evaluated from a network node's point of view, independent of a generation unit's size. The proposed methodology presents an approach to assess the benefits of dynamic hosting capacity versus static hosting capacity, with the latter being determined via conservative regulatory criteria currently applied in Spain, considered representative of common as-usual conservative criteria for SHC computations. DHC is subject to the operating conditions derived from RES and load which are represented as hourly curves to capture the variability throughout the year.
2. **Technologically neutral evaluation of HC:** Both SHC and DHC are calculated from a network perspective, i.e., technologically neutral, as DSOs require. This means that hosting capacity is presented as a network node's HC rather than the HC for a specific generation technology under evaluation. The modelling of DHC accounts for the uncertainty of renewable energy availability by employing several sample years in a combinatorial analysis and the time variability of the demand throughout the year. DHC and SHC are compared in terms of energy injection into the network.
3. **Definition of security-aware dynamic hosting capacity to account for network contingencies' probabilities impact on DHC:** The model includes an evaluation of the impact of contingency considerations for a holistic comparison with existing regulations. DHC is assessed one by one for all network assets' N-1 failures. The network nodes' security-aware dynamic hosting capacity is introduced. It is derived by determining the DHC for each N-1 contingency, accounting for the respective probability of occurrence of the N-1 contingency scenario. It is presented as an hourly annual curve instead of a single threshold, allowing RES promoters to plan their investment optimally.

The rest of the paper is organised as follows: the modelling methodology of SHC, DHC and SDHC is presented in 2, and the case study design, including model inputs, is presented in 3. Section 4 presents the results of the case study on the benefits of SDHC over SHC. Section 5 concludes the paper.

2. Methodology

This work assesses the benefits of a flexible definition of nodal HC that accounts for realistic operating conditions resulting from the variability of RES and load throughout the year. The results of the analysis are limited to the node under evaluation, similar to hosting capacities published by DSOs [9,10,11,12,13]. The following definitions of different HC concepts are employed throughout this paper:

- **Static hosting capacity (SHC)**: single HC threshold derived via conservative criteria of minimum load and maximum availability of existing generation.
- **Dynamic hosting capacity (DHC)**: hourly curve of HC accounting for operating results based on load and existing generation profiles.
- **Security-aware hosting capacity (SDHC)**: hourly curve of HC accounting for DHC under N-1 contingencies of all normally closed network elements and their probabilities of occurrence.

Fig. 1 summarises the methodology for obtaining HC in its different definitions. Network reconfigurations r are employed to account for N-1 contingencies of the network assets compared to normal operating conditions N, while hours h convert HC from a static threshold to a dynamic definition.

A network node's hosting capacity is determined as the maximum injectable active power. The nodal maximum injectable energy is obtained via optimal power-flow (OPF) analysis to ensure that operational security limits are not violated. Secure network operation is guaranteed via thermal line limits and maximum voltage deviations. Note that although voltage regulation mechanisms such as tap changers and inverter controls may provide additional value to implementing a DHC approach, they have been excluded from the study since not all distribution grid zones may be able to resort to these devices. Consequently, the results shown are conservative and focus on the impact of RES and load variability alone.

The OPF's objective function seeks the minimisation of system costs. Hence, ascending cost signals are employed to ensure the merit order within the network. This will not result in an economic dispatch of the system components but is used to ensure that the cost minimisation algorithm does not curtail preexisting generators or load to increase HC. Cost signals rank the merit order as follows:

1. **Existing generation capacity:** preexisting generators in the network must not be curtailed to inject more energy at the node under HC evaluation.
2. **HC evaluation node:** energy injected at the HC evaluation node.
3. **Import from the external grid:** electricity imports from the upstream network to cover local demand.

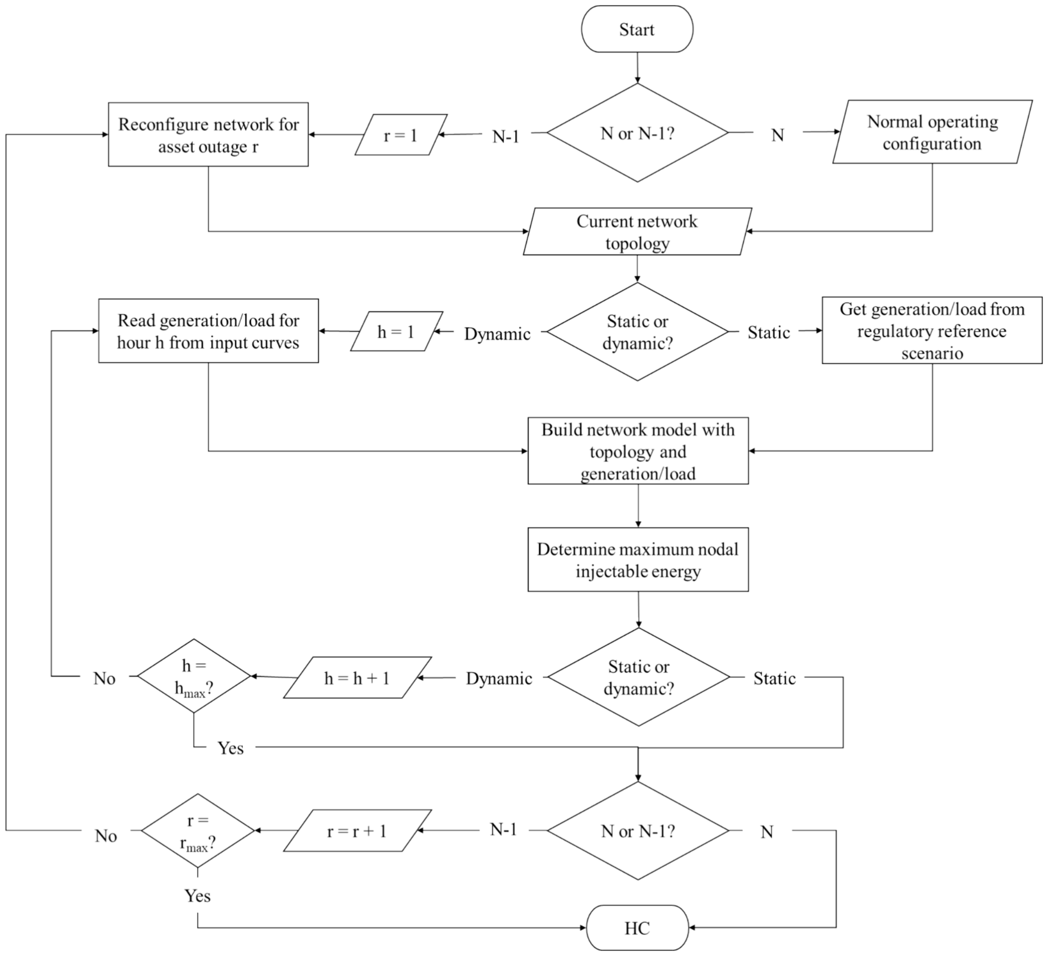

Fig. 1. Model flowchart for obtaining HC.

4. **Energy non-served:** load curtailments represent a last-resort mechanism to ensure the safe operation of the network within security limits.

Furthermore, some countries' regulations require the evaluation of HC accounting for short-circuit currents. For example, Spanish regulation defines the short-circuit ratio (SCR) for each distribution network node as [28] presented in Eq. (1), where Scc represents three-phase short-circuit power, and P_{MPEi} is the capacity of all N generation units connected at the node under analysis. SCR considerations are limited to the static evaluation under normal operating network configuration. Dynamic SCR due to different reconfigurations and varying demand/generation patterns are out of the scope of this work.

$$SCR = \frac{S_{cc}}{\sum_i^N P_{MPE_i}} \tag{1}$$

The result of the optimisation represents nodal HC. Different network nodes are evaluated in this study to obtain a broader understanding of SHC, DHC and SDHC. In this section, the criteria for the calculation of the different hosting capacities are described. SHC is calculated according to the regulatory requirements described in 2.1, and DHC modelling is described in 2.2. SDHC modelling is described in 2.3.

2.1. Static hosting capacity according to regulatory requirements

A node's SHC is the maximum injectable energy for the reference scenario without violating the operational security limits. Static hosting capacity is evaluated based on peak generation and valley load to guarantee the available HC at all hours. As for considerations of network unavailability, worst-case SHC is assessed under N-1 contingency conditions. SHC under N-1 contingencies is evaluated, including network reconfigurations to ensure service availability in case of asset failure. Dynamic network reconfiguration (DNR) is considered according to [29]. The multi-objective, multi-period DNR model aims to optimise the network topology by minimising the overall operation cost of a distribution system. The objective function considers the cost components outlined in [29]: i) Network power losses, and ii) Costs associated with lines and transformers overloading, and bus voltage violations. The DNR objective function is subject to four groups of constraints: power balance, power flow limits, switching operations, and topological constraints such as radiality. In this work, the employment of DNR is limited to the reconfiguration after asset failures and not as a HC enhancement technology to guarantee that the conclusions obtained result from the variability of RES and load.

SHC results are assessed for normal operating conditions (SHC N) and asset contingencies (SHC N-1).

2.2. Dynamic hosting capacity

Dynamic hosting capacity (DHC) is evaluated as the maximum hourly injectable energy without violating the operational security limits. The evaluated energy injection does not follow a PV or wind generation profile but is modelled as an infinite generator available at maximum capacity throughout all hours of the year. This allows to determine the technologically neutral maximum injectable energy from a grid perspective, maintaining operative security limits. The determined DHC can then be used optimally by installations of different technologies (e.g. PV, wind, batteries), including hybridisation. RES uncertainty in the model refers to the output of preexisting generation units. Various yearly conditions of PV and wind resource availability are identified and employed combinatorically, i.e. every sample year of PV availability is evaluated against every sample year of wind availability due to often low correlations between PV and wind availability [30,31,32]. All preexisting generators are granted priority over the new generator under evaluation, i.e. HC cannot be enhanced by curtailing existing generation capacity (see merit order in 2).

Similar to SHC, DHC for normal operating conditions (DHC N) is contrasted with available DHC in the case of asset failures (DHC N-1). N-1 contingencies are modelled including network reconfigurations to ensure service availability in case of asset failure [29]. DHC N-1 is defined hour by hour as the minimum HC obtained from computing all N-1 contingencies.

2.3. Security-aware dynamic hosting capacity

Security-aware dynamic hosting capacity is defined as the network node's DHC accounting for N-1 contingencies and their probabilities. Instead of defining HC as the deterministic minimum value obtained throughout contingency operation, SDHC accounts for the failure probabilities of network assets. Similar to DHC, it represents an hourly curve for each node. SDHC assessment does not consider the mean time to failure of network assets. Instead, the optimal network configurations corresponding to N-1 contingency scenarios are simulated for each combination of yearly conditions. N-1 contingency HC is defined via DHC N-1 obtained for each network asset as described in 2.2.

Eq. (2) details the calculation of SDHC, where h represents the hour of the year,j represents the number of network assets accounted for SDHC calculation (i.e. all normally closed lines and transformers), and i indexes the network component under N-1 contingency.FOR represents the forced outage rate of the normally closed network assets.

$$SDHC_h = DHC_h^N \left[\prod_{j=1}^{N} (1 - FOR_j) \right] + \sum_{i \in \Omega_{N-1}} DHC_{h,i}^{N-1} * FOR_i * \left[\prod_{\substack{j=1 \\ j \neq i}}^{N} (1 - FOR_j) \right] \tag{2}$$

3. Case study design

The modelling methodology is implemented in MATPOWER 7.1, employing the MATPOWER Interior Point Solver (MIPS) [33]. This section proceeds to present the distribution network employed for the case study (3.1) and details the input profiles for both load and existing RES generation (3.2), as well as the forced outage rate assumptions for N-1 modelling (3.3).

3.1. CIGRE benchmark network

Nodal HC is assessed with the CIGRE MV network with DER [34,35,36]. This radial benchmark distribution system operates at 20 kV (Fig. 2) and accounts for two downstream low voltage (LV) networks at nodes 1 and 12. This work defines security operating criteria according to the Spanish regulation. For this, thermal line limits are set to 70 % of a line's maximum capacity and maximum voltage deviations are limited to ± 7 % [37]. These limits align with UNE-EN 50,160 and are to be maintained during all static and dynamic hosting capacity scenarios. According to Spanish regulation, the specifications for HC assessment define that the SCR for each distribution network node must be greater than or equal to 6 [37]. These limits are applied to the CIGRE MV benchmark network.

Three sample nodes are selected for hosting capacity evaluation. The nodes are highlighted in yellow in Fig. 2. Node 3 is selected due to its proximity to the external grid, node 5 due to its location downstream in feeder 1, and node 14 due to its location in feeder 2.

N-1 contingencies are modelled under consideration of network reconfiguration using switches S1-S3 (Fig. 2). Failures of every normally

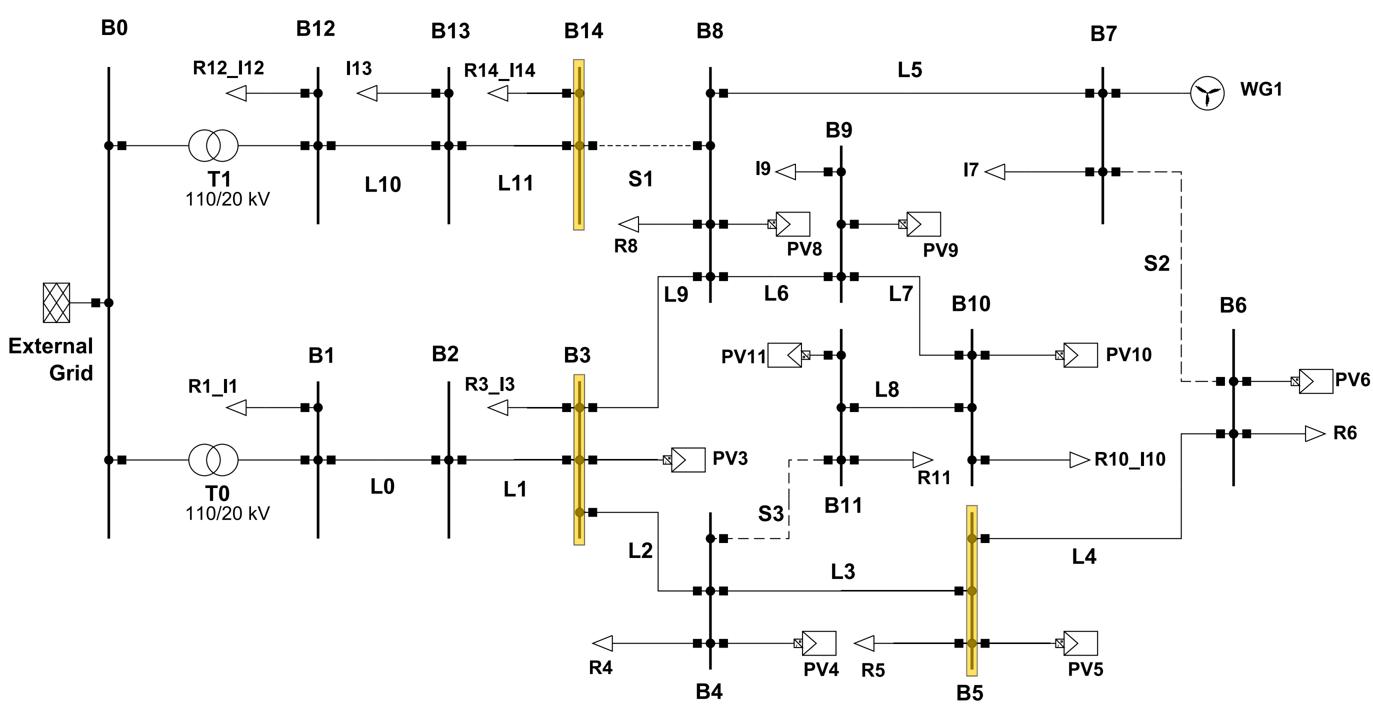

Fig. 2. Line diagram of the network.

closed line (L0 to L11) and both transformers are considered. Network reconfiguration is obtained via optimisation as in [29], and the results are annexed in Table 14.

3.2. Generation and load

3.2.1. Static reference scenario

The scenario for the calculation of SHC is determined according to Spanish regulation. Spanish DSOs are to evaluate the hosting capacity of their networks according to a reference scenario defined in regulation [28]. The scenario hypotheses are:

- **Minimum demand**: this demand is defined as 55 % of peak demand but can be substituted with minimum simultaneous system demand if sufficient data is available.
- **Maximum RES availability**: all generators connected to the grid and with permissions for connection granted are to be considered. At the node at which hosting capacity is evaluated, generators are considered at 100 % of their granted access capacity. At all other network nodes, generators are considered at 90 % of their granted access capacity.

3.2.2. Hourly load

Hourly load pu curves are extracted from the Spanish transparency platform ESIOS [38]. Residential load is assumed to follow the low voltage load curves, while commercial demand is assumed to follow the tariff category 6.1A, representing MV consumers [39]. Hourly curves are evaluated from 2015 to 2021 to determine the years with the greatest difference. A correlation analysis of the pre-crisis years shows no significant deviations in demand profiles throughout most of the years. Consequently, the pre-crisis year of 2019 is selected for load profiles. Furthermore, 2017 shows a seasonal variation from 2019 (Table 6) and is included in the analysis. Additionally, the load curves of 2021 are included in this analysis to account for the energy crisis years.

3.2.3. Hourly RES generation

The impact of RES generation uncertainty on HC is one of the key parameters to consider. Hence, several input profiles are selected to analyse the effect of RES stochasticity on the network's DHC. All curves represent RES availability in Almería, Spain and are derived from [40,41]. PV and wind curves evaluated for model input range from 2010 to 2022. In this work, RES variability is modelled via a combinatorial analysis of PV and wind generation profiles. Consequently, the 12 years of data on resource availability would lead to 144 RES years to model, leading to a total of 432 years due to the assessment of three load profile years. Due to the computational complexity of this issue, the amount of years to sample is reduced. Reducing the number of input curves is required for computational feasibility, as this analysis is carried out as a combinatorial analysis. The reduction of time series data is common in the literature [42]. The methodology for selecting sample years in this case study is not a novel contribution. It is chosen to select the sample years with a maximum variety. Thus, it allows to reduce computational effort while accounting for the variability of RES resource availability. In all cases, a very low correlation between solar and wind availability was observed (see Table 7 in the Annex).

As for PV, there is no significant variation throughout the years. The annexed Table 8 shows the correlations of the PV availabilities throughout the years 2010 to 2022. The lowest correlation is of 0.90. Hence, this metric is considered insufficient for selecting the study's sample years. Instead, years are selected based on the annual equivalent hours of the resource availability (Table 9). The years selected represent:

- High annual equivalent hours (2029 h in 2019)
- Medium annual equivalent hours (1972 h in 2016)
- Low annual equivalent hours (1911 h in 2010)

Table 1
Multi-criterion selection of wind resource sample years.

Year selected	Criteria
Y2014	Average annual equivalent hours; low CF at night, high CF during the afternoon; high CF in first months of the year
Y2015	Lowest annual equivalent hours
Y2016	Negative correlations with all years from 2018 onwards
Y2018	Highest monthly CF detected (March & April)
Y2021	Highest annual equivalent hours; high CF during night hours
Y2022	Low overall correlation with other years

For wind, the correlation analysis points out the randomness of resource availability (Table 10). Hence, a multi-criterion evaluation is carried out to reduce the sample years of wind resource availability. Criteria are annual equivalent hours (Table 11), average capacity factor (CF) per month of the year to express seasonality (Table 13), and average CF per hour of day (Table 13). The analysis allows to reduce the input profiles to six sample years, as explained in Table 1. As a result of the selection of sample years, DHC is derived from a combinatorial analysis of 3 load * 3 PV * 6 wind = 54 sample years instead of 432.

3.3. Network asset forced outage rates

For the computation of N-1 contingencies, the components' forced outage rates (FORs) are calculated. These FORs of the system components represent the probability of each N-1 contingency to happen. The probabilities are then applied to calculate the security-aware DHC.

Component failure rates are assumed to be of typical orders of magnitudes [43]. Table 2 shows an overview of the failure rate and the mean time to repair (MTTR) for overhead lines (OHL), cables and transformers.

These failure rates and the MTTR are applied to all normally closed network elements. Table 3 shows the resulting forced outage rates (FORs). The highest FOR is that of L1, with 0.057 %.

Table 2
Component failure rates [43].

Component	Failure rate λ *(per circuit mile and year)*	MTTR *(h)*
OHL	0.1	4
Cable	0.07	10
Transformer	0.04	40

Table 3
Forced outage rates of system components.

Element	Name	Type	Length *(km)*	FOR
L0	Line 1–2	Cable	2.82	0.036 %
L1	Line 2–3	Cable	4.42	0.057 %
L2	Line 3–4	Cable	0.61	0.008 %
L3	Line 4–5	Cable	0.56	0.007 %
L4	Line 5–6	Cable	1.54	0.020 %
L5	Line 7–8	Cable	1.67	0.021 %
L6	Line 8–9	Cable	0.32	0.004 %
L7	Line 9–10	Cable	0.77	0.010 %
L8	Line 10–11	Cable	0.33	0.004 %
L9	Line 3–8	Cable	1.3	0.017 %
L10	Line 12–13	OHL	4.89	0.036 %
L11	Line 13–14	OHL	2.99	0.022 %
T0	Transformer 0–1	25 MVA	–	0.018 %
T1	Transformer 0–12	25 MVA	–	0.018 %

4. Case study results

4.1. Static hosting capacity

As a first step of nodal HC assessment, SHC is determined according to the regulatory reference methodology. SHC is calculated for the reference scenario (section 2.1) under normal operating conditions (N), under N-1 contingencies, and according to the short-circuit ratio limitation. The minimum system demand of 13.7 MVA is detected on the 3rd of April of 2021 at 3 am, with commercial and residential loads at 30 % of their contracted capacity [34].

Fig. 3 shows an example of SHC determination under N-1 contingencies at node 5. The SHC for each contingency is compared to the reference scenario's SHC without contingency. The failure of lines connecting nodes 3 and 5 (L2 and L3) reduces the connectivity from node 5 with the rest of the network, reducing available HC. A failure in L9 has the same effect. Furthermore, failures affecting any line between L2 and L5 lead to the closure of S2. This is significant in the N-1 contingency scenario of L5, as it leads to a power flow from the wind farm towards the HC evaluation node, decreasing hosting capacity due to the priority of existing generation capacity. The smallest SHC at node 5 under N-1 contingency is 2.51 MW at a failure of L5.

Table 4 summarises the findings for the three nodes under evaluation. The N-1 criterion is the most limiting criterion at all of the nodes. This is hardly visible for node 3 but significantly reduces the SHC determined at nodes 5 and 14. As a result, the connection of new generation capacity to these network nodes is limited due to contingency considerations with minor FORs. At node 5, the minimum SHC is determined for the N-1 contingency at L5, as described above. At node 14, the N-1 contingency at $L11$ reduces the connectivity of node 14 and the residential demand feeder located at node 12, resulting in a SHC reduction of 2.02 MW from the 4.90 MW of SHC under normal operating conditions N.

Relaxing the SHC evaluation to normal operating conditions allows for + 30 % of injectable energy at node 5. At node 14, the additional injectable energy under SHC N compared to SHC N-1 is significant due to the magnitude of the reduction of SHC pointed out above. Compared to the restrictive SHC limited by contingency considerations at $L11$, SHC under normal operating conditions increases the injectable energy at node 14 by as much as 70 %. This finding underlines the value of introducing flexibility to be activated in low-probability events, i.e. relaxing the contingency consideration criterion for SHC assessment.

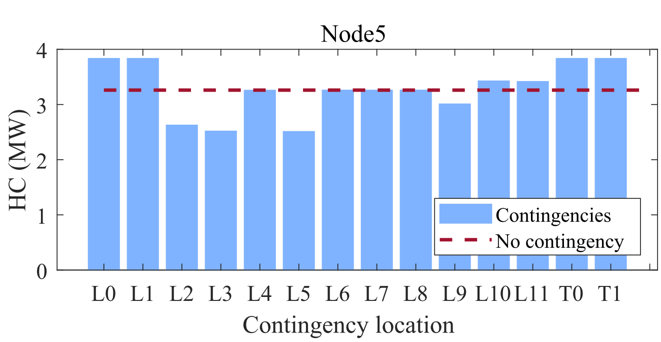

Fig. 3. SHC under N-1 contingencies for HC evaluation at node 5.

Table 4
SHC thresholds (MW) for each criterion of regulatory evaluation.

	Node 3	Node 5	Node 14
SHC N	3.25	3.26	4.90
SHC N-1	3.25	2.51	2.87
SCR	6.47	5.88	7.95
Limiting criterion	N-1 (L9)	N-1 (L5)	N-1 ($L11$)
Increase N vs N-1	0.13 %	+30 %	+70 %

4.2. Dynamic hosting capacity under normal operating conditions

After determining the SHC according to Spanish regulation, the network nodes' DHC is determined. The 18 years of hourly maximum injectable energy at the HC evaluation bus are evaluated as a load duration curve and compared to the SHC thresholds derived from regulation. For the sake of brevity, the analysis is carried out exemplary for one of the nodes under evaluation and compared to the other two nodes afterwards.

Fig. 4 presents the exemplary DHC load duration curves over the 54 sample years for node 5. DHC is compared to the different SHC thresholds according to the regulatory criteria. The figure shows the deviation between SHC N and the most restrictive SHC N-1 result mentioned previously (Table 4). Furthermore, the threshold derived from the short-circuit ratio is included in the figure. The filled blue area in Fig. 4 represents the maximum additional injectable energy in the case of DHC compared to the N-1 contingency SHC. The filled area represents an annual average of 67 % of injectable energy compared to the allowed injection under the N-1 restricted SHC.

Fig. 5 presents an analysis of DHC at node 5 throughout the hours of the day. This analysis is carried out to evaluate the dependence of HC and the input profiles. Hourly HC outputs of all 54 sample years are included in the boxplots. The figure points out that node 5 HC shows two peaks that coincide with the demand peaks of the Spanish electricity system, which does not vary throughout the sample years. The influence of the varying RES input profiles is not noticeable. The correlation between hourly hosting capacity and residential load is 0.99 at node 5. The correlations with RES profiles are insignificant: below 0.05 with wind and 0.35 with PV. The latter is influenced by the PV output peak coinciding with the central hours of the day when residential demand also peaks from 10:00 to 15:00.

Table 5 provides an overview of DHC under normal operating conditions N at the three nodes under analysis. DHC at all nodes is above the SHC threshold defined according to regulatory requirements, as indicated by the DHC N range in Table 5. DHC at node 14 shows a smaller range (4.64 MW to 5.2 MW) than the other nodes. Throughout the 54 sample years, DHC at node 14 is below SHC N for 83 h (0.018 %). At the other nodes, DHC is always above the regulatory reference scenario SHC N, pointing out the conservative assumptions of minimum load and

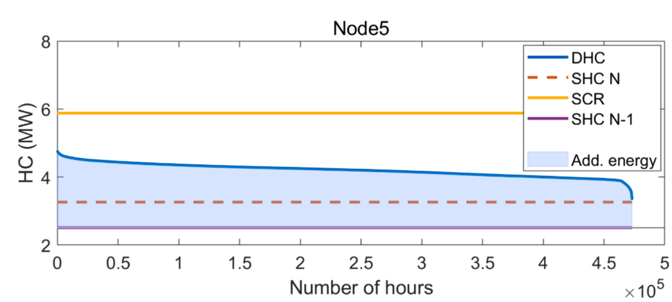

Fig. 4. Node 5 DHC load duration curve.

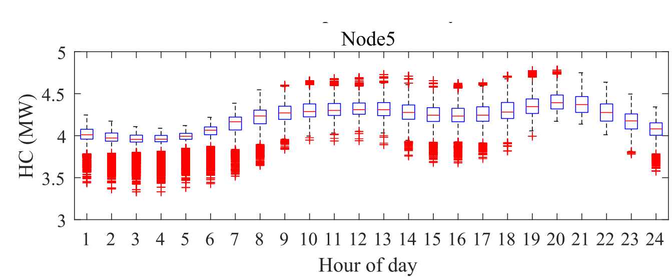

Fig. 5. Node 5 HC according to the hour of the day.

Table 5
Comparison of DHC results of nodes 3, 5 and 14 under normal operating conditions.

	Node 3	Node 5	Node 14
DHC range (N)	3.32 MW to 6.47 MW	3.33 to 4.78 MW	4.62 MW to 5.2 MW
Influent pu profiles	Residential load, wind	Residential load	Commercial load
Add. Energy/yr(DHC vs SHC N-1)	+62 %	+67 %	+76 %
Add. Energy/yr(DHC N-1 vs SHC N-1)	+34 %	+19 %	+27 %

maximum generation required for the reference scenario (2.1). DHC at node 5 ranges from 3.33 to 4.78 MW, while DHC at node 3 shows a significantly larger range (3.32 to the SCR cap of 6.47 MW). Node 3 is the only node where the SCR criterion limits DHC under normal operating conditions. The upstream location of node 3 close to the transformer station with a connected LV network increases the injectable energy. Node 14 is located in feeder 2, with no RES generation, resulting in HC depending on demand curves only, with a lower variability throughout the year. However, the increase from SHC to DHC is especially noticeable at node 14 due to the restrictive N-1 SHC result discussed in 4.1.

The evaluation of the impact of the input profiles on DHC results gives different results for the three nodes. At node 3, DHC depends on the residential load profile and the wind farm's energy output. The correlation with the wind profile is strongly negative (−0.7), indicating that HC at node 3 is reduced whenever the wind generator at node 7 injects energy into the network. This is explained by the location of the wind turbine in the network, which is relatively close to node 3. Power flow from the wind generator flows from node 7 to node 8, limiting the capacity of power flowing from node HC evaluation node 3 towards node 8. Furthermore, the correlations with load are positive, indicating that hours of high demand allow for a higher energy injection at network node 3. Correlations are higher with residential load (∼0.6 to 0.7, depending on the load year) than commercial load (∼0.4 to 0.5) due to residential load representing a higher share of network load. HC at node 14 again shows high correlations with load profiles. At this node, the commercial load profile has a higher impact on HC (correlation of > 0.9) than the residential load (∼0.65 to 0.8, depending on the load year) due to the location of commercial loads at nodes 13 and 14. Injection at bus 14 allows for a decrease in imports from the upstream network to cover these loads. RES profiles do not impact DHC at node 14, as no generation capacity is located in feeder 2.

Furthermore, Table 5 includes the average annual injectable energy from the most restrictive SHC to DHC (represented as filled blue area in Fig. 4). The annual average is obtained by dividing the total additional injectable energy by 54 sample years. It is presented in MWh and as a percentual increase compared to the most restrictive SHC criterion. The lowest available additional injectable energy is of 62 % at node 3, representing a significant increase compared to the SHC. This additional injectable energy reaches as much as 76 % at node 14, where regulatory SHC is severely limited due to the N-1 contingency considerations.

4.3. Dynamic hosting capacity under N-1 contingencies

In the first step of the contingency analysis, DHC under N-1 contingencies is assessed individually for each N-1 contingency. The analysis evaluates the distribution functions of the 54 sample years of DHC for each contingency. Fig. 6 represents the cumulative distribution functions (CDFs) of DHC under N-1 contingencies for the three nodes under analysis. The CDF under normal operating conditions N is included. At node 3, N-1 failures in lines L0, L1 and L9 have a decreasing effect on the DHC, shifting the CDF towards the left. A failure in L0 or L1 results in the unavailability of node 3 to supply the demand in node 1, which represents loads of an entire LV system connected downstream of the MV grid. A contingency in L9 affects the downstream power flow from the node under HC consideration. Contingencies on feeder 2 (*L*10, *L*11, T1) have an increasing effect on DHC at node 3 due to the closure of S1 in these contingencies. This allows the supply of additional loads on feeder 2 via energy injection at node 3. The same is the case under the contingency of T0. The CDFs of both transformer contingencies show that energy injection is at the SCR limit during all hours. However, it should be noted that failures of the transformer stations lead to a significant amount of non-served energy despite increasing DHC at node 3. The remaining contingencies do not affect the DHC at node 3.

At node 5, no N-1 contingency leads to an increase in DHC. Contingencies in lines L2 to L5 lead to a decrease in HC. The maximum shift of the CDF to the left is observed at L3, followed by L5. Failures affecting any line between L2 and L5 lead to the closure of S2. This is significant in the N-1 contingency scenario of L5, as it leads to a power flow from the wind turbine towards node 5, decreasing hosting capacity due to the

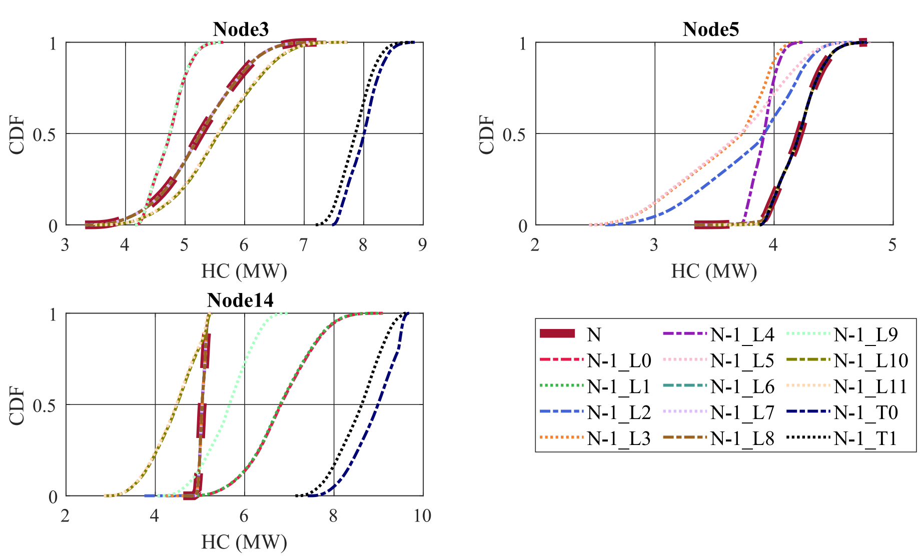

Fig. 6. Cumulative distribution functions of DHC under N-1 contingencies.

priority of existing generation capacity. The remaining contingencies do not affect the DHC at node 5.

At node 14, DHC increases at contingencies in L0 and L1 are significant. This is due to the closure of S1, allowing to supply the loads at feeder 1 via injecting energy at node 14. The same effect is observed in the case of a contingency at L9, although the increase is lower than in the case of L0 and L1. Similar to the observations at node 3, contingencies at the transformer stations increase the injectable energy at node 14 at the expense of significant amounts of non-served energy. The CDFs for both transformer contingencies are at the SCR during almost all hours. Contingencies located at feeder 2 ($L10$ and $L11$) reduce the connection of node 14 from the downstream LV network located at node 12, reducing hosting capacity under these contingencies. The remaining contingencies do not affect the DHC at node 14.

Table 5 includes information on the additional injectable energy for DHC N-1, derived from the least favourable N-1 HC for each hour of the year. The annual additional injectable energy is 34 % at node 3, 19 % at node 5, and 27 % at node 14. These percentages are based on the minimum N-1 contingency DHC result for each hour of the year, disrespecting the low probabilities of occurrence of these contingencies (Table 3).

4.4. Security-aware dynamic hosting capacity

DHC results are evaluated under N-1 contingencies to obtain security-aware DHC. The SDHC is obtained by computing Eq. (2) with the FORs of each N-1 contingency (Table 3). Fig. 7 presents the annual SDHC for each node under evaluation. Furthermore, the N-1 range indicates the minimum and maximum hosting capacity under contingencies detected for each hour of the year. The dashed line represents the regulatory SHC (section 4.1). The 54 sample years are reduced to 8760 h by assigning each year equal weight.

The figure points out that, at nodes 3 and 14, maximum energy injections are limited by the short circuit ratio (SCR) threshold. SDHC at node 3 reaches the maximum SCR threshold several times throughout the year, while at node 14, only N-1 contingencies activate the SCR injection limit. All minimum SDHC values are above the threshold of SHC determined according to regulation.

The SDHC of node 3 shows the highest variability due to the negative correlation with the wind resource. Contrarily, the SDHC at node 14 shows the lowest variability throughout the year due to the high correlation with the commercial load profile and the lack of correlation with RES generation profiles. At node 5, the SDHC is at the upper bound of the N-1 range. N-1 contingencies only lower DHC at this node, as shown in Fig. 6.

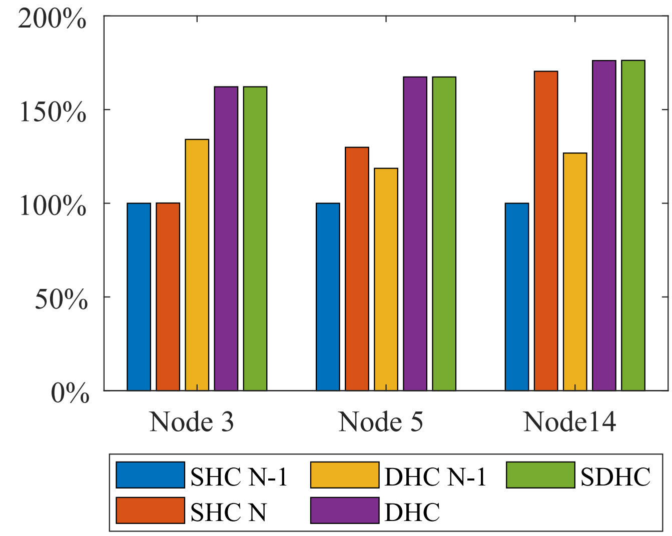

Fig. 8. Relative injectable energy – SHC, DHC and SDHC.

Fig. 8 compares the annual injectable energy at each HC evaluation node. SHC under N-1 restrictions, SHC under normal operating conditions N, most limiting N-1 DHC, DHC under normal operating conditions, and SDHC are compared. The DHC N-1 data refers to the lowest line of the DHC range shown in Fig. 7. The energy injection in the SHC N-1 case is used as a baseline (100 %). The figure points out the potential of relaxing the N-1 contingency criteria for calculating SHC (see section 4.1). Furthermore, the figure points out the significant increase in injectable energy when comparing DHC to SHC (see section 4.2). Even the deterministic consideration of hourly worst-case N-1 DHC leads to an increase of annual injectable energy of at least 19 %. Due to the low values of FOR, SDHC does not show a significant variation from DHC. The variation is below 0.1 % at all three HC evaluation nodes. Consequently, compared to the N-1 restricted SHC, SDHC allows for an additional injectable energy of 62 %, 67 %, and 76 % at nodes 3, 5 and 14, respectively (i.e. the same values observed for DHC, Table 5). These values point out that, despite the N-1 range showing noticeable deviations from SDHC (Fig. 7), N-1 contingencies do not significantly affect DHC due to low FORs.

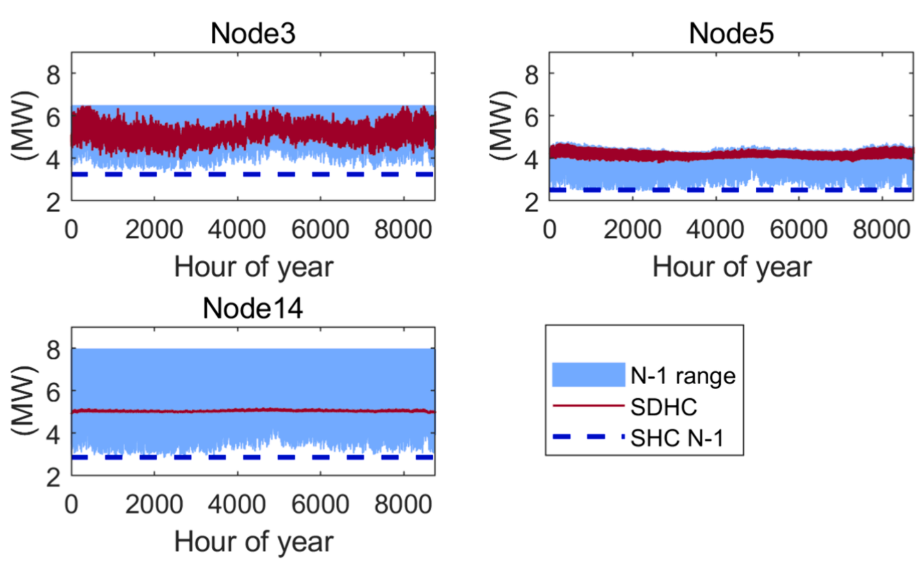

Fig. 7. Security-aware annual DHC.

5. Conclusions

This paper presents an analysis of a distribution network's security-aware dynamic hosting capacity under the uncertainty of RES generation profiles considering N-1 network contingencies. SDHC introduces a concept of dynamic hosting capacity accounting for N-1 asset contingencies and their probabilities. Dynamic hosting capacity allows to assess a network node's capacity for additional energy injection based on hourly values of demand and generation capacity instead of a static threshold derived via conservative operative assumptions. Hourly SDHC throughout the year is compared to the static hosting capacity threshold calculated according to Spanish regulatory requirements. The analysis is carried out for three different nodes of the CIGRE benchmark MV grid. Node 3 is selected due to its proximity to the external grid, node 5 due to its location downstream in feeder 1, and node 14 due to its location in feeder 2.

The evaluation of SHC shows that the regulatory requirement for considering N-1 network contingencies translates to a significant reduction of available HC despite forced outage rates of below 0.06 %. Consequently, DSOs are required to severely limit connections to their network based on considerations that are very unlikely to happen. Relaxing the contingency criteria for evaluating a network's hosting capacity could significantly increase the available HC of current electricity distribution grids. This study finds increases in annual injectable energy of up to 70 % when relaxing the N-1 contingency criterion, i.e. implementing low-probability event flexibility. This finding is based on the consideration of SHC according to conservative requirements without allowing for a more dynamic definition of hosting capacity.

The benefits of DHC are evaluated as hourly DHC over 54 sample years of different PV and wind generation profile years as well as load, obtained via a combinatorial analysis of three PV profiles and six wind profiles. Wind profiles are considered with a higher amount of sample years due to the randomness of the resource. A comparison of DHC with SHC under normal operating conditions shows that DHC falls below SHC thresholds only at node 14 and only during 0.018 % of the hours considered in the analysis. This observation points out the conservative assumptions of the regulatory reference scenario for evaluating SHC (close to maximum generation and minimum system demand).

The hourly computation of N-1 network asset failures' impact on DHC leads to the definition of the N-1 range. Even the worst-case DHC, that is the minimum hourly N-1 DHC, leads to an increase of annual injectable energy of at least 19 % when compared to N-1 SHC.

This paper defines the concept of security-aware dynamic hosting capacity as DHC accounting for the network's N-1 contingencies and their FORs. The evaluation of SDHC shows that some contingencies may even temporarily increase a network node's HC. However, due to low FORs, the variation of SDHC from average DHC under normal operating conditions is below 0.01 % of annual injectable energy. The analysis of N-1 contingencies and their probabilities highlights the conservative regulatory requirements for evaluating distribution network hosting capacity. A dynamic definition of hosting capacity instead of imposing restrictive N-1 SHC thresholds due to low contingency probabilities allows injecting significant additional energy into existing distribution networks without requiring reinforcement. This additional injectable energy under SDHC ranges from 62 % to 78 %.

Dynamic hosting capacity represents a valuable tool for an efficient electricity network integration of RES. It is especially relevant in the context of high connection times due to permitting associated with network reinforcement processes derived from conservative grid operating assumptions. This work contributes a methodology for the evaluation of DHC and the impact of N-1 contingencies on available DHC. The methodology is generalisable to other networks to evaluate the impact of asset FOR on DHC. For doing so, asset failure rate and MTTRmust be provided together with N-1 contingency configurations. Future research should evaluate the utility of the additional available injectable energy under SDHC for different RES technologies and their associated generation profile. Furthermore, allocating SDHC to a connection seeker requires transparency regarding curtailment probabilities and procedures. Different forms of flexible connection agreements should be investigated to foster the utilisation of the available hosting capacity of existing networks via SDHC.

CRediT authorship contribution statement

Leslie Herding: Writing – original draft, Visualization, Methodology, Investigation, Formal analysis. **Leonel Carvalho:** Writing – review & editing, Validation, Methodology, Conceptualization. **Rafael Cossent:** Writing – review & editing, Validation, Supervision, Conceptualization. **Michel Rivier:** Writing – review & editing, Validation, Supervision, Funding acquisition, Conceptualization.

Declaration of competing interest

The authors declare the following financial interests/personal relationships which may be considered as potential competing interests: Leslie Herding reports financial support was provided by Iberdrola Chair on Energy and Innovation. If there are other authors, they declare that they have no known competing financial interests or personal relationships that could have appeared to influence the work reported in this paper.

Data availability

All data used is publicly available in the referenced sources.

Acknowledgements

The authors would like to thank Orlando Valarezo for providing scenario input data, and Lukas Sigrist for the patience and support throughout the modelling process. The authors appreciate the funding for the mobility of professors and researchers in foreign research centres obtained from Universidad Pontificia Comillas.

This research has been carried out thanks to the Iberdrola Chair on Energy and Innovation and the funding of the RETOS COLABORACIÓN programme of the Spanish Ministry of Science and Innovation and the Spanish State Research Agency (project “Platform of innovative models to accelerate the energy decarbonisation of the economy (MODESC)”, with reference number RTC2019- 007315-3).

Appendix. Load sample year selection

Table 6
Average residential load (pu) per month of the year.

	Y2015	Y2016	Y2017	Y2018	Y2019	Y2020	Y2021
January	0.69	0.66	0.67	0.64	0.69	0.67	0.65
February	0.68	0.67	0.61	0.67	0.63	0.58	0.55
March	0.58	0.63	0.55	0.60	0.56	0.54	0.53
Abril	0.50	0.57	0.49	0.53	0.54	0.47	0.48
May	0.50	0.53	0.49	0.49	0.50	0.45	0.46
June	0.54	0.57	0.57	0.53	0.53	0.50	0.48
July	0.66	0.64	0.59	0.59	0.63	0.62	0.54
August	0.57	0.62	0.58	0.60	0.59	0.59	0.53
September	0.52	0.60	0.52	0.55	0.54	0.52	0.49
October	0.51	0.54	0.50	0.51	0.52	0.51	0.46
November	0.56	0.62	0.57	0.58	0.60	0.55	0.54
December	0.60	0.68	0.65	0.61	0.63	0.64	0.57

PV and wind pu sample year selection.

Table 7
Annual correlations of PV and wind availability.

	Y2010	Y2011	Y2012	Y2013	Y2014	Y2015	Y2016	Y2017	Y2018	Y2019	Y2020	Y2021	Y2022
CORREL (PV,wind)	0.00	−0.03	−0.02	−0.02	−0.04	−0.01	0.01	−0.03	−0.02	−0.05	−0.02	−0.06	−0.03

Table 8
Correlations of PV availability between different years considered in the study.

	Y2010	Y2011	Y2012	Y2013	Y2014	Y2015	Y2016	Y2017	Y2018	Y2019	Y2020	Y2021	Y2022
Y2010		0.90	0.90	0.91	0.90	0.91	0.92	0.91	0.90	0.91	0.91	0.90	0.90
Y2011	0.90		0.92	0.92	0.92	0.92	0.93	0.92	0.92	0.92	0.92	0.91	0.91
Y2012	0.90	0.92		0.93	0.93	0.93	0.92	0.92	0.92	0.93	0.93	0.92	0.92
Y2013	0.91	0.92	0.93		0.93	0.93	0.93	0.93	0.92	0.93	0.92	0.91	0.93
Y2014	0.90	0.92	0.93	0.93		0.93	0.93	0.93	0.93	0.94	0.93	0.92	0.91
Y2015	0.91	0.92	0.93	0.93	0.93		0.93	0.93	0.92	0.94	0.93	0.92	0.93
Y2016	0.92	0.93	0.92	0.93	0.93	0.93		0.93	0.92	0.93	0.93	0.91	0.92
Y2017	0.91	0.92	0.92	0.93	0.93	0.93	0.93		0.92	0.93	0.93	0.91	0.92
Y2018	0.90	0.92	0.92	0.92	0.93	0.92	0.92	0.92		0.93	0.92	0.92	0.91
Y2019	0.91	0.92	0.93	0.93	0.94	0.94	0.93	0.93	0.93		0.93	0.93	0.92
Y2020	0.91	0.92	0.93	0.92	0.93	0.93	0.93	0.93	0.92	0.93		0.91	0.92
Y2021	0.90	0.91	0.92	0.91	0.92	0.92	0.91	0.91	0.92	0.93	0.91		0.91
Y2022	0.90	0.91	0.92	0.93	0.91	0.93	0.92	0.92	0.91	0.92	0.92	0.91	

Table 9
Equivalent hours of solar PV availability.

	Y2010	Y2011	Y2012	Y2013	Y2014	Y2015	Y2016	Y2017	Y2018	Y2019	Y2020	Y2021	Y2022
Eq. hours	1911	1949	2007	2007	2020	1989	1972	2017	1959	2029	1967	1951	1899

Table 10
Correlations of wind availability between different years considered in the study.

	Y2010	Y2011	Y2012	Y2013	Y2014	Y2015	Y2016	Y2017	Y2018	Y2019	Y2020	Y2021	Y2022
Y2010		-0.01	0.00	0.08	0.03	0.07	0.06	0.12	0.06	0.05	0.01	0.08	0.01
Y2011	-0.01		0.05	0.13	0.02	0.01	-0.01	0.10	0.16	0.10	0.02	-0.04	0.05
Y2012	0.00	0.05		0.00	0.10	0.06	0.06	0.07	0.07	0.04	0.06	-0.02	0.03
Y2013	0.08	0.13	0.00		0.12	0.03	0.01	0.08	0.06	0.07	0.04	0.06	0.08
Y2014	0.03	0.02	0.10	0.12		0.00	0.07	0.02	0.14	0.01	0.01	-0.01	0.05
Y2015	0.07	0.01	0.06	0.03	0.00		0.06	0.09	-0.02	0.00	0.07	0.06	0.00
Y2016	0.06	-0.01	0.06	0.01	0.07	0.06		0.04	-0.04	-0.04	-0.04	-0.04	-0.05
Y2017	0.12	0.10	0.07	0.08	0.02	0.09	0.04		0.07	-0.04	0.03	-0.01	0.00
Y2018	0.06	0.16	0.07	0.06	0.14	-0.02	-0.04	0.07		0.01	0.05	0.04	0.09
Y2019	0.05	0.10	0.04	0.07	0.01	0.00	-0.04	-0.04	0.01		0.08	0.05	0.01
Y2020	0.01	0.02	0.06	0.04	0.01	0.07	-0.04	0.03	0.05	0.08		0.03	0.02
Y2021	0.08	-0.04	-0.02	0.06	-0.01	0.06	-0.04	-0.01	0.04	0.05	0.03		0.05
Y2022	0.01	0.05	0.03	0.08	0.05	0.00	-0.05	0.00	0.09	0.01	0.02	0.05	

Table 11
Equivalent hours of wind availability.

	Y2010	Y2011	Y2012	Y2013	Y2014	Y2015	Y2016	Y2017	Y2018	Y2019	Y2020	Y2021	Y2022
Eq. hours	3742	3741	3401	3763	3546	3244	3634	3466	3654	3564	3421	3792	3644

Table 12
Average wind capacity factor per month of the year.

Month	Y2010	Y2011	Y2012	Y2013	Y2014	Y2015	Y2016	Y2017	Y2018	Y2019	Y2020	Y2021	Y2022
January	0.54	0.42	0.33	0.50	0.51	0.35	0.42	0.36	0.46	0.38	0.27	0.49	0.48
February	0.59	0.37	0.41	0.50	0.54	0.61	0.64	0.54	0.36	0.44	0.30	0.58	0.40
March	0.46	0.58	0.42	0.67	0.54	0.33	0.32	0.39	0.68	0.49	0.50	0.53	0.55
Abril	0.41	0.50	0.56	0.47	0.38	0.49	0.44	0.48	0.65	0.48	0.49	0.48	0.47
May	0.49	0.50	0.41	0.37	0.44	0.41	0.44	0.54	0.34	0.41	0.48	0.40	0.41
June	0.37	0.37	0.37	0.46	0.33	0.42	0.37	0.44	0.40	0.37	0.47	0.40	0.46
July	0.42	0.34	0.38	0.34	0.32	0.22	0.45	0.31	0.28	0.41	0.40	0.34	0.34
August	0.33	0.42	0.30	0.33	0.27	0.34	0.49	0.33	0.34	0.28	0.30	0.31	0.41
September	0.31	0.45	0.44	0.38	0.34	0.38	0.32	0.33	0.38	0.34	0.37	0.33	0.34
October	0.30	0.38	0.29	0.27	0.44	0.32	0.34	0.29	0.38	0.27	0.33	0.40	0.35
November	0.47	0.47	0.45	0.38	0.45	0.31	0.39	0.29	0.44	0.55	0.31	0.46	0.39
December	0.45	0.33	0.33	0.50	0.32	0.28	0.38	0.46	0.29	0.47	0.45	0.48	0.39

Table 13
Average wind capacity factor per hour of the day.

Hour	Y2010	Y2011	Y2012	Y2013	Y2014	Y2015	Y2016	Y2017	Y2018	Y2019	Y2020	Y2021	Y2022
1	0.40	0.41	0.37	0.41	0.39	0.36	0.39	0.38	0.41	0.41	0.38	0.41	0.41
2	0.40	0.41	0.37	0.41	0.39	0.35	0.40	0.39	0.41	0.41	0.38	0.41	0.41
3	0.40	0.41	0.37	0.42	0.38	0.35	0.40	0.39	0.41	0.40	0.39	0.42	0.41
4	0.40	0.41	0.37	0.42	0.38	0.36	0.40	0.39	0.40	0.40	0.38	0.42	0.41
5	0.41	0.42	0.37	0.43	0.37	0.36	0.40	0.39	0.40	0.40	0.38	0.42	0.41
6	0.42	0.42	0.37	0.43	0.36	0.37	0.40	0.39	0.39	0.39	0.38	0.42	0.40
7	0.42	0.42	0.36	0.42	0.36	0.37	0.40	0.39	0.38	0.38	0.38	0.42	0.39
8	0.42	0.42	0.36	0.42	0.35	0.36	0.40	0.39	0.37	0.38	0.37	0.42	0.39
9	0.42	0.42	0.36	0.42	0.35	0.36	0.40	0.38	0.37	0.37	0.36	0.41	0.39
10	0.42	0.42	0.36	0.42	0.35	0.35	0.40	0.38	0.38	0.37	0.37	0.41	0.39
11	0.42	0.42	0.37	0.42	0.37	0.36	0.40	0.39	0.39	0.38	0.37	0.42	0.40
12	0.43	0.42	0.38	0.42	0.39	0.36	0.41	0.39	0.41	0.39	0.38	0.42	0.41
13	0.44	0.43	0.39	0.43	0.41	0.37	0.42	0.40	0.43	0.40	0.39	0.43	0.42
14	0.44	0.44	0.40	0.44	0.43	0.38	0.43	0.40	0.45	0.42	0.40	0.44	0.43
15	0.45	0.44	0.41	0.44	0.45	0.39	0.44	0.41	0.46	0.44	0.41	0.46	0.44
16	0.46	0.45	0.42	0.45	0.46	0.40	0.45	0.42	0.46	0.45	0.42	0.46	0.44
17	0.47	0.45	0.43	0.46	0.47	0.41	0.46	0.43	0.47	0.45	0.43	0.47	0.45
18	0.47	0.46	0.44	0.47	0.47	0.41	0.46	0.43	0.47	0.46	0.44	0.48	0.45
19	0.46	0.46	0.43	0.46	0.46	0.40	0.45	0.42	0.45	0.44	0.43	0.47	0.44
20	0.44	0.44	0.42	0.45	0.45	0.39	0.43	0.40	0.44	0.43	0.41	0.46	0.43
21	0.43	0.42	0.40	0.43	0.43	0.37	0.42	0.39	0.42	0.41	0.39	0.44	0.41
22	0.42	0.42	0.39	0.42	0.42	0.37	0.40	0.38	0.42	0.40	0.38	0.43	0.41
23	0.41	0.41	0.39	0.41	0.41	0.36	0.40	0.38	0.41	0.40	0.38	0.42	0.41
24	0.40	0.41	0.38	0.41	0.40	0.36	0.39	0.38	0.41	0.41	0.38	0.42	0.41

Network reconfiguration.

Table 14
N-1 contingency reconfigurations (Line: failure element, column: state of each element in case of failure).

	L0	L1	L2	L3	L4	L5	L6	L7	L8	L9	L10	L11	T0	T1
L0	0	1	1	1	1	1	1	1	1	1	1	1	1	1
L1	1	0	1	1	1	1	1	1	1	1	1	1	1	1
L2	1	1	0	1	1	1	1	1	1	1	1	1	1	1
L3	1	1	1	0	1	1	1	1	1	1	1	1	1	1
L4	1	1	1	1	0	1	1	1	1	1	1	1	1	1
L5	1	1	1	1	1	0	1	1	1	1	1	1	1	1
L6	1	1	1	1	1	1	0	1	1	1	1	1	1	1
L7	1	1	1	1	1	1	1	0	1	1	1	1	1	1
L8	1	1	1	1	1	1	1	1	0	1	1	1	1	1
L9	1	1	1	1	1	1	1	1	1	0	1	1	1	1
L10	1	1	1	1	1	1	1	1	1	1	0	1	1	1
L11	1	1	1	1	1	1	1	1	1	1	1	0	1	1
L12	0	0	1	1	1	1	0	0	0	0	0	0	0	0
L13	0	0	0	0	0	0	1	1	1	0	0	0	0	0
L14	1	1	0	0	0	0	0	0	0	1	1	1	1	1
T0	1	1	1	1	1	1	1	1	1	1	1	1	0	1
T1	1	1	1	1	1	1	1	1	1	1	1	1	1	0

References

[1] European Commission, *Proposal for a COUNCIL REGULATION laying down a framework to accelerate the deployment of renewable energy*. 2022. Accessed: Sep. 13, 2023. [Online]. Available: https://eur-lex.europa.eu/legal-content/EN/TXT/?uri=CELEX%3A52022PC0591&qid=1669020920010.

[2] European Commission, COMMISSION RECOMMENDATION on speeding up permit-granting procedures for renewable energy projects and facilitating Power Purchase Agreements. 2022. Accessed: Sep. 13, 2023. [Online]. Available: https://eur-lex.europa.eu/legal-content/EN/TXT/?uri=PI_COM%3AC%282022%293219&qid=1653033569832.

[3] Deloitte, 'La planificación y la tramitación de las infraestructuras eléctricas para la Transición Energética', Deloitte Spain. Accessed: Oct. 21, 2022. [Online]. Available: https://www2.deloitte.com/es/es/pages/energy-and-resources/articles/planificacion-y-tramitacion-infraestructuras-electricas.html.

[4] Herding L, Cossent R, Rivier M, Chaves-Ávila JP, Gómez T. Assessment of electricity network investment for the integration of high RES shares: a Spanish-like case study. Sustainable Energy Grids Networks 2021;28:100561. https://doi.org/10.1016/j.segan.2021.100561.

[5] CEER, 'CEER Paper on Alternative Connection Agreements'. Accessed: Dec. 11, 2023. [Online]. Available: https://www.ceer.eu/documents/104400/-/-/e473b6de-03c9-61aa-2c6a-86f2e3aa8f08.

[6] Alturki M, Khodaei A, Paaso A, Bahramirad S. Optimization-based distribution grid hosting capacity calculations. Appl Energy Jun. 2018;219:350–60. https://doi.org/10.1016/j.apenergy.2017.10.127.

[7] M.H.J. Bollen N. Etherden Overload and overvoltage in low-voltage and medium-voltage networks due to renewable energy — Some illustrative case studies in 2011 2nd IEEE PES International Conference and Exhibition on Innovative Smart Grid Technologies 2011 1 8 10.1109/ISGTEurope.2011.6162645.

[8] European Commission, 'COM(2023) 757 final'. Accessed: Nov. 29, 2023. [Online]. Available: https://eur-lex.europa.eu/legal-content/EN/TXT/PDF/?uri=COM:2023:757:FIN.

[9] Scottish Power Ltd., 'Getting Connected-SP MANWEB HEAT MAPS', Getting Connected-SP MANWEB HEAT MAPS. [Online]. Available: https://www.spenergynetworks.co.uk/pages/sp_manweb_heat_maps.aspx.

[10] SP Energy Network, 'Getting Connected - SP DISTRIBUTION HEAT MAPS', SPEnergyNetworks. Accessed: May 11, 2021. [Online]. Available: <%=GetPageUrl %>.

[11] ENERGA-OPERATOR SA, 'Informacje o stanie przyłączeń w sieci'. Accessed: Dec. 09, 2020. [Online]. Available: https://energa-operator.pl/uslugi/przylaczenie-do-sieci/informacje-o-stanie-przylaczen.

[12] i-DE, 'Mapa de Capacidad'. Accessed: Feb. 13, 2023. [Online]. Available: https://www.i-de.es/conexion-red-electrica/produccion-energia/mapa-capacidad-acceso.

[13] E-REDES, 'Información sobre la Capacidad de la red E-REDES'. Accessed: Feb. 13, 2023. [Online]. Available: https://www.eredesdistribucion.es/instalaciones/informacion-sobre-la-capacidad-de-la-red.

[14] Gómez T, Cossent R, Chaves-Avila JP. Flexible network access, local flexibility market mechanisms and cost-reflective tariffs: three regulatory tools to foster decarbonized electricity networks. Oxford Energy Forum 2020;124:18–23. https://www.iit.comillas.edu/publicacion/mostrar_publicacion_working_paper.php.es?id=387.

[15] ENA, 'Rising to Britain's Net Zero Challenge'. Accessed: Dec. 14, 2023. [Online]. Available: https://www.energynetworks.org/assets/images/Publications/2023/231211-ena-rising-to-connections.pdf?1702549332.

[16] Ofgem, 'Access and Forward-Looking Charges Significant Code Review – Summer 2019 working paper', Access and Forward-Looking Charges Significant Code Review – Summer 2019 working paper. Accessed: Aug. 07, 2020. [Online]. Available: https://www.ofgem.gov.uk/publications-and-updates/access-and-forward-looking-charges-significant-code-review-summer-2019-working-paper.

[17] European Commission, 'Digitalisation of the European Energy System | Shaping Europe's digital future'. Accessed: Dec. 20, 2023. [Online]. Available: https://digital-strategy.ec.europa.eu/en/policies/digitalisation-energy.

[18] N. Etherden, M. Bollen, S. Ackeby, and O. Lennerhag, 'The transparent hosting-capacity approach – overview, applications and developments', presented at the International Conference and Exhibition on Electricity Distribution : 15/06/2015 - 18/06/2015, 2015. Accessed: May 10, 2021. [Online]. Available: http://urn.kb.se/resolve?urn=urn:nbn:se:ltu:diva-39121.

[19] Ismael SM, Abdel Aleem SHE, Abdelaziz AY, Zobaa AF. 'State-of-the-art of hosting capacity in modern power systems with distributed generation'. Renew Energy 2019;130:1002–20. https://doi.org/10.1016/j.renene.2018.07.008.

[20] Koirala A, Van Acker T, Dhulst R, Van Hertem D. 'Hosting capacity of photovoltaic systems in low voltage distribution systems: a benchmark of deterministic and stochastic approaches'. Renew Sustain Energy Rev 2022;155:111899. https://doi.org/10.1016/j.rser.2021.111899.

[21] Herding L, Cossent R, Rivier M. 'Enhancing RES grid connection via dynamic hosting capacity and hybridization', presented at the. IEEE Belgrade PowerTech Belgrade, Serbia: IEEE 2023;2023. https://doi.org/10.1109/PowerTech55446.2023.10202726.

[22] D. Fang et al. Deterministic and Probabilistic Assessment of Distribution Network Hosting Capacity for Wind-Based Renewable Generation in 2020 International Conference on Probabilistic Methods Applied to Power Systems (PMAPS), Aug 2020 1 6 10.1109/PMAPS47429.2020.9183525.

[23] Naciri S, Moufid I, El Markhi H. Dynamic hosting capacity of photovoltaic system analysis and enhancement using distributed SVC and STATCOM compensators: case study of a university building. Renewable Energy Focus 2023;45:123–32. https://doi.org/10.1016/j.ref.2023.03.002.

[24] Ding F, Mather B. On distributed PV hosting capacity estimation, sensitivity study, and improvement. IEEE Trans Sustainable Energy Jul. 2017;8(3):1010–20. https://doi.org/10.1109/TSTE.2016.2640239.

[25] Yuan J, Weng Y, Tan C-W. Determining maximum hosting capacity for PV systems in distribution grids. Int J Electr Power Energy Syst 2022;135:107342. https://doi.org/10.1016/j.ijepes.2021.107342.

[26] Hajeforosh S, Khatun A, Bollen M. Enhancing the hosting capacity of distribution transformers for using dynamic component rating. Int J Electr Power Energy Syst 2022;142:108130. https://doi.org/10.1016/j.ijepes.2022.108130.

[27] Jain AK, et al. Dynamic hosting capacity analysis for distributed photovoltaic resources—framework and case study. Appl Energy Dec. 2020;280:115633. https://doi.org/10.1016/j.apenergy.2020.115633.

[28] CNMC, 'Resolución de 20 de mayo de, de la Comisión Nacional de los Mercados y la Competencia, por la que se establecen las especificaciones de detalle para la determinación de la capacidad de acceso de generación a la red de transporte y a las redes de distribución' https://www.boe.es/eli/es/res/2021/05/20/ (4) 2021 Accessed: Sep. 13, 2021. [Online]. Available.

[29] Valarezo O, Chaves-Ávila JP, Gómez T. 'Multi-objective distribution network reconfiguration: application to a real large-scale distribution system'. Appl Energy 2024. vol. Under review.

[30] Widen J. Correlations between large-scale solar and wind power in a future scenario for sweden. IEEE Trans Sustainable Energy 2011;2(2):177–84. https://doi.org/10.1109/TSTE.2010.2101620.

[31] Couto A, Estanqueiro A. Assessment of wind and solar PV local complementarity for the hybridization of the wind power plants installed in Portugal. J Clean Prod 2021;319:128728. https://doi.org/10.1016/j.jclepro.2021.128728.

[32] Harrison-Atlas D, Murphy C, Schleifer A, Grue N. Temporal complementarity and value of wind-PV hybrid systems across the United States. Renew Energy 2022;201:111–23. https://doi.org/10.1016/j.renene.2022.10.060.

[33] R. D. Zimmermann and C. E. Murillo-Sánchez, 'MATPOWER User's Manual, Version 7.1'. Accessed: Jul. 24, 2023. [Online]. Available: https://matpower.org/docs/MATPOWER-manual.pdf.

[34] CIGRE, 'Benchmark Systems for Network Integration of Renewable and Distributed Energy Resources', e-cigre. Accessed: Oct. 26, 2023. [Online]. Available: https://e-cigre.org/publication/ELT_273_8-benchmark-systems-for-network-integration-of-renewable-and-distributed-energy-resources.

[35] K. Rudion, A. Orths, Z. A. Styczynski, and K. Strunz, 'Design of benchmark of medium voltage distribution network for investigation of DG integration', in *2006 IEEE Power Engineering Society General Meeting*, Jun. 2006, p. 6 pp.-. doi: 10.1109/PES.2006.1709447.

[36] University of Kassel and Fraunhofer IEE, 'CIGRE Networks — pandapower 2.4.0 documentation'. Accessed: Oct. 26, 2023. [Online]. Available: https://pandapower.readthedocs.io/en/v2.13.1/networks/cigre.html.

[37] CNMC 'Circular 1/2021' Accessed: Sep. 19 2021 [Online]. Available: https://www.boe.es/eli/es/cir/2021/01/20/1/con.

[38] REE, 'Bienvenido | ESIOS electricidad datos transparencia'. Accessed: Oct. 23, 2023. [Online]. Available: https://www.esios.ree.es/es.

[39] CNMC, *Resolución de 18 de marzo de 2021, de la Comisión Nacional de los Mercados y la Competencia, por la que se establecen los valores de los peajes de acceso a las redes de transporte y distribución de electricidad de aplicación a partir del 1 de junio de 2021*, vol. BOE-A-2021-4565. 2021, pp. 33575–33593. Accessed: Oct. 23, 2023. [Online]. Available: https://www.boe.es/eli/es/res/2021/03/18/(3).

[40] Pfenninger S, Staffell I. Long-term patterns of European PV output using 30 years of validated hourly reanalysis and satellite data. Energy 2016;114:1251–65. https://doi.org/10.1016/j.energy.2016.08.060.

[41] Staffell I, Pfenninger S. Using bias-corrected reanalysis to simulate current and future wind power output. Energy 2016;114:1224–39. https://doi.org/10.1016/j.energy.2016.08.068.

[42] Novo R, Marocco P, Giorgi G, Lanzini A, Santarelli M, Mattiazzo G. Planning the decarbonisation of energy systems: the importance of applying time series clustering to long-term models. Energy Conversion and Management: X 2022;15:100274. https://doi.org/10.1016/j.ecmx.2022.100274.

[43] R.E. Brown Electric power distribution reliability 2nd ed. 2017 CRC Press Boca Raton 10.1201/9780849375682.

7.5 Paper 5

- We propose a methodology to assess a promoter perspective on flexible connections.
- Four different hosting capacity (HC) concepts and hybridisation are assessed.
- Investor risk is accounted for via the Conditional Value-at-Risk (CVaR) of profits.
- Relaxing HC calculation criteria increases installed capacities and profits.
- Combining HC relaxation and hybridisation increases average profits by 75%.

Local renewable capacity investment planning under distribution grid hosting capacity uncertainty via Conditional Value-at-Risk

Leslie Herding*[,a], Leonel Carvalho[b], Rafael Cossent[a], Michel Rivier[a]

[a]Institute for Research in Technology (IIT), ICAI School of Engineering, Universidad Pontificia Comillas, C/Santa Cruz de Marcenado 26, 28015 Madrid, Spain

[b]Universidade Lusófona - Centro Universitário do Porto, Rua Augusto Rosa, 24, 4000-098 Porto, Portugal

[*] Corresponding author: lherding@comillas.edu

Abstract

Electricity distribution grids have been identified as a potential bottleneck for the rapid rollout of distributed generation. This paper assesses the impact of relaxing the hosting capacity (HC) calculation criteria on the expected profits of local generation capacity. Additionally, the potential of combining HC relaxation with hybridising renewable generation technologies is quantified. The methodology accounts for uncertainty surrounding HC, renewable resource availability, and market prices. The investor risk is represented via Conditional Value-at-Risk. The case study points out that the relaxation of HC calculation criteria unlocks the electricity grid's capacity to absorb more energy and incentivises the increase of installed generation capacity for maximising investor profits. Moving from a contingency-restricted static HC to a dynamic HC definition leads to an additional energy injection of 65%, increasing average investor profits by 64%. Combining the HC relaxation with hybridisation increases the optimal portfolio capacity by 127% and average investor profits by 75%. Sensitivity analyses are performed to assess the robustness of the results. The results highlight the potential of unlocking electricity distribution grid capacity by relaxing HC calculation criteria while guaranteeing profitability for investors.

Keywords

Distribution grids; Distributed generation; Hosting capacity; Flexible connections; Conditional Value-at-Risk

1 Introduction

Ambitious decarbonisation targets call for a rapid electricity grid integration of renewable energy sources (RES). The rollout of distributed generation (DG) and the electrification of energy demands puts a special focus on distribution networks. These grids have previously been identified as a potential bottleneck for the energy transition [1]. Significant additional grid capacity is one option to safely integrate the new distributed energy resources (DER), requiring investment and time. Conversely, operating the networks more flexibly has been identified as an efficient means to increase the use of existing grid capacity, effectively allowing to speed up the grid integration of new resources [2]. Flexible connections are one tool that enables distribution system operators (DSOs) to operate the grid more dynamically [3]. It allows DSOs to adjust the injection and withdrawal into and from their grids to actual operating conditions rather than limit the integration of DER based on worst-case considerations [4].

DSOs evaluate the so-called hosting capacity (HC) when assessing a potential new connection to their networks. HC describes the capacity that can be connected to a network node without deteriorating performance indicators such as voltage magnitude or power quality beyond the pre-established limits [5]. Usually, HC is calculated for a conservative scenario of grid operation to guarantee that grid service can be provided at all times. These conservative assumptions increase the need for new grid assets for integrating RES despite those assets being used only a few hours per year, if ever [4]. However, the increasing digitalisation of electricity networks allows for a more dynamic operation based on the time-variable conditions of generation and demand.

Consequently, the HC can also be defined dynamically, introducing dynamic hosting capacity (DHC) [6]. DHC has been shown to enhance the capacity which can be connected to a network node. The authors of [7] present a dynamic HC evaluation that allows for temporary violations of the operational limits of the network. This method allows for a photovoltaic (PV) HC enhancement of 60% to 200% compared to the value of static hosting capacity (SHC). The authors of [8] show how implementing dynamic transformer ratings allows connecting PV capacity above the transformer's rated capacity. In [9], a network node's DHC is compared to the node's SHC. The dynamic operation of the network allows an increase of HC by 62% to 67%, depending on the characteristics of the network node.

If HC is defined more dynamically, RES promoters need to optimise the capacity to install in response to the corresponding profile of the node's dynamic HC. Throughout the literature, RES capacity planning is often carried out as generation expansion planning (GEP). The GEP process optimises the capacity mix of the power system by looking at the bulk power system as a whole. This might be combined with transmission expansion planning (TEP). GEP & TEP for the Saudi Arabian power system are carried out in [10], GEP for the Australian power grid focusing on generation-storage requirements and the optimal storage sizing is presented in [11]. The authors of [12] propose a GEP algorithm that accounts for different load characteristics for computationally efficient power system planning. The paper includes a case study of Thailand's power system. The impact of policies on capacity planning in the north-western power grid in China is assessed in [13]. The authors of [14] evaluate the effect of phasing out RES remuneration support schemes on the speed of capacity deployment on the system level.

The aforementioned GEP studies determine the optimal generation portfolio of an entire power system from a minimisation of total costs point of view, i.e., from a centralised perspective. They do not, however, consider the optimisation for each separate generation capacity investment incurred throughout the system. The authors of [15] propose a methodology to plan an optimal hybrid energy. The algorithm accounts for PV, wind, battery storage and diesel units to optimise the cost of an isolated system. The authors of [16] optimise a household-scale hybrid RES system via a multi-objective genetic algorithm. The algorithm's objective function considers carbon footprint, product environmental footprint and the net present cost of the system to be optimised. The optimal sizing of DG is assessed in [17]. The work accounts for uncertainty in renewable generation availability and load. Contrary to common GEP, the previous works allow for sizing individual DG installations. They do, however, not consider any risk related to future market prices.

One approach of risk assessment is Conditional Value-at-Risk (CVaR). CVaR represents a metric to assess a portfolio's average worst-case losses. It is a variation of the Value-at-Risk metric and allows for a more accurate consideration of the probability distribution of economic losses [18]. Hence, it offers effectiveness even in cases where losses do not follow a Normal distribution [19].

CVaR-based risk assessment has already been applied to various aspects of power systems. The authors of [20] assess independent, locally operated battery energy storage systems (BESSs) as a solution to alleviate intermittent RES-related grid challenges. The paper employs CVaR to represent the risk surrounding the uncertainty of the scheduling problem. In [21], the optimal geographically diverse storage portfolio for a merchant is determined. The upper level of the tri-level optimisation problem minimises the intermediary merchant's risk of losses via CVaR. The mid-level maximises profits, and the lower level clears the day-ahead market. In [22], CVaR is included in TEP to determine the concept of Conditional Value-at-Risk of Energy Not Supplied to assess the risk of power supply of a planning scheme. The authors of [23] apply CVaR to the day-ahead scheduling of home energy management systems to reduce the risk of exposure to market prices and PV uncertainty. Optimal investment decisions on a candidate facility for an energy hub, comprised of various generation and demand technologies, are determined in [24]. CVaR is considered in the objective function. The study assesses the optimal technological composition of the energy hub under different risk adversity levels, expressed by the weight of CVaR in the objective function.

Those previous studies have shown that CVaR represents a suitable metric for risk assessment in power system analyses. This study employs CVaR to determine the optimal generation capacity mix for profit maximisation under various sources of uncertainty. Uncertainties range from HC and RES resource availability to market prices. The installed capacity is optimised for maximum profits to evaluate an investor's perspective on relaxing the criteria for HC calculation according to the HC concepts presented in [9]. Investor risk is accounted for by optimising Conditional Value-at-Risk surrounding the expected profits of the candidate generation capacity portfolios. In this study, the generation capacity mix composed of one or various generation technologies installed together behind the same grid connection point is denominated portfolio. Different definitions of HC and their impact on the optimal generation capacity portfolio are assessed. HC concepts range from static to dynamic definitions and include different reliability considerations. Additionally, the effect of the hybridisation of different RES generation technologies on the optimal generation portfolio is quantified for each HC concept.

This paper's contributions can be summarised as follows:

- Local generation capacity investment optimisation under hosting capacity uncertainty: Local RES capacity is optimised to maximise profits under uncertainties regarding the available hosting capacity, renewable resource availability and future market process.
- Development of a methodology to assess the impact of flexible connection schemes and hybridisation on optimal local RES capacity investment planning: The proposed model optimises local RES capacity for four different HC concepts, including a baseline defined according to current regulation. The methodology allows to assess the

benefits of relaxing regulatory HC calculation requirements, moving towards a more flexible definition of distribution network HC. Further, the proposed methodology allows to quantify the impact of the relaxation of the local hybridisation of different RES technologies, and the combination of HC relaxation and RES hybridisation on the optimal local RES capacity investment.

- **Quantification of measures to increase the use of existing electricity distribution network capacity**: A case study quantifies the increase of the use of the existing electricity network via HC calculation relaxation and local RES hybridisation. The impact is quantified in terms of installed capacity, annual energy injection and average annual investor profits.
- **Sensitivity analysis to enhance robustness**: Several sensitivities are performed to ensure the robustness of the results to the different input parameters.

The remainder of this paper is structured as follows: section 2 presents the methodology of RES capacity investment planning under HC uncertainty. Case study inputs are presented in 3, and the results in 4. Section 5 concludes the paper.

2 Local RES capacity investment planning methodology with limited and uncertain HC

The local RES capacity investment planning methodology under uncertainty presented in this paper is composed of several optimisation steps. The methodology is summarised in Figure 1 and will be described in more detail throughout this section. The figure presents a flowchart of the local RES capacity investment planning process and summarises the inputs, calculation steps and results. Further, the number of scenarios managed in each methodology step is shown in the figure. In this paper, *local* refers to the optimisation of RES capacity of different technologies to be installed downstream of the same grid connection point.

In order to properly understand the methological approach represented in Figure 1, it is essential to keep in mind that the CVaR approach adopted in this study requires the assessment of many possible RES investment candidate portfolios (ICP) with respect to the whole set of possible uncertain scenarios that may materialise ex-post. The main uncertainty factors taken into consideration are:

1. The network node’s HC. The hourly DHC profile will depend on the load and production variability of previously connected assets to the distribution network under study,
2. The own variability of the candidate RES investment primary source (solar radiation and wind), that is one to one correlated with the production variability of the RES previously connected to the grid and used to determined the DHC, and
3. The hourly remuneration for the injection of electricity into the network, depending on energy market prices.

The proposed methodology builds a full set of RES ICPs by optimising the investment making decision for each individual possible scenario, i.e. each combinatorial set of each individual HC hourly profile scenario with each individual energy market price hourly profile scenario. The whole set of resulting ICPs is assessed thoughout the whole set of possible combinations of scenarios, leading to a probability distribution function of the expected profits for each ICP. Then, a CVaR maximisation approach is adopted to select the unique optimal investment decision made by the RES investor.

Thus, the approach can be summarised in four steps, as shown in Figure 1. As a first step, an Optimal Power Flow (OPF) is employed to derive a node's hourly HC [25]. As mentioned before, the HC result will depend on load and RES hourly variability profiles, represented via input curves. The analysis is combinatorial in order to address the flexible HC uncertainty faced by the RES investor. It considers *d* hourly demand profile scenarios, and p and w solar PV and wind RES hourly variability profile scenarios, respectively, leading to $m = d*p*w$ different HC hourly profiles. Besides, the OPF analysis is carried out for several different conceptual approaches of HC, which will be evaluated in this paper. Details of the HC concepts considered in this work are introduced in section 2.1.

In a second step, the resulting HC outputs feed a local RES investment model that optimises the renewable capacity installed for each one of the *m* HC curves computed in Step 1 and for each one of the *s* energy market price profiles considered in the study. Thus $n = m*s$ RES ICPs are computed at this stage. The investment model is presented in more detail in 2.2. In this work, the term portfolio describes the resulting investment mix generation and storage capacity to be installed downstream of the grid interconnection point. A portfolio may consist of a technology mix if deemed optimal by the investment model. An ICP describes a portfolio that represents the optimal decision for an individual scenario. Thus, n ICPs are computed for each one of the *n* scenarios with their associated RES availability, HC, and energy market prices.

In Step 3, each ICP is assessed throughout all the different scenarios of RES and HC availability and market prices considered in the study. The *n* ICPs derived from the investment model in Step 2 are assessed via an operational evaluation, detailed in section 2.3. The operational assessment provides the ICPs' profits throughout all *n* scenarios, allowing to determine the average profits and CVaR of each ICP. These outputs represent the ICPs' performances in various scenarios of grid and market conditions. The results of the operational evaluation represent the input for the investment decision (Step 4), which is presented in more detail in 2.4.

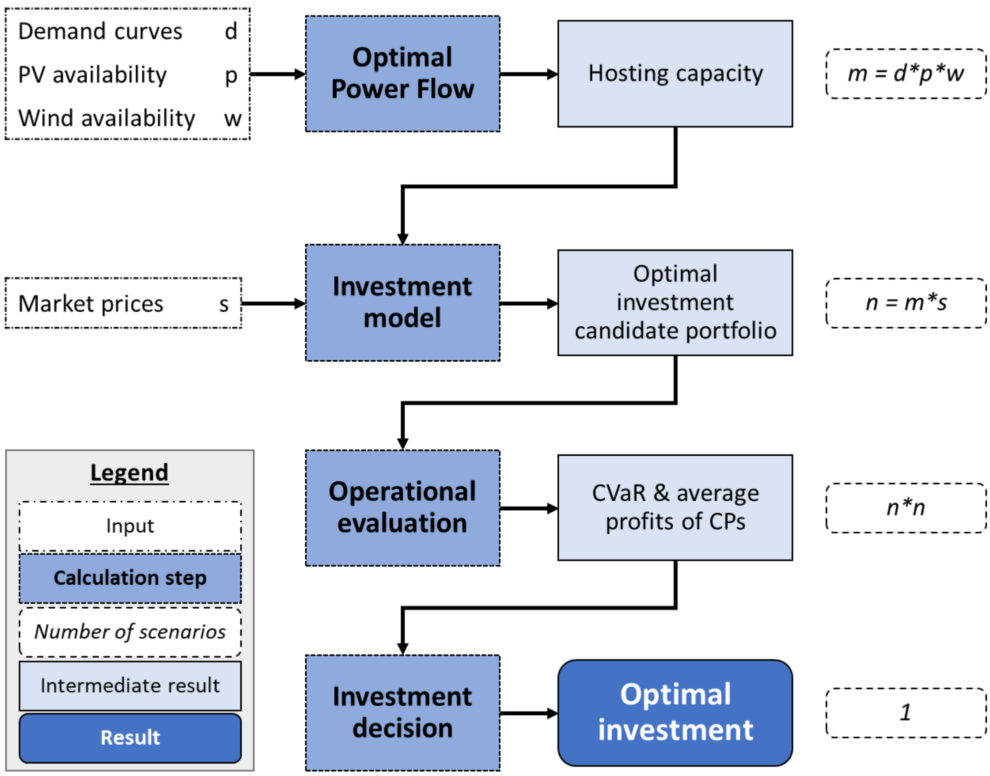

Figure 1: Flowchart of the local RES capacity investment planning methodology

2.1 Step1: Hosting capacity calculation

The nodal hosting capacity concepts considered for the RES capacity investment planning are derived from previous work [9]. HC concepts are differentiated in terms of time granularity and reliability considerations. The concepts are summarised in Table 1. In the SHC concepts, a fixed threshold is applied throughout all hours of the year. This threshold is usually derived via conservative maximum generation/minimum load considerations or vice versa [26]. Hence, *m* is reduced to 1 in the case of SHC.

In contrast to SHC, DHC is represented with a time-series. This allows to consider the variable operating conditions of the network in terms of load and pre-existing generation connected to the distribution network under consideration. As stated in 2, a total of *m* scenarios of different loads and outputs of pre-existing generators are simulated to address the intrinsic DHC uncertainty faced by a RES investor facing flexible connection schemes.

Additionally, the concepts of SHC and DHC are combined with two different reliability concepts. SHC N and DHC N represent the network node's static and dynamic HC under normal operating conditions. That means all network assets are considered operative. The N-1 concepts assume the worst-case asset failure. The N-1 concept is based on the definition of distribution grid HC in Spanish regulation [26]. N-1 contingencies modelling accounts for network reconfigurations to ensure service availability in case of asset failure [27]. All asset failures are simulated individually and the minimum value of energy that can be injected without violating the network's operating limits is the node's HC. In the case of SHC N-1, this is a single threshold obtained via the maximum generation/minimum load scenario [26]. DHC N-1 is derived by simulating all asset failures throughout all timesteps. The minimum value of obtained HC is selected timestep by timestep to form the DHC N-1 concept. The local RES capacity investment planning methodology is carried out independently for each of the HC concepts, allowing to analyse the optimal investment decision under changing HC capacity calculation criteria.

Table 1: Hosting capacity concepts assessed in this work

HC concept	Time granularity	Reliability considerations
SHC N-1	Snapshot	Worst-case N-1
SHC N	Snapshot	-
DHC N-1	Time-series	Worst-case N-1
DHC N	Time-series	-

2.2 Step 2: RES Investment candidate portfolio determination under HC constraints

The investment model used for local RES generation capacity planning under HC constraints represents an evolution of previous work by the authors presented in [6].An ICP is determined in accordance with the HC restrictions introduced in the previous section. Further, the model allows to assess the impact of the hybridisation of RES technologies and batteries. For the same HC concept, one non-hybrid and one hybrid ICP are determined. In the non-hybrid case, the investment model determines the optimal generation capacity for the most fitting technology. In the hybrid case, the model decides the optimal capacity mix in which all available generation technologies may be combined to maximise profits. Generation technologies considered for the non-hybrid capacity installation are PV or wind. In the hybrid case, the model may also choose to install 4-hour batteries to hybridise the RES capacity mix.

The model maximises profits by evaluating investment and operation and maintenance (O&M) costs, and the income generated from the energy injection into the network. The objective function is represented in Eq. 1. Profits are determined by multiplying the energy injection E_inj_h by the available hourly remuneration Rem_h, with h indexing the time steps. Investment costs depend on the unit investment costs *Inv* and the resulting installed capacity *P*, for each RES generation technology *t* and for 4-hours batteries *b*. Furthermore, the O&M terms represent additional cost terms for all involved technologies to be considered in the objective function.

$$max\left[\sum_h (E\_inj_h * Rem_h) - \sum_t (P_t * Inv_t) - \sum_t (P_t * O\&M_t) - P_b * Inv_b - P_b * O\&M_b\right] \qquad \text{Eq. 1}$$

In each timestep, the energy injection is limited by *HC* (Eq. 2). In the case of DHC, HC takes on the corresponding time-series. In the case of SHC, the threshold is fixed by a static value throughout all hours of the year.

$$E\_inj_h \leq HC_h \qquad \text{Eq. 2}$$

The energy available from PV and wind depends on the resulting installed capacity and the unitary resource availability of each technology $pu_{t,h}$ (Eq. 3).

$$E\_avail_h = \sum_t \left(P_t * pu_{t,h}\right) \qquad \text{Eq. 3}$$

The available HC conditions the net energy injection to the grid E_inj_h and triggers curtailments in case the available energy surpasses the available HC. This is indicated in Eq. 4 where *E_avail* represents the available energy, *E_curt* the energy subject to curtailment, and *E_BSSin* and *E_BSSout* represent the charge and discharge of the energy storage system, if installed.

$$E\_inj_h = E\_avail_h - E\_curt_h - E\_BSSin_h + E\_BSSout_h \qquad \text{Eq. 4}$$

The unitary remuneration Rem_h (EUR/MWh) is modelled according to a RES expansion auction scheme (Eq. 5) [28]. The unitary remuneration is set as a combination of the auction clearing price *CP* (which is an input parameter to the model) and the market price MP_h. Those two values are coupled via a coupling coefficient *CC*, as employed in the Spanish auctions for renewables [29]. This adjustment allows for limited exposure to market volatility while providing certainty for the portfolio's remuneration. By adjusting *CC*, the model is able to represent any possible scheme ranging from a null to a full energy market price exposure (i.e. from PPA to a merchant scheme).

$$Rem_h = CP + CC * (MP_h - CP) \qquad \text{Eq. 5}$$

Classical restrictions for storage operation are modelled according to [30]. In the case of the non-hybrid investment model, binary variables are employed to ensure that only one of the technologies *t* is deployed [6].

As described in 2, the model considers the *m* different scenarios of HC. Further, *s* years of different *MP* curves are considered, leading to a total of $n = m*s$ scenarios assessed by the investment model, resulting in *n* ICPs. Each ICP represents the investment decision under the scenario restrictions of HC and RES availability and market prices. For a thorough assessment of the investment candidate portfolios, the portfolio's performance needs to be assessed throughout different operating scenarios. The operational evaluation is described in the following section.

2.3 Step 3: Operational evaluation of each investment candidate portfolio

Every ICP obtained from the investment model is assessed across different operational scenarios to ensure the robustness of the expected profits and build a profit probability distribution function to feed the subsequent CVaR analysis. For the operational evaluation, the ICP's generation capacity obtained from the investment model is fixed. The energy injection and the corresponding profits of the fixed capacity are determined throughout the other operating scenarios with different HC and RES availability and market prices.

Table 2 shows the scheme of the operational evaluation. The second line shows the *n* ICPs derived from the investment model in step 2. Those ICPs are subject to the input curves of RES and HC availability and remuneration considered for the computation of the investment model and represent the optimal investment decision for those inputs. Each ICP's operational performance is assessed throughout all other scenarios of RES and HC availability and remuneration to determine the optimal ICPs. This can be read column-wise from the table. For example, the first column shows that the ICP obtained from the first combination of input curves is fixed (ICP_1), and profits are assessed with all other combinations of input curves ($Op_{1,1}$ to $Op_{1,n}$). The evaluation is repeated for each of the *n* ICPs to determine which yields the best performance throughout the variety of input scenarios.

Table 2: Operational evaluation scheme for comparing capacity investment candidate portfolios

	Investment candidate portfolio				
	ICP_1	…	…	…	ICP_n
Operational evaluation	$Op_{1,1}$	…	…	…	$Op_{n,1}$
	…	…	…	…	…
	…	…	…	…	…
	$Op_{1,n}$	…	…	…	$Op_{n,n}$

The profits obtained throughout all operational scenarios are then assessed via Conditional Value-at-Risk, or expected shortfall. CVaR is a measure that expresses the average expected losses of a portfolio in the worst q%. It is a variation of Value-at-Risk (VaR). VaR describes the losses or profit of a portfolio with a probability of q%, hence representing the q^{th} quantile of the probability distribution function (PDF) that defines the losses. However, VaR does not provide any information on the kurtosis of the PDF. Kurtosis is a measure to describe the tailedness of a distribution function and how it deviates from a normal distribution function [31]. Not accounting for this information might lead to an incorrect estimation of worst-case losses.

The CVaR method represents a means to overcome that shortcoming of the VaR method. CVaR is defined as the average value of portfolio loss when the portfolio loss exceeds a given VaR value of probability δ [19]. CVaR can hence be described as in Eq. 6, where f(x,y) describes the loss function, represented by the decision variables x and the random model parameters y [32]. The CVaR method aims to determine the optimal value of x to minimise the losses f(x,y), subject to the uncertainty in y.

$$CVaR^{\delta} = E_y\big(f(x,y)|f(x,y) \geq VaR^{\delta}\big) \qquad \text{Eq. 6}$$

CVaR describes the area under the PDF of profits up to the VaR cut-off [33]. In this methodology, the CVaR method is applied to the profits obtained from the operational evaluation of each candidate portfolio. Hence, the magnitude of CVaR is impacted not only by the choice of VaR but also by the kurtosis of the profit PDF. The uncertainty y is caused by variations in HC, RES availability and market prices.

2.4 Step 4: Investment decision

The optimal investment decision is derived from the CVaR analysis. Commonly, CVaR is employed to assess the worst-case losses of a given portfolio under consideration [34]. However, in this case, CVaR is determined over the profits obtained by the different ICPs thoughout the various operating scenarios (Eq. 1). Hence, an ICP's CVaR represents the worst-case profits in this paper. Negative profits indicate that the ICP generates losses in some of the operating scenarios under consideration. Accordingly, the investment decision carried out in this work seeks to maximise CVaR, i.e. worst-case profits. Worst-case profits represent the left-hand tail of the PDF of profits. Hence, maximising CVaR might lead to different investment decisions than maximising average profits, usually a more conservative one with less installed capacity. A CVaR > 0 of an investment decision ensures that profits are still ensured, even in the worst operating conditions.

3 Case study inputs

As mentioned in 2.2, the investment model is applied to *n* different scenarios. In this work, the scenarios represent different variations of the input parameters in the form of annual houtly curves. Hence, the timeframe of each scenario is one year and the timesteps *h* represent the hours of each year.

3.1 Hosting capacity

Hosting capacity is an input from [9]. HC is derived for three nodes of the CIGRE benchmark 20 kV network with DER [35], [36], [37]. This work presents the exemplary RES capacity investment assessment for the results obtained for node 5. Nodes 3 and 14 are addressed in the form of a sensitivity analysis. In [9], nodal DHC is assessed over a total of $m = d*p*w$ sample years and is comprised of three different load curves ($d = 3$), three annual curves of PV availability ($p = 3$), and six curves of wind availability ($w = 6$). The chronological DHC curves are an input for the investment model, as highlighted in 2. Consequently, $m = 54$ sample years are assessed for DHC. For SHC, *m* is reduced to 1 and represents the static regulatory reference scenario.

Table 3 summarises the average annual injectable energy at the three network nodes for each of the four HC concepts under evaluation. Average annual injectable energy represents the average of the 54 sample years of load and RES variability considered for DHC evaluation. The table further presents the percentual increase of injectable energy compared to the regulatory reference HC, SHC N-1. The results highlight the potential of less restrictive HC definitions to speed up the network integration of new generation assets.

Table 3: Average annual injectable energy (GWh/yr) [9]

	Node3	**Node5**	**Node14**
SHC N-1	28.47	21.99	25.14
SHC N	28.51 *(+0.13%)*	28.58 *(+30%)*	42.74 *(+70%)*
DHC N-1	38.15 *(+34%)*	26.17 *(+19%)*	31.93 *(+27%)*
DHC N	46.12 *(+62%)*	36.72 *(+67%)*	44.25 *(+76%)*

3.2 Renewable generation

The corresponding input is required to adequately represent the two RES generation technologies (i.e., PV, wind) and the storage the model considers. The batteries are modelled as 4-hour batteries with an efficiency of 85% [38]. As pointed out in 2, various sample years are modelled to express the variability of PV and wind resource availability. The sample years are the same as those employed for HC determination in [9]. As described in 3.1, PV availability is represented with *p = 3* sample years. Wind availability is represented with *w = 6* sample years to capture the higher randomness of the resource. The RES availability curves represent Almería, Spain [39], [40]. The selected years and their variety of full-load hours are summarised in Figure 2.

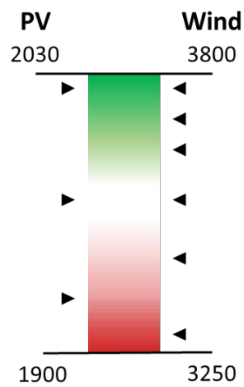

Figure 2: Full-load hours of PV and wind availability sample years

3.3 Investment and operation costs

The investment model requires input on CAPEX and OPEX of the generation technologies. The input for the annual scenario evaluation is summarised in Table 4. The costs represent 2022 generation costs and are annualised with a weighted average cost of capital of 7.5% [41] and the lifetime shown in the table. PV and wind-related costs are based on [41], and battery-related costs on [38].

Table 4: RES and storage investment cost model input

	Annualised investment (EUR/MW*yr)	**O&M (EUR/kW*yr)**	**Lifetime (years)**
PV	66,375	7.99	25
Wind	98,112	28.53	25
4h-Battery	255,876	56.47	15

3.4 Remuneration

The *CP* input is based on recent auction results throughout Europe, due to the small amount of data available for Spain. Results are reported to be between 30 and 95 EUR/MWh for wind and PV [42]. The few available Spanish auction results represent the lowest observed results, so the remuneration is considered at 60 EUR/MWh for the base case. Furthermore, a sensitivity of 40 EUR/MWh is included in the analysis, as Spanish auction results have been reported to be below 37 EUR/MWh.

The *CC* presented in Eq. 5 has been set to 5% for non-controllable and 25% for controllable generation units in previous auctions [43]. Accordingly, the coefficient is set to 5% in the base case, but a sensitivity analysis will analyse levels of 25%, 50%, 75% and 100%. A 100% coupling coefficient represents a merchant installation fully exposed to market prices. Different sample years of market prices are included to assess the increasing exposure to market volatility. The last five years ($s = 5$) of Spanish SPOT market prices are evaluated in this analysis [44]. Figure 3 presents the histograms which point out the variability among the market price input years. As stated in 2.2, the investment model is evaluated for all $m = 54$ HC years with the corresponding PV and wind availability and the five market price years. The analysis is combinatorial to express the uncertainty related to future resource availability and market prices, leading to a total of $n = 54*5 = 270$ ICPs.

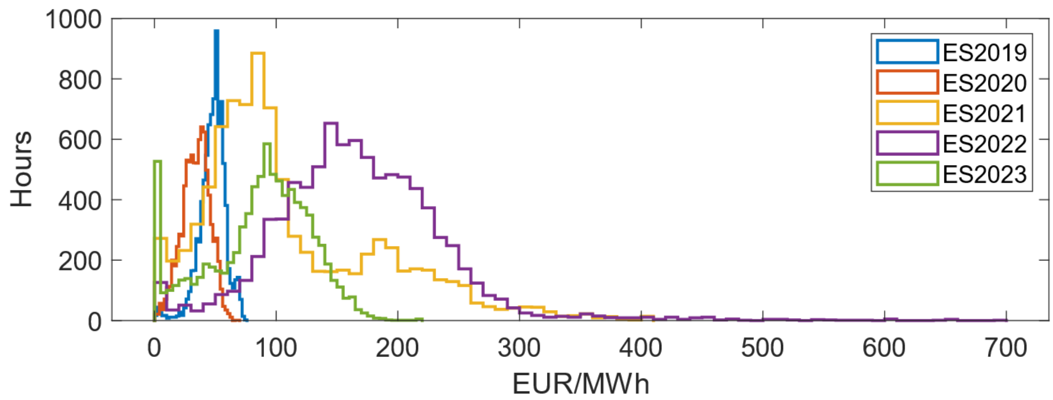

Figure 3: Market price input histograms

3.5 Operational evaluation

The operational evaluation is carried out for the *n = 270* scenarios of HC and RES availability and market prices introduced in 3.4. Accordingly, each ICP's performance is assessed by calculating the energy injection and the corresponding profits throughout the 270 sample years (Table 2). Conditional Value-at-Risk is then determined for the worst 5% (*δ = 5%*) of profits obtained from the operational evaluation [20]. For computing CVaR, all 270 sample years are considered equally probable.

3.6 Sensitivity assessment

As highlighted throughout the previous sections, the methodology is first performed on a base case. After that, the robustness of the findings is enhanced via several sensitivities. An overview of the characteristics evaluated in the sensitivity analysis is provided in Table 5. As shown in the table, the sensitivities seek to assess the dependency of the results on the network node (i.e. HC availability, section 3.1), the *CP* and the *CC* input for the remuneration (section 3.4). The sensitivity on the *CP* is performed on all three nodes assessed in the nodal sensitivity. The *CC* is evaluated only over the base case for brevity.

Table 5: Overview of base case and sensitivity characteristics

Sensitivity case	Node	Clearing price	Coupling coefficient
Base case	5	40 EUR/MWh	5%
Nodal sensitivities	3, 14	40 EUR/MWh	5%
Clearing price sensitivities	3, 5, 14	60 EUR/MWh	5%
Coupling coefficient sensisitivities	5	60 EUR/MWh	25%, 50%, 75%, 100%

4 Case study results

In the course of this section, the case study results are presented. First, the base case will be analysed in detail. For clarity, the results are shown and analysed step by step. As described in 2.1, the HC is a result from a previous work and used as an input to the computation process. Hence, in this section, the investment model outputs (Step 2) represent the first results. The resulting ICPs are assessed in 4.1, followed by the operational evaluation (Step 3) in 4.2 and the investment decision (Step 4) in 4.3. Section 4.4 presents the results of the sensitivity analyses.

4.1 Step 2: Investment candidate portfolios

In Step 2 of the proposed methodology, the investment optimisation model is run independently for the 270 sample years, providing 270 ICPs. The analysis is carried out individually for all HC concepts, resulting in 270 ICPs for each of the four HC concepts. Additionally, capacity investment is optimised once for non-hybrid installations and once for hybridisation between PV, wind and 4h-batteries. Figure 4 shows a boxplot of the investment model results for the base case at node 5 of the 20 kV CIGRE benchmark network. The boxes represent the total installed capacities of the ICPs obtained from the investment model for the 270 sample years in MW. The scenario names are composed of the HC concept (i.e. SHC and DHC; N-1 and N) and an indicator of whether the results represent the non-hybrid (NH) or the hybrid (H) results of the investment model. Installed capacities range from 3.2 MW in the case of SHC N-1 NH to over 8 MW in the case of DHC N H. In the non-hybrid cases, more capacity is installed at SHC N than at DHC N-1. This aligns with the increase in injectable energy presented in Table 3. This trend is not visible in the hybrid cases, as different ratios of PV and wind capacity eliminate the effect. Both non-hybrid and hybrid point out the potential of less conservative HC restrictions, as installed capacities show a notable increase. It is important to note that all hybrid capacity portfolios are composed of PV and wind capacity. In none of the cases does the model install batteries due to the magnitude of its CAPEX.

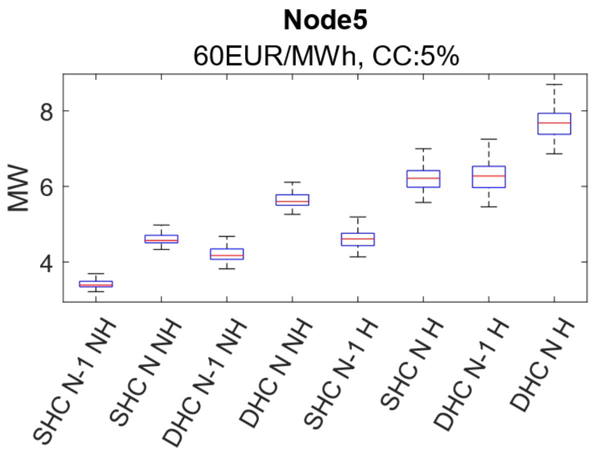

Figure 4: Investment model results

4.2 Step 3: Operational evaluation

The operational evaluation helps to assess the ICPs presented in the previous section. The boxes in Figure 4 contain 270 investment decisions for each HC and hybridisation case. The decisions depend on the sample years, which differ in RES availability, market prices and HC. As indicated in 2.2, each investment decision for a candidate portfolio is based on one of the sample years, and the operational evaluation determines the profits of the given portfolio throughout all other sample years (section 2.3). Those profits then allow the calculation of the ICP's Conditional Value-at-Risk.

Figure 5 shows the results of the operational evaluation by summarising the CVaR and the average profits obtained by each of the 270 ICPs for each HC concept, once for the non-hybrid and once for the hybrid capacity installations. The figure shows that the relation between CVaR and average profits is linear within each HC and hybridisation case due to the low coupling coefficient to market prices. That means that the maximum average profits and the maximum CVaR (i.e. worst-case profits) are obtained from the same ICP.

Also, Figure 5 points out that the impact of moving from N-1 to N reliability criteria for HC calculation on CVaR and average profits is more pronounced than the impact of hybridisation. Combining hybridisation and DHC (i.e. DHC N H) allows for a significant increase in CVaR and average profits compared to SHC N-1 NH.

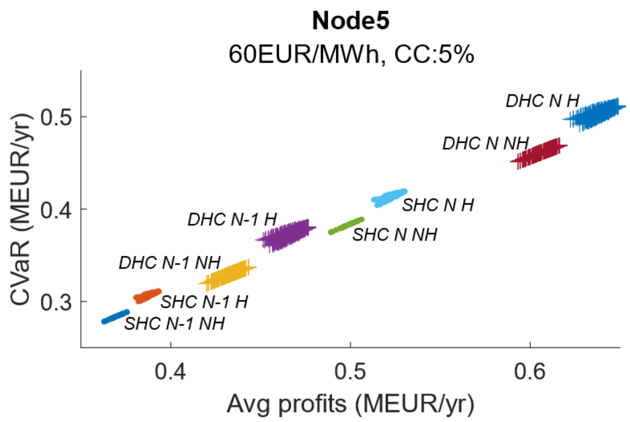

Figure 5: Operational evaluation

4.3 Step 4: Investment decision

The candidate portfolio's operational evaluation allows to draw conclusions on the optimal portfolio investment decision. The chosen generation capacity portfolios for each case represent the investment decisions leading to maximum values of CVaR and average profits (Figure 5). Figure 6 shows the results of the investment decisions for the base case at node 5. The figure shows the installed capacities (left axis) and the optimal portfolio's average annual energy injection obtained throughout all sample years (right axis). In all non-hybrid cases, the model installs wind capacity. The hybrid results show a capacity portfolio of wind and PV. As mentioned in 4.1, no battery capacity is installed.

PV accounts for 36% of the non-hybrid portfolios in most cases. Only at DHC N-1 H, PV accounts for 45% of the capacity. These shares indicate the complementarity of the RES resources to make a more efficient use of a given network node's HC. This is underlined by the increase in energy injection. Average annual energy injection increases around 12% for the portfolios with 36% PV participation compared to the non-hybrid portfolio of the same HC concept (i.e. SHC N H vs SHC N NH). In the case of DHC N-1 H, where PV represents 45% of the portfolio, the average annual energy injection is increased by 18%. This increase in energy injection leads to a rise in average annual profits of 5%, 7% in the case of DHC N-1 H. In line with profits, CVaR increases by 8% to 13%.

The relaxation of HC calculation criteria significantly impacts installed capacities and energy injection, increasing profits and CVaR, as seen in Figure 5. DHC N NH leads to a 65% increase in installed capacity and energy injection compared to SHC N-1 NH. CVaR and average annual profits are increased by 62% and 64%, respectively. Relaxing only the reliability constraint but not the time granularity constraint (i.e. SHC N NH) increases all indicators under evaluation by 35%. These increases from SHC N-1 align with the increases in injectable energy derived from the node's HC (Table 3).

When accounting for hybridisation, the previous findings are amplified. DHC N H leads to a 127% increase in installed capacity compared to SHC N-1 NH. The average annual energy injection increases by 86%, and CVaR and average annual profits increased by 77% and 73%, respectively. Even without relaxing the time constraint, the increase is notable. SHC N H shows an 81% increase in installed capacity and 51% additional average annual energy injection compared to SHC N-1 NH. CVaR and average profits are increased by 45% and 41%, respectively.

These findings highlight how the mechanisms of relaxing HC calculation restrictions and the hybridisation of generation portfolios allow for a more efficient use of hosting capacity. The combination of hybridisation and the relaxation of HC calculation criteria leads to the most significant increases in the use of the existing electricity distribution network capacity. All increases in the use of HC, i.e., installed capacities and energy injections, are accompanied by increases in average profits and CVaR (i.e. worst-case profits) of the portfolios.

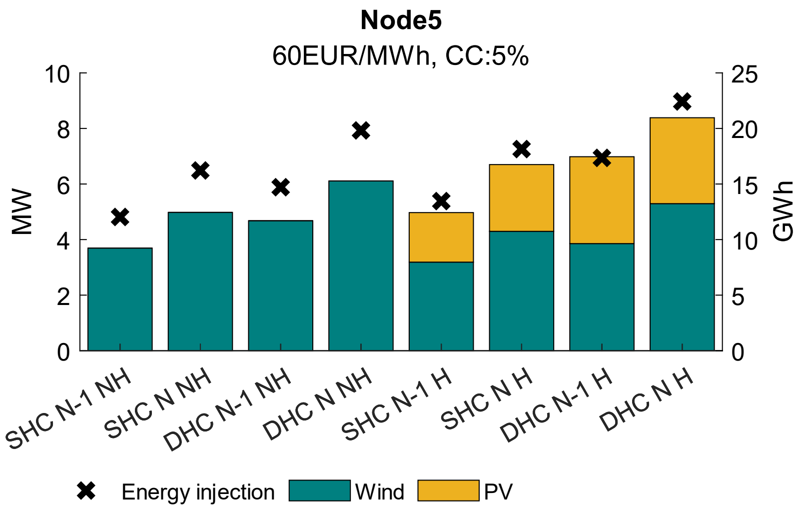

Figure 6: Investment decision - base case

4.4 Sensitivity analysis

Several sensitivities are performed to assess the dependence of the results on certain input assumptions. Figure 7 shows the sensitivity results for the portfolio optimisation at different network nodes and the variation of the auction clearing price. Three different nodes of the

20 kV CIGRE benchmark network are compared, each at a clearing price of 60 EUR/MWh (base case) and 40 EUR/MWh.

The figure provides information on the final portfolios' average annual profits. In line with the scope of this work, the results are presented as increases with respect to the corresponding result for the case of SHC N-1 NH. The numerical results in the column on the left of the incremental representation provide the total magnitudes obtained for the corresponding SHC N-1 NH case. This means that at node 5, at *CP = 60 EUR/MWh*, the optimal portfolio for SHC N-1 NH yields an annual average profit of 0.38 MEUR/yr. Each numerical result in the figure is based on the optimal generation capacity's performance over the *n = 270* years considered for the operational evaluation.

The figure also shows that, for all nodes, the increases are aligned for both *CP* sensitivities. The clearing price influences the magnitude of the installed capacity and its energy injection and profits, but not the relative relation between the different HC concepts. The nodal sensitivities yield a more significant variation of the impact of relaxing HC calculation criteria and hybridisation. However, for each node, the increases in energy injection and profits align with the increases in injectable energy derived from the HC assessment (Table 3). The findings show that the benefits of relaxing HC calculation criteria previously assessed from a network perspective (i.e. injectable energy) can be translated to benefits for promoters seeking profit maximisation (i.e. energy injection and profits).

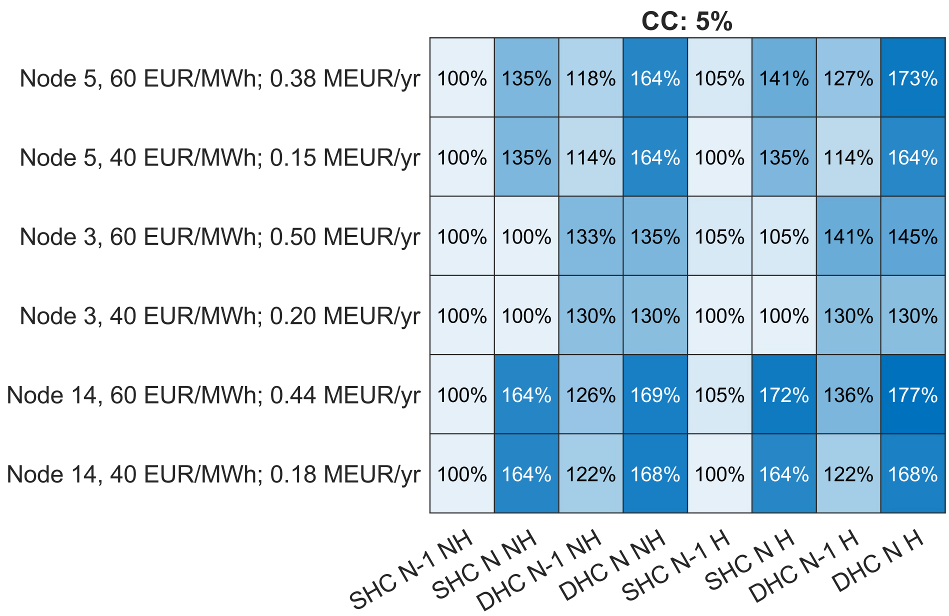

Figure 7: Nodal and ICP sensitivity analysis – average profits

Figure 8 presents the operational evaluation of CVaR and average profits for the market coupling coefficient sensitivity. Results are presented for the base case assumptions of node 5 and a clearing price of 60 EUR/MWh, as indicated in Table 5. The sensitivity gradually increases the market coupling coefficient (Eq. 5) from 5% to 100%, including interim values of 25%, 50% and 75%. The operational evaluation of CVaR (i.e. worst-case profits) over average profits of the performance of the candidate portfolios for all sample years gradually deviates from the linearity observed at *CC = 5%*. High *CC*s have a higher impact on the linearity of profits and CVaR than the HC concept or hybridisation. Hence, a RES generation capacity investment's risk derived from the exposure to market prices is more significant than the risk due to uncertainty surrounding HC and RES availability.

Higher exposure to market prices allows higher profits by overdimensioning the candidate portfolio for years where the average price captured is extraordinarily high. However, the exposure also increases the risk related to incorrect market forecasts. This can be seen especially in the case of *CC = 100%*. The results show up to 1.31 MEUR of average annual profits in the case of DHC N H. However, the majority of CVaR results are negative, indicating losses. As a consequence, the investment decision is less straightforward for *CC > 25%* due to the loss of linearity. The maximisation of average profits and the maximisation of CVaR no longer result in the same candidate portfolio being selected.

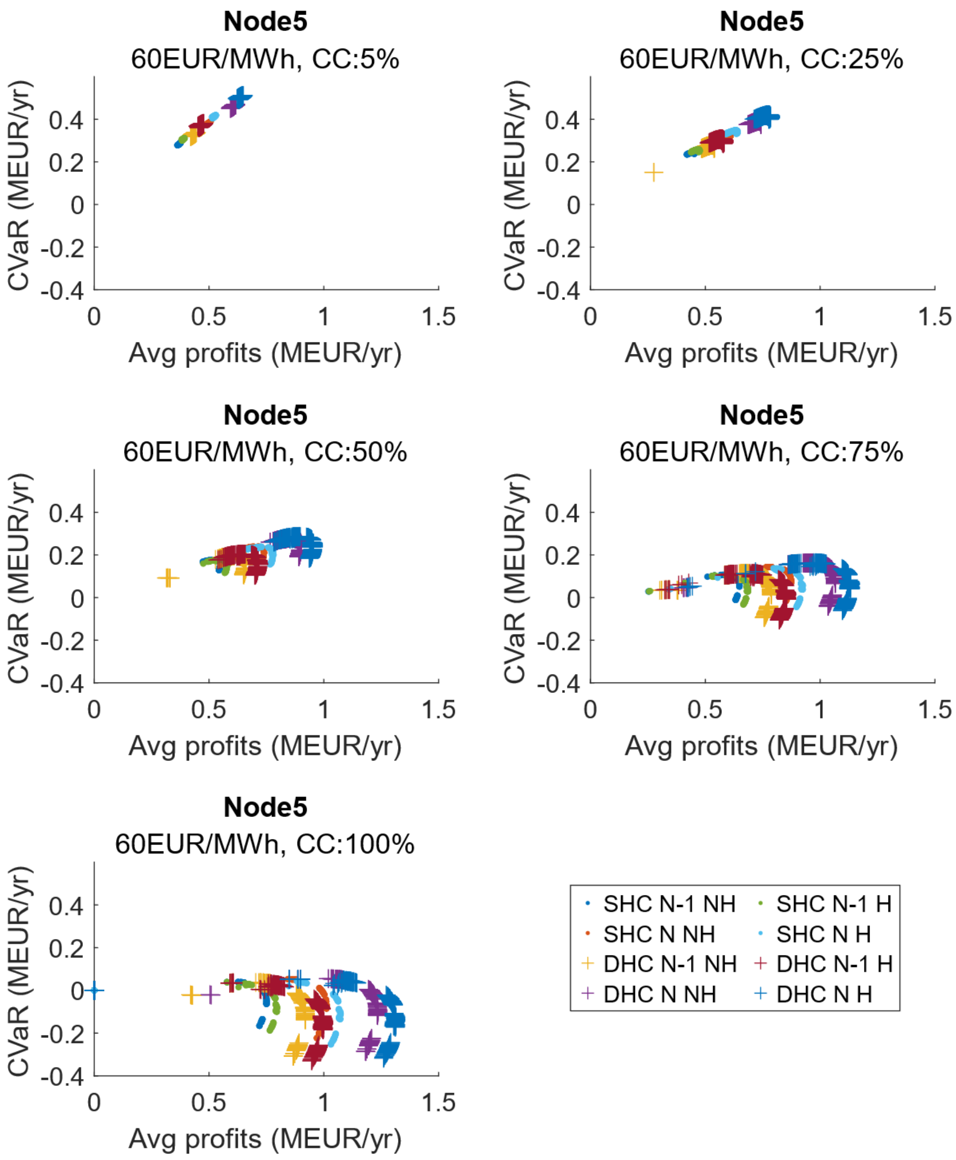

Figure 8: Market coupling coefficient sensitivity - operational evaluation

Figure 9 provides an exemplary evaluation of the operational results of DHC N H. The figure shows the results of CVaR and average profits of all ICPs derived for DHC N H at 75% *CC*. The resulting data indicate the existence of a Pareto front that supports the identification of the optimal investment decision. The ICPs on the Pareto front are characterised by the fact that there is no other ICP which shows higher CVaR and average profits. Of the 270 ICPs subject to the operational evaluation, 54 ICPs form the Pareto front. CVaR of the ICPs on the Pareto front ranges from 0.064 MEUR/yr to 0.162 MEUR/yr (+157% from the minimum CVaR), and average profits range from 0.983 MEUR/yr to 1.132 MEUR/yr (+15% from the minimum average profits). Further, the ICPs on the Pareto front can be grouped into three groups similar in CVaR and average profits, as supported by the visualisation in Figure 9.

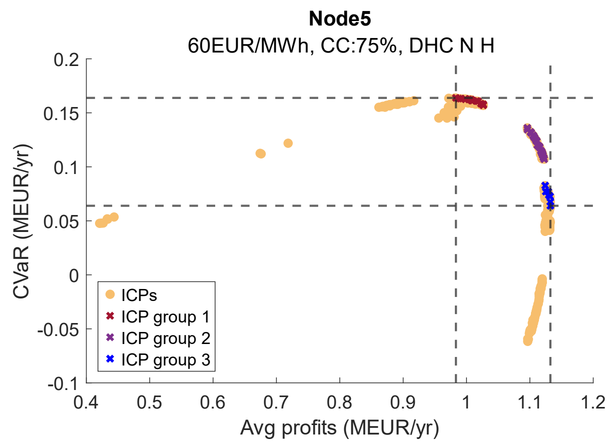

Figure 9: Pareto front on operational evaluation at high CC

Figure 10 provides more insight into the ICPs on the Pareto front. The figure shows the composition of the capacity mixes according to the group identified previously. The total amount of DG installed supports the division into the three groups. Group 1 represents the group with the highest CVaR values (Figure 9) and the lowest total capacity installed (Figure 10). In this group, worst-case average profits are maximised via smaller investments (i.e. lower capacity investments). Group 2 is on the opposite side of the investment decision spectrum and shows the lowest CVaR values (Figure 9) and the highest total capacity installed (Figure 10). Here, average profits are maximised by increasing the energy injection into the network (i.e. higher market revenue). Group 3 represents intermediate values for CVaR (Figure 9) and installed DG capacity (Figure 10).

In cases such as the one at hand, the final investment decision depends on the risk-aversion or risk-prone attitude of the investor. A more risk-averse investor would opt for an ICP of group 1, as the ICPs have the highest CVaR and the lowest investment requirements, i.e. capital at risk. Installing more capacity means moving towards ICP group 2. This implies reducing CVaR, i.e. worst-case profits. As highlighted above, the span of average profits obtained by the ICPs on the Pareto front increases by 15% from the lowest to the highest value. However, CVaR increases by 157%. ICPs of group 1 yield similar average profits while requiring less investment due to the lower installed capacities. Given all the above, the capacity mixes of the ICPs in group 1 seem the most reasonable investment choice. Wind is predominant in these ICPs, ranging from 4.7 to 4.9 MW. These capacities are complemented by 1.1 to 2.3 MW of PV.

A more risk-prone investor might opt for an ICP in group 3. This group is characterised by intermediate values of CVaR and average profits. The average profits of group 3 almost reach the maximum average profits of the ICPs on the Pareto front while maintaining CVaR at a higher level. In group 3, PV capacities range from 2.2 to 3.3 MW and wind capacities from 5.6 to 6.1 MW. The ICP choice with a CVaR closest to group 1 results in 2.5 MW of PV and 5.6 MW of wind. This ICP yields a CVaR of 0.136 MEUR/yr and average profits of 1.096 MEUR/yr.

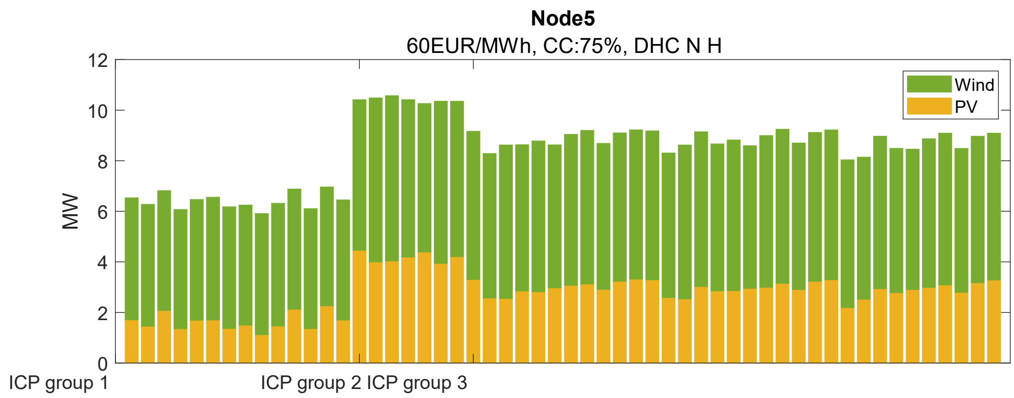

Figure 10: Capacity composition on the Pareto front

The analysis of the *CC* sensitivity highlights the contribution of the CVaR method for determining an optimal RES capacity investment decision while accounting for risk. Investment decisions based on average profits alone would have resulted in a higher total investment. Further, considering a too small amount of sample years might even lead to investment decisions with losses (see the ICPs on the bottom right in Figure 9).

5 Conclusions

This paper contributes a RES generation capacity investor perspective on the ongoing discussion of a more efficient use of existing electricity distribution network capacity for a successful energy transition. A cascade methodology is employed to point out how a more flexible definition of hosting capacity and the hybridisation of PV and wind energy can help increase the use of existing network capacity. The methodology accounts for investment risk via the CVaR metric, which is applied to the operational profits of the ICPs, ensuring a maximisation of a portfolio's worst-case profits.

Four different HC concepts with different temporal granularity and reliability considerations are evaluated: SHC N-1, SHC N, DHC N-1 and DHC N. 54 years of load and RES variability are considered for determining DHC variations. Five years of different market price assumptions are included in the analysis, leading to a total of 54*5 = 270 sample years assessed during portfolio optimisation.

The case study performed on nodes of the CIGRE 20 kV benchmark system quantifies the benefits of relaxing HC calculation criteria. For the base case, DHC N leads to a 65% increase in installed capacity and, consequently, to a 65% increase in energy injection. This increase is accompanied by a 62% higher CVaR and 64% higher average profits. Combined with hybridisation, the generation portfolio grows by 127%, leading to an 87% average annual energy injection increase. DHC N H allows an increase in CVaR and average profits by around 75% compared to SHC N-1 NH.

Sensitivity analyses assess the robustness of the findings to the network node under consideration, the clearing price of the auction result modelled at the investment model stage, and the market coupling coefficient of the remuneration to market prices. The results of the first two sensitivities confirm the findings of the base case: despite different absolute magnitudes, both average annual energy injection and average annual profits increase in line with the increases of injectable energy of the corresponding node when relaxing the calculation criteria of HC. The last sensitivity highlights how increasing market price coupling coefficients complicate the investment decision as CVaR and average profits are no longer in a linear relationship. *CCs ≥ 75%* show high average profits at the cost of negative CVaRs, stressing the risk associated with incorrect future market price assumptions at high exposures.

This work contributes a new perspective on relaxing the HC calculation criteria and shows that, despite increased uncertainty, DHC is of interest to RES investors. All proposed HC concepts show an increase in installed capacity and profits from the regulatory HC criterion. The corresponding increase in injected energy underlines the relevance of the HC concepts in speeding up the energy transition by enhancing the use of existing electricity distribution grids without endangering a safe network operation. Further, the uncertainty surrounding the investment in RES generation capacity requires an approach that allows to account for investment risk. This work proposes a methodology adaptable to different investor risk-adversity levels.

Future work should address the uncertainty of HC for new generators under load growth related to different new load vectors. Further, carrying the concepts of relaxing nodal HC to the operation of a network with various customers connected under this new regulatory regime requires further research. Additionally, combining DHC with other HC enhancement techniques could further speed up the distribution grid integration of DER. Applying the existing methodology to demand instead of generation represents another promising research line.

6 Acknowledgements

The authors appreciate the funding for the mobility of professors and researchers in foreign research centres obtained from Universidad Pontificia Comillas.

This research has been carried out thanks to the Iberdrola Chair on Energy and Innovation and the funding of the RETOS COLABORACIÓN programme of the Spanish Ministry of Science and Innovation and the Spanish State Research Agency (project "Platform of innovative models to accelerate the energy decarbonisation of the economy (MODESC)", with reference number RTC2019- 007315-3).

7 References

[1] Eurelectric, 'Grids for speed - Eurelectric Power Summit 2024'. Accessed: May 23, 2024. [Online]. Available: https://powersummit2024.eurelectric.org/grids-for-speed/

[2] Eurelectric, 'Electrification Action Plan'. Accessed: Sep. 24, 2024. [Online]. Available: https://www.eurelectric.org/wp-content/uploads/2024/06/electrification-action-plan-final.pdf

[3] CEER, 'CEER Paper on Alternative Connection Agreements'. Accessed: Dec. 11, 2023. [Online]. Available: https://www.ceer.eu/documents/104400/-/-/e473b6de-03c9-61aa-2c6a-86f2e3aa8f08

[4] T. Gómez, R. Cossent, and J. P. Chaves-Avila, 'Flexible network access, local flexibility market mechanisms and cost-reflective tariffs: three regulatory tools to foster decarbonized electricity networks', *Oxford Energy Forum*, vol. 124, pp. 18–23, May 2020, doi: https://www.iit.comillas.edu/publicacion/mostrar_publicacion_working_paper.php.es?id=387.

[5] M. H. J. Bollen and N. Etherden, 'Overload and overvoltage in low-voltage and medium-voltage networks due to renewable energy — Some illustrative case studies', in *2011 2nd IEEE PES International Conference and Exhibition on Innovative Smart Grid Technologies*, Dec. 2011, pp. 1–8. doi: 10.1109/ISGTEurope.2011.6162645.

[6] L. Herding, R. Cossent, and M. Rivier, 'Enhancing RES Grid Connection via Dynamic Hosting Capacity and Hybridization', presented at the 2023 IEEE Belgrade PowerTech, Belgrade, Serbia: IEEE, 2023. doi: 10.1109/PowerTech55446.2023.10202726.

[7] A. K. Jain *et al.*, 'Dynamic hosting capacity analysis for distributed photovoltaic resources—Framework and case study', *Applied Energy*, vol. 280, p. 115633, Dec. 2020, doi: 10.1016/j.apenergy.2020.115633.

[8] S. Hajeforosh, A. Khatun, and M. Bollen, 'Enhancing the hosting capacity of distribution transformers for using dynamic component rating', *International Journal of Electrical Power & Energy Systems*, vol. 142, p. 108130, Nov. 2022, doi: 10.1016/j.ijepes.2022.108130.

[9] L. Herding, L. Carvalho, R. Cossent, and M. Rivier, 'A security-aware dynamic hosting capacity approach to enhance the integration of renewable generation in distribution networks', *International Journal of Electrical Power & Energy Systems*, vol. 161, p. 110210, Oct. 2024, doi: 10.1016/j.ijepes.2024.110210.

[10] M. Alraddadi, A. J. Conejo, and R. M. Lima, ‘Expansion Planning for Renewable Integration in Power System of Regions with Very High Solar Irradiation’, *Journal of Modern Power Systems and Clean Energy*, vol. 9, no. 3, pp. 485–494, May 2021, doi: 10.35833/MPCE.2019.000112.

[11] R. A. Shaikh, D. J. Vowles, A. Allison, and D. Abbott, ‘Evaluation of Australia’s Generation-Storage Requirements in a Fully Renewable Grid With Intermittent and Flexible Generation’, *IEEE Access*, vol. 11, pp. 64201–64218, 2023, doi: 10.1109/ACCESS.2023.3286037.

[12] R. Diewvilai and K. Audomvongseree, ‘Enhancing Generation Expansion Planning With Integration of Variable Renewable Energy and Full-Year Hourly Multiple Load Levels Balance Constraints’, *IEEE Access*, vol. 12, pp. 41143–41167, 2024, doi: 10.1109/ACCESS.2024.3377660.

[13] X. Chen, J. Lv, M. B. McElroy, X. Han, C. P. Nielsen, and J. Wen, ‘Power System Capacity Expansion Under Higher Penetration of Renewables Considering Flexibility Constraints and Low Carbon Policies’, *IEEE Transactions on Power Systems*, vol. 33, no. 6, pp. 6240–6253, Nov. 2018, doi: 10.1109/TPWRS.2018.2827003.

[14] M. Melliger and E. Chappin, ‘Phasing out support schemes for renewables in neighbouring countries: An agent-based model with investment preferences’, *Applied Energy*, vol. 305, p. 117959, Jan. 2022, doi: 10.1016/j.apenergy.2021.117959.

[15] F. S. Mahmoud *et al.*, ‘Optimal sizing of smart hybrid renewable energy system using different optimization algorithms’, *Energy Reports*, vol. 8, pp. 4935–4956, Nov. 2022, doi: 10.1016/j.egyr.2022.03.197.

[16] M. J. Mayer, A. Szilágyi, and G. Gróf, ‘Environmental and economic multi-objective optimization of a household level hybrid renewable energy system by genetic algorithm’, *Applied Energy*, vol. 269, p. 115058, Jul. 2020, doi: 10.1016/j.apenergy.2020.115058.

[17] H. HassanzadehFard and A. Jalilian, ‘Optimal sizing and location of renewable energy based DG units in distribution systems considering load growth’, *International Journal of Electrical Power & Energy Systems*, vol. 101, pp. 356–370, Oct. 2018, doi: 10.1016/j.ijepes.2018.03.038.

[18] R. T. Rockafellar and S. Uryasev, ‘Optimization of conditional value-at-risk’, *Journal of Risk*, vol. 2, no. 3, pp. 21–41, 2020.

[19] M. Zhang, Y. Tang, L. Liu, and D. Zhou, ‘Optimal investment portfolio strategies for power enterprises under multi-policy scenarios of renewable energy’, *Renewable and Sustainable Energy Reviews*, vol. 154, p. 111879, Feb. 2022, doi: 10.1016/j.rser.2021.111879.

[20] H. Saber, H. Heidarabadi, M. Moeini-Aghtaie, H. Farzin, and M. R. Karimi, ‘Expansion Planning Studies of Independent-Locally Operated Battery Energy Storage Systems (BESSs): A CVaR-Based Study’, *IEEE Transactions on Sustainable Energy*, vol. 11, no. 4, pp. 2109–2118, Oct. 2020, doi: 10.1109/TSTE.2019.2950591.

[21] E. Mortaz, ‘Portfolio Diversification for an Intermediary Energy Storage Merchant’, *IEEE Transactions on Sustainable Energy*, vol. 11, no. 3, pp. 1539–1547, Jul. 2020, doi: 10.1109/TSTE.2019.2929947.

[22] Z. Qi, Q. Junjie, Y. Dahai, X. Heng, L. Hengwei, and Z. Hongsheng, ‘Risk Assessment for Transmission Network Planning Scheme based on Conditional Value-at-Risk’, in *2018 8th*

International Conference on Power and Energy Systems (ICPES), Dec. 2018, pp. 49–53. doi: 10.1109/ICPESYS.2018.8626970.

[23] S. Paul and N. P. Padhy, 'Resilient Scheduling Portfolio of Residential Devices and Plug-In Electric Vehicle by Minimizing Conditional Value at Risk', *IEEE Transactions on Industrial Informatics*, vol. 15, no. 3, pp. 1566–1578, Mar. 2019, doi: 10.1109/TII.2018.2847742.

[24] A. Xuan, X. Shen, Q. Guo, and H. Sun, 'A conditional value-at-risk based planning model for integrated energy system with energy storage and renewables', *Applied Energy*, vol. 294, p. 116971, Jul. 2021, doi: 10.1016/j.apenergy.2021.116971.

[25] R. D. Zimmermann and C. E. Murillo-Sánchez, 'MATPOWER User's Manual, Version 7.1'. Accessed: Jul. 24, 2023. [Online]. Available: https://matpower.org/docs/MATPOWER-manual.pdf

[26] CNMC, 'Resolución de 20 de mayo de 2021, de la Comisión Nacional de los Mercados y la Competencia, por la que se establecen las especificaciones de detalle para la determinación de la capacidad de acceso de generación a la red de transporte y a las redes de distribución'. Accessed: Sep. 13, 2021. [Online]. Available: https://www.boe.es/eli/es/res/2021/05/20/(4)

[27] O. Valarezo, J. P. Chaves-Ávila, and T. Gómez, 'Multi-objective distribution network reconfiguration: application to a real large-scale distribution system', *Applied Energy*, vol. Under review.

[28] IEA, 'Renewable electricity capacity remuneration policy types, 2020-2025 – Charts – Data & Statistics', IEA. Accessed: Oct. 10, 2024. [Online]. Available: https://www.iea.org/data-and-statistics/charts/renewable-electricity-capacity-remuneration-policy-types-2020-2025-2

[29] MITECO, 'Real Decreto 960/2020'. Accessed: Dec. 09, 2020. [Online]. Available: https://boe.es/buscar/doc.php?id=BOE-A-2020-13591

[30] K. Antoniadou-Plytaria, D. Steen, L. A. Tuan, O. Carlson, and M. A. Fotouhi Ghazvini, 'Market-Based Energy Management Model of a Building Microgrid Considering Battery Degradation', *IEEE Transactions on Smart Grid*, vol. 12, no. 2, pp. 1794–1804, Mar. 2021, doi: 10.1109/TSG.2020.3037120.

[31] J. Lee, 'Statistics, Descriptive', in *International Encyclopedia of Human Geography*, R. Kitchin and N. Thrift, Eds., Oxford: Elsevier, 2009, pp. 422–428. doi: 10.1016/B978-008044910-4.00534-4.

[32] R. Khodabakhsh and S. Sirouspour, 'Optimal Control of Energy Storage in a Microgrid by Minimizing Conditional Value-at-Risk', *IEEE Transactions on Sustainable Energy*, vol. 7, no. 3, pp. 1264–1273, Jul. 2016, doi: 10.1109/TSTE.2016.2543024.

[33] J. Garcia-Gonzalez, E. Parrilla, and A. Mateo, 'Risk-averse profit-based optimal scheduling of a hydro-chain in the day-ahead electricity market', *EUROPEAN JOURNAL OF OPERATIONAL RESEARCH*, vol. 181, no. 3, pp. 1354–1369, Sep. 2007, doi: 10.1016/j.ejor.2005.11.047.

[34] S. Sarykalin, G. Serraino, and S. Uryasev, 'Value-at-Risk vs. Conditional Value-at-Risk in Risk Management and Optimization', *INFORMS TutORials in Operations Research*, Oct. 2014, doi: 10.1287/educ.1080.0052.

[35] CIGRE, ‘Benchmark Systems for Network Integration of Renewable and Distributed Energy Resources’, e-cigre. Accessed: Oct. 26, 2023. [Online]. Available: https://e-cigre.org/publication/ELT_273_8-benchmark-systems-for-network-integration-of-renewable-and-distributed-energy-resources

[36] K. Rudion, A. Orths, Z. A. Styczynski, and K. Strunz, ‘Design of benchmark of medium voltage distribution network for investigation of DG integration’, in *2006 IEEE Power Engineering Society General Meeting*, Jun. 2006, p. 6 pp.-. doi: 10.1109/PES.2006.1709447.

[37] University of Kassel and Fraunhofer IEE, ‘CIGRE Networks — pandapower 2.4.0 documentation’. Accessed: Oct. 26, 2023. [Online]. Available: https://pandapower.readthedocs.io/en/v2.13.1/networks/cigre.html

[38] NREL, ‘Annual Technology Baseline - Commercial Battery Storage’, 2023. doi: 10.2172/1665769.

[39] S. Pfenninger and I. Staffell, ‘Long-term patterns of European PV output using 30 years of validated hourly reanalysis and satellite data’, *Energy*, vol. 114, pp. 1251–1265, Nov. 2016, doi: 10.1016/j.energy.2016.08.060.

[40] I. Staffell and S. Pfenninger, ‘Using bias-corrected reanalysis to simulate current and future wind power output’, *Energy*, vol. 114, pp. 1224–1239, Nov. 2016, doi: 10.1016/j.energy.2016.08.068.

[41] IRENA, ‘Renewable power generation costs in 2022’, 2023.

[42] IEA, ‘Renewable electricity – Renewable Energy Market Update - May 2022 – Analysis’, IEA. Accessed: Oct. 23, 2024. [Online]. Available: https://www.iea.org/reports/renewable-energy-market-update-may-2022/renewable-electricity

[43] MITECO, ‘Subastas del Régimen Económico de Energías Renovables’, Ministerio para la Transición Ecológica y el Reto Demográfico. Accessed: Nov. 08, 2024. [Online]. Available: https://www.miteco.gob.es/content/miteco/es/es/energia/renovables/regimen-economico.html

[44] REE, ‘Bienvenido | ESIOS electricidad · datos · transparencia’. Accessed: Oct. 23, 2023. [Online]. Available: https://www.esios.ree.es/es

7.6 Conference paper

Enhancing RES grid connection via dynamic hosting capacity and hybridization

Leslie Herding*, Rafael Cossent, Michel Rivier,

Institute for Research in Technology (IIT), ICAI School of Engineering, Universidad Pontificia Comillas, C/Santa Cruz de Marcenado 26, 28015 Madrid, Spain

*) Corresponding author: lherding@comillas.edu

Abstract

Decarbonizing the energy sector requires the rapid integration of significant renewable generation capacity into electricity grids. The enhancement of existing grid capacity, avoiding reinforcement, represents an interesting alternative to accelerate the grid integration of new capacity. Dynamic hosting capacity (DHC) allows distribution system operators to move away from conservative definitions of available grid capacity. Hybridization allows promoters to combine different renewable generation and storage technologies at the same connection point to maximize the injection of energy into the grid. This work proposes a model to analyze the two mechanisms to enhance existing hosting capacity and presents results for a case study at three different connection points and locations in Spain. A dynamic definition of grid hosting capacity is found to increase the renewable energy sources (RES) installed capacity as well as their injected energy by up to 9%. The hybridization of photovoltaic (PV) and wind capacity increases installed capacity by 9% to 54%, injecting up to 20% more energy into the network. Combining dynamic hosting capacity and hybridization increases total RES installed capacity by up to 62%, injecting up to 29% more energy into the grid. Assumed battery investment costs result in the economic infeasibility of storage installation.

Keywords

Electricity sector decarbonization, non-firm access, hosting capacity, dynamic line rating, hybridization

Parameter	Definition	Unit
HC	Electricity grid hosting capacity	MW
Inv_t / Inv_b	Annualized Investment cost	MEUR/yr
pu_{th}	Availability of RES resource	-
$Pmax$	Maximum installed capacity threshold	MW
Rem_h	Remuneration for injected energy	EUR/MWh
Variables		
$Binary\_Inv\_Dec_t$	Binary investment decision variable per technology	[0, 1]
E_avail_h	Energy available	MWh
E_BSSin_h	Battery storage charge	MWh
E_BSSout_h	Battery storage discharge	MWh
E_curt_h	Energy curtailed	MWh
E_inj_h	Energy injected into the electricity grid	MWh
P_t	Installed RES & storage capacity per technology	MW
Sets		
h	Hour	
t	Technology (PV, wind)	
b	Batteries	

1. Introduction

The European energy policy seeks to increase the European climate ambition for 2030. In the course of this ambition, European countries detail their energy transition objectives within National Energy and Climate Plans (NECPs) [1]. One of the topics included in the NECPs is the transition towards a more sustainable, decarbonized energy sector. Electricity grids play a major role in accommodating high shares of intermittent renewable energy sources (RES) generation. The new installations challenge current electricity networks with a high number of connection requests [2]–[4], requiring grid reinforcement to accommodate the increased amount of RES capacity [5] or leading to the rejection of access requests to network nodes where reinforcement is not possible.

Even though electricity grid reinforcement is not the critical investment necessary for electricity grid decarbonization [6], constructing electricity lines implies a prolonged connection time. Hence, alternative mechanisms for enhancing the electricity grid's capacity to integrate high RES shares are worth investigating.

The capacity of the electricity network to integrate further generation or demand is denominated as hosting capacity (HC). For the determination of available HC, the impact of connecting a new unit on performance indicators such as power quality is considered [7]. The introduction of RES generation will affect the performance index. Up to a certain limit, deterioration of the index is tolerated as long as it does not endanger the safe operation of the grid. However, when the limit is exceeded, reinforcement is required to guarantee the system's safety, especially with increasing shares of RES. The capacity of RES that can be connected to the grid without exceeding the limit of the performance index is the network's HC [8].

The common criteria employed by distribution system operators (DSOs) for calculating HC are conservative as they seek to guarantee the safe operation of the grid at all times [9]. Many European DSOs apply a single HC value obtained via conservative scenarios [10]. Using a single value of HC at all hours is considered static hosting capacity (SHC). There are several means to connect capacity above the SHC threshold, such as a dynamic definition of HC and the hybridization of generation installations by installing several technologies.

This work presents a model that quantifies the impacts of DHC and hybridization on integrating RES capacity into electricity distribution networks. It provides a case study for three Spanish locations, accounting for different potentials of photovoltaic (PV) and wind generation.

The remaining part of the paper is structured as follows: section II summarizes the measures of HC enhancement analyzed in this work, section III presents the development of the model, and section IV describes the scenarios. The case study and its results are presented in sections V and VI, respectively. Section VII sums up the conclusions.

2. Hosting capacity enhancement

2.1 Reinforcement

The first and most common approach for enhancing a network's HC is the reinforcement of the grid. Usually this means that connection-seekers meet costly reinforcement requirements for assets that might be used only during a reduced number of hours a year, if ever [9]. Also, high reinforcement requirements might lead to the economic infeasibility of small generation units when facing excessive connection costs (e.g. the upgrade of a transformer station) [9], [11], [12].

2.2 Dynamic hosting capacity

An alternative approach is enhancing the use of existing HC. Dynamic hosting capacity (DHC) allows the DSO to consider the variations of hosting capacity in different operating scenarios and provides the connection-seeker with more but one static threshold of HC. Variations in HC might be driven by seasonal differences in electricity line capacity due to varying weather conditions [13], [14], for example. Operational conditions of the network, such as the magnitude of demand, may also lead to congestions, reducing the available HC during some hours of the year.

2.3 Hybridization

Another mechanism to accelerate the integration of RES into electricity networks is the hybridization of generation installations. This means that installations of different electricity generation technologies share one connection point and are considered the same installation from the network operating perspective. Spanish regulation recently introduced this option for generators as long as the installation is hybridized with a renewable technology and the owner of the installation is the same [15]. Hybridization allows promoters to enhance the use of the electricity grid access they have been assigned by complementing intermittent

RES output profiles with another technology, including storage. In locations with low simultaneity of PV and wind production, a hybrid installation of these two technologies might be promising.

3. Model development

This work proposes a model to evaluate the optimal RES and storage capacity to be installed for each technology in the technology catalogue for a grid connection point with a given HC under the condition that the promoter's benefits are maximized. The electricity grid connection is modelled via the grid's hourly capacity for energy injection, electric power flows are not included in the model. Different criteria for the definition of restrictions allow to analyze the impact of DHC and hybridization on installed capacities and prices captured by the installations. Traditional reinforcement (section II.A) is not analyzed in this study as the greater use of existing HC is evaluated. The RES generator's access to the electricity grid model is designed as a mixed integer programming optimization model in GAMS applying the gurobi solver.

The following assumptions are implicit inputs to the model:

1. No maximum RES and storage installable capacity is fixed: the optimization model can install as much capacity as economically feasible, provided the grid HC restrictions are not violated. This means promoters are considered free to overdimension their installation behind the connection point as long as they deem it economically feasible.
2. No maximum curtailment level is fixed: the resulting curtailment can be as high as economically optimal while maximizing the promoter's benefit.
3. Independent of the amount of capacity installed, the model employs the hypothesis of a price-taker approach. This means wholesale market prices are not influenced by the total capacity of RES and storage installed at this connection point.
4. Electricity grid hosting capacity is provided for a high voltage (HV) distribution network consisting of overhead lines.

The model is designed to maximize promoter profits, considering the investment in generation and storage capacity. Incomes stem from the hourly selling of electricity injected into the grid at a defined hourly energy price. The objective function is defined in (1).

$$max\left[\sum_h (E\_inj_h * Rem_h) - \sum_t (P_t * Inv_t) - P_b * Inv_b\right] \quad (1)$$

Subject to

$$E\_inj_h \leq HC_h \quad (2)$$

$$E\_avail_h = \sum_t \left(P_t * pu_{t,h}\right) \quad (3)$$

$$E\_inj_h = E\_avail_h - E\_curt_h - E\_BSSin_h + E\_BSSout_h \quad (4)$$

The technology catalogue allows the model to invest in PV and wind generation capacity. Hourly energy injected into the grid is limited by the hourly available grid capacity as an upper bound (2). Hourly available energy depends on each technology's installed capacity and the resource's local availability at each hour of the year (3). Hence, this equation is applied to PV and wind capacity, not to batteries. Battery charge/discharge, State-of-Energy and efficiency are modelled according to [16]. The hourly energy balance determines the magnitude of curtailment (4).

4. Scenarios

In this section, the scenarios for the evaluation of hosting capacity enhancement via DHC and hybridization are presented. Also, the additional model restrictions employed for the different scenarios are described.

Table 1 gives an overview of the scenarios. The single-technology model result for static hosting capacity (SHC N_Hyb) is considered as baseline scenario to evaluate the impact of DHC and hybridization.

When modelling SHC, the hourly HC component in (2) restricting the maximum energy injected is considered constant at the minimum value of available hosting capacity throughout all hours. At no moment of the year is the generator allowed to inject more energy but the minimum value of HC available.

The hybridization (Hyb) of generation installations is evaluated as a second approach to enhance the grid's HC. The model can combine photovoltaic (PV), wind generation, and energy storage.

Table 1: Scenario overview

Scenario name	Hosting capacity	Hybridization option
SHC N_Hyb	Static	No
DHC N_Hyb	Dynamic	No
SHC Hyb	Static	Yes
DHC Hyb	Dynamic	Yes

For the non-hybrid scenarios (N_Hyb), additional restrictions prevent the model from installing more than one technology. Binary variables are employed for this restriction, as shown in (5). Pmax represents an auxiliary threshold of capacity applied as a parameter to restrict the model to install one technology only. With the auxiliary parameter, the optimization can be computed as linear. The parameter is defined as a large number to ensure it does not limit the capacity installed by the model. (6) guarantees that the model cannot invest in more than one technology as the sum of binary investment decisions must not be greater than unity. (5) and (6) are activated only for non-hybrid scenarios. Additionally, investment in battery capacity is set to 0 in N_Hyb scenarios.

$$P_t \leq Binary\_Inv\_Dec_t * Pmax \tag{5}$$

$$\sum_t Binary\_Inv\_Dec_t \leq 1 \tag{6}$$

5. Case study

The model is tested with a case study that evaluates the potential of the regulatory mechanisms to enhance RES grid integration into Spanish electricity networks. The economic input parameters (A) and the definition of RES potential at different case study locations (C) are presented in this section.

All optimizations are carried out as greenfield approaches with no pre-existing capacity of any technology.

5.1 Economic input parameters

A first economic input to the model is the investment costs of the three technologies considered in this case study, as shown in Table 2. The model considers costs on an annualized basis to facilitate the comparison of technologies with different lifetimes. The discount rate is fixed at 7%, and the assumptions on technology lifetime are included in the table.

Table 2: Technology investment costs and lifetime [17]

	Investment (€/kW)	Lifetime (years)	Annualized investment (€/kW-yr)
PV	500	25	42.91
Wind	950	30	76.56
4h Batteries	961	10	136.82

The available hourly remuneration for the injection of electricity into the grid is defined as price-taker under a merchant income scheme. These prices are set in this case study as the 2019 Spanish electricity SPOT market prices [18] before the pandemic and the gas crisis. Fig. 1 shows the load duration curve of 2019 Spanish SPOT prices. The price ranks from 74.74 to 0.03 €/MWh with a standard deviation of 10.88 €/MWh. The weighted average price for the 2019 electricity demand is 48.58 €/MWh.

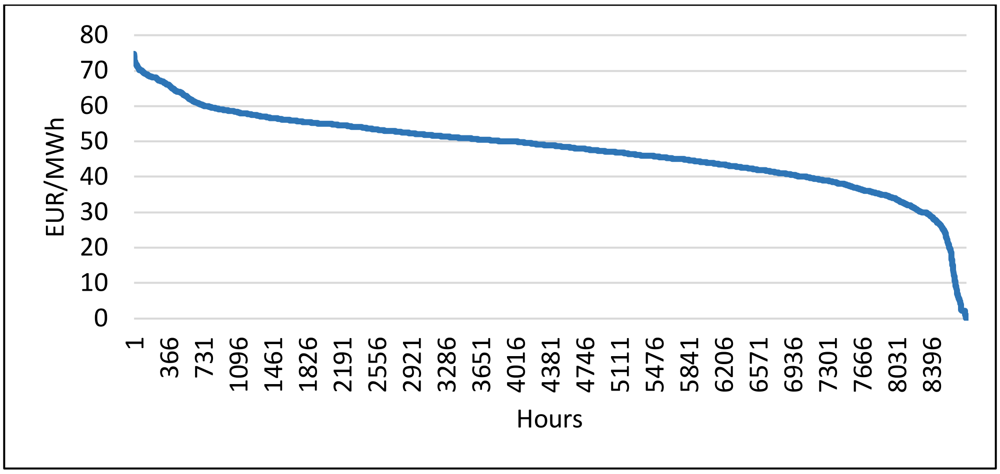

Fig. 1: Load duration curve of 2019 Spanish SPOT prices

5.2 Grid hosting capacity

The baseline electricity grid hosting capacity is set to 100 MW. This threshold is employed throughout all hours for the SHC scenarios.

The dynamic definition of hosting capacity allows considering hourly variations of the electricity grid's availability to evacuate energy injected. According to ENTSO-E, Dynamic Line Rating (DLR) allows to increase line capacity of overhead lines to up to 200%. Throughout

Europe, up to 15% gain can be observed over 90% of the time [19]. This estimation is applicable to the case study, as the 100 MW hosting capacity is part of the high voltage (HV) grid. The HV grid (below 220 kV) is considered part of the distribution grid in Spain and is commonly built as overhead lines [20].

As a conservative approximation to these numbers, hourly hosting capacities for this case study are considered to increase to 115 MW during colder winter months from November to April. HC is applied to 50% of the hours of the year instead of the 90% stated by ENTSO-E to account for high Spanish temperatures from spring to autumn.

The seasonal HC variation is the only oscillation considered. HC is set to the same at all hours of the day. Consequently, the average hosting capacity is increased from 100 to 107.5 MW by increasing hourly HC from 100 MW to 115 MW from November to April.

5.3 RES potential

The model is evaluated with an exemplary case study with hourly RES availability per unit (pu) curves for three locations in Spain, selected according to their PV and wind potential recorded in 2019 [21], [22]: A Coruña, Almería and Linares. The capacity factors (CFs) and the resulting levelized cost of energy (LCOE) are shown in Table 3. A Coruña represents a site with high wind but low PV potential, Almería shows good CFs for both technologies, and Linares is a good PV site with a low wind CF compared to the other sites.

Table 3: CF and LCOE at the three Spanish locations

Location	Capacity factor (CF)			LCOE (€/MWh)	
	PV	Wind	Ratio PV/Wind	PV	Wind
A Coruña	0.17	0.45	0.38	28.81	19.42
Almería	0.23	0.41	0.58	21.14	21.48
Linares	0.21	0.23	0.91	23.32	38.00

6. Results

The results of the case study are presented in the following. First, the effect of DHC is evaluated for non-hybrid installations (A). After that, the hybridization is assessed under the SHC scheme (B). In C, the combination of DHC and hybridization is analyzed.

The scenarios are evaluated based on the installed capacity of each technology, the amount of available energy injected, the curtailment levels, and the average energy price captured by the installation. This last value expresses the ratio of the total income obtained and energy injected into the grid.

6.1 Static vs dynamic hosting capacity

Fig. 2 compares the installed capacity for SHC and DHC without hybridization. In A Coruña and Almería, the model chooses to install wind capacity. Only in Linares, with high CF for PV and low wind potential, the model selects a PV installation. The installed technologies in A Coruña and Linares correspond to the technologies with lower LCOE, as identified in Table 3. In Almería, the LCOE of PV is slightly lower than that of wind. Still, the model prefers to install wind as the concentration of PV output in the central hours of the day would result in higher curtailment levels than the more random output of wind energy obtained at a similar LCOE.

Another striking observation from the model is that even the static definition of HC, resulting in 100 MW hosting capacity at all times, results in capacity installations of at least 150 MW. The possibility to inject energy during more hours compensates for the curtailment whenever available energy surpasses the 100 MW of HC. Curtailment levels in the SHC No_Hyb scenarios range from 6% to 18%. Overdimensioning the generation installations maximizes the generators' income, even under the SHC scheme.

Increasing the network hosting capacity by 15% during the winter months (November to April) leads to an increase in installed capacity in all locations. For the PV location of Linares, the observed increase is the lowest, with 6% more PV capacity in the DHC scenario. In the high-wind locations A Coruña and Almería, installed wind capacity increases by 9% and 8%, respectively. The higher wind CF of A Coruña leads to a higher installed capacity increase than Almería. The higher growth in the wind systems compared to the PV system of Linares indicates that the PV output profile concentrated to only some hours of the day leaves less room for making use of the increased hosting capacity. The energy injected into the grid is subject to growth coefficients similar to those of installed capacity, while curtailment levels (measured in %) are not affected by the change from SHC to DHC.

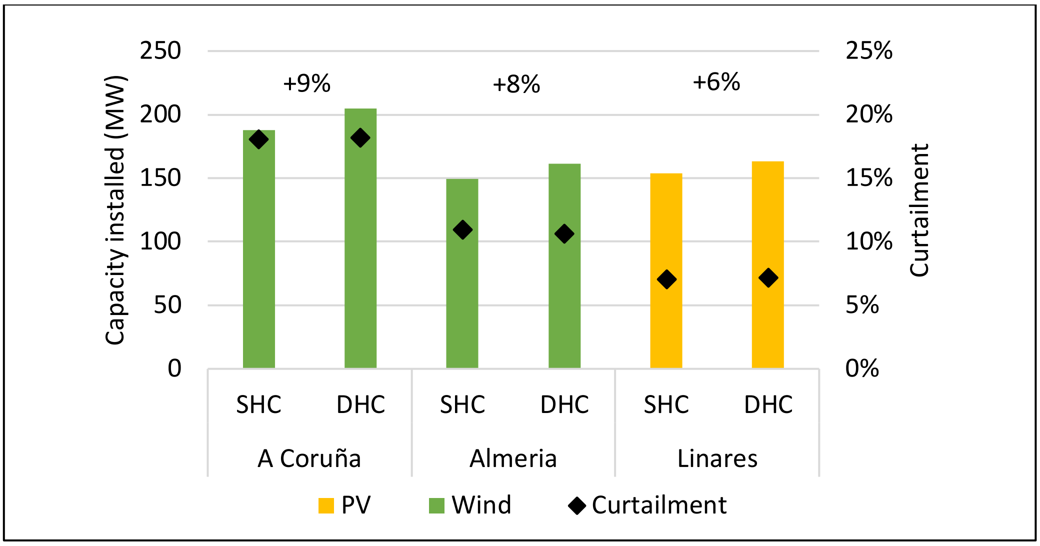

Fig. 2: Installed PV & wind capacities and curtailment levels when moving from SHC to DHC

Fig. 5 provides an overview of the energy injected to the grid in each of the scenarios. Injected energy is considered with respect to the N_Hyb SHC scenario, hence values greater than 100% represent an increase of injected energy.

The average price captured by each scenario is summarized in Fig. 5. The PV installation in Linares captures an average remuneration price of 49 €/MWh, compared to 46 €/MWh for the wind installations.

6.2 Single-technology vs hybridization

The results of allowing the model to invest in an optimal capacity mix of PV, wind and batteries are presented in Fig. 3. The baseline scenario SHC N_Hyb is compared to the optimal capacity mix when the model is allowed to hybridize (Hyb) the installation, maintaining the static definition of HC. A first conclusion is that, at 2019 SPOT remuneration, battery investment costs impede storage from representing an attractive solution. No battery capacity is installed in any of the scenarios.

All locations are suitable for the hybridization of PV and wind capacity. The capacity mix proportion correlates with the generation technologies' capacity factors. The higher the CF of PV compared to the CF of wind, the higher the participation of PV in the final capacity mix. Consequently, A Coruña remains a wind-dominated location, and Linares remains PV-dominated. In Almería, where the CF of PV reaches 58% of the magnitude of the CF of wind (Table 3), the final capacity mix includes 46% of PV capacity.

In A Coruña, hybridization increases the optimal total installed capacity by 17%. In Almería, installed capacity is increased by 54% and in Linares by 9%. The more diverse the hybrid capacity mix, the higher the total capacity increase from non-hybrid to hybrid. In A Coruña, a total of 20% of PV is contained in the hybrid capacity mix. In Almería, this share increases to 46%. The hybrid installation in Linares includes 12% of wind capacity.

The energy injected into the grid (Fig. 5) is increased only slightly in the case of A Coruña (4%). Almería and Linares see more significant increases of injected energy, 20% and 11%, respectively. The increase in Linares is especially striking due to the comparatively low growth in installed capacity. Adding wind capacity at the PV-dominant location allows using the grid capacity at off-peak hours of PV production, significantly increasing injected energy. The comparatively low CF of PV in A Coruña (Table 3) explains the contrary observation at this site.

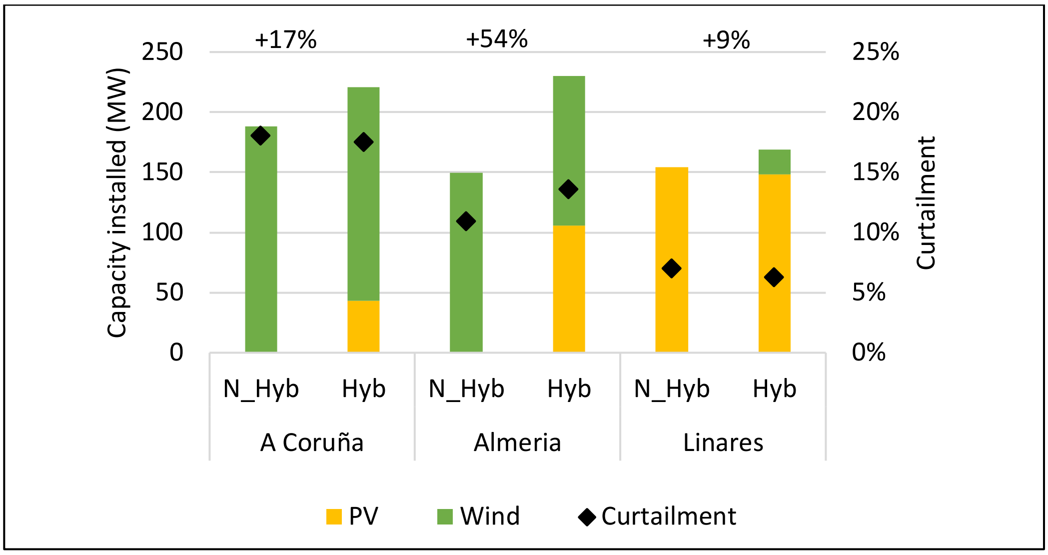

Fig. 3: Installed PV & wind capacities and curtailment levels when allowing hybridization (Hyb) under SHC

The curtailment level is seeing a notable impact in Almería only. A 54% capacity increase leads to a 3% curtailment increase. The average HC of 107.5 MW throughout the year is met by a total of 230 MW of installed capacity.

The average price captured in the wind-dominated locations increases from 46 to 47 €/MWh. The 49 €/MWh captured in Linares remain unchanged by the hybridization (Fig. 5).

6.3 Dynamic access for hybrid installations

Fig. 4 summarizes the benefits of DHC as well as hybridizing RES installations. Moving from a non-hybrid regime with SHC to allowing hybridization and the usage of DHC increases installed capacity of at least 19%. In Almería, the installed capacity increase is as high as 65%.

Even when combining DHC and hybridization, investment into battery capacity is still no option for the model.

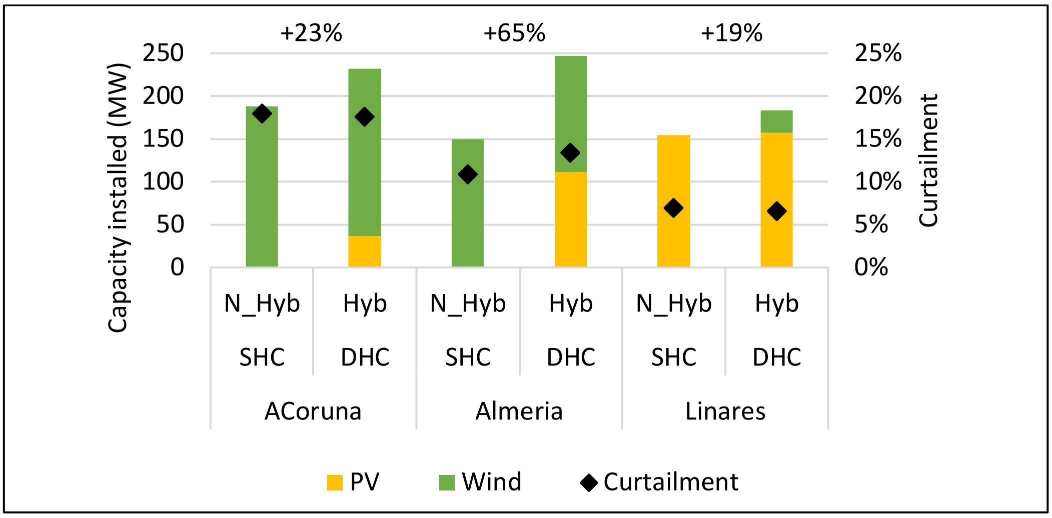

Fig. 4: Comparison of installed capacities and curtailment when moving from a non-hybrid SHC scheme to hybrid DHC

Injected energy is increased notably at all locations. As already observed in the previous section, the smallest increase in injected energy is obtained in A Coruña (12%) due to a rather low CF of PV. In Linares, the participation of 14% of wind capacity to the mix allows injecting 21% more energy when moving from SHC N_Hyb to DHC Hyb (Fig. 5). In Almería, this increase reaches the maximum of 29% due to the high increase in installed capacity and the high capacity factors of both technologies.

Curtailment levels in the DHC Hyb scenarios are the same as in the SHC Hyb scenarios presented in B. The average price captured does not change by combining DHC and hybridization (Fig. 5).

7. Conclusions

This paper proposes a model to evaluate the introduction of regulatory mechanisms for enhancing the use of the existing electricity network to accelerate the electricity grid integration of high shares of renewable generation capacity, avoiding reinforcements. The analyzed mechanisms to enhance grid hosting capacity are the introduction of dynamic hosting capacity and hybrid RES installations. A case study analyses the mechanisms at three Spanish generation sites with different RES potentials.

Both mechanisms allow to increase the optimal capacity installed and the total RES energy injected to the grid while ensuring the economic viability of the installation from the promoter's perspective. The parameter most sensitive to considering DHC and hybridization is the magnitude of installed generation capacity. The increased installed capacity allows to inject more electricity into the grid while only moderately impacting curtailment levels and the average price captured. Overdimensioning the installation behind the connection point to the electricity grid yields higher benefits, even though up to 18% of the available energy is subject to curtailment.

The introduction of DHC in single-technology (N_Hyb) systems increases installed capacity and energy injected into the grid by below 10%. Allowing for hybridization under a static definition of grid HC increases installed capacity by up to over 50%, injecting up to 20% more energy into the network. The combination of DHC and hybridization yields the highest installed capacities, increasing the capacity from the base case (SHC N_Hyb) by up to 65% and injecting up to 29% more energy.

DHC and hybrid RES installations represent a suitable tool to accelerate the integration of RES generation capacity into existing electricity grids. Regulators and RES promoters can benefit from these regulatory mechanisms. RES promoters by increasing their earnings as defined in the model's objective function. Regulators by reducing the complexity of the grid access process via the avoidance of reinforcement works, facilitating compliance with national targets of rapid RES rollout.

Future work should enhance the analysis of the profitability of the proposed regulatory mechanisms under different remuneration schemes, such as Power Purchase Agreements (PPAs) or Contracts for Differences (CfDs). A contrast with SPOT prices i) affected by the gas crisis and ii) shifting away from the price taker approach (i.e. including RES availability influencing prices) represent further future work to be carried out. Also, a more precise definition of DHC accounting for weather effects or grid operating conditions seems promising for an in-depth analysis of the potential of DHC for enhancing electricity grid hosting capacity and avoiding reinforcement.

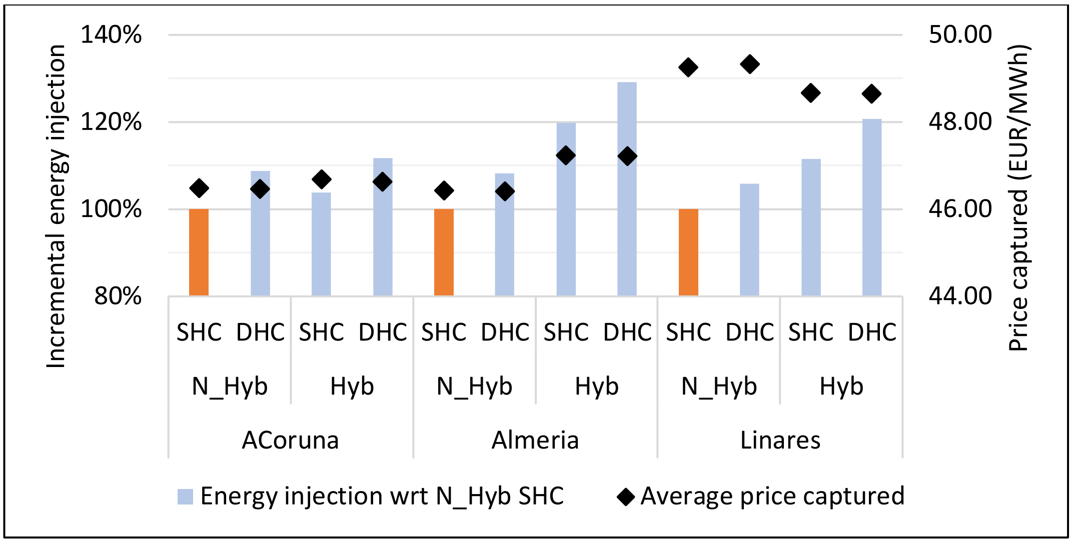

Fig. 5: Injected energy and average price captured per scenario

8. References

[1] European Commission, 'National energy and climate plans (NECPs)', *National energy and climate plans (NECPs)*, Jan. 23, 2019. https://ec.europa.eu/energy/topics/energy-strategy/national-energy-climate-plans_en (accessed Oct. 05, 2020).

[2] R. Roca, '¿Burbuja renovable o proyectos fantasma? Los permisos de acceso concedidos por REE superan los 121 GW, pero más del 60% no dispone aún de punto de conexión', Jun. 25, 2020. https://elperiodicodelaenergia.com/burbuja-renovable-o-proyectos-fantasma-los-permisos-de-acceso-concedidos-por-ree-superan-los-121-gw-pero-mas-del-60-no-dispone-aun-de-punto-de-conexion/ (accessed Oct. 05, 2020).

[3] R. Roca, 'Atascazo monumental en la red ante la avalancha de nuevas renovables: REE da el punto de acceso a 1 GW mientras rechaza 12 GW solo en diciembre', Feb. 03, 2020. https://elperiodicodelaenergia.com/atascazo-monumental-en-la-red-ante-la-avalancha-de-nuevas-renovables-ree-da-el-punto-de-acceso-a-1-gw-mientras-rechaza-12-gw-solo-en-diciembre/ (accessed Oct. 05, 2020).

[4] L. Ojea, 'Locura renovable en España: quieren instalarse más de 87 GW, la mitad ya con el permiso de acceso concedido por REE', Jan. 31, 2019. https://elperiodicodelaenergia.com/locura-renovable-en-espana-quieren-instalarse-mas-de-87-gw-la-mitad-ya-con-el-permiso-de-acceso-concedido-por-ree/ (accessed Oct. 05, 2020).

[5] Redacción El Periódico de la Energía, 'REE invertirá 118 millones en la red de transporte de la Comunidad Valenciana hasta 2023', Sep. 18, 2020. https://elperiodicodelaenergia.com/ree-invertira-118-millones-en-la-red-de-transporte-de-la-comunidad-valenciana-hasta-2023/ (accessed Oct. 05, 2020).

[6] L. Herding, R. Cossent, M. Rivier, J. P. Chaves-Ávila, and T. Gómez, 'Assessment of electricity network investment for the integration of high RES shares: A Spanish-like case study', *Sustainable Energy, Grids and Networks*, vol. 28, p. 100561, Dec. 2021, doi: 10.1016/j.segan.2021.100561.

[7] M. Alturki, A. Khodaei, A. Paaso, and S. Bahramirad, ‘Optimization-based distribution grid hosting capacity calculations’, *Applied Energy*, vol. 219, pp. 350–360, Jun. 2018, doi: 10.1016/j.apenergy.2017.10.127.

[8] M. H. J. Bollen and N. Etherden, ‘Overload and overvoltage in low-voltage and medium-voltage networks due to renewable energy — Some illustrative case studies’, in *2011 2nd IEEE PES International Conference and Exhibition on Innovative Smart Grid Technologies*, Dec. 2011, pp. 1–8. doi: 10.1109/ISGTEurope.2011.6162645.

[9] T. Gómez, R. Cossent, and J. P. Chaves-Avila, ‘Flexible network access, local flexibility market mechanisms and cost-reflective tariffs: three regulatory tools to foster decarbonized electricity networks’, *Oxford Energy Forum*, vol. 124, pp. 18–23, May 2020, doi: https://www.iit.comillas.edu/publicacion/mostrar_publicacion_working_paper.php.es?id=387.

[10] J. P. Chaves Avila *et al.*, ‘EUniversal D5.1 - Identification of relevant market mechanisms for the procurement of flexibility needs and grid services’, Jan. 2021, doi: https://euniversal.eu/wp-content/uploads/2021/02/EUniversal_D5.1.pdf.

[11] MIT, ‘The Future of Solar Energy’, 2015. http://energy.mit.edu/wp-content/uploads/2015/05/MITEI-The-Future-of-Solar-Energy.pdf (accessed Apr. 06, 2020).

[12] R. C. Knight, J. P. Montez, F. Knecht, and T. Bouquet, ‘Distributed generation connection charging within the European Union’, Sep. 2005. https://www.ceer.eu/documents/104400/-/-/cacc41c3-7177-7652-71f7-b2b2ef3472a9 (accessed Jul. 09, 2020).

[13] IRENA, ‘Dynamic Line Rating: Innovation Landscape Brief’. 2020. [Online]. Available: https://www.irena.org/-/media/Files/IRENA/Agency/Publication/2020/Jul/IRENA_Dynamic_line_rating_2020.pdf?la=en&hash=A8129CE4C516895E7749FD495C32C8B818112D7C

[14] US DOE, ‘Dynamic Line Rating’, Jun. 2019. https://www.energy.gov/sites/prod/files/2019/08/f66/Congressional_DLR_Report_June2019_final_508_0.pdf (accessed Jul. 07, 2022).

[15] MITECO, ‘Real Decreto 1183/2020’, Dec. 30, 2020. https://boe.es/buscar/doc.php?id=BOE-A-2020-17278 (accessed Jan. 02, 2021).

[16] K. Antoniadou-Plytaria, D. Steen, L. A. Tuan, O. Carlson, and M. A. Fotouhi Ghazvini, ‘Market-Based Energy Management Model of a Building Microgrid Considering Battery Degradation’, *IEEE Transactions on Smart Grid*, vol. 12, no. 2, pp. 1794–1804, Mar. 2021, doi: 10.1109/TSG.2020.3037120.

[17] IEA, ‘World Energy Outlook 2019 – Analysis’, *IEA*, Nov. 2019. https://www.iea.org/reports/world-energy-outlook-2019 (accessed Feb. 10, 2021).

[18] REE, ‘ESIOS: Precio mercado SPOT diario’. https://www.esios.ree.es/es?locale=es (accessed Oct. 27, 2021).

[19] ENTSO-E, ‘Dynamic Line Rating (DLR) - ENTSO-E’. https://www.entsoe.eu/Technopedia/techsheets/dynamic-line-rating-dlr (accessed Jun. 02, 2022).

[20] G. Prettico, F. Gangale, A. Mengolini, A. Lucas, and G. Fulli, ‘DISTRIBUTION SYSTEM OPERATORS OBSERVATORY: From European Electricity Distribution Systems to Representative Distribution Networks’. EUR 27927 EN; 10.2790/701791, 2016. [Online]. Available: https://publications.jrc.ec.europa.eu/repository/bitstream/JRC101680/ldna27927enn.pdf

[21] S. Pfenninger and I. Staffell, ‘Long-term patterns of European PV output using 30 years of validated hourly reanalysis and satellite data’, *Energy*, vol. 114, pp. 1251–1265, Nov. 2016, doi: 10.1016/j.energy.2016.08.060.

[22] I. Staffell and S. Pfenninger, ‘Using bias-corrected reanalysis to simulate current and future wind power output’, *Energy*, vol. 114, pp. 1224–1239, Nov. 2016, doi: 10.1016/j.energy.2016.08.068.